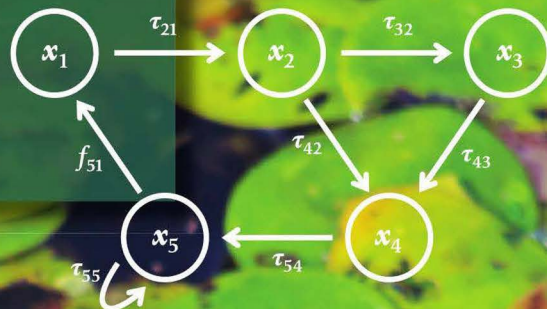


STUDENT MATHEMATICAL LIBRARY
Volume 106



Matrix Models for Population, Disease, and Evolutionary Dynamics

J. M. Cushing



AMERICAN
MATHEMATICAL
SOCIETY

Matrix Models for Population, Disease, and Evolutionary Dynamics

STUDENT MATHEMATICAL LIBRARY
Volume 106

Matrix Models for Population, Disease, and Evolutionary Dynamics

J. M. Cushing



AMERICAN
MATHEMATICAL
SOCIETY

Providence, Rhode Island

EDITORIAL COMMITTEE

John McCleary
Rosa C. Orellana (Chair)

Paul Pollack
Kavita Ramanan

2020 *Mathematics Subject Classification.* Primary 92D25, 92D30, 39A50; Secondary 37N25, 15B99.

The bullfrog cover photo is courtesy of Diane Labombarbe / E+ via Getty Images.

For additional information and updates on this book, visit
www.ams.org/bookpages/stml-106

Library of Congress Cataloging-in-Publication Data

Names: Cushing, J. M. (Jim Michael), 1942- author.
Title: Matrix models for population, disease, and evolutionary dynamics / J.M. Cushing.
Description: Providence, Rhode Island : American Mathematical Society, [2024] | Series: Student mathematical library, 1520-9121 ; volume 106 | Includes bibliographical references and index.
Identifiers: LCCN 2023050951 | ISBN 9781470473341 (paperback) | 9781470476434 (ebook)
Subjects: LCSH: Biology--Mathematical models. | Matrices. | AMS: Biology and other natural sciences -- Genetics and population dynamics -- Population dynamics (general). | Biology and other natural sciences -- Genetics and population dynamics -- Epidemiology. | Difference and functional equations -- Difference equations -- Stochastic difference equations. | Dynamical systems and ergodic theory -- Applications -- Dynamical systems in biology. | Linear and multilinear algebra; matrix theory -- Special matrices -- None of the above, but in this section.
Classification: LCC QH323.5 .C88 2024 | DDC 578.01/5129434-de23
LC record available at <https://lccn.loc.gov/2023050951>

Copying and reprinting. Individual readers of this publication, and nonprofit libraries acting for them, are permitted to make fair use of the material, such as to copy select pages for use in teaching or research. Permission is granted to quote brief passages from this publication in reviews, provided the customary acknowledgment of the source is given.

Republication, systematic copying, or multiple reproduction of any material in this publication is permitted only under license from the American Mathematical Society. Requests for permission to reuse portions of AMS publication content are handled by the Copyright Clearance Center. For more information, please visit www.ams.org/publications/pubpermissions.

Send requests for translation rights and licensed reprints to reprint-permission@ams.org.

© 2024 by the American Mathematical Society. All rights reserved.
The American Mathematical Society retains all rights
except those granted to the United States Government.
Printed in the United States of America.

⊗ The paper used in this book is acid-free and falls within the guidelines
established to ensure permanence and durability.
Visit the AMS home page at [https://www.ams.org/](http://www.ams.org/)

This book is dedicated to
Lucia, Lara, Jesse, Alina, and Deirdre.

Contents

Preface	xii
Table of Symbols	xv
Chapter 1. Population Models	1
§1.1. Linear Difference Equations	2
§1.2. Nonlinear Difference Equations	7
§1.3. Applications	31
§1.4. Concluding Remarks	37
§1.5. Exercises	37
Chapter 2. Linear Matrix Models for Structured Populations	43
§2.1. Modeling Methodology	44
§2.2. The Fundamental Theorem of Demography	50
§2.3. The Reproduction Number R_0	60
§2.4. Sensitivity and Elasticity Analysis	69
§2.5. Applications	74
§2.6. Concluding Remarks	84
§2.7. Exercises	85
Chapter 3. Nonlinear Matrix Models for Structured Populations	91
§3.1. Modeling Methodology	91

§3.2. Equilibria and the Linearization Principle	98
§3.3. The Extinction Equilibrium and Its Stability	102
§3.4. Positive Equilibria: A Basic Bifurcation Theorem	108
§3.5. Secondary Bifurcations	119
§3.6. Imprimitive Projection Matrices	134
§3.7. Applications	142
§3.8. Concluding Remarks	160
§3.9. Exercises	161
 Chapter 4. Disease and Epidemic Models	167
§4.1. Preliminaries	167
§4.2. Disease-Free Equilibria and R_0	171
§4.3. Examples	172
§4.4. Endemic Equilibria: A Basic Bifurcation Theorem	182
§4.5. Applications	187
§4.6. Concluding Remarks	199
§4.7. Exercises	199
 Chapter 5. Darwinian Dynamics	201
§5.1. Modeling Methodology	202
§5.2. Extinction Equilibria	214
§5.3. A Basic Bifurcation Theorem	217
§5.4. The ESS Maximum Principle	221
§5.5. R_0 for Darwinian Models	227
§5.6. Applications	231
§5.7. Concluding Remarks	250
§5.8. Exercises	251
 Appendix A. Appendices	255
§A.1. Jury Conditions for 2×2 Matrices	255
§A.2. The Linearization Principle	257
§A.3. The Implicit Function Theorem	258
§A.4. Mean Trait Dynamics	259

Contents

ix

Bibliography 263

Index 271

Preface

This book offers an introduction to the use of matrix theory and linear algebra in modeling the dynamics of biological populations. Matrix algebra has been used in population dynamics since the seminal work of H. Bernardelli [8], E. G. Lewis [103], and P. H. Leslie [100], [101] in the 1940s. Particularly influential was Leslie's work on the dynamics of populations structured by age categories. Later, in 1965, L. P. Lefkovitch demonstrated how the methodology can be applied to populations structured by other means as well, such as body size or weight, life cycle stages, disease states, spatial location, and/or any number of physiological and behavioral characteristics [99]. Today matrix models continue to play an expanding major role in theoretical and applied population dynamics [13], [14], [15], [28], [106].

The book does not serve as a broad introduction to the subject of structured population dynamics. That would entail covering a large variety of other types of mathematical equations, including partial differential equations, delay or functional differential equations, integral equations, and integro-differential equations [9], [10], [12], [28], [55], [83], [84], [94], [105], [109], [110], [122], [130], [133], and require more mathematical background (and a much larger book). With a focus on matrix models, the book requires only first courses in multivariable calculus and matrix theory (or linear algebra) as prerequisites. Additional material needed that might not be found in a first course in these subjects is

covered when required (e.g., topics from Perron–Frobenius theory). Although a student would benefit from a first course in differential equations (in that basic topics in dynamics would then be familiar), the book is mathematically self contained with regard to dynamical systems concepts (equilibria, stability, bifurcations, etc.). It is aimed at the upper-division undergraduate or first-year graduate student level of mathematical maturity. The book could be used in a variety of ways, including as

- a text for a special topics course;
- a supplement to a mathematical biology course;
- a resource for a general modeling course;
- independent reading and research projects;
- a source of applications of matrix theory and difference equations.

I have used the material in the book, over many decades, in a variety of teaching and mentoring settings at the University of Arizona, including an undergraduate biomathematics course in the Department of Mathematics and a mathematical modeling course in the Department of Ecology and Evolutionary Biology; undergraduate independent study courses for both mathematics and biological majors; undergraduate honors projects and theses; REU research projects; and research training courses for first-year graduate students in the Interdisciplinary Program in Applied Mathematics.

In this book, a student will learn the basics of modeling methodology (i.e., how to set up a matrix model from biological underpinnings) and the fundamentals of the analysis of discrete time dynamical systems (equilibria, stability, bifurcations, etc.). In addition to numerous examples that illustrate these fundamentals, several applications appear at the end of each chapter that illustrate the full cycle of model setup, mathematical analysis, and interpretation. These applications were carefully selected so as to illustrate not only the mathematical techniques and theorems presented in the chapter but to showcase some specific questions and problems of historical and/or contemporary interest in theoretical and applied population dynamics.

A focus throughout the book is on the long-term fate of a population (i.e., its asymptotic dynamics), and a central recurrent theme in all chapters concerns the problem of extinction versus survival. Which of these

outcomes a model equation predicts typically depends on the parameters (coefficients) appearing in the model equation, and a change in one (or more) of these parameters can change the predicted outcome from extinction to survival or vice versa. Bifurcation theory is a mathematical discipline that focuses specifically on dynamic changes caused by changes in an equation's parameters; hence, bifurcation theory serves as a natural context in which to study population dynamic models, including the basic question of extinction versus survival. Each chapter has as its centerpiece a basic bifurcation theorem that addresses the issue of extinction versus survival. (A twist occurs in Chapter 4 on epidemic models where the extinction state is replaced by a so-called disease-free state.) The strength of these basic bifurcation theorems is their generality and relative ease of application. They therefore serve as a baseline starting point for the analysis of virtually any model. The shortcoming of the basic bifurcation theorems is that they do not give a complete global picture of a model's dynamics. This global picture depends heavily on the particular details of the model equation under consideration and requires further analysis.

The topics presented in the Chapters 1–3 are, in my view, the bare bones of matrix models and structured population dynamics, both the modeling methodology and the analysis of model equations. These chapters give a student a solid foundation on which to pursue further topics, either in higher level textbooks and scientific/mathematical literature or as original research projects. Although the models and equations treated are in discrete time and deal with populations structured by discrete classes only, they serve as a starting point for more general models involving continuous time and/or population structuring, which are mathematically more difficult and challenging.

Chapters 4 and 5 give two example directions for further topic development in structured population dynamics. Models of diseases, used in the study of epidemics, are structured population models (the structuring done with respect to disease states). While commonly done using ordinary differential equations, discrete time models are also used (e.g., see [9]). Chapter 4 gives an introduction to this topic for discrete disease classes. (Discrete time models with continuously distributed disease classes lead to integro-difference equation type models [e.g., see [94], [108]]). Chapter 5 extends population dynamic models to include Darwinian evolution by natural selection. The modeling methodology given

in this chapter has only recently been developed for discrete time models [129] and, to my knowledge, appears at this time in no student level book. Both of these chapters open the door to innumerable research projects for young investigators, given that there are so many pathogens and diseases that threaten any biological population and given that evolution is the central principle in biology.

There are numerous other topics of interest and importance in population dynamics that are not covered in this book. For example, models that include immigration/emigration and harvesting, periodic (seasonal) or stochastically fluctuating parameters, a spatial component, or multispecies interactions are not covered. The reasons, besides the length of the book, are that these topics demand higher mathematical prerequisites or, in some case, are not yet so well developed for matrix models. The topics covered in the book will, however, give a student a solid foundation on which to pursue these and other topics found in higher level textbooks or in the scientific/mathematical literature.

I am highly grateful for the comments that I received from several reviewers of early drafts of the book. Their critiques and suggestions were very helpful in preparing an improved final version.

Jim Michael Cushing
Professor Emeritus
Department of Mathematics
Interdisciplinary Program in Applied Mathematics
University of Arizona
Tucson, AZ 85721 USA

Table of Symbols

$x = \text{col}(x_i)$	an m -dimensional column vector with $x_i \in R$
$x^T = \text{row}(x_i)$	the transpose of $x = \text{col}(x_i)$
R^m	m -dimensional Euclidean space
$x \geq 0_m$	means $x \in R^m$ has nonnegative entries $x_i \geq 0$
$x > 0_m$	means $x \in R^m$ has positive entries $x_i > 0$
R_+^m	the set of nonnegative vectors $x \geq 0_m$ in R^m
$\text{int}(R_+^m)$	the set of positive vectors $x > 0_m$
∂R_+^m	$R_+^m/\text{int}(R_+^m)$ = the boundary of R_+^m
$R = R^1$	the set of real numbers
$R_+ = R_+^1$	the set of nonnegative real numbers
$\text{int}(R_+)$	the set of positive real numbers
Z_+	the set of nonnegative integers $\{0, 1, 2, \dots\}$
$C(\Delta : \Theta)$	the set of continuous functions from Δ to Θ
$C^q(\Delta : \Theta)$	$\begin{cases} \text{the set of } q\text{-times continuously differentiable} \\ \text{functions from a } \Delta \text{ to } \Theta \end{cases}$
∂_x	the derivative with respect to x
∇_x	the gradient of a function of x (a column vector)
$M = [m_{ij}]$	an $m \times n$ matrix with entries m_{ij}
$M^T = [\bar{m}_{ji}]$	the conjugate transpose of M
$\rho(\mathbf{M})$	$\begin{cases} \text{the spectral radius of } \mathbf{M} \\ \max\{ \lambda_i \} \text{ where } \lambda_i \text{ are the eigenvalues of } \mathbf{M} \end{cases}$
$M \odot N = [m_{ij}n_{ij}]$	the Hadamard product of $M = [m_{ij}]$, $N = [n_{ij}]$
$w \cdot v = \sum_{i=1}^m w_i v_i$	the inner product of $w, v \in R^m$
$\ x\ = \sum_{i=1}^m x_i $	the vector norm we will use
\coloneqq	means “is defined to be”
$\gtrsim (\lesssim)$	means “greater (less) than and close to”

$x \leq y$ ($x \geq y$)	means $x_i \leq y_i$ ($x_i \geq y_i$) for all i
$M \leq N$ ($M \geq N$)	means $m_{ij} \leq n_{ij}$ ($m_{ij} \geq n_{ij}$) for all i, j
I_m	is the $m \times m$ identity matrix

Chapter 1

Population Models

The basic goal of population dynamics is to account for changes in a biological population over time. In order to set up a mathematical model for this purpose, one needs to decide what population measure to use and at what points in time to track it. A single quantity such as the total population size (or density) of individuals, biomass, or dry weight is a coarse measurement that ignores differences among individuals. However in many (if not most) biological populations, individual organisms differ in a variety of ways that significantly affect their fitness (fertility, survival, etc.), which in turn affect the dynamics of the population as a whole. At an opposite extreme is a model that tracks every individual over time. For all but those populations with a small number of individuals, such individual-based models consist of so many equations that their analysis is intractable and their study reliant on computer simulations, from which it is difficult to attain rigorous and broad insight into their properties and implications. A middle ground is a structured population model in which all individuals are categorized by a finite set of classes based on one or more characteristics, such as chronological age, body size or weight, life cycle stage, gender, state of health relative to some disease, behavioral activity, genetic composition, and so on. The population is then represented by the finite-dimensional, vector of population densities in each class. If this demographic vector is censused at discrete time units, then a mathematical model that predicts the vector from one time step to the next will take the form of a so-called **difference equation**

(or a recursion formula). Often, as we will see, this prediction is mathematically calculated by a matrix multiplication of the vector and, as a result, the resulting model for the dynamics of this structured population is called a **matrix population model** [13], [28]. Mathematically, such a model is an example of a discrete time dynamical system [95].

The distribution of individuals could be described by a continuously varying characteristic and tracked continuously through time. In that case, the mathematical model for the dynamics of the distribution takes the form of a partial differential equation [28], [110]. Another alternative is to track a continuous characteristic in discrete time, an approach that leads to integro-difference equations [94]. As an introduction to structured population dynamics, this book will focus on discrete time and structuring. For a discussion contrasting discrete versus continuous time modeling of structured populations, see [13].

Before delving into a study of matrix population models for structured populations, we take a brief look in this introductory chapter at the unstructured population case, as modeled by a single difference equation. We do this for pedagogical reasons, namely so that the reader will become familiar, in the lowest-dimensional setting, with modeling methodologies for discrete-time population dynamics, with basic mathematical techniques used to analyze discrete time models, and with some fundamental biological questions that can be addressed by the models. This look at single difference equation models is not intended to be a wide survey of this topic but is instead intended to provide only a framework and some guidelines for the study of matrix equations in subsequent chapters. We will not, therefore, dwell on any specific applications of single difference equations but instead focus on model derivation methodology and some basic mathematical methods of analysis.

1.1. Linear Difference Equations

Let $x(t)$ denote population density at time t . From a knowledge of $x(t)$, our goal is to predict the population density at a future point in time, say $t + 1$. The unit of time is at the modeler's discretion and could, for example, simply be a convenient time for a follow-up census (daily, monthly, annually, etc.) or be related to some significant biological or physiological process, such as a generation or maturation period. The model derivation method we use is based on the following simple accounting

principle: at time $t + 1$ two types of individuals will be present in the population census, namely individuals who were not present in the previous census at time t (new arrivals such as newborns and immigrants) and individuals who were present at time t (survivors); thus,

$$(1.1) \quad x(t+1) = \text{new arrivals} + \text{survivors}.$$

To build a mathematical model, we need to provide mathematical expressions for the new arrivals and for the survivors. These expressions will depend, of course, on the biological circumstances we wish to consider. In the introduction to discrete-time population dynamics undertaken here, we will focus on populations closed to immigration (or seed-ing) and not subject to emigration (or harvesting). In this way, new ar-rivals in equation (1.1) are due to births only, and survivors are individ-uals present at time t who do not die and are present at time $t + 1$.

Suppose each individual alive at time t produces $b_0 > 0$ newborns that survive to time $t + 1$. Then the total number of newborns contributed at time $t + 1$ by all individuals alive at time t is $b_0x(t)$. Note that this term has both a reproduction and a survival component since newborns between census times need to survive to the next census in order to be counted in $x(t + 1)$. Thus, b_0 is viewed as an individuals expected num-ber of births in a unit of time multiplied by the probability that the new-born survives to the next census time. While keeping this in mind, we will refer to the model parameter b_0 as a **(per capita) fertility rate**. Fi-nally, with regard to the survivors present in the census at t , we assume that the fraction of individuals that survive a unit of time is s_0 , where $0 \leq s_0 \leq 1$; hence, the total of all survivors is $s_0x(t)$. (We can also view s_0 as the probability an individual survives a unit of time.) We call the model parameter s_0 the **(per capita) survival rate**. (The reason for the zero subscripts will become clear later.) We will always assume

$$(1.2) \quad b_0 > 0 \quad \text{and} \quad 0 \leq s_0 < 1$$

so that some reproduction occurs and that some post-reproduction loss occurs by death.

Under these modeling assumptions, equation (1.1) becomes

$$(1.3) \quad x(t+1) = b_0x(t) + s_0x(t)$$

or

$$(1.4) \quad x(t+1) = r_0x(t),$$

where we define

$$r_0 := b_0 + s_0 > 0.$$

This difference equation determines, by recursive application, a unique sequence of future predictions of the population density $x(t)$ once an initial population density $x(0)$ is provided. It defines what is called a **discrete time dynamical system**. We call the sequence $x(t)$ a **solution** of equation (1.4). Equation (1.4) together with an initial condition $x(0)$ is called an **initial value problem**.

A straightforward induction yields a formula for the solution of the difference equation (1.4), which permits a prediction of $x(t)$ directly from $x(0)$:

$$(1.5) \quad x(t) = x(0) r_0^t.$$

We call the model parameter r_0 the **population growth rate**. We can also write this formula as

$$x(t) = x(0) r_0^t = x(0) e^{t \ln r_0}.$$

We call $\ln r_0$ the **exponential population growth rate** $\ln r_0$ or **fitness**.¹

It is clear from both equation (1.4) and the solution formula (1.5) that if $x(0) \geq 0$, then $x(t) \geq 0$ for all $t \in \mathbb{Z}_+$. If $x(0) = 0$, then the population remains at zero (i.e., $x(t) = 0$ for all $t \in \mathbb{Z}_+$). A constant solution, such as this, is called an **equilibrium** (or a **fixed point**). We will denote equilibria by x_e . The particular equilibrium $x_e = 0$ we call the **extinction equilibrium**. On the other hand if $x(0) > 0$, then it is clear from (1.5) that

$$(1.6) \quad \lim_{t \rightarrow +\infty} x(t) = \begin{cases} 0 & \text{if } 0 < r_0 < 1 \\ x(0) & \text{if } r_0 = 1 \\ +\infty & \text{if } 1 < r_0 \end{cases}.$$

In the first case when $0 < r_0 < 1$, the population tends asymptotically to extinction, while in the third case when $1 < r_0$, it grows (exponentially) without bound. In the first case, we say that the extinction equilibrium is an **attractor**, while in the third case, we say it is a **repeller**. Thus, as the value of the population growth rate r_0 increases through 1, the population's long-term fate (its asymptotic dynamic) significantly changes from extinction to survival (in the form of unlimited exponential growth), and because of this, we say a **bifurcation** has occurred.

¹Often throughout the book we will use the notation $\exp(x)$ for e^x . So, in this case, we can also write $r_0^t = \exp(t \ln r_0)$.

Notice that when $r_0 = 1$, the population remains fixed at its initial condition (that is, $x(t) = x(0)$) for all $t \in \mathbb{Z}_+$. In this case, *every* solution (1.5) is an equilibrium.

These facts are geometrically summarized in Figure 1.1, which shows a plot of all equilibria of (1.4) in the (r_0, x) -plane. This graph shows the intersection of two branches of equilibria at the point $(r_0, x) = (1, 0)$, namely the branch of extinction equilibrium points $(r_0, x_e) = (r_0, 0)$ for all r_0 and the branch of nonextinction equilibrium points $(r_0, x_e) = (1, x_e)$ for all values of x_e . This plot is called a **bifurcation diagram**, and the intersection point is called a **bifurcation point** (or more specifically a **transcritical bifurcation point** since it occurs at the intersection of two transversely crossing branches of equilibrium points). The bifurcation point $(r_0, x_e) = (1, 0)$ and its critical bifurcation value $r_0 = 1$ of the population growth rate r_0 are of fundamental importance biologically since it represents the threshold between extinction (when $r_0 < 1$) and survival (when $r_0 > 1$) of the population.

Some simple algebra shows

- $r_0 > 1$ if and only if $b_0 \frac{1}{1 - s_0} > 1$,
- $r_0 < 1$ if and only if $b_0 \frac{1}{1 - s_0} < 1$, and
- $r_0 = 1$ if and only if $b_0 \frac{1}{1 - s_0} = 1$.

The quantity

$$(1.7) \quad R_0 := b_0 \frac{1}{1 - s_0}$$

is called the **reproduction number**.² Its biological interpretation can be seen from the alternative formula

$$R_0 = \sum_{i=1}^{\infty} b_0 s_0^i,$$

which is obtained from the sum $(1 - s_0)^{-1}$ of the geometric series $\sum_{i=1}^{\infty} s_0^i$, by noting that s_0^i is the probability an individual survives i consecutive time steps. Thus, $b_0 s_0^i$ is the probability of surviving i time units multiplied by the reproductive reward for doing so. The sum of these expected reproductive outputs R_0 is then the *expected number of offspring*

² R_0 has been also called the reproductive number or value and sometimes the net reproduction number.

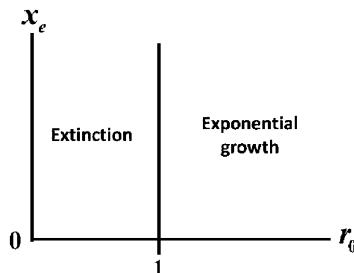


Figure 1.1. The bifurcation diagram for the linear equation (1.4) using r_0 as the bifurcation parameter. The same vertical bifurcation diagram occurs at 1 if R_0 is used as the bifurcation parameter. A similar bifurcation diagram results if b_0 is used as the bifurcation parameter with bifurcation point relocated from 1 to $1 - s_0$.

produced by an individual over its entire life span. It is no surprise, then, that population extinction occurs if $R_0 < 1$, since it means each individual is not expected to replace itself over its lifetime.

Remark 1.1. There are two model parameters, b_0 and s_0 , in equation (1.3). The quantities r_0 and R_0 are both quantities derived from these model equation parameters. As we have seen, either of these quantities can serve as a diagnostic that will determine the long-term fate of the population. Another point of view is to consider the model's asymptotic dynamics as determined by the fertility rate b_0 , while holding the survival rate s_0 fixed. The result is an equilibrium bifurcation diagram identical to that in Figure 1.1 with r_0 replaced by b_0 and the bifurcation point 1 replaced by $1 - s_0$. Or, similarly, we could fix b_0 and use s_0 as the bifurcation parameter. Then the result is again a bifurcation diagram as in Figure 1.1 but with r_0 replaced by s_0 and 1 replaced by $1 - b_0$. However, given the interpretation of s_0 and its corresponding constraint $0 \leq s_0 < 1$, a bifurcation occurs in this case only if $b_0 < 1$. Our point here is that in addition to quantities derived from model parameters, any individual parameter in a population model is a possible bifurcation parameter, to be chosen at the whim of the modeler (as might be dictated by available data or what can be manipulated in experiments). The choice of bifurcation parameter will become an even more central issue in later chapters where many more parameters typically appear in models.

1.2. Nonlinear Difference Equations

Equation (1.4) is called a **linear difference equation** because $x(t+1)$ is a linear function of $x(t)$. As a population model, it predicts asymptotic survival of the population only if $r_0 > 1$ (equivalently $R_0 > 1$), in which case the population grows exponentially. Exponential growth is not, obviously, a sustainable long-term dynamic, since the population density will exceed all bounds.³ The model allows for a long-term sustainable (i.e., asymptotically bounded) population only in the (highly unlikely or “nongeneric”) case that r_0 exactly equals 1. To have a model that more realistically allows for bounded and sustainable population growth, r_0 cannot remain constant over time.

There are many reasons why fertility and/or survival, and hence r_0 , might change over time: changes in environmental factors such as temperature and humidity (regular and periodic or irregular and stochastic), habitat and food resource availability, interactions with other biological species, the occurrence of diseases, etc. A general principle in population dynamics is that, even in the absence of such environmental factors, fertility and/or survival can also change due to changes in the population’s density. This can be due, for example, to overcrowding and competition for resources (food, mates, habitat, etc.). This is usually referred to as **density dependence** (or self regulation). For evidence of this in natural populations, see [21]. Mathematically, we express this phenomenon by letting $b(x)$ and $s(x)$ denote the fertility and survival rates of an individual in a population of density x , thereby obtaining from equation (1.1) the difference equation

$$(1.8) \quad x(t+1) = b(x(t))x(t) + s(x(t))x(t).$$

Here a modeler needs to specify mathematical expressions for $b(x)$ and $s(x)$ in such a way that $b(x) \geq 0$ and $0 \leq s(x) \leq 1$, at least for $x \geq 0$. When not both $b(x)$ and $s(x)$ are constant functions of x , then equation (1.8) is a **nonlinear difference equation** (because the right side $b(x)x + s(x)x$ of equation (1.8) is a nonlinear function of x).

A general way to model population self regulation is to introduce factors that modify the density-free fertility and survival rates b_0 and s_0 :

$$(1.9) \quad b(x) = b_0\beta(x) \quad \text{and} \quad s(x) = s_0\sigma(x),$$

³The British economist and philosopher Kenneth Boulding (a Nobel Prize nominee) is attributed with the comment: “Anyone who believes exponential growth can go on forever in a finite world is either a madman or an economist.”

where $\beta(x)$ and $\sigma(x)$ describe the effect that population density has on fertility and survival respectively. We assume

$$(1.10) \quad \beta(0) = 1 \quad \text{and} \quad \sigma(0) = 1$$

so that b_0 and s_0 retain their biological interpretations as the density-free fertility and survival rates, which for that reason, we refer to as **inherent rates** (or intrinsic rates). With expressions (1.9), equation (1.8) becomes

$$(1.11) \quad x(t+1) = b_0\beta(x(t))x(t) + s_0\sigma(x(t))x(t).$$

Clearly, given their biological meaning, we must assume that both **density factors** $\beta(x)$ and $\sigma(x)$ are nonnegative valued functions and that $s_0\sigma(x) \leq 1$ for all values of $x \geq 0$. Other mathematical properties of $\beta(x)$ and $\sigma(x)$ depend on biological assumptions and mechanisms a modeler wishes to incorporate into the model equation.

Commonly used density factors are

$$(1.12) \quad e^{-cx}, \quad c > 0$$

and

$$(1.13) \quad \frac{1}{1+cx}, \quad c > 0.$$

Each of these choices, and any other choice that is a decreasing function of $x > 0$, implies that any increase in population density is deleterious in the sense that it has a suppressing or negative effect on fertility and/or survival. There are, however, biological situations when increased population density, particularly when it is low, has a positive effect on one or both of these vital rates. Such a phenomenon is known as a **component Allee effect**. This can occur, for example, when increasing a low population density enhances mating possibilities or improves survival by means of group protection from predators [26]. Example rational functions that can be used as a density factor with an Allee component include

$$(1.14) \quad \frac{1+ax^q}{1+sax^q}$$

and

$$(1.15) \quad \frac{1+ax}{1+ax^2},$$

where $a, p > 0$ and $0 < s < 1$ are real numbers and $q \geq 1$ is an integer. The factor (1.14) is an increasing function of $x > 0$, rising from 1 to $1/s$ as $x \rightarrow +\infty$. The factor (1.15) at first increases as a function of

$x > 0$ before it decreases to 0 as $x \rightarrow +\infty$. Another Allee factor, found in [85], is

$$(1.16) \quad 1 + p \frac{x^q}{a + x^q}.$$

Throughout this chapter, we assume that the inherent vital rates and the population regulation factors in equation (1.11) have the following properties.

Assumption 1.2. The inherent fertility and survival rates b_0 and s_0 satisfy (1.2), and the population density factors satisfy $\beta, \sigma \in C^2(R : R_+)$. In addition to the normalizations (1.10), assume that $s_0\sigma(x) \leq 1$ and that $\beta(x)x$ is bounded for all $x \in R_+$.

The requirement that $\beta(x)x$ be bounded is the biologically reasonable assumption that there is an upper bound on the total number of newborns the population being modeled can produce per unit time, no matter what the population density is. This implies $\lim_{x \rightarrow \infty} \beta(x) = 0$, which means that the effect is to decrease an individual's fertility for large population densities to the extent that fertility asymptotically ceases as the population density increases without bound.

An initial condition $x(0) \in R_+$ associated with the difference equation (1.11) defines an **initial value problem**. By recursive iteration of the equation, starting with the initial condition $x(0)$, we obtain a unique sequence $x(t)$ for $t \in Z_+$, which we call a **solution** of the initial value problem.

Remark 1.3. R_+ is (forward) invariant under Assumption 1.2. By this is meant that all solutions of equation (1.11) with an initial condition $x(0) \geq 0$ satisfy $x(t) \geq 0$ for all $t \in Z_+$. Thus, in so far as applications of the equation to population dynamics, the values of the density factors $\beta(x)$ and $\sigma(x)$ for $x < 0$ are irrelevant. This means that we can redefine these factors in any way we want for $x < 0$ without affecting the dynamics of solutions with $x(0) \geq 0$ and hence any biological conclusions drawn from the equation. We mention this because some density factors commonly used in population models are not defined and smooth for all $x < 0$ as required by Assumption 1.2. The factor (1.13), which we will frequently use, is an example. When such factors are used we will always assume (even if not explicitly mentioned) that they are redefined for $x < 0$ in such a way that

they satisfy Assumption 1.2 (i.e., are twice continuously differentiable for all $x \in R$). See Exercise 1.29.

Example 1.4. The Discrete Logistic Equation. Suppose the time unit in the population equation (1.11) is the reproductive period for all individuals in the population, and suppose that post-reproduction survival is not possible (i.e., $s_0 = 0$). Such a population called **semelparous** (or in the case of plants **monocarpic**). Annual plants are an example, as are some longer-lived plants such as the century plants (agaves) and some species of bamboo. Examples of semelparity among animals include the famous Pacific salmon as well as many species of molluscs (such as some squid and octopi), insects, and arachnids. If we use (1.13) for the the fertility factor $\beta(x)$ and assume the reproductive period is one time unit in the model, then we get the equation

$$(1.17) \quad x(t+1) = b_0 \frac{1}{1 + cx(t)} x(t),$$

a difference equation called the **discrete logistic equation** (or sometimes the **Beverton-Holt equation**). Notice that

$$\beta(x)x = \frac{1}{1 + cx}x$$

is an increasing function that (by L'Hôpital's Rule) approaches $1/c$ as $x \rightarrow \infty$, and therefore, $\beta(x)x \leq 1/c$ for all $x \in R_+$. Since in this example $s_0\sigma(x) \equiv 0$, we see that Assumption 1.2 is satisfied (see Remark 1.3).

This famous equation can also be considered when post-reproduction survival is allowed (i.e., the population is **iteroparous**) by assuming that both adult reproduction and survival density factors are affected identically by population density so that both $\beta(x)$ and $\sigma(x)$ are given by (1.13) (e.g., see [101]). In this case, equation (1.11) becomes

$$x(t+1) = r_0 \frac{1}{1 + cx(t)} x(t),$$

which is identical to equation (1.17) with b_0 replaced by $r_0 := b_0 + s_0$. \square

The existence, uniqueness, and nonnegativity of solutions—basic properties of solutions needed for a mathematical model of population dynamics—require mathematical proofs for models based on differential equations but are obvious for difference equations. Therefore, when using difference equations as population models, we can directly turn

our attention to properties of solutions and what their biological implications are. Basic properties of interest are whether solutions blow-up, decay, equilibrate, or oscillate.

Example 1.5. It is uncommon that a formula for the solutions of initial value problems is available. An exception is the linear difference equation (1.4) with its solution formula (1.5). Another notable exception is the (nonlinear) discrete logistic equation (1.17). The reader is asked in Exercise 1.31 to verify that the solution of (1.17) with initial condition $x(0) \geq 0$ is

$$(1.18) \quad x(t) = \begin{cases} \frac{x(0)b_0^t}{x_e - x(0) + x(0)b_0^t} x_e & \text{if } b_0 \neq 1 \\ \frac{x(0)}{1 + cx(0)t} & \text{if } b_0 = 1 \end{cases},$$

where

$$x_e := \frac{b_0 - 1}{c}.$$

Using this formula, we can deduce several interesting facts about the solutions of the discrete logistic equation.

First, note that $b_0 \leq 1$ implies $\lim_{t \rightarrow \infty} x(t) = 0$ for all $x(0) > 0$. Suppose, on the other hand, that $b_0 > 1$. Rewriting the solution formula as

$$x(t) = x_e \frac{x(0)}{(x_e - x(0)) b_0^{-t} + x(0)}$$

and noting that $\lim_{t \rightarrow \infty} b_0^{-t} = 0$, we find that $\lim_{t \rightarrow \infty} x(t) = x_e$ for all nonzero initial conditions $x(0) > 0$. Notice that the initial condition $x(0) = x_e$ produces the constant solution $x(t) \equiv x_e$ for all $t \in \mathbb{Z}_+$ (called an equilibrium solution or fixed point). We conclude in this case that the population no longer goes extinct but instead equilibrates (i.e., is or approaches the equilibrium x_e as $t \rightarrow \infty$).

Moreover (letting t range continuously for the moment) from the derivative

$$\frac{dx(t)}{dt} = (x_e - x_0) \frac{x_0 x_e (\ln b_0) b_0^t}{(x_e - x_0 + b_0^t x_0)^2},$$

we see that when $b_0 > 1$, solutions with initial conditions $0 < x(0) < x_e$ are increasing to x_e and those with $x(0) > x_e$ are decreasing to x_e . It is this dynamic similarity with the famous logistic differential equation from which equation (1.17) derives its name. \square

The discrete logistic equation is exceptional in that we have a formula for the solutions of initial value problems. As seen in Example 1.5, we can use this formula to determine the properties of solutions and their biological implications. For virtually all other model difference equations, however, solution formulas are not available and other analytic methods are needed to study solution properties. This is the main topic of the next section.

1.2.1. Equilibria and Local Stability. A basic biological question to ask of a population model is, What does it predict about the long-term fate of the population? Does the model predict the population will go extinct or survive? And if the population is predicted to survive, what are the characteristics of its dynamics? Will the population grow indefinitely (as predicted by the linear equation (1.4)), equilibrate to a steady state (as predicted by the discrete logistic equation (1.17)), or oscillate in some manner (as we will see in Section 1.2.3 can be predicted by some models). In this section we develop some general analytical tools to address the questions of extinction and survival by equilibration.

An **equilibrium** (or fixed point) is a constant solution $x(t) = x_e$ for all $t \in \mathbb{Z}_+$. Clearly $x_e = 0$ is an equilibrium of the general population model equation (1.11), no matter what the factors $\beta(x)$ and $\sigma(x)$ or the inherent vital rates b_0 and s_0 are. All equilibria are found by solving the **equilibrium equation**

$$x = [b_0\beta(x) + s_0\sigma(x)]x$$

associated with equation (1.11). Nonzero equilibria are roots $x \neq 0$ of the algebraic equation

$$(1.19) \quad b_0\beta(x) + s_0\sigma(x) = 1.$$

If we were to solve this equation for x , the answer would in general depend on the inherent rates b_0 and s_0 . To study how equilibria depend on these model parameters, let us fix the survival rate s_0 and consider equilibria (roots of (1.19)) as they depend on the fertility rate b_0 , a dependence we could write as $x(b_0)$.

We can geometrically display the dependence of equilibria on b_0 , as we did for the linear equation in Section 1.1, by plotting $x(b_0)$ in the (b_0, x) -plane to obtain a **bifurcation (or equilibrium) diagram**. However, without explicit formulas for the factors $\beta(x)$ and $\sigma(x)$, we obviously cannot hope to solve the equation (1.19) explicitly for x . So, let us

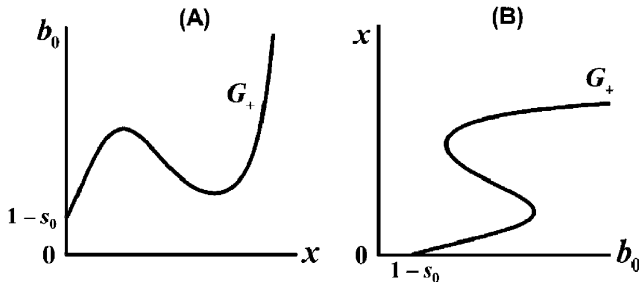


Figure 1.2. The graph G_+ of Equation (1.20) in the (x, b_0) -plane shown in (A), when reflected through the $b_0 = x$ line, produces the part G_+ of the graph G in the first quadrant of the (b_0, x) -plane shown in (B). From intersection points of G_+ with a vertical line drawn from a selected value of b_0 in (B) one learns whether or not there exists a positive equilibrium of the population equation (1.11) for that value of b_0 and, if so, how many there are.

reverse our point of view and solve for $b_0 = b_0(x)$ as a function of x . The answer is easy enough to obtain, namely

$$(1.20) \quad b_0(x) = \frac{1 - s_0 \sigma(x)}{\beta(x)},$$

and we can get the desired equilibrium/bifurcation diagram by plotting the graph G of this function of $x \in R_+$ in the (x, b_0) -plane and then interchanging the coordinate axes (for example, by reflecting through the line $x = b_0$).

Note that the point $(1 - s_0, 0)$ lies on the graph G and on the axes $x = 0$ in the diagram. The axes $x = 0$ is also the graph of the extinction equilibria $x_e = 0$ for all values of b_0 . These two equilibria graphs, that is the extinction equilibria and the positive (survival) equilibria from G , intersect at the point $(1 - s_0, 0)$ in the (b_0, x) -plane, which is called a **(transcritical) bifurcation point**.

For a population model, we are interested only in $x \geq 0$, so we will denote that portion of G (i.e., the graph of (1.20) for $x \geq 0$) by G_+ . See Figure 1.2 for a generic picture of how these graphs might look.

Remark 1.6. Assumption 1.2 implies $b_0(x) > 0$ for all x and satisfies $b_0(0) = 1 - s_0$ and $\lim_{x \rightarrow \infty} b_0(x) = \infty$ (since $\lim_{x \rightarrow \infty} \beta(x) = 0$). Thus, the range of the function $b_0(x)$ is the half-line $b_0 \geq b_0^* > 0$, where $b_0^* :=$

$\min_{x \geq 0} b_0(x) \leq 1 - s_0$. **Assumption 1.2 implies there exists at least one positive equilibrium for each value of $b_0 \geq b_0^*$.**

Remark 1.7. Given the simple linear relationship between the inherent population growth rate $r_0 = b_0 + s_0$ and the inherent fertility rate b_0 , the equilibrium diagrams in Figure 1.2 will look the same when drawn in the (r_0, x) -plane (as in Figure 1.1) but with intersection (bifurcation) point $1 - s_0$ replaced by 1. The same is true if they are drawn in the (R_0, x) -plane where $R_0 = b_0 / (1 - s_0)$ is the inherent reproduction number.

Before looking at examples of equilibrium bifurcation diagrams constructed from the graph G , we consider nonequilibrium solutions and the question of whether or not they approach an equilibrium. For this purpose, we introduce the following formal definitions.

Definition 1.8. Assume $f \in C(\Omega : \Omega)$, where $\Omega \subseteq \mathbb{R}$ is an open set, and assume $x_e \in \Omega$ is an equilibrium of the difference equation

$$(1.21) \quad x(t+1) = f(x(t)),$$

that is to say $x = x_e$ solves the **equilibrium equation** $x = f(x)$.

- (a) x_e is **locally stable** if to any real number $\varepsilon > 0$ there corresponds a real number $\delta(\varepsilon) > 0$ such that $|x(0) - x_e| < \delta(\varepsilon)$ implies $|x(t) - x_e| < \varepsilon$ for all $t \in \mathbb{Z}_+$. It is **unstable** if it is not locally stable.
- (b) x_e is **attracting** if there exists a real number $\delta^* > 0$ such that $|x(0) - x_e| < \delta^*$ implies $\lim_{t \rightarrow +\infty} |x(t) - x_e| = 0$.
- (c) x_e is **locally asymptotically stable** if it is both locally stable and attracting.⁴
- (d) The **basin of attraction** \mathcal{B} of x_e is the set of initial conditions $x(0) \in \Omega$ for which $\lim_{t \rightarrow +\infty} |x(t) - x_e| = 0$.

Local stability means, roughly speaking, that a solution will remain as close as you want to the equilibrium for all future time provided it is initially sufficiently close to the equilibrium. To be locally asymptotically stable means that, in addition, solutions will tend to the equilibrium as $t \rightarrow +\infty$ if they start sufficiently close to the equilibrium.

Remark 1.9. In this book when we say that an equilibrium is **stable**, we always mean it is locally asymptotically stable.

⁴It is possible for an equilibrium to be locally attracting but not locally stable.

While Definition 1.8 provides a concise description of what stability means, it is not in general an easy task to establish the stability or instability of an equilibrium by direct application of these criteria. Instead we rely on analytic techniques that supply conditions that are sufficient to determine the stability properties of an equilibrium. The most basic technique used for this purpose is the Linearization Principle described in the following theorem (a proof of which can be found in Appendix A.2). Throughout this book, ∂_x denotes differentiation with respect to x (see Table of Symbols).

Theorem 1.10. The Linearization Principle. *Assume x_e is an equilibrium of a difference equation (1.21) where $f \in C^1(\Omega : \Omega)$ is continuously differentiable on an open interval $\Omega \subseteq \mathbb{R}$ containing x_e . Then x_e is (locally asymptotically) stable if $|\partial_x f(x_e)| < 1$ and is unstable if $|\partial_x f(x_e)| > 1$ where*

$$\partial_x f(x_e) := \partial_x f(x)|_{x=x_e}.$$

It is important to note that the Linearization Principle provides a sufficient, but not necessary, condition for local asymptotic stability. This is because an application of Theorem 1.10 requires $|\partial_x f(x_e)| \neq 1$. An equilibrium for which this inequality holds is called an **hyperbolic equilibrium**. The stability properties of a nonhyperbolic equilibrium, when $|\partial_x f(x_e)| = 1$, cannot be determined by the Linearization Principle. That is to say, a **nonhyperbolic equilibrium** can be stable, or it can unstable; other methods must be used to determine which is the case.

Example 1.11. For the discrete logistic equation (1.17),⁵

$$f(x) = b_0 \frac{1}{1 + cx} x$$

and

$$\partial_x f(x) = b_0 \frac{1}{(1 + cx)^2}.$$

For the extinction equilibrium $x_e = 0$, we have $|\partial_x f(x_e)| = b_0$, and Theorem 1.10 (with $\Omega = \mathbb{R}$) implies this equilibrium is (locally asymptotically) stable if $b_0 < 1$ and unstable if $b_0 > 1$. For the positive (survival) equilibrium $x_e = (b_0 - 1)/c$ that exists for $b_0 > 1$, we find that $|\partial_x f(x_e)| = 1/b_0$. Theorem 1.10 implies this equilibrium is (locally

⁵Recall Remark 1.3.

asymptotically) stable. These conclusions are consistent with those derived from the solution formula in Example 1.5. \square

Using the Linearization Principle in Theorem 1.10, we can obtain a general result for the general model equation (1.11).

Theorem 1.12. *Assume Assumption 1.2 and fix the inherent survival rate s_0 in the population model equation (1.11). The extinction equilibrium is (locally asymptotically) stable for $b_0 < 1 - s_0$ and unstable for $b_0 > 1 - s_0$.*

Proof. With

$$(1.22) \quad f(x) = [b_0\beta(x) + s_0\sigma(x)]x,$$

we calculate

$$\partial_x f(0) = b_0\beta(0) + s_0\sigma(0) = b_0 + s_0,$$

and the results follow from Theorem 1.10. \square

It turns out that we can get some stability information about positive equilibria of the general model equation (1.11) on the graph G_+ from some simple observations about the geometry of the graph G_+ in its bifurcation diagram. A *critical point* (x^*, r_0^*) on the equilibrium graph G_+ is a point where

$$\partial_x b_0(x^*) := \partial_x b_0(x)|_{x=x^*} = 0.$$

In the (x, b_0) -plane, critical points correspond to points where the slope equals 0 (i.e., where local extrema or inflection points occur), while in the (b_0, x) -plane, they correspond to points with vertical tangents.

Theorem 1.13. *Assume Assumption 1.2 and fix the inherent survival rate s_0 in the population model equation (1.11).*

- (a) *If G_+ is decreasing at a point (x_e, b_0) (specifically, if $\partial_x b_0(x_e) < 0$), then the equilibrium x_e of the population equation (1.11) is unstable.*
- (b) *Suppose G_+ is increasing at a point (x_e, b_0) (specifically, if $\partial_x b_0(x_e) > 0$). Then the equilibrium x_e is stable if the point (x_e, b_0) is sufficiently close to the bifurcation point $(0, 1 - s_0)$ or to a critical point of G_+ .*

Proof. A positive equilibrium $x_e > 0$ satisfies

$$b_0\beta(x_e) + s_0\sigma(x_e) = 1$$

with $b_0 = b_0(x_e)$ given by (1.20). To apply the Linearization Principle in Theorem 1.10 to equation (1.11), the derivative of $f(x)$, given by (1.22), is

$$\partial_x f(x) = [b_0\beta(x) + s_0\sigma(x)] + [b_0\partial_x\beta(x) + s_0\partial_x\sigma(x)]x,$$

which when evaluated at an equilibrium $x_e > 0$ gives

$$\partial_x f(x_e) = 1 + [b_0\partial_x\beta(x_e) + s_0\partial_x\sigma(x_e)]x_e.$$

The equilibrium x_e corresponds to $b_0 = b_0(x_e)$ so that we can write

$$(1.23) \quad \partial_x f(x_e) = 1 + [b_0(x_e)\partial_x\beta(x_e) + s_0\partial_x\sigma(x_e)]x_e.$$

From (1.20) and (1.19) we know

$$b_0(x)\beta(x) + s_0\sigma(x) = 1$$

for all positive equilibria. If we differentiate both sides of this equation with respect to x and evaluate the answer $x = x_e$, we get

$$\partial_x b_0(x_e)\beta(x_e) + b_0(x_e)\partial_x\beta(x_e) + s_0\partial_x\sigma(x_e) = 0$$

or

$$b_0(x_e)\partial_x\beta(x_e) + s_0\partial_x\sigma(x_e) = -\partial_x b_0(x_e)\beta(x_e).$$

From (1.23), we get

$$\partial_x f(x_e) = 1 - \partial_x b_0(x_e)\beta(x_e)x_e.$$

From this formula, we can obtain the following two conclusions.

- (a) $\partial_x b_0(x_e) < 0$ implies $\partial_x f(x_e) > 1$; hence, x_e is unstable by Theorem 1.10. Geometrically, $\partial_x b_0(x_e) < 0$ means the graph G_+ is decreasing at the equilibrium point (x_e, b_0) .
- (b) If $\partial_x b_0(x_e) > 0$, then $\partial_x b_0(x_e) < 1$. Let $\beta_m > 0$ be an upper bound on $\beta(x)x$ for $x \geq 0$, which is guaranteed by Assumption 1.2. If

$$(1.24) \quad 0 < \partial_x b_0(x_e) < 2/\beta_m,$$

then

$$\begin{aligned} \partial_x f(x_e) &= 1 - \partial_x b_0(x_e)\beta(x_e)x_e \\ &> 1 - \partial_x b_0(x_e)\beta_m > 1 - \frac{2}{\beta_m}\beta_m > -1. \end{aligned}$$

Consequently, $|\partial_x f(x_e)| < 1$ and x_e is stable by Theorem 1.10. The inequalities (1.24) hold if (x_e, b_0) is sufficiently near a critical point (where $\partial_x b_0(x_e) = 0$) on the graph G . The inequality

$|\partial_x f(x_e)| < 1$ also holds if $x_e > 0$ is sufficiently small, since then $\partial_x f(x_e)$ is close to 1.

□

Remark 1.14. From the proof, we can be more specific in Theorem 1.13(b) about how close a point (x_e, b_0) needs to be to a critical point, or in other words how close $\partial_x b_0(x_e) > 0$ needs to be to 0, in order to guarantee the stability of a positive equilibrium. Namely, $x_e > 0$ is stable if $0 < \partial_x b_0(x_e) < 2/\beta_m$.

For the discrete logistic model, the equation (1.20) becomes $b_0(x) = 1 + cx$ for $x \geq 0$, and G_+ is the graph of this linear equation. See Figure 1.3(A). Here is another example.

Example 1.15. The Ricker Equation. In the discrete logistic model, if we replace the density factor (1.13) by the exponential factor (1.12), we get the so-called Ricker equation

$$(1.25) \quad x(t+1) = b_0 e^{-cx(t)} x(t).$$

Theorem 1.12 tells us that the extinction equilibrium destabilizes as b_0 increases through 1. With regard to positive equilibria, the equilibrium graph G_+ is the plot of the function (1.20) $b_0(x) = e^{cx}$ for $x \geq 0$. This graph (shown in Figure 1.3(B)) is increasing for all $x > 0$, which tells us that there exists a positive equilibrium for and only for $b_0 > 1$ and that there is only one positive equilibrium for each $b_0 > 1$. Moreover, we know from Theorem 1.13(b) that the positive equilibrium is stable at least for r_0 close 1 (i.e., near the transcritical bifurcation point $(b_0, x) = (1, 0)$).

We can learn more about equation (1.25) by applying the Linearization Principle. Using the formula for the positive equilibria, namely $x_e = c^{-1} \ln b_0$ for $b_0 > 1$, we find that $\partial_x f(x_e) = 1 - \ln b_0 < 1$; hence, $|\partial_x f(x_e)| < 1$ if (and only if) $b_0 < e^2$. We conclude that the positive equilibria of the Ricker equation are (locally asymptotically) stable for $1 < b_0 < e^2$ and are unstable if $b_0 > e^2$.

This example illustrates that positive equilibria located at increasing segments of the equilibrium graph G are not always stable. □

The bifurcation graphs shown in Figure 1.3(A) and (B) for the discrete logistic equation and the Ricker equation are both examples of a

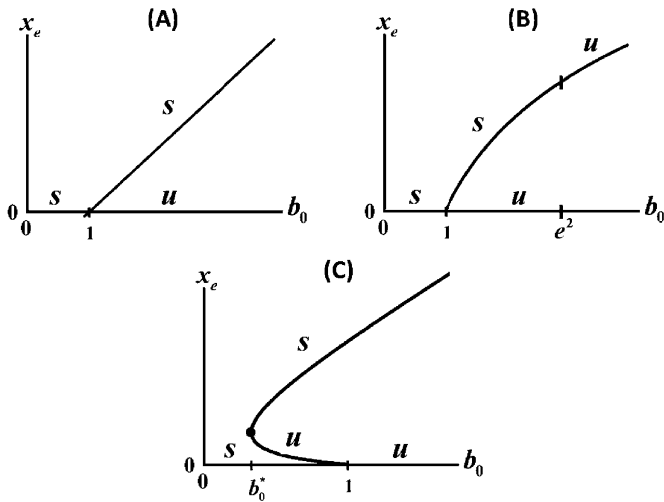


Figure 1.3. The equilibrium bifurcation diagrams for (A) the discrete logistic equation (1.17), (B) the Ricker equation (1.15), and (C) equation (1.27). The notation s indicates a stable equilibrium, and u indicates an unstable equilibrium. In all cases the extinction equilibrium, which forms the horizontal b_0 -axis, destabilizes as b_0 increases through 1. In (A), the bifurcation is forward-stable, and positive equilibria are stable for all $b_0 > 1$. In (B), the bifurcation is forward-stable, but positive equilibria are stable only for $1 < b_0 < e^2$. In (C), the bifurcation is backward-unstable. In this case, the positive equilibria on the decreasing segment are unstable, and those on the increasing segment are stable.

forward bifurcation, by which is meant that near the bifurcation point $(b_0, x) = (1, 0)$, the positive equilibria on G_+ exist for $b_0 > 1$. The next example illustrates a **backward bifurcation**, where the positive equilibria on G_+ near the bifurcation point $(b_0, x) = (1, 0)$ exist for $b_0 < 1$.

Example 1.16. A Model with an Allee Component. For a semelparous population ($s_0 = 0$) with fertility density factor (1.15)

$$(1.26) \quad \beta(x) = \frac{1 + ax}{1 + cx^2},$$

we have the difference equation

$$(1.27) \quad x(t+1) = b_0 \frac{1 + ax(t)}{1 + cx^2(t)} x(t).$$

This model implies that an increase in low density will increase fertility from the density-free level of b_0 to a maximum value of $\beta(x^*)$, where

$$x^* := \frac{1}{a} \left(-1 + \sqrt{1 + \frac{1}{c} a^2} \right) > 0.$$

For densities $x > x_m$, fertility decreases and approaches 0 as $x \rightarrow \infty$. Thus, increased population density is a positive effect at low densities but a negative effect at high densities.

Theorem 1.12 tells us that the extinction equilibrium destabilizes as b_0 increases through 1. With regard to positive equilibria, the equilibrium graph G_+ is the plot of the function (1.20):

$$b_0(x) = \frac{1 + cx^2}{1 + ax}$$

for $x \geq 0$. This graph is decreasing for x ranging from 0 to the critical point x^* where it has a global minimum, after which the graph increases without bound as $x \rightarrow \infty$. This leads to the graph G_+ as depicted in Figure 1.3(C). This bifurcation graph, together with Theorem 1.13, tells us several things.

First, with regard to positive equilibria, there is exactly one positive equilibrium $x_1 > 0$ for $b_0 \geq 1$ and exactly two positive equilibria $0 < x_2 < x_1$ for $b_0^* < b_0 < 1$, where

$$b_0^* := 2 \frac{-c + \sqrt{c^2 + ca^2}}{a^2} > 0.$$

Secondly, because the graph G_+ is decreasing at the smaller equilibria $x_2 < x^*$, it follows that these equilibria are unstable. Finally, because the graph is increasing at the larger equilibria, they are stable at least near the critical point (i.e., for $b_0 \gtrsim b_0^*$). \square

Example 1.16 illustrates what can be learned about equilibria from the equilibrium graph G_+ alone. More can be learned, of course, by applying other methods and analysis. For example, in Exercise 1.30 the reader is challenged to calculate a formula for the equilibrium x_1 of equation (1.27) and use it with the Linearization Principle to show that x_1 is in fact stable for *all* values of $b_0 > b_0^*$.

Note the special role played by the point b_0^* in Example 1.16 as graphically seen in Figure 1.3(C). It is as if the two equilibria x_1 and x_2 collide and annihilate each other as b_0 decreases through b_0^* . This change in the

existence count of positive equilibria at b_0^* is a bifurcation call a **tangent or blue-sky bifurcation**.⁶ Such bifurcations occur at (local) maxima and minima of the graph G^+ when plotted in the (x, b_0) -plane. The critical b_0 points where they occur are called **tipping or turning points**.

The examples of forward and backward bifurcations shown in Figure 1.3 are illustrative of the general connection between the **direction of bifurcation** (forward or backward) and the stability of the positive equilibria that arise from the bifurcation (i.e., the positive equilibria on G_+ near the bifurcation point $(b_0, x) = (1 - s_0, 0)$). Clearly, the bifurcation is forward if the slope of G_+ at this point is positive (i.e., if $\partial_x b_0(0) > 0$), and Theorem 1.13 tells us that the positive equilibria on G_+ near the bifurcation point are stable. In this case, we say the **bifurcation is stable**. Conversely, if $\partial_x b_0(0) < 0$, then Theorem 1.13 tells us that the positive equilibria on G_+ near the bifurcation point are unstable, and we say the **bifurcation is unstable**. In a nutshell, the *direction of bifurcation tells us the stability of the equilibria*.

From the definition (1.20) of $b_0(x)$ and the normalizations $\beta(0) = \sigma(0) = 1$ in Assumption 1.2, we calculate

$$\partial_x b_0(0) = -[(1 - s_0) \partial_x \beta(0) + s_0 \partial_x \sigma(0)].$$

From this, we see that the sign of the weighted average $(1 - s_0) \partial_x \beta(0) + s_0 \partial_x \sigma(0)$ of the sensitivities $\partial_x \beta(0)$ and $\partial_x \sigma(0)$ determines the direction and stability of the bifurcation of positive equilibria at $(r_0, x) = (1, 0)$. We summarize these results in the following theorem. With the burden of some extra notation, but with an eye toward matrix models in subsequent chapters, we let κ denote $\partial_x b_0(0)$:

$$(1.28) \quad \kappa := -[(1 - s_0) \partial_x \beta(0) + s_0 \partial_x \sigma(0)].$$

Theorem 1.17. *Assume Assumption 1.2 and fix the inherent survival rate s_0 in the population model equation (1.11). The bifurcation of positive equilibria from the extinction equilibrium $x_e = 0$ at the point $b_0 = 1 - s_0$ is forward and stable if $\kappa > 0$ and backward and unstable if $\kappa < 0$.*

Example 1.16 illustrates some significant features of a backward-unstable bifurcations in general. First, there are values of the inherent fertility rate $b_0 < 1$ for which there exists a stable positive equilibrium

⁶Other names include blue-sky catastrophe bifurcation, fold bifurcation, or **+1** bifurcation (because $\partial_x f(x_e) = +1$ at this point). It is also sometimes called a saddle-node bifurcation, although this name is appropriate for the higher-dimensional context of systems of difference equations and not for a single difference equation.

(i.e., for which the population can survive). Secondly, since $b_0 < 1$ implies that the extinction equilibrium is also stable, it follows that survival in this case is **initial-condition dependent**. Specifically, survival requires that $x(0) > 0$ not be in the basin of attraction of the extinction equilibrium $x_e = 0$, which in Example 1.16 is the interval $0 < x(0) < x_1$. The boundary of the basin of attraction (i.e., the unstable equilibrium $x_1 > 0$) is a threshold below which a population must not drop if it is to survive. A third significant feature of the backward-unstable bifurcation in Example 1.16 is the presence of the tipping point b_0^* . Its presence threatens a population with an abrupt collapse and extinction if b_0 were to decrease below b_0^* (as might be caused, for example, by environmental degradation).

Definition 1.18. A **strong Allee effect** occurs when both the extinction equilibrium and a positive equilibrium are stable.⁷

Equation (1.27) in Example 1.16 is an example of a model equation with a strong Allee effect. This is a consequence of the backward bifurcation caused by the Allee component in the fertility density factor (1.26), which since $\partial_x \beta(0) > 0$ (and $s_0 = 0$), implies $\kappa < 0$ in Theorem 1.17. The presence of an Allee component in an equation does not, however, necessarily imply that a strong Allee effect occurs. When a strong Allee effect does not occur in a model that has an Allee component, as in Example 1.19, a **weak Allee effect** is said to occur. Here is an example.

Example 1.19. Consider the population model equation (1.11) with density factors

$$\beta(x) = \frac{1}{1 + cx} \quad \text{and} \quad \sigma(x) = \frac{1 + x(t)}{1 + \frac{1}{2}x(t)}$$

under the assumption that the inherent survival rate s_0 satisfies

$$(1.29) \quad s_0 < \frac{1}{2}.$$

This model has a negative density effect on fertility (the same as that in the discrete logistic equation) and an Allee component effect in survival since $\beta(x)$ and $\sigma(x)$ are decreasing and increasing functions of $x \geq 0$, respectively. Note that density-dependent survival $s_0\sigma(x)$ increases from

⁷More generally, a strong Allee effect occurs if the extinction equilibrium is stable and there also exists a positive (survival) attractor, which need not be an equilibrium [33]. See Section 3.5.4 in Chapter 3 for an example.

s_0 to $2s_0 < 1$ as population density x increases without bounded. A straightforward calculation shows that

$$\kappa = (1 - s_0)c - \frac{1}{2}s_0,$$

and by Theorem 1.17, the bifurcation at $b_0 = 1 - s_0$ is forward-stable if

$$(1.30) \quad c > \frac{1}{2} \frac{s_0}{1 - s_0}.$$

Following our procedure in Section 1.2.1 for analyzing positive equilibria, we solve the equilibrium equation for b_0 to obtain (from (1.20))

$$b_0(x) = (1 + cx) \frac{(1 - 2s_0)x + 2(1 - s_0)}{x + 2}.$$

Performing some calculus on this function of x , we find under the assumptions (1.29) and (1.30) that $b_0(x)$ is a monotone increasing function of $x > 0$, ranging from $1 - s_0$ to $+\infty$. It follows that there exists a positive equilibrium for and only for $b_0 > 1 - s_0$, and as a result, a strong Allee effect does not occur in this model equation under these assumptions. \square

The following theorem shows that a strong Allee effect and the existence of a tipping point are general features of backward bifurcations in a population equation (1.11).

Theorem 1.20. *Assume Assumption 1.2 and fix the inherent survival rate s_0 in the population model equation (1.11). If the bifurcation at $b_0 = 1 - s_0$ is backward (and hence unstable), then there exists a tipping point b_0^* , $0 < b_0^* < 1$, and a strong Allee effect occurs (at least) for $b_0 \gtrsim b_0^*$.*

Proof. Assumption 1.2 implies that $\lim_{x \rightarrow \infty} \beta(x) = 0$; hence, $\lim_{x \rightarrow \infty} b_0(x) = \infty$. Since a backward bifurcation implies $b_0(x) < 1$ for $x \gtrsim 0$, it follows that $b_0(x)$ has a global minimum at some $x = x^* > 0$. The point $(b_0^*, x^*) = (b_0(x^*), x^*)$ is a critical point of G^+ ; hence, b_0^* is a tipping point. For $b_0 \lesssim b_0^*$, there are no points on G_+ and hence no positive equilibria. For each $b_0 \gtrsim b_0^*$, there exist (at least) two points (b_0, x_1) and (b_0, x_2) , with $x_1 < x^* < x_2$, on G^+ at which G^+ is decreasing and increasing, respectively. By Theorem 1.13, x_1 is unstable and x_2 is stable. \square

Theorem 1.20 implies that a strong Allee effect (with a tipping point) always occurs in a population equation (1.11) when the bifurcation at

$b_0 = 1$ is backward. The next example shows, however, that it is also possible for a strong Allee effect to occur even when the bifurcation is forward.

Example 1.21. Hysteresis. The model equation

$$(1.31) \quad x(t+1) = b_0 \left(1 + p \frac{x^q(t)}{a + x^q(t)} \right) x(t) + s_0 \frac{1}{1 + cx(t)} x(t)$$

incorporates an Allee component (1.16) in the fertility factor $\beta(x)$ and a negative population regulation effect on the post reproductive survival factor $\sigma(x)$. We consider the case when the integer $q \geq 2$. By Theorem 1.12, the extinction equilibrium loses stability as b_0 increases through $1 - s_0$. A calculation shows $\kappa = -s_0 c < 0$, and we see by Theorem 1.13 that a forward, stable bifurcation of positive equilibria occurs.

While no tractable formula exists for the positive equilibria, one can learn a great deal about their existence and stability from the geometry of the equilibrium graph G_+ and from Theorem 1.13. The graph G_+ defined by (1.20) can be sketched using methods from calculus and analytic geometry or, for selected values of the coefficients, obtained with the aid of a graphing program. Two examples are shown in Figure 1.4 with $q = 2$. In this case,

$$r(x) = b_0 \left(1 + p \frac{x^2}{a + x^2} \right) + s_0 \frac{1}{1 + cx},$$

and the bifurcation graph G_+ is the graph of the equation

$$b_0 = \left(1 - s_0 \frac{1}{1 + cx} \right) \left(1 + p \frac{x^2}{a + x^2} \right)^{-1}$$

in the (b_0, x) -plane. These examples show what is called **hysteresis**, whereby the equilibrium graph has the S-shape bend in it, giving rise to multiple equilibria for certain b_0 values and two tipping points for b_0 .

In Figure 1.4(A), positive equilibria exist for and only for $b_0 > 1$. Because of the S-shaped bend in the equilibrium graph, we see that there is an interval of b_0 values for which there exist three positive equilibria. This interval is bordered by two tipping points (critical points of G_+). The stability information obtainable from Theorem 1.13 is also indicated in the graph. For another example of this hysteresis phenomenon, see Section 1.3.2.

Figure 1.4(B) shows another example in which the S-shape bend in the equilibrium graph is so extreme that positive equilibria (in fact two

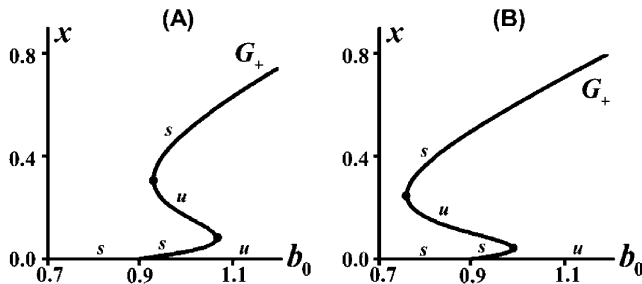


Figure 1.4. The equilibrium graphs of Equation (1.31) with parameter values $q = 2$, $c = 0.5$, $s_0 = 0.1$. In plot (A) $a = 0.1$ and in (B) $a = 0.05$. By Theorem 1.13 equilibria on the decreasing segments are unstable and those on increasing segments near the critical points (indicated by solid circles) are stable.

positive equilibria) exist for values b_0 on an interval $b_0^* < b_0 < 1$, where b_0^* is a tipping point. For these values of b_0 the extinction equilibrium is stable, which shows that a strong Allee effect can occur in a population equation (1.11) even when the bifurcation at $b_0 = 1 - s_0$ is forward. \square

Remark 1.22. Because of the simple relationships between b_0 and the inherent population growth rate $r_0 = b_0 + s_0$ and the inherent reproduction number $R_0 = b_0 / (1 - s_0)$, Theorems 1.12, 1.13, 1.17, and 1.20 could be restated with b_0 replaced by either r_0 or R_0 . In either case, the bifurcation point $b_0 = 1 - s_0$ is then replaced by 1.

1.2.2. Global Asymptotic Stability. It is important to remember that the stability of an equilibrium, as defined by Definition 1.8 and as determined by the Linearization Principle, is a local phenomena in that it concerns the dynamic properties of only those solutions with initial conditions close to the equilibrium. That a stable equilibrium does not necessarily attract all solutions is clearly illustrated by Examples 1.16 and 1.21 which, for some values of b_0 , have multiple stable and unstable equilibria.

Definition 1.23. Assume $x_e \in \Omega$ is an equilibrium of a difference equation (1.21) with $f \in C^1(\Omega : \Omega)$, where Ω is an open interval containing x_e , and let $\mathbb{B} \subseteq \Omega$ be its basin of attraction. We say x_e is **globally asymptotically stable on a set Λ** if it is locally asymptotically stable and $\Lambda \subseteq \mathbb{B}$.

Example 1.24. In Example 1.11, we applied the Linearization Principle to the extinction equilibrium $x_e = 0$ and the positive (survival) equilibrium

$$x_e = \frac{b_0 - 1}{c}$$

of the discrete logistic equation (1.17) to show that they are locally asymptotically stable for $b_0 < 1$ and $b_0 > 1$, respectively. In Example 1.5, we saw that $x(0) > 0$ implies $\lim_{t \rightarrow \infty} x(t) = 0$ for $b_0 < 1$ and $\lim_{t \rightarrow \infty} x(t) = x_e$ for $b_0 > 1$. Thus, $x = 0$ is globally asymptotically stable on $\Lambda = \text{int}(R_+)$ for $b_0 < 1$, and x_e is globally asymptotically stable on $\Lambda = \text{int}(R_+)$ for $b_0 > 1$. \square

In general, it is not an easy problem to determine the basin of attraction \mathbb{B} of an equilibrium or if it is globally asymptotically stable on a set of interest. Solution formulas are not in general available for nonlinear difference equations, as in Example 1.24, so other methods are required for the study of global attractivity [62], [63], [98]. With regard to the extinction equilibrium, here is a theorem that is often applicable.

Theorem 1.25. *In addition to Assumption 1.2, suppose the density factors in equation 1.11 satisfy*

$$(1.32) \quad \beta(x) \leq \beta(0) = 1 \quad \text{and} \quad \sigma(x) \leq \sigma(0) = 1 \quad \text{for all } x \geq 0.$$

Then $r_0 = b_0 + s_0 < 1$ implies that the extinction equilibrium $x_e = 0$ is globally asymptotically stable on $\Lambda = R_+$.

Proof. For any initial condition $x(0) \in \mathbb{R}_+$, the solution $x(t)$ of equation (1.11) satisfies $x(t) \geq 0$ for all $t \in \mathbb{Z}_+$ and, by (1.32), the inequalities

$$0 \leq x(t+1) \leq b_0 x(t) + s_0 x(t) = r_0 x(t).$$

An induction argument shows $0 \leq x(t) \leq r_0^t x(0)$ for all $t \in \mathbb{Z}_+$, and it follows that $\lim_{t \rightarrow \infty} x(t) = 0$ (i.e., that $x_e = 0$ is attracting on \mathbb{R}_+). Since it is also locally asymptotically stable by Theorem 1.12, it follows that $x_e = 0$ is globally asymptotically stable. \square

With regard to other equilibria, the following theorem (which the reader is challenged to prove in Exercise 1.39) is often useful.

Theorem 1.26. *Assume $f \in C(\Omega : \Omega)$ with*

$$\Omega = \{x \in R : 0 < x < \beta \leq +\infty\}$$

and has a fixed point $x_e \in \Omega$.

- (a) If, for all $x \in \Omega$, the function $f(x)$ satisfies the two conditions
- $x < f(x) < x_e$ when $x < x_e$ and
 - $f(x) < x$ when $x > x_e$,
- then x_e is globally asymptotically stable on Ω .
- (b) If $\partial_x f(x) > 0$ and $\partial_x^2 f(x) < 0$ on Ω , then conditions (i) and (ii) in part (a) hold.

The density factors

$$\beta(x) = \frac{1}{1+cx} \quad \text{and} \quad \sigma(x) = 1$$

in the discrete logistic equation (in which $s_0 = 0$) for a semelparous population

$$x(t+1) = b_0 \frac{1}{1+cx(t)} x(t)$$

satisfy the inequalities (1.32); hence, by Theorem 1.25, the extinction equilibrium is globally asymptotically stable if $r_0 = b_0 < 1$. For $r_0 = b_0 > 1$, we saw in Example 1.24, by making use of the solution formula (1.18), that the positive equilibrium

$$x_e = \frac{b_0 - 1}{c}$$

is globally asymptotically stable on $\text{int}(R_+)$. This conclusion can be reached without the solution formula by applying Theorem 1.26(b) with $\Omega = \text{int}(R_+)$ and $f(x) = b_0x/(1+cx)$ for which

$$\partial_x f(x) = \frac{b_0}{(1+cx)^2} > 0 \quad \text{and} \quad \partial_x^2 f(x) = -2 \frac{cb_0}{(1+cx)^3} < 0$$

for all $x > 0$.

Example 1.27. The density factors

$$\beta(x) = e^{-cx} \quad \text{and} \quad \sigma(x) = 1$$

in the Ricker equation (in which $s_0 = 0$) for a semelparous population

$$x(t+1) = b_0 e^{-cx(t)} x(t),$$

satisfy the inequalities (1.32); hence, the extinction equilibrium is globally asymptotically stable if $r_0 = b_0 < 1$.

We saw in Example 1.15 that the positive equilibrium

$$(1.33) \quad x_e = \frac{\ln b_0}{c}$$

exists and is locally asymptotically stable for $1 < b_0 < e^2$ (and unstable for $b_0 > e^2$). Is it globally asymptotically stable on $\text{int}(R_+)$? To apply Theorem 1.26, we calculate the derivatives

$$\partial_x f(x) = b_0(1 - cx)e^{-cx} \quad \text{and} \quad \partial_x^2 f(x) = cb_0(cx - 2)e^{-cx}$$

and find that the conditions $\partial_x f(x) > 0$ and $\partial_x^2 f(x) < 0$ hold on the interval

$$\Omega = \left\{ x : 0 < x < \frac{1}{c} \right\}.$$

Theorem 1.26(b) applies if $f(x) = b_0 e^{-cx} x$ maps Ω into itself and if $x_e \in \Omega$. The first condition holds if

$$\max_{\Omega} f(x) = f\left(\frac{1}{c}\right) = b_0 e^{-1} \frac{1}{c} < \frac{1}{c},$$

that is to say if $0 < b_0 < e$. It is not difficult to see that $x_e \in \Omega$ for this same interval of b_0 values. We conclude, by invoking Theorem 1.26(b), that the positive equilibrium (1.33) is globally asymptotically stable on the interval Ω for all b_0 on the interval $0 < b_0 < e$.

When b_0 lies in the interval $0 < b_0 < e$, all solutions with positive initial conditions $x(0) \in \text{int}(R_+)$ satisfy $x(t) \in \Omega$ for $t \geq 1$ since $\max_{\Omega} f(x) < 1/c$. So it follows that x_e is globally attracting, hence globally asymptotically stable, on the larger interval $\text{int}(R_+)$.

In fact, it turns out that x_e is globally asymptotically stable on $\text{int}(R_+)$ for all b_0 in the larger interval $0 < b_0 < e^2$, but this is more difficult to prove; see [64]. \square

1.2.3. Cycles and Chaos. The discrete logistic equation (1.17) predicts population extinction if $b_0 < 1$ and survival by equilibration for all $b_0 > 1$. The Ricker equation (1.25), on the other hand, predicts survival by equilibrium only if $b_0 > 1$ and less than e^2 . So what does the Ricker equation predict when $b_0 > e^2$? The sample solution for this case shown in Figure 1.5 illustrates that while the population does survive, it does not equilibrate. Instead it (seemingly) settles into a cyclic oscillation of period 2. This is typical for difference equations (1.21) when changes in a coefficient causes an equilibrium x_e to lose stability because $\partial_x f(x_e)$ decreases through -1 , which is what happens, for example, to the positive equilibrium of the Ricker equation as b_0 increases through e^2 (see Example 1.15). In general when this occurs, periodic solutions of period 2 (called **2-cycles**) come into existence by a bifurcation from the equilibrium (either forward or backward). This bifurcation is called a

period-doubling bifurcation.⁸ This is in contrast to the bifurcation of equilibria when the extinction equilibrium loses stability when $\partial_x f(x_e)$ increases through +1, as in Theorem 1.17. Moreover, the sample solution shown in Figure 1.5(B) approaches a period 2 oscillation as time goes on, which suggests that the 2-cycle is an attractor. In the bifurcation diagram in Figure 1.5, we see even more than a period-doubling bifurcation at $b_0 = e^2$. As b_0 continues to increase, the period 2 solutions give way (by another period-doubling bifurcation) to solutions of period 4 (called 4-cycles), which in turn give way to solutions of period 8 (8-cycles), and so on. This period-doubling cascade seemingly goes on indefinitely but in fact does come to an end, and solutions ultimately oscillate wildly with no discernible pattern; see Figure 1.5(E). (Such a bifurcation sequence is often called a “route-to-chaos.”)

A *p*-cycle is a solution of $x(t+1) = f(x(t))$ for which there exists a positive integer p (called the period) such that $x(t+p) = x(t)$ for all $t \in \mathbb{Z}_+$. An equilibrium is, of course, a solution of period $p = 1$ (or of any period, for that matter), a solution of period 2 is also solution of period 4 (or any multiple of 2), and so on. In this book, a *p*-cycle is a periodic solution whose *minimal period* is p . So, for example, $x_0 \neq x_1$ for a 2-cycle. A *p*-cycle is characterized by p points $x_i := x(i)$ (for $i = 0, 1, \dots, p-1$) that are indefinitely repeated.

The existence of a *p*-cycle can be mathematically studied by noting that its initial point x_0 (or, indeed, any point x_i in the cycle) is fixed point of the p th composite $f^{(p)}(x)$ of $f(x)$. For example, a 2-cycle consists of two points $x_0 \neq x_1 = f(x_0)$ for which $x_0 = f^{(2)}(x_0)$, where

$$f^{(2)}(x) := f(f(x)).$$

We say a 2-cycle is stable (or unstable) if x_0 it is a stable (or unstable) equilibrium of the difference equation $x(t+1) = f^{(2)}(x(t))$ constructed from the composite. Noting that the chain rule gives

$$\partial_x f^{(2)}(x) = \partial_x f(f(x)) \partial_x f(x),$$

we see that the Linearization Principle implies a 2-cycle is stable if

$$|\partial_x f(f(x_0)) \partial_x f(x_0)| = |\partial_x f(x_1) \partial_x f(x_0)| < 1$$

⁸Other names are a 2-cycle or a flip or -1 bifurcation.

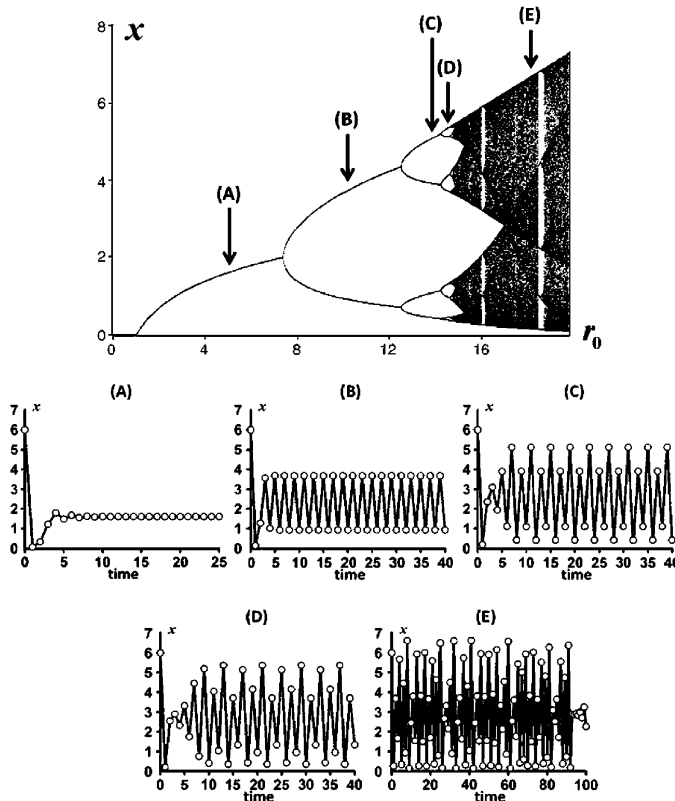


Figure 1.5. The bifurcation diagram for the Ricker equation (1.25) with $c = 1$ is shown together with a sample solution (initial condition $x(0) = 10$) for five selected $r_0 = b_0$ values: (A) $r_0 = 5$, (B) $r_0 = 10$, (C) $r_0 = 14$, (D) $r_0 = 14.6$, (E) $r_0 = 18$. The graph shows, above each b_0 value, the number of points in the attractor. For example, for (B) there are two points, indicating the attractor is a 2-cycle (not two equilibria) and for (C) and (D) there are four and eight points, indicating the attractors are a 4-cycle and 8-cycle respectively. At b_0 such as (E) the diagram indicates a large number of points in the attract, which could mean a cycle of very large period or a nonperiodic ("chaotic") attractor.

and unstable if $|\partial_x f(x_1) \partial_x f(x_0)| > 1$. More generally, for a p -cycle x_0, x_1, \dots, x_{p-1} , we apply the Linearization Principle to the p th composite equation $x_{t+1} = f^{(p)}(x_t)$ and utilize the derivative

$$\partial_x f^{(p)}(x_1) = \partial_x f(x_{p-1}) \cdots \partial_x f(x_1) \partial_x f(x_0)$$

when applying the Linearization Principle. We get that a p -cycle is stable if

$$|\partial_x f(x_{p-1}) \cdots \partial_x f(x_1) \partial_x f(x_0)| < 1$$

and unstable if

$$|\partial_x f(x_{p-1}) \cdots \partial_x f(x_1) \partial_x f(x_0)| > 1.$$

When $|\partial_x f^{(p)}(x_0)| \neq 1$, and hence the Linearization Principle applies, the p -cycle is called a **hyperbolic p -cycle**. See Exercise 1.41 for more on p -cycles.

We will not pursue a rigorous study of cycles nor of more complicated attractors, as this lies beyond the mathematical goals of this book; readers are referred to [62], [63]. We will, however, on occasion employ this method of utilizing the composite map to study periodic cycles.

1.3. Applications

1.3.1. Trade-Off Between Fertility and Post-Reproduction Survival. Trade-offs are a fundamental principle in life history strategies, and one of the most basic involves reproductive effort [119]. To funnel more resources and effort into reproduction comes at a cost of fewer resources that can be allocated to other important processes that enhance an individual's survival, health, growth, etc. Consider a simple model, based on the model equation (1.11), in which a food resource is allocated between an individual's inherent fertility and its survival. Specifically, assume the inherent birth rate has the form $b_0 = n\rho\varphi$, where ρ is amount of food resources consumed (per unit time), φ is the fraction of consumed resource allocated to reproduction, and n is number of surviving newborns per adult per unit resource. Suppose the remaining fraction $1 - \varphi$ of the resource is allocated toward post-reproductive survival so that $s_0 = s(1 - \varphi)$, where s is the maximal possible post-reproduction survival rate. Finally, if we assume competition for the food resource is modeled logically with $\beta(x) = 1/(1 + cx)$ and that post-reproductive survival is density-free ($\sigma(x) \equiv 1$), then the general model equation (1.11) becomes

$$(1.34) \quad x(t+1) = n\rho\varphi \frac{1}{1 + cx(t)} x(t) + s(1 - \varphi) x(t)$$

with

$$n, \rho, c > 0, \quad 0 < s < 1, \quad \text{and} \quad 0 \leq \varphi \leq 1.$$

Since the only density factor ($\beta(x) = 1/(1+cx)$) in equation (1.34) is a decreasing function of x (in particular, is strictly decreasing at $x_e = 0$), we conclude that $\kappa > 0$ and, by Theorem 1.17, that the bifurcation of positive equilibria that occurs when the extinction equilibrium destabilizes as

$$r_0 = n\rho\varphi + s(1 - \varphi)$$

increases through 1 is forward and stable. Thus, the extinction equilibrium is (locally asymptotically) stable if $r_0 < 1$ and unstable if $r_0 > 1$ when there exists a (locally asymptotically) stable positive equilibrium, at least for $r_0 \gtrsim 1$.

We can say more for this equation since it is not algebraically difficult to solve the equilibrium equation

$$x = n\rho\varphi \frac{1}{1+cx} x + s(1-\varphi)x$$

for the (unique) positive root

$$x_e = \frac{1}{c} \frac{r_0 - 1}{1 - s(1 - \varphi)},$$

which shows there exists a (unique) positive equilibrium for all $r_0 > 1$. Moreover, using

$$f(x) = n\rho\varphi \frac{1}{1+cx} x + s(1-\varphi)x$$

and $I = \text{int}(R_+)$ and calculating the derivatives

$$\partial_x f(x) = n\rho\varphi \frac{1}{(1+cx)^2} + s(1-\varphi) > 0 \quad \text{and}$$

$$\partial_x^2 f(x) = -2cn\rho \frac{\varphi}{(1+cx)^3} < 0,$$

we conclude from Theorem 1.26(b) that x_e is globally asymptotically stable on $\text{int}(R_+)$ for all $r_0 > 1$.

If a species had a “choice,” what life history strategy would it choose: high fertility with low post-reproduction survival or vice versa? The answer depends of course on what the goal is. If, for example, the goal were to obtain the largest population level at equilibrium, then we see from the formula for x_e and r_0 that

$$\frac{dx_e}{d\varphi} = n\rho \frac{1-s}{c(1-s(1-\varphi))^2} > 0.$$

Consequently, x_e is maximized at $\varphi = 1$.

The maximum equilibrium population density is attained, according to the model (1.34), by choosing a semelparous life history strategy.

However, iteroparous species are abundant in nature despite the fact that some theoretical arguments, such as the one here, argue in favor of semelparity (this is known as Cole's Paradox [22]). We will revisit this issue in Chapter 5 when we allow φ to be subject to natural selection (rather than somehow “chosen” by the species or a modeler).

1.3.2. A Spruce-Budworm Model. The spruce budworm is a widely distributed defoliator of coniferous trees (mainly spruce and fir) whose periodic outbreaks cause millions of acres of damage throughout North America. The occurrence of outbreaks are associated with the beetle’s interaction with predator species, mostly birds who feed on the juvenile stages (larvae and pupae). A famous differential equation model based on the assumption of a constant predator population density p exhibits a hysteresis effect that is instrumental in explaining the periodic outbreaks of spruce budworm infestations [107]. Here, we will consider a discrete time model based on the same basic modeling assumptions.

We modify the discrete logistic equation for a semelparous population (such as the spruce budworm) by including an additional factor α that accounts for the loss of newborns due to predation:

$$x(t+1) = b_0 \frac{1}{1 + cx(t)} \alpha x(t),$$

where α is the fraction of newborns that escape predation. Following [49], we model α using what is called a Holling III functional response as follows. The amount of prey consumed by the predator population (in a unit of time) is

$$(1.35) \quad \frac{apx^2}{1 + aT_h x^2},$$

where $T_h < 1$ is the *handling time* (the time spent by a predator consuming a prey) and a is called the *prey discovery time*. We assume that

$$p < 2\sqrt{\frac{T_h}{a}} := p_{\max}$$

so that the amount of prey consumed (1.35) does not exceed the amount x available. The amount of prey that survive predation is

$$x - \frac{apx^2}{1 + aT_h x^2} = \left(1 - \frac{apx}{1 + aT_h x^2}\right)x,$$

which implies that the fraction of the prey that survive is

$$\alpha = 1 - \frac{apx}{1 + aT_h x^2}.$$

Thus, we arrive at the equation

$$(1.36) \quad x(t+1) = b_0 \frac{1}{1 + cx(t)} \left(1 - \frac{apx(t)}{1 + aT_h x^2(t)}\right) x(t).$$

Since the density factor

$$\beta(x) = \frac{1}{1 + cx} \left(1 - \frac{apx}{1 + aT_h x^2}\right)$$

satisfies $\partial_x \beta(0) = -(c + ap) < 0$, we find by Theorems 1.12 and 1.17 that the extinction equilibrium loses stability as $r_0 = b_0$ increases

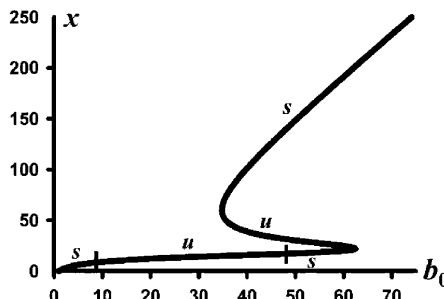


Figure 1.6. The equilibrium diagram for the spruce-budworm equation (1.36) with parameter values (1.38) exhibits an S-shape hysteresis curve. The letters s and u indicate (local asymptotic) stability and instability, respectively. Notice the instability of the equilibria along the segment delineated by the hash marks. This is not inconsistent with Theorem 1.13, which guarantees stability along increasing segments near bifurcation points.

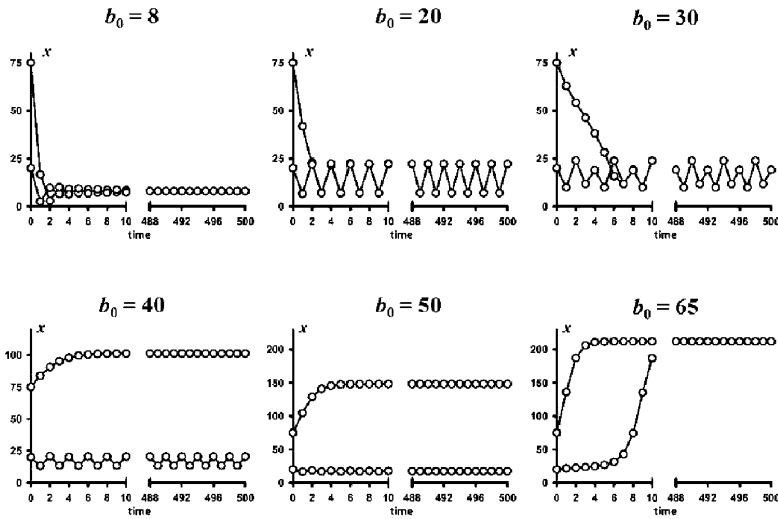


Figure 1.7. The time series plots of two sample solutions of spruce-budworm equation (1.36) with parameter values (1.38) are shown for six selected b_0 values. In each plot, the graphs of two solutions with initial conditions $x(0) = 20$ and 75 are shown. For $b_0 = 8$, both solutions tend to an equilibrium; for $b_0 = 20$ and 30, they are 2-cycle and 4-cycle, respectively; for $b_0 = 40$, one solution tends to a 2-cycle while the other to an equilibrium; for $b_0 = 50$, they tend to different equilibria; and for $b_0 = 65$, they tend to the same equilibrium.

through 1 and that the resulting bifurcation of positive equilibria is forward and stable.

We can get a global picture of the equilibria using Theorem 1.13 from the graph G_+ of (1.20), which in this case is $b_0(x) = 1/\beta(x)$ or

$$(1.37) \quad b_0(x) = (1 + cx) \frac{1 + aT_h x^2}{1 - apx + aT_h x^2}.$$

There are two cases: either the graph G_+ is monotonic or it has two critical points and a cubic polynomial-like shape (see Exercise 1.42). The latter case corresponds to a hysteresis S-shape in a bifurcation diagram in the (b_0, x) -plane, similar to that in Example 1.21 and Figure 1.4. Figure 1.6 shows an equilibrium bifurcation diagram that illustrates the latter

case using parameter values

$$(1.38) \quad c = 0.25, \quad a = 0.01, \quad T_h = 0.25, \quad \text{and} \quad p = 9$$

(for which $p_{\max} = 10$). The graph in Figure 1.6 has a hysteresis S-shape for which there are multiple positive equilibria for b_0 ranging from $b_0 \approx 34.78$ to 62.46 . By Theorem 1.13, equilibria on the decreasing segment in the graph are unstable equilibria, and the equilibria on either of the two increasing segments are stable, at least near the three bifurcation points at $b_0 = 1$ and $b_0 \approx 34.78$ and 62.46 . Numerical simulations suggest that the equilibria on the upper increasing branch are stable for all $b_0 \gtrsim 34.78$, whereas the positive equilibria on the lower increasing branch are stable only near $b_0 \gtrsim 1$ and $b_0 \lesssim 62.46$ (as guaranteed by Theorem 1.13). There occurs a period-doubling bifurcation at $b_0 \approx 9.14$, and the resulting 2-cycles are stable near this bifurcation point, but they undergo a period-doubling bifurcation to a 4-cycle at $b_0 \approx 22.29$. This sequence of bifurcations is reversed as b_0 continues to increase and pass through $b_0 \approx 48.70$, after which the equilibrium is restabilized (until it disappears for $b_0 \gtrsim 62.46$). (In Exercise 1.43, you are asked to use the Linearization Principle for these numerical examples to verify the stability and instability of equilibria.) Sample time series solutions in Figure 1.7 and the bifurcation diagram in Figure 1.8 illustrate these bifurcation phenomena.

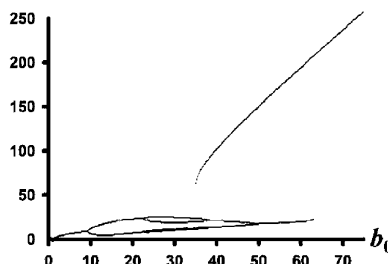


Figure 1.8. The bifurcation diagram for the spruce-budworm equation (1.36) with parameter values (1.38) exhibits an S-shape hysteresis curve.

1.4. Concluding Remarks

The goal of this introductory chapter is to introduce basic methods for deriving discrete-time population dynamic models and to present several basic concepts and theorems for the analysis of their asymptotic dynamics. A focus was on equilibria, both survival and extinction equilibria, and their stability properties as they depend on the parameters b_0 and s_0 (the inherent fertility and survival rates) in the general model equation (1.8)–(1.9). The mathematical approach was that of bifurcation theory. While b_0 was primarily used as the bifurcation parameter, we could have used other parameters, such as s_0 and the derived quantities r_0 and R_0 , in which case the bifurcation diagrams would be similar but with different bifurcation points; see Remark 1.1.

For pedagogical purposes, this introduction is done in the simplest (lowest dimensional) case using models described by a single difference equation which, while adequate for these introductory purposes, is inadequate in many important ways as a model for biological populations. Such an equation describes a population by means of a single quantity (state variable) for population density, which therefore in effect treats all individuals in the population as identical with regard to their physical state and life cycle stage. In the following chapters we will explore what are called discrete-time *structured* population models that account for differences among individuals in a population. This will entail describing a population by more than just a single aggregated state variable. As a result, the dynamics of the population will be described mathematically by more than one difference equation for whose analysis we will employ matrix notation and analysis.

1.5. Exercises

Exercise 1.28. Under Assumption 1.2, prove that the general population equation (1.11) has at least one positive equilibrium for each $r_0 = b_0 + s_0 > 1$.

Exercise 1.29. A factor $\beta(x)$ given by (1.13) has a (nonremovable) singularity at $x = -1/c$. Choose c_1 and c_2 so that the redefinition of this factor for $x < 0$ given as follows is defined and differentiable for all $x \in R$,

in keeping with Remark 1.3:

$$\beta(x) = \begin{cases} \frac{1}{1+cx} & \text{for } x \geq 0 \\ x^2 + c_1x + c_2 & \text{for } x < 0 \end{cases}.$$

How would you do the redefinition to obtain a twice differentiable factor? (HINT: Use a cubic polynomial.)

Exercise 1.30. Solve the equilibrium equation for equation (1.27) in Example 1.16 to find formulas for the positive equilibria x_2 and x_1 . Use your formulas and the Linearization Principle (Theorem 1.10) to show that the equilibrium x_1 is stable for all values of $r_0 > r_0^*$ and equilibrium x_2 is unstable for all values of r_0 satisfying $r_0^* < r_0 < 1$.

Exercise 1.31. (a) Verify that (1.18) is a formula for the solution of the discrete logistic equation (1.17) where $x_e = (b_0 - 1)/c$. (b) Derive the formula (1.18) by making the change of variable $y(t) = 1/x(t)$, obtaining a linear difference equation for $y(t)$, and finding a formula for its solution by induction.

Exercise 1.32. Consider a modification of the discrete logistic model equation that allows for (population density free) post-reproductive survival (iteroparity)

$$x(t+1) = b_0 \frac{1}{1+cx(t)} x(t) + s_0 x(t)$$

with $0 < s_0 < 1$. Use the Linearization Principle (Theorem 1.10) to prove the following facts about this model: (a) the extinction equilibrium $x_e = 0$ destabilizes as $r_0 = b_0/(1-s_0)$ increases through 1; (b) there exists no positive equilibria if $r_0 < 1$, and there exists a unique positive equilibrium $x_e > 0$ if $r_0 > 1$; and (c) the positive equilibria for $r_0 > 1$ are locally asymptotically stable. Draw a bifurcation diagram for equilibria, using b_0 as the bifurcation parameter.

Exercise 1.33. Repeat parts (a) and (b) of Exercise 1.32 for the equation iteroparous version of the Ricker equation

$$x(t+1) = b_0 e^{-cx(t)} x(t) + s_0 x(t)$$

with $0 < s_0 < 1$. Use the Linearization Principle (Theorem 1.10) to prove the positive equilibria $x_e > 0$ are locally asymptotically stable for $1 < r_0 < \exp(2/(1-s_0))$. Draw a bifurcation diagram for equilibria, using r_0 as the bifurcation parameter. Show that $\partial_x f(x_e) = -1$ when $r_0 = \exp(2/(1-s_0))$.

Exercise 1.34. Analyze the equilibria, and their stability properties, of the equations

$$x(t+1) = b_0 x(t) + s_0 \frac{1}{1 + cx(t)} x(t) \quad \text{and}$$

$$x(t+1) = b_0 x(t) + s_0 e^{-cx} x(t)$$

and draw a bifurcation diagram for each equation.

Exercise 1.35. Use the Linearization Principle (Theorem 1.10) to prove Theorem 1.13.

Exercise 1.36. Apply Theorems 1.13, 1.17, and 1.20 to each of the following equations (all coefficients are positive with $0 < s_0 < 1$):

- (a) $x(t+1) = b_0 \frac{1}{1 + c_1 x(t)} x(t) + s_0 \frac{1}{1 + c_2 x(t)} x(t);$
- (b) $x(t+1) = b_0 e^{-c_1 x(t)} x(t) + s_0 e^{-c_2 x(t)} x(t);$
- (c) $x(t+1) = b_0 \frac{1 + ax(t)}{1 + c_1 x^2(t)} x(t) + s_0 \frac{1}{1 + c_2 x(t)} x(t);$
- (d) $x(t+1) = b_0 \frac{1 + \phi a x^2(t)}{1 + a x^2(t)} x(t) + s_0 x(t).$

Exercise 1.37. Apply Theorems 1.13, 1.17, and 1.20 to the equation

$$x(t+1) = b_0 \frac{1}{1 + cx(t)} \frac{1 + \phi a x^2(t)}{1 + a x^2(t)} x(t) + s_0 x(t)$$

and draw its bifurcation diagram G for each of the following sets of parameters:

- (a) $c = 1, a = 1, \phi = 4,$ and $s_0 = 0.5;$
- (b) $c = 2, a = 3, \phi = 3,$ and $s_0 = 0.5;$
- (c) $c = 3, a = 0.5, \phi = 2,$ and $s_0 = 0.5.$

Exercise 1.38. In a first course on ordinary differential equations, students typically encounter the so-called logistic differential equation $x' = r(1 - x/K)x$ and learn to calculate the formula

$$x(t) = \begin{cases} K \frac{x_0 e^{rt}}{K - x_0 + x_0 e^{rt}} & \text{if } x_0 \neq K \\ K & \text{if } x_0 = K \end{cases}$$

for the solution of the initial value problem $x(0) = x_0 > 0.$ Evaluating this formula at the discrete sampling times $t \in \mathbb{Z}_+,$ we obtain a sequence $x(t).$ Show that this sequence satisfies the discrete logistic equation (1.17) with $b_0 = e^r$ and $c = (b_0 - 1)/K.$

Exercise 1.39. Assume $f : I \rightarrow I$ is continuous on an open interval

$$I = \{x \in R : 0 < x < \beta \leq +\infty\}.$$

- (a) Prove that if $x(t)$ is a solution of the difference equation $x(t+1) = f(x(t))$ that converges to a limit x^* as $t \rightarrow \infty$, then x^* is an equilibrium.
- (b) Assume $f(x)$ has a fixed point $x_e \in I$ and that $f(x)$ satisfies the following two conditions for all $x \in I$: (i) $x < x_e$ implies $x < f(x) < x_e$ and (ii) $x > x_e$ implies $f(x) < x$. Prove that x_e is globally attracting on I . (HINTS: First show that $x(0) < x_e$ yields an increasing sequence that satisfies $x(t) < x_e$ for all t . Second, show that if $x(0) > x_e$, then either $x(t)$ is a decreasing sequence that satisfies $x(t) > x_e$ for all t or there is a time t^* after which $x(t) \leq x_e$ is increasing for all $t \geq t^*$.) It is known that if x_e is globally attracting, then it is stable (Theorem 4.7 in [62]); thus, under the conditions (i) and (ii), x_e is globally asymptotically stable on I .
- (c) Show that (i) and (ii) from part (b) hold if $\partial_x f(x) > 0$ and $\partial_x^2 f(x) < 0$ on I .
- (d) Use (c) to show that when $r_0 > 1$, the positive equilibrium of the discrete logistic equation (1.17) is globally asymptotically stable.
- (e) Use (c) to find parameter values $b_0 = r_0$ and c in the Ricker equation (1.25) for which the positive equilibrium is globally asymptotically stable.

Exercise 1.40. Apply Theorems 1.25 and 1.26 to the equations

$$x(t+1) = b_0 \frac{1}{1 + cx(t)} x(t) + s_0 x(t) \quad \text{and}$$

$$x(t+1) = b_0 x(t) + s_0 \frac{1}{1 + cx(t)} x(t).$$

Exercise 1.41. Consider the following definitions: a p -cycle x_1, x_2, \dots, x_p of the difference equation (1.21) is

- (a) **locally stable** if to any real number $\varepsilon > 0$ there corresponds a real number $\delta(\varepsilon) > 0$ such that $\sum_{i=0}^{p-1} |x(i) - x_i| < \delta(\varepsilon)$ implies $\sum_{i=t_p}^{t_p+p-1} |x(i) - x_i| < \varepsilon$ for all $t \in Z_+$, and it is **unstable** if it is not locally stable;

- (b) **attracting** if there exists a real number $\delta^* > 0$ such that $\sum_{i=0}^{p-1} |x(i) - x_i| < \delta^*$ implies $\lim_{t \rightarrow +\infty} \sum_{i=t_p}^{tp+p-1} |x(i) - x_i| = 0$;
- (c) **locally asymptotically stable** (or simply **stable**) if it is both locally stable and attracting.

Prove that a p -cycle is stable (or unstable) by these definitions if and only if x_0 is a stable (or unstable) equilibrium of the p th composite equation (as defined in Definition 1.8).

Exercise 1.42. Show that as a function of $x > 0$, the expression in (1.37) is either monotonic or has two critical points. (HINT: Show the derivative with respect to x is a quotient whose numerator is a fourth order polynomial in x and apply Descartes' Rule of Signs.)

Exercise 1.43. Use a computer to calculate the equilibria for the spruce-budworm equation (1.36) with parameter values (1.38) and the six values of b_0 used in Figure 1.7. Then numerically calculate $\partial_x f(x)$ and use it, with the Linearization Principle, to determine the stability of each equilibrium.

Chapter 2

Linear Matrix Models for Structured Populations

In most biological populations, there is diversity, indeed often a great deal of diversity, among individual organisms. This diversity can be found in innumerable physiological and behavioral characteristics, such as age, weight, body size, gender, life cycle stages, mobility, food requirements, foraging efficiency, genetics, state of health (e.g., in the presence of a disease) ... the list is virtually endless. Any of these characteristics, or set of characteristics, can play a significant role in an individual's fitness and, as a result, the dynamics of the population as a whole. At the opposite extreme of using an aggregated state variable to account for all individuals (as in the models found in Chapter 1), one could envision a model in which every individual organism is a state variable. In this case, the methodology that dynamically tracks every individual is called individual-based modeling. These kinds of models obviously involve, for a population of any significant size, a very large number of state variable equations and, as a result, are in general analytically intractable. Their study relies on computer simulations, which makes it difficult to obtain a thorough and rigorous understanding of the model's implications and predictions. An intermediate point of view and modeling methodology is to specify a finite set of categories or classes of individuals, defined with regard to characteristics of importance for the

population to be studied, and to track the dynamics of each class. A basic example is to track a finite set of classes based on chronological age. These kinds of models are called **structured population models** and they are the main subject of the remaining chapters.

Following the format of Chapter 1, we first consider (in this chapter) linear structured population models in which vital fertility and survival rates are constant over time and then consider nonlinear models (in Chapter 3) in which they are dependent on population density. In both chapters, we will be guided by the basic properties of linear and nonlinear models that we discovered in Chapter 1 for unstructured population models. For example, we saw in Section 1.1 that linear difference equations predict either exponential decay (to extinction) or unbounded growth except when r_0 exactly equals 1, results that are represented in the vertical bifurcation diagram in Figure 1.1. For nonlinear equations, on the other hand, the bifurcation diagram is (in general) no longer vertical, but is bent in such a way as to allow sustained survival at a finite equilibrium for some values of r_0 (as in Figures 1.2 and 1.3). We will find (among many other things) that these two basic features remain basically in tact for matrix models of structured populations as well.

2.1. Modeling Methodology

Suppose each individual in a population is placed in exactly one of finitely many classes and let $x_i(t)$ be the population density of the i th class at time $t \in \mathbb{Z}_+$. We follow each class density $x_i(t)$ through time by using the accounting principle (1.1). We consider populations closed to immigration or seeding, in which the new arrivals in our basic modeling accounting procedure (1.1) are newborns only. For each j -class individual alive at time t , let $f_{ij} \geq 0$ denote the number of i -class newborns it produces and that are present at the next census time $t + 1$. Then the new i -class arrivals in total equal $\sum_{j=1}^m f_{ij}x_j(t)$, where m is the number of classes. Next we let τ_{ij} denote the fraction of j -class individuals alive at time t that are alive and in the i th class at time $t + 1$. Thus, τ_{ij} entails both the probability that a j -class individual survives and the probability that it moves to class i . Then by (1.1)

$$(2.1) \quad x_i(t+1) = \sum_{j=1}^m f_{ij}x_j(t) + \sum_{j=1}^m \tau_{ij}x_j(t)$$

for each $i = 1, 2, \dots, m$, where

$$(2.2) \quad f_{ij} \geq 0, \quad 0 \leq \tau_{ij} \leq 1, \quad \text{and} \quad \sum_{i=1}^m \tau_{ij} \leq 1$$

for all i and $j = 1, 2, \dots, m$. The latter inequality holds because the total number of j -class individuals that survive to $t + 1$, namely $\sum_{i=1}^m \tau_{ij} x_i(t)$, must be less or equal to the number $x_j(t)$ that was present at time t .

We can write all the equations (2.1) more concisely by using matrix notation:

$$(2.3) \quad \mathbf{x}(t+1) = \mathbf{P}\mathbf{x}(t),$$

where $\mathbf{x}(t) = \text{col}(x_i(t))$, $\mathbf{P} = \mathbf{F} + \mathbf{T}$, and

$$\mathbf{F} = [f_{ij}] \quad \text{and} \quad \mathbf{T} = [\tau_{ij}]$$

are $m \times m$ matrices. The matrix $\mathbf{P} = [p_{ij}]$, where $p_{ij} = f_{ij} + \tau_{ij}$, is called the **population projection matrix**. We call \mathbf{P} , \mathbf{F} , and \mathbf{T} **nonnegative matrices** because all their entries are nonnegative real numbers. We denote these matrix properties by writing $\mathbf{P} \geq \mathbf{0}_{m \times m}$, $\mathbf{F} \geq \mathbf{0}_{m \times m}$, and $\mathbf{T} \geq \mathbf{0}_{m \times m}$, where $\mathbf{0}_{m \times m}$ is the $m \times m$ matrix of zeros. We call \mathbf{F} the **fertility matrix** and \mathbf{T} the **transition matrix**.

Note that each initial condition $\mathbf{x}(0)$ produces a unique sequence $\mathbf{x}(t)$ by repeated application of the **matrix difference equation** (2.3). We call this sequence a **solution** of the matrix equation. Since the projection matrix \mathbf{P} is nonnegative, the solution of an initial value problem with a nonnegative initial condition $\mathbf{x}(0) \in R_+^m$ remains nonnegative (i.e., $\mathbf{x}(t) \in R_+^m$ for all $t \in Z_+$). Thus, each nonnegative initial condition is associated with a unique nonnegative solution.

The iconic example of a structured population is the Leslie model for an age-structured population [100], [101]. In this model, individuals are classified by a finite set of age class of equal length and the population is censused sequentially at time intervals equal to this length, which we take without loss in generality to be 1. Newborns belong to class $i = 1$ so that

$$(2.4) \quad \mathbf{F} = \begin{bmatrix} b_1 & b_2 & \cdots & b_{m-1} & b_m \\ 0 & 0 & \cdots & 0 & 0 \\ 0 & 0 & \cdots & 0 & 0 \\ \vdots & \vdots & & \vdots & \vdots \\ 0 & 0 & \cdots & 0 & 0 \end{bmatrix}$$

and surviving individuals necessarily advance to the next age class so that \mathbf{T} is the sub-diagonal matrix

$$(2.5) \quad \mathbf{T} = \begin{bmatrix} 0 & 0 & \cdots & 0 & 0 \\ s_1 & 0 & \cdots & 0 & 0 \\ 0 & s_2 & \cdots & 0 & 0 \\ \vdots & \vdots & & \vdots & \vdots \\ 0 & 0 & \cdots & s_{m-1} & 0 \end{bmatrix},$$

where, for notational simplification, we have defined

$$b_i := f_{1i} \quad \text{and} \quad s_i := \tau_{i+1,i}.$$

Matrices (2.4) and (2.5) yield the **Leslie matrix** [100], [101]

$$(2.6) \quad \mathbf{P} = \mathbf{F} + \mathbf{T} = \begin{bmatrix} b_1 & b_2 & \cdots & b_{m-1} & b_m \\ s_1 & 0 & \cdots & 0 & 0 \\ 0 & s_2 & \cdots & 0 & 0 \\ \vdots & \vdots & & \vdots & \vdots \\ 0 & 0 & \cdots & s_{m-1} & 0 \end{bmatrix}$$

with $b_i \geq 0$ and $0 < s_i \leq 1$

in which b_i is the number of newborns (class 1 individuals) produced by age class i individuals (per unit time) and s_i is the fraction of (probability that) an age class i individual survives a unit of time.

The Leslie model with projection matrix (2.6) assumes no individual lives beyond the m th age class, which accounts for the 0 appearing in the lower-right corner in the transition matrix (2.5). For example, in human demographic models, the age classes are typically 10 years in length so that in a Leslie model of dimension m it is assumed no individual is older than $10m$ years. Such a Leslie model with $m = 10$ assumes no individual lives past age 100. Leslie models arise in applications that redefine the m th class to be individuals of age older than $m - 1$ units, which allows individuals to live to any age. The modified transition matrix has a positive survival probability s_m in its lower-right corner

$$(2.7) \quad \mathbf{T} = \begin{bmatrix} 0 & 0 & \cdots & 0 & 0 \\ s_1 & 0 & \cdots & 0 & 0 \\ 0 & s_2 & \cdots & 0 & 0 \\ \vdots & \vdots & & \vdots & \vdots \\ 0 & 0 & \cdots & s_{m-1} & s_m \end{bmatrix}.$$

The resulting projection matrix

$$(2.8) \quad \mathbf{P} = \begin{bmatrix} b_1 & b_2 & \cdots & b_{m-1} & b_m \\ s_1 & 0 & \cdots & 0 & 0 \\ 0 & s_2 & \cdots & 0 & 0 \\ \vdots & \vdots & & \vdots & \vdots \\ 0 & 0 & \cdots & s_{m-1} & s_m \end{bmatrix}$$

with $b_i \geq 0$, $0 < s_m \leq 1$, and $0 < s_i \leq 1$ for $i = 1, 2, \dots, m - 1$

is called an **extended Leslie matrix**.

Instead of using chronological age, suppose we structure a population according to some measure of body size (height, girth, weight, etc.). We choose a time unit so that an individual can advance at most one size class per unit time. We also assume that a surviving individual cannot shrink in size and that all newborns are in the smallest size class. The fertility matrix \mathbf{F} is again given by (2.4), but the transition matrix \mathbf{T} is now a bidiagonal matrix

$$(2.9) \quad \mathbf{T} = \begin{bmatrix} \tau_{11} & 0 & 0 & \cdots & 0 & 0 \\ \tau_{21} & \tau_{22} & 0 & \cdots & 0 & 0 \\ 0 & \tau_{32} & \tau_{33} & \cdots & 0 & 0 \\ \vdots & \vdots & \vdots & & \vdots & \vdots \\ 0 & 0 & 0 & \cdots & \tau_{m-1,m-1} & 0 \\ 0 & 0 & 0 & \cdots & \tau_{m,m-1} & \tau_{mm} \end{bmatrix},$$

where τ_{ii} is the probability a surviving i -class individual remains in the i -class and $\tau_{i+1,i}$ is the probability it grows to the next larger size class. The resulting projection matrix

$$(2.10) \quad \mathbf{P} = \begin{bmatrix} b_1 + \tau_{11} & b_2 & b_3 & \cdots & b_{m-1} & b_m \\ \tau_{21} & \tau_{22} & 0 & \cdots & 0 & 0 \\ 0 & \tau_{32} & \tau_{33} & \cdots & 0 & 0 \\ \vdots & \vdots & \vdots & & \vdots & \vdots \\ 0 & 0 & 0 & \cdots & \tau_{m-1,m-1} & 0 \\ 0 & 0 & 0 & \cdots & \tau_{m,m-1} & \tau_{mm} \end{bmatrix}$$

defines the **Usher matrix model [124]** (or the **standard size structured model [13]**). Note that, from a mathematical point of view, a Leslie model is a special case of the Usher model with $\tau_{ii} = 0$.

Example 2.1. In [111], the 3×3 Leslie matrix

$$(2.11) \quad \mathbf{P} = \begin{bmatrix} 0 & 0 & 1.893 \\ 0.6310 & 0 & 0 \\ 0 & 0.0631 & 0.6272 \end{bmatrix}$$

is used in an application to the stingray species *Dasyatis violacea*. The time unit is one year, and individuals are juveniles (nonreproducing) for the first two years. The 8×8 Usher matrix

$$(2.12) \quad \mathbf{P} = \begin{bmatrix} 0 & 0 & 0 & 0 & 0 & 0.042 & 0.069 & 0.069 \\ 0.716 & 0.567 & 0 & 0 & 0 & 0 & 0 & 0 \\ 0 & 0.149 & 0.567 & 0 & 0 & 0 & 0 & 0 \\ 0 & 0 & 0.149 & 0.605 & 0 & 0 & 0 & 0 \\ 0 & 0 & 0 & 0.235 & 0.560 & 0 & 0 & 0 \\ 0 & 0 & 0 & 0 & 0.225 & 0.678 & 0 & 0 \\ 0 & 0 & 0 & 0 & 0 & 0.249 & 0.851 & 0 \\ 0 & 0 & 0 & 0 & 0 & 0 & 0.016 & 0.860 \end{bmatrix}$$

is used to study the population dynamics of the endangered desert tortoise (*Gopherus agassizii*) by the authors in [60]. Here, the time unit is one year, and the size classes are defined as: yearling, juvenile 1, juvenile 2, immature 1, immature 2, subadult, adult 1, and adult 2. Finally, in [131], the 7×7 projection matrix

$$(2.13) \quad \mathbf{P} = \begin{bmatrix} 0 & 0 & 0 & 0 & 0 & 0 & 431 \\ 0.748 & 0 & 0 & 0 & 0 & 0 & 0 \\ 0 & 0.966 & 0 & 0 & 0 & 0 & 0 \\ 0.008 & 0.013 & 0.010 & 0.125 & 0 & 0 & 0 \\ 0.070 & 0.007 & 0 & 0.125 & 0.238 & 0 & 0 \\ 0.002 & 0.008 & 0 & 0.038 & 0.245 & 0.167 & 0 \\ 0 & 0 & 0 & 0 & 0.023 & 0.750 & 0 \end{bmatrix}$$

is used to study the population dynamics of wild teasel (*Dipsacus sylvestris*) with a one-year time unit. Here, the classification scheme is based on the life cycle stages: new seeds, 1-year dormant seeds, 2-year dormant seeds, small rosettes, medium rosettes, large rosettes, and flowering plants.

A basic question to ask about each of these matrix models is whether the population is growing or whether it is decreasing and in danger of extinction. We will learn techniques for answering this question in Section 2.2. \square

In addition to the matrix formulation of a structured population dynamic model, as carried out previously, we can geometrically represent

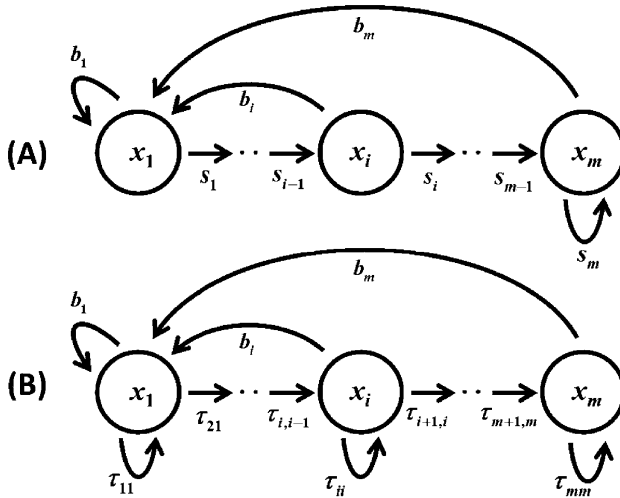


Figure 2.1. The life cycle graphs associated with (A) the Leslie age-structured model and (B) the Usher size-structured model.

the model by means of a directed graph, called the **life cycle graph**. We draw a circle (a node) for each class and then draw a directed arc from circle i to circle j if a transition from class i to class j is possible or if individuals in class i produce offspring in class j , that is to say if the entry p_{ij} from the projection matrix is positive. Figure 2.1 shows the life cycle graphs associated with the Leslie and Usher matrix models.

As a final remark in this introductory section, we point out that a projection matrix is called **irreducible** if, in its corresponding life cycle graph, there is a path from every node to every other node. (Such a graph is called strongly connected.) In this case, every class is reachable from every class by either transition or births. *In this book, we consider only irreducible projection matrices*, as they are overwhelmingly the ones that arise in applications.

As an example, we obtain the following result from inspection of the life cycle graphs in Figure 2.1.

Theorem 2.2. *Leslie and Usher projection matrices are irreducible if (and only if) $s_i > 0$ for all i and $b_m > 0$.*

Throughout this and the remaining chapters, we use the a superscript T to denote the (complex) transpose of a vector or a matrix, and

we use the so-called L_1 vector norm

$$\|\mathbf{v}\| = \sum_{i=1}^m |v_i|$$

for $\mathbf{v} \in \mathbb{R}^m$. (See the Table of Symbols.) Thus, in applications of a matrix equation (2.3) with a nonnegative projection matrix, $\|\mathbf{x}(t)\| = \sum_{i=1}^m x_i(t)$ is the **total population size**.

2.2. The Fundamental Theorem of Demography

By a straightforward induction argument (Exercise 2.24), one can derive the formula

$$(2.14) \quad \mathbf{x}(t) = \mathbf{P}^t \mathbf{x}(0), \quad t \in \mathbb{Z}_+$$

for the solution of the matrix equation (2.3) with projection matrix \mathbf{P} .

Example 2.3. Consider the projection matrix

$$(2.15) \quad \mathbf{P} = \begin{bmatrix} 0 & 0 & 1.893 \\ 0.6310 & 0 & 0 \\ 0 & 0.0631 & 0.6272 \end{bmatrix}$$

from the stringray application in Example 2.1. If we start with a population consisting of only 10 adults

$$\mathbf{x}(0) = \begin{bmatrix} 0 \\ 0 \\ 10 \end{bmatrix},$$

we obtain by iteration of the matrix equation (2.3) the demographic vectors (rounded to 4 significant digits):

$$\begin{aligned} \mathbf{x}(1) &= \begin{bmatrix} 18.93 \\ 0 \\ 6.272 \end{bmatrix}, & \mathbf{x}(2) &= \begin{bmatrix} 11.87 \\ 11.95 \\ 3.934 \end{bmatrix}, \\ \mathbf{x}(3) &= \begin{bmatrix} 7.447 \\ 7.492 \\ 3.221 \end{bmatrix}, \text{ and } & \mathbf{x}(4) &= \begin{bmatrix} 6.097 \\ 4.699 \\ 2.493 \end{bmatrix}. \end{aligned}$$

Notice that the component population densities appear to be decreasing with time, as do the total population densities:

$$\begin{aligned} \|\mathbf{x}(1)\| &= 25.20, & \|\mathbf{x}(2)\| &= 27.75, \\ \|\mathbf{x}(3)\| &= 18.16, \text{ and } & \|\mathbf{x}(4)\| &= 13.29. \end{aligned}$$

Using formula (2.14), we can see further evidence of this from

$$\mathbf{x}(10) = \begin{bmatrix} 1.166 \\ 0.9705 \\ 0.4670 \end{bmatrix}, \quad \mathbf{x}(20) = \begin{bmatrix} 7.328 \times 10^{-2} \\ 6.098 \times 10^{-2} \\ 2.935 \times 10^{-2} \end{bmatrix},$$

$$\mathbf{x}(30) = \begin{bmatrix} 4.606 \times 10^{-3} \\ 3.833 \times 10^{-3} \\ 1.845 \times 10^{-3} \end{bmatrix}, \text{ and } \mathbf{x}(40) = \begin{bmatrix} 2.8948 \times 10^{-4} \\ 2.4089 \times 10^{-4} \\ 1.1596 \times 10^{-4} \end{bmatrix}$$

and their total population sizes

$$\|\mathbf{x}(10)\| = 2.603, \quad \|\mathbf{x}(20)\| = 1.636 \times 10^{-1},$$

$$\|\mathbf{x}(30)\| = 1.028 \times 10^{-2}, \text{ and } \|\mathbf{x}(40)\| = 6.463 \times 10^{-4}.$$

Another interesting observation to make from these calculations concerns the normalized population distribution $\mathbf{x}(t) / \|\mathbf{x}(t)\|$ (which give the proportions of the population in each of the three classes at each time t). Despite the fact that the population appears to be going extinct, the normalized population distribution appears to stabilize:

$$\frac{\mathbf{x}(1)}{\|\mathbf{x}(1)\|} = \begin{bmatrix} 0.7511 \\ 0 \\ 0.2489 \end{bmatrix}, \quad \frac{\mathbf{x}(2)}{\|\mathbf{x}(2)\|} = \begin{bmatrix} 0.4278 \\ 0.4304 \\ 0.1418 \end{bmatrix},$$

$$\frac{\mathbf{x}(3)}{\|\mathbf{x}(3)\|} = \begin{bmatrix} 0.4101 \\ 0.4126 \\ 0.1774 \end{bmatrix}, \quad \frac{\mathbf{x}(4)}{\|\mathbf{x}(4)\|} = \begin{bmatrix} 0.4588 \\ 0.3536 \\ 0.1876 \end{bmatrix},$$

$$\frac{\mathbf{x}(10)}{\|\mathbf{x}(10)\|} = \begin{bmatrix} 0.4478 \\ 0.3728 \\ 0.1794 \end{bmatrix}, \quad \frac{\mathbf{x}(20)}{\|\mathbf{x}(20)\|} = \begin{bmatrix} 0.4479 \\ 0.3727 \\ 0.1794 \end{bmatrix},$$

$$\frac{\mathbf{x}(30)}{\|\mathbf{x}(30)\|} = \begin{bmatrix} 0.4479 \\ 0.3727 \\ 0.1794 \end{bmatrix}, \text{ and } \frac{\mathbf{x}(40)}{\|\mathbf{x}(40)\|} = \begin{bmatrix} 0.4479 \\ 0.3727 \\ 0.1794 \end{bmatrix}.$$

As we will see in Theorem 2.7, this is not a coincidence. □

Suppose the $m \times m$ projection matrix \mathbf{P} is diagonalizable (i.e., has m linearly independent right eigenvectors \mathbf{v}_i and m linearly independent left eigenvectors \mathbf{w}_i^T). Then we can write any initial condition $\mathbf{x}(0)$ as a linear combination of the eigenvectors:

$$(2.16) \quad \mathbf{x}(0) = \sum_{i=1}^m c_i \mathbf{v}_i,$$

where the coefficients c_i are given by the formula

$$(2.17) \quad c_i = \frac{\mathbf{w}_i^T \mathbf{x}(0)}{\mathbf{w}_i^T \mathbf{v}_i}.$$

(See Exercise 2.25.) By a repeated application of (2.14), we obtain a solution formula

$$(2.18) \quad \mathbf{x}(t) = \sum_{i=1}^m c_i \lambda_i^t \mathbf{v}_i, \quad t \in \mathbb{Z}_+.$$

expressed in terms of the eigenvalues and eigenvectors. From this formula, we see that the asymptotic dynamics of the solution $\mathbf{x}(t)$ depends on asymptotic dynamics of the exponentials λ_i^t . Obviously, as $t \rightarrow \infty$, λ_i^t tends to 0 if $|\lambda_i| < 1$ or increases without bound if $|\lambda_i| > 1$.

If \mathbf{P} has complex eigenvalues and eigenvectors, then they appear in complex conjugate pairs. Since the sum of complex conjugates is two times their real parts, the solution formula (2.18) will be real valued, even when complex eigenvalues occur.

Example 2.4. Using a computer program, we find that the eigenvalues of the projection matrix in Example 2.3 are

$$\begin{aligned} \lambda_1 &= 0.7583, & \lambda_2 &= -0.06554 + 0.3084i, \\ \text{and } \lambda_3 &= -0.06554 - 0.3084i. \end{aligned}$$

Notice that

$$|\lambda_1| = 0.7583 < 1 \quad \text{and} \quad |\lambda_2| = |\lambda_3| = 0.3153 < 1,$$

and it follows from the solution formula (2.18) that $\lim_{t \rightarrow \infty} \mathbf{x}(t) = \mathbf{0}_3$. This corroborates the speculation in Example 2.3 that the population model predicts extinction.

Eigenvalues associated with the eigenvalues, normalized so that $\|\mathbf{v}_i\| = 1$, are (rounded to 4 significant digits)

$$\begin{aligned} \mathbf{v}_1 &= \begin{bmatrix} 0.4479 \\ 0.3727 \\ 0.1794 \end{bmatrix}, & \mathbf{v}_2 &= \begin{bmatrix} 0.3157 \\ -0.1313 - 0.6180i \\ -0.01093 + 0.05142i \end{bmatrix}, \\ \text{and } \mathbf{v}_3 &= \begin{bmatrix} 0.3157 \\ -0.1313 + 0.6180i \\ -0.01093 - 0.05142i \end{bmatrix}, \end{aligned}$$

and we can write the initial condition

$$\mathbf{x}(0) = \begin{bmatrix} 0 \\ 0 \\ 10 \end{bmatrix}$$

used in Example 2.3 as $\mathbf{x}(0) = c_1\mathbf{v}_1 + c_2\mathbf{v}_2 + c_3\mathbf{v}_3$ with coefficients

$$c_1 = 41.42, \quad c_2 = -29.38 - 18.74i,$$

$$\text{and } c_3 = -29.38 + 18.74i.$$

Using the solution formula (2.18), we rewrite the normalized population distribution

$$\frac{\mathbf{x}(t)}{\|\mathbf{x}(t)\|} = \frac{c_1\lambda_1^t\mathbf{v}_1 + c_2\lambda_2^t\mathbf{v}_2 + c_3\lambda_3^t\mathbf{v}_3}{\left\|c_1\lambda_1^t\mathbf{v}_1 + c_2\lambda_2^t\mathbf{v}_2 + c_3\lambda_3^t\mathbf{v}_3\right\|}$$

as

$$\frac{\mathbf{x}(t)}{\|\mathbf{x}(t)\|} = \frac{c_1\mathbf{v}_1 + c_2\left(\frac{\lambda_2}{\lambda_1}\right)^t\mathbf{v}_2 + c_3\left(\frac{\lambda_3}{\lambda_1}\right)^t\mathbf{v}_3}{\left\|c_1\mathbf{v}_1 + c_2\left(\frac{\lambda_2}{\lambda_1}\right)^t\mathbf{v}_2 + c_3\left(\frac{\lambda_3}{\lambda_1}\right)^t\mathbf{v}_3\right\|}$$

and find, since

$$\left|\frac{\lambda_2}{\lambda_1}\right| = \left|\frac{\lambda_3}{\lambda_1}\right| = 0.4158 < 1,$$

that

$$\lim_{t \rightarrow \infty} \frac{\mathbf{x}(t)}{\|\mathbf{x}(t)\|} = \frac{c_1\mathbf{v}_1}{\|c_1\mathbf{v}_1\|} = \mathbf{v}_1.$$

This corroborates the speculation in Example 2.3 that normalized population distribution stabilizes and in fact approaches the eigenvector \mathbf{v}_1 . \square

To make any general pronouncements about the asymptotic dynamics of the matrix equation (2.3) with regard to the eigenvalues and eigenvectors of the projection matrix \mathbf{P} , we need more information about the eigenvalues and eigenvectors of nonnegative, irreducible matrices. The list of facts in the following Theorem 2.5 come from a large collection of known facts about nonnegative matrices called **Perron–Frobenius theory** (see for example [7], [80], [125]). An eigenvalue λ_i of a matrix is called **dominant** if $|\lambda_i| \geq |\lambda_j|$ for all j . Recall an eigenvalue is simple means that it is an algebraically simple (i.e., nonrepeated) root of the matrix's characteristic polynomial. (An algebraically simple eigenvalue is necessarily a geometrically simple eigenvalue [i.e., its eigenspace is one dimensional].)

Theorem 2.5.

- (a) A nonnegative matrix has a real nonnegative, dominant eigenvalue and associated nonnegative right and left eigenvectors.
- (b) If a nonnegative matrix is irreducible, then the dominant eigenvalue is positive and simple, and it has associated positive right and left eigenvectors. Moreover, no other eigenvalue has a non-negative eigenvector.

Remark 2.6. If λ_i are the eigenvalues of a matrix M , then

$$\rho[\mathbf{M}] = \max\{|\lambda_i|\} \geq 0$$

is called the spectral radius of the matrix. For a nonnegative matrix M , Theorem 2.5 implies the spectral radius $\rho[\mathbf{M}]$ is in fact an eigenvalue; it is often called the Perron eigenvalue. We assume the eigenvalues are ordered so that $\lambda_1 = \rho[\mathbf{M}]$. In population models, the dominant, Perron eigenvalue of the projection matrix P is often also denoted by $r_0 = \rho[\mathbf{M}]$.

Suppose the projection matrix \mathbf{P} in the matrix equation (2.3) is non-negative and irreducible, and let \mathbf{v} and \mathbf{w}^T denote positive right and left eigenvectors associated with the dominant eigenvalue $r_0 > 0$. Without loss in generality, we order the eigenvalues λ_i so that $\lambda_1 = r_0$, $\mathbf{v}_1 = \mathbf{v}$, and $\mathbf{w}_1^T = \mathbf{w}^T$ and then write the solution formula (2.18) as

$$(2.19) \quad \mathbf{x}(t) = c_1 r_0^t \mathbf{v} + \sum_{i=2}^m c_i \lambda_i^t \mathbf{v}_i.$$

Note that if $\mathbf{x}(0)$ is a nonnegative and nonzero initial condition, then the coefficient $c_1 = \mathbf{w}^T \mathbf{x}(0) > 0$. If the dominant eigenvalue $\lambda_1 = r_0$, which by definition satisfies $r_0 \geq |\lambda_i|$ for all $i \neq 1$, happens to satisfy the strict inequalities $r_0 > |\lambda_i|$ for all $i \neq 1$, then it is called **strictly dominant** and the matrix is then called **primitive**. Primitive population projection matrices play a leading role in matrix models, although **imprimitive** projection matrices do arise in applications (as we will see). Here is a basic theorem about the asymptotic dynamics of solutions of linear matrix models with primitive projection matrices and about their **normalized population distributions** $\mathbf{x}(t)/\|\mathbf{x}(t)\|$ (which consist of the fractions of the total population $\|\mathbf{x}(t)\|$ in each class).

Theorem 2.7. The Fundamental Theorem of Demography or the Strong Ergodic Theorem. Assume the projection matrix \mathbf{P} in the matrix

equation (2.3) is primitive. If $r_0 > 0$ is the strictly dominant eigenvalue and \mathbf{w}^T and \mathbf{v} are associated left and right, positive eigenvectors, then for all solutions with nonzero, nonnegative initial condition $\mathbf{x}(0) \in R_+^m$,

$$\lim_{t \rightarrow \infty} \frac{\mathbf{x}(t)}{r_0^t} = \mathbf{w}^T \mathbf{x}(0) \mathbf{v} > \mathbf{0} \quad \text{and} \quad \lim_{t \rightarrow \infty} \frac{\mathbf{x}(t)}{\|\mathbf{x}(t)\|} = \frac{\mathbf{v}}{\|\mathbf{v}\|}.$$

We give a proof of this theorem under the assumption that \mathbf{P} is diagonalizable (i.e., has m independent eigenvectors). For a proof when this is not the case, see [82].

Proof. Note that $r_0 > |\lambda_i|$ for all $i \neq 1$ implies $\lim_{t \rightarrow \infty} (\lambda_i/r_0)^t = 0$ for all $i \neq 1$. The first limit follows immediately from

$$\frac{\mathbf{x}(t)}{r_0^t} = c_1 \mathbf{v} + \sum_{i=2}^m c_i \left(\frac{\lambda_i}{r_0} \right)^t \mathbf{v}_i,$$

obtained from (2.19). To verify the second limit, we divide the numerator and denominator of the normalized distribution

$$\frac{\mathbf{x}(t)}{\|\mathbf{x}(t)\|} = \frac{c_1 \mathbf{v} r_0^t + \sum_{i=2}^m c_i \lambda_i^t \mathbf{v}_i}{\left\| c_1 \mathbf{v} r_0^t + \sum_{i=2}^m c_i \lambda_i^t \mathbf{v}_i \right\|}$$

by r_0^t to obtain

$$\frac{\mathbf{x}(t)}{\|\mathbf{x}(t)\|} = \frac{c_1 \mathbf{v} + \sum_{i=2}^m c_i \left(\frac{\lambda_i}{r_0} \right)^t \mathbf{v}_i}{\left\| c_1 \mathbf{v} + \sum_{i=2}^m c_i \left(\frac{\lambda_i}{r_0} \right)^t \mathbf{v}_i \right\|},$$

from which follows

$$\lim_{t \rightarrow \infty} \frac{\mathbf{x}(t)}{\|\mathbf{x}(t)\|} = \frac{c_1 \mathbf{v}}{\|c_1 \mathbf{v}\|} = \frac{\mathbf{v}}{\|\mathbf{v}\|}$$

since $c_1 = \mathbf{w} \cdot \mathbf{x}(0) > 0$. \square

Theorem 2.7 says several important things concerning the long-term fate of a population governed by equation (2.3) with a primitive projection matrix \mathbf{P} . From

$$\lim_{t \rightarrow \infty} \frac{\|\mathbf{x}(t)\|}{r_0^t} = \mathbf{w}^T \mathbf{x}(0) \|\mathbf{v}\| > 0,$$

we see that there are three case for the asymptotic dynamics:

$$\lim_{t \rightarrow \infty} \|\mathbf{x}(t)\| = \begin{cases} 0 & \text{if } 0 < r_0 < 1 \\ \mathbf{w}^T \mathbf{x}(0) \|\mathbf{v}\| & \text{if } r_0 = 1 \\ +\infty & \text{if } 1 < r_0 \end{cases}.$$

These are the same three possibilities as we found for scalar ($m = 1$) linear equations in Chapter 1 (see equation (1.6)). Geometrically, we have the same (vertical) bifurcation diagram as in Figure 1.1, but in this case, the plot would include the total population size at equilibria $\|\mathbf{x}_e\|$ against r_0 . For $r_0 \neq 1$, the total population $\|\mathbf{x}(t)\|$ is proportional to r_0^t for large t , and we call r_0 the **population growth rate**.

Another important fact that follows from Theorem 2.7 is that, regardless of whether the population is growing ($r_0 > 1$) or decaying ($r_0 < 1$), the proportions in each class stabilize to the normalized eigenvector $\mathbf{v}/\|\mathbf{v}\|$ as $t \rightarrow \infty$. This normalized distribution (whose entries form a partition of unity) is historically called the **stable demographic distribution**. (The word “stable” here is not to be confused with “asymptotically stable” in Definition 1.8.)

Before looking at some examples, we list some methods for determining the irreducibility and primitivity of a nonnegative matrix in the following theorem. A path in a life cycle graph that begins and ends at the same node is called a **loop**.

Theorem 2.8. Suppose \mathbf{M} is a nonnegative matrix.

- (a) \mathbf{M} is irreducible if and only if $(\mathbf{I}_m + \mathbf{M})^{m-1}$ is a positive matrix (where \mathbf{I}_m is the $m \times m$ identity matrix).
- (b) \mathbf{M} is primitive if and only if there exists an integer $p \geq 1$ such that \mathbf{M}^p is a positive matrix.
- (c) If \mathbf{M} is irreducible, then it is primitive if either of the following holds:
 - (i) There exists a positive diagonal entry.
 - (ii) 1 is the greatest common divisor of the lengths of its loops.

Remark 2.9. It turns out that if \mathbf{M} is primitive, then \mathbf{M}^{m^2-2m+2} is positive. This means the smallest integer for which \mathbf{M}^p is positive is less than or equal to $m^2 - 2m + 2$, so that when applying this power test for primitivity in Theorem 2.8(b), one needs consider powers no higher than $m^2 - 2m + 2$. (This fact, by the way, implies that each class is connected to any other class by a path of length no longer than $m^2 - 2m + 2$.)

Example 2.10. The Leslie and Usher matrices (2.11) and (2.12) introduced in Example 2.1 as matrix models for stingray and desert tortoise populations, respectively, are both irreducible by Theorem 2.2. An application of part (i) in Theorem 2.8(c) with $\mathbf{M} = \mathbf{P}$ shows that both of these projection matrices are primitive. The matrix (2.13) in Example 2.1, used to model wild teasel, is neither a Leslie nor an Usher matrix. With the aid of a computable algebra program, we can determine its irreducibility by applying Theorem 2.8(a) with $m = 7$ and $\mathbf{M} = \mathbf{P}$ to find that

$$(\mathbf{I}_7 + \mathbf{P})^6 = \begin{bmatrix} 169.3 & 78.32 & 2.926 & 536.7 & 2599 & 11300. & 33130 \\ 57.50 & 36.54 & 0.7111 & 218.9 & 1227 & 5807 & 9979 \\ 22.37 & 18.16 & 1.098 & 68.70 & 484.6 & 3744 & 6646 \\ 1.147 & 0.8646 & 0.09124 & 5.504 & 21.54 & 135.1 & 263.6 \\ 6.280 & 3.883 & 0.09959 & 24.49 & 134.8 & 676.5 & 1196 \\ 1.166 & 0.6815 & 0.02236 & 4.314 & 24.38 & 162.3 & 319.9 \\ 0.621 & 0.2748 & 0.01245 & 1.906 & 9.628 & 62.03 & 169.3 \end{bmatrix}$$

is a positive matrix. Then an application of part (i) in Theorem 2.8(c) shows this projection matrix is primitive. \square

Example 2.11. A Juvenile-Adult Model. A basic structuring of many biological populations can be based on the two classes: juveniles x_1 and adults x_2 . If we assume the attainment of reproductive maturity correlates with chronological age and use the maturation period as the unit of time, then we have the 2×2 fertility matrix

$$\mathbf{F} = \begin{bmatrix} 0 & b_2 \\ 0 & 0 \end{bmatrix} \text{ with } b_2 > 0,$$

where b_2 is the per adult number of juveniles produced per adult (per unit time). Assuming juvenile status cannot be again attained by a mature adult, we have the transition matrix

$$\mathbf{T} = \begin{bmatrix} 0 & 0 \\ s_1 & s_2 \end{bmatrix},$$

where s_1 and s_2 are juvenile and adult survival probabilities, respectively. Clearly, the population cannot survive if $b_2 = 0$ (there is no reproduction) or if $s_1 = 0$ (no juvenile reaches maturity). The projection matrix of this juvenile-adult matrix model is the $m = 2$

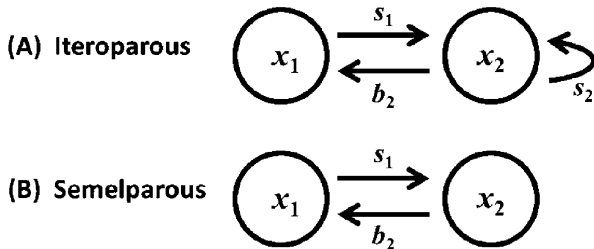


Figure 2.2. The life cycle graphs associated with the juvenile-adult projection matrix (2.20). The iteroparous case (A) is primitive, and the semelparous case (B) is imprimitive.

dimensional Leslie matrix (2.6)

$$(2.20) \quad \mathbf{P} = \mathbf{F} + \mathbf{T} = \begin{bmatrix} 0 & b_2 \\ s_1 & s_2 \end{bmatrix} \quad \text{with } b_2 > 0, \quad 0 < s_1 \leq 1, \quad \text{and } 0 \leq s_2 \leq 1.$$

It is easy to see that from the life cycle graph in Figure 2.2 that \mathbf{P} is irreducible (there is a path connecting the juveniles to adults and vice versa), which we can also verify from Theorem 2.8(a) and the calculation

$$(\mathbf{I}_m + \mathbf{P})^{m-1} = \begin{bmatrix} 1 & b_2 \\ s_1 & 1 + s_2 \end{bmatrix} > 0.$$

A calculation shows

$$\mathbf{P}^2 = \begin{bmatrix} b_2 s_1 & b_2 s_2 \\ s_1 s_2 & s_2^2 + b_2 s_1 \end{bmatrix}.$$

By Theorem 2.8(a), we arrive at the following conclusions.

The juvenile-adult model projection matrix (2.20) is:

- *primitive if $s_2 > 0$;*
- *imprimitive if $s_2 = 0$.*

We refer to the case $s_2 > 0$ as the **iteroparous juvenile-adult model** since it implies an adult can have multiple reproductive episodes. The case $s_2 = 0$, when an adult has only one reproductive time unit, we call the **semelparous juvenile-adult model**.

For an $m = 2$ dimensional projection matrix, algebraic formulas for its eigenvalues are analytically tractable by means of its quadratic characteristic polynomial model. Primitivity can also be determined by investigating the eigenvalues, which for the juvenile-adult projection matrix (2.20) are real:

$$\lambda_1 = \frac{1}{2}s_2 + \frac{1}{2}\sqrt{s_2^2 + 4b_2s_1} \quad \text{and} \quad \lambda_2 = \frac{1}{2}s_2 - \frac{1}{2}\sqrt{s_2^2 + 4b_2s_1}.$$

It is easy to see that $\lambda_1 > 0$ and $\lambda_1 > \lambda_2$. It is left as an exercise to show that $\lambda_1 \geq |\lambda_2|$ so that

$$(2.21) \quad r_0 = \frac{1}{2}s_2 + \frac{1}{2}\sqrt{s_2^2 + 4b_2s_1}$$

and that $\lambda_1 > |\lambda_2|$ (i.e., \mathbf{P} is primitive) if and only if $s_2 > 0$. \square

The juvenile-adult in Example 2.11 is the lowest-dimensional case of the Leslie model with projection matrix (2.6). Leslie matrices of higher dimensions are widely used in population modeling (in, for example, human demography). The next theorem follows from parts (i) and (ii) of Theorem 2.8(c).

Theorem 2.12. *Consider an irreducible extended Leslie matrix (2.8) with $s_i > 0$ for $1 \leq i \leq m - 1$ and $b_m > 0$.*

- (a) *It is primitive if either $b_1 > 0$ or $s_m > 0$.*
- (b) *If both $b_1 = s_m = 0$, then it is primitive if (and only if) the greatest common divisor of the set of indices for which $b_i > 0$ equals 1. For example, it is primitive if two consecutive classes are fertile (i.e., there exists an i such that b_i and b_{i+1} are both positive).*

Example 2.13. A Leslie model with $b_i = 0$ for all $i = 1, 2, \dots, m - 1$ can be used to describe a population whose juvenile stages pass through $m - 1$ stages before reaching maturity at age m . These stages could be, for example, egg, larval instars, and pupal stages in an insect. We see from Theorem 2.12 that such a Leslie matrix is primitive if and only if $s_m > 0$, in which case the population is iteroparous.

An example is the **linear LPA model** (LPA stands for larva-pupa-adult)

$$(2.22) \quad \mathbf{P} = \begin{bmatrix} 0 & 0 & b_3 \\ s_1 & 0 & 0 \\ 0 & s_2 & s_3 \end{bmatrix} \quad \text{with } b_3 > 0 \text{ and } 0 < s_1, s_2 \leq 1,$$

which is primitive if and only if $s_3 > 0$. Another example is the imprimitive Leslie model

$$(2.23) \quad \mathbf{P} = \begin{bmatrix} 0 & 0 & \cdots & 0 & b_m \\ s_1 & 0 & \cdots & 0 & 0 \\ 0 & s_2 & \cdots & 0 & 0 \\ \vdots & \vdots & & \vdots & \vdots \\ 0 & 0 & \cdots & s_{m-1} & 0 \end{bmatrix} \text{ with } b_m > 0 \text{ and } 0 < s_i \leq 1,$$

which is called a **semelparous Leslie model**. Nonlinear versions of these two models have played significant roles in the study of certain insects—flour beetles (various species of the genus *Tribolium*) and periodical cicadas (various species of the genus *Magicicada*), respectively—as we will see in Chapter 3. \square

2.3. The Reproduction Number R_0

If the projection matrix \mathbf{P} in the linear model (2.3) is primitive, then the inherent growth rate r_0 of the population is the strictly dominant eigenvalue (the Perron eigenvalue) of \mathbf{P} . By Theorem 2.7, the population will grow (exponentially without bound) or decay (to extinction) if $r_0 > 1$ or $r_0 < 1$, respectively. The eigenvalues of \mathbf{P} are the roots of its characteristic polynomial, which has degree m , and as a result, it can be difficult to calculate r_0 for large m . If \mathbf{P} is a numerical matrix, then computer programs are available for this purpose, but if \mathbf{P} contains entries that are not numerically specified, then an algebraic formula for r_0 in terms of the entries in \mathbf{P} is in general impossible to obtain for $m \geq 5$. Alternatively, there is another quantity that can be used to determine population growth or decay. This quantity is often analytically tractable, even for large values of m , and also has a biological meaning that is informative and amenable to calculation from data. We encountered the reproduction number R_0 in Chapter 1 for the case $m = 1$. In this section, we define and learn how to calculate R_0 for structured models of dimension $m > 1$.

2.3.1. The Definition and Calculation of R_0 . Consider an initial distribution $\mathbf{x}(0)$ that consists of only newborns. The distribution of survivors from an initial condition $\mathbf{x}(0)$ after one time step is $\mathbf{T}\mathbf{x}(0)$, after two time steps is $\mathbf{T}(\mathbf{T}\mathbf{x}(0)) = \mathbf{T}^2\mathbf{x}(0)$, and after i times steps is $\mathbf{T}^i\mathbf{x}(0)$.

The distribution of newborns that will be produced by the initial newborn distribution $\mathbf{0}_m \neq \mathbf{x}(0) \in R_+^m$ is $\mathbf{F}\mathbf{x}(0)$. After another time step, the initial distribution becomes $\mathbf{T}\mathbf{x}(0)$, which will produce the distribution $\mathbf{FT}\mathbf{x}(0)$ of newborns; after another time step, the initial distribution becomes $\mathbf{T}^2\mathbf{x}(0)$, which will produce the distribution $\mathbf{FT}^2\mathbf{x}(0)$ of newborns; and so on. Over the lifetime of the newborns in the initial distribution, the distribution of accumulated newborns for which they are responsible is

$$(2.24) \quad \mathbf{Fx}(0) + \mathbf{FTx}(0) + \mathbf{FT}^2\mathbf{x}(0) + \cdots = \mathbf{F} \left(\sum_{i=0}^{\infty} \mathbf{T}^i \right) \mathbf{x}(0)$$

provided the series

$$\mathbf{I}_m + \mathbf{T} + \mathbf{T}^2 + \cdots = \sum_{i=0}^{\infty} \mathbf{T}^i$$

converges. We assume the spectral radius of the nonnegative transition matrix \mathbf{T} satisfies $\rho(\mathbf{T}) < 1$. Since $\rho(\mathbf{T})$ is the dominant eigenvalue of \mathbf{T} (cf. Theorem 2.5(a)), this assumption implies 1 is not an eigenvalue of \mathbf{T} . Thus, $\mathbf{I}_m - \mathbf{T}$ is nonsingular and $(\mathbf{I}_m - \mathbf{T})^{-1}$ exists. In fact

$$(2.25) \quad (\mathbf{I}_m - \mathbf{T})^{-1} = \sum_{i=0}^{\infty} \mathbf{T}^i$$

(see Exercise 2.31), and as a result, the distribution of accumulated newborns (2.24) equals

$$\mathbf{Fx}(0) + \mathbf{FTx}(0) + \mathbf{FT}^2\mathbf{x}(0) + \cdots = \mathbf{F}(\mathbf{I}_m - \mathbf{T})^{-1} \mathbf{x}(0).$$

If we view this distribution of all newborns, obtained from the initial distribution of newborns $\mathbf{x}(0)$, as a new generation, then we see from this that the matrix $\mathbf{F}(\mathbf{I}_m - \mathbf{T})^{-1}$ maps a generation of newborns to the next generation of newborns. For this reason, $\mathbf{F}(\mathbf{I}_m - \mathbf{T})^{-1}$ is called the **next generation matrix**.

Definition 2.14. Assume that the fertility and transition matrices satisfy (2.2) and that $\rho(\mathbf{T}) < 1$. The **reproduction number** associated with the projection matrix $\mathbf{P} = \mathbf{F} + \mathbf{T}$ is the spectral radius of the next generation matrix:

$$R_0 := \rho(\mathbf{F}(\mathbf{I}_m - \mathbf{T})^{-1}).$$

We expect that repeated generations will grow or decay according to whether R_0 is greater than or less than 1. In Chapter 1, we observed that this is indeed true for the case $m = 1$ since r_0 and R_0 are on the same side of 1. In [39], this is proved for $m > 1$. The following theorem, found in [104], provides a slightly stronger version of this fact.

Theorem 2.15. *Assume $\rho(\mathbf{T}) < 1$ for a nonnegative matrix model $\mathbf{P} = \mathbf{F} + \mathbf{T}$ satisfying (2.2). Then one of the following holds:*

$$1 < r_0 \leq R_0, \quad 0 \leq R_0 \leq r_0 < 1, \quad \text{or} \quad r_0 = R_0 = 1.$$

If in addition \mathbf{P} is irreducible, then $R_0 > 0$.

Example 2.16. For the juvenile-adult model in Example 2.11, we have that

$$\mathbf{F} = \begin{bmatrix} 0 & b_2 \\ 0 & 0 \end{bmatrix} \quad \text{and} \quad \mathbf{T} = \begin{bmatrix} 0 & 0 \\ s_1 & s_2 \end{bmatrix}$$

with $b_2 > 0$, $0 < s_1 \leq 1$, and $0 \leq s_2 < 1$

and that the projection matrix $\mathbf{P} = \mathbf{F} + \mathbf{T}$ is primitive. The next generation matrix is

$$\begin{aligned} \mathbf{F}(\mathbf{I}_m - \mathbf{T})^{-1} &= \begin{bmatrix} 0 & b_2 \\ 0 & 0 \end{bmatrix} \left(\begin{bmatrix} 1 & 0 \\ 0 & 1 \end{bmatrix} - \begin{bmatrix} 0 & 0 \\ s_1 & s_2 \end{bmatrix} \right)^{-1} \\ &= \begin{bmatrix} 0 & b_2 \\ 0 & 0 \end{bmatrix} \begin{bmatrix} 1 & 0 \\ s_1 \frac{1}{1-s_2} & \frac{1}{1-s_2} \end{bmatrix} \\ &= \begin{bmatrix} b_2 s_1 \frac{1}{1-s_2} & b_2 \frac{1}{1-s_2} \\ 0 & 0 \end{bmatrix}. \end{aligned}$$

The eigenvalues of this matrix are 0 and

$$(2.26) \quad R_0 = b_2 s_1 \frac{1}{1 - s_2}.$$

By Theorem 2.15, the population grows without bound (i.e., $r_0 > 1$) if $R_0 > 1$ and decays to the origin (i.e., $r_0 < 1$) if $R_0 < 1$.

In this particular example, these conclusions can also be established directly from the formula for r_0 (2.21) in Example 2.11. \square

Notice in Example 2.11 that the 2×2 fertility matrix has a row of zeros and, as a result, so does the next generation matrix $\mathbf{F}(\mathbf{I}_m - \mathbf{T})^{-1}$. In fact, this is true for fertility and next generation matrices of any dimension $m \geq 2$. That is to say, *if all newborns belong to one and only one*

class, which without loss in generality we can label as the first class, then all but the first row in \mathbf{F} consist entirely of zeros. It follows that this is also true of the next generation matrix $\mathbf{F}(\mathbf{I}_m - \mathbf{T})^{-1}$, which means that 0 is an $m - 1$ times repeated eigenvalue and that the remaining eigenvalue R_0 appears in the upper-left corner of $\mathbf{F}(\mathbf{I}_m - \mathbf{T})^{-1}$. A result of this observation is that R_0 equals the inner product of the first row

$$\mathbf{f}_1^T = [f_{11} \quad f_{12} \quad \cdots \quad f_{1m}]$$

of \mathbf{F} with the first column of $(\mathbf{I}_m - \mathbf{T})^{-1}$, which we denote by \mathbf{n}_1 . Then
(2.27)
$$R_0 = \mathbf{f}_1^T \mathbf{n}_1,$$

and the main task involved in calculating R_0 is to obtain the first column \mathbf{n}_1 of $(\mathbf{I}_m - \mathbf{T})^{-1}$.

For example, when $m = 2$, the first row of

$$\mathbf{F} = \begin{bmatrix} f_{11} & f_{12} \\ 0 & 0 \end{bmatrix}$$

is

$$\mathbf{f}_1^T = [f_{11} \quad f_{12}],$$

and the first column of

$$(\mathbf{I}_m - \mathbf{T})^{-1} = \begin{bmatrix} 1 - \tau_{11} & -\tau_{12} \\ -\tau_{21} & 1 - \tau_{22} \end{bmatrix}^{-1}$$

is

$$\mathbf{n}_1 = \begin{bmatrix} \frac{1 - \tau_{22}}{(1 - \tau_{11})(1 - \tau_{22}) - \tau_{21}\tau_{12}} \\ \frac{\tau_{21}}{(1 - \tau_{11})(1 - \tau_{22}) - \tau_{21}\tau_{12}} \end{bmatrix}.$$

Thus, for an $m = 2$ dimensional matrix model with a single newborn class, the reproduction number is

$$\begin{aligned} R_0 &= \mathbf{f}_1^T \mathbf{n}_1 \\ &= f_{11} \frac{1 - \tau_{22}}{(1 - \tau_{11})(1 - \tau_{22}) - \tau_{21}\tau_{12}} + f_{12} \frac{\tau_{21}}{(1 - \tau_{11})(1 - \tau_{22}) - \tau_{21}\tau_{12}}. \end{aligned}$$

Here is an m -dimensional example.

Example 2.17. The first row of the fertility matrix F in the extended m -dimensional Leslie model (2.8) is

$$\mathbf{f}_1^T = [b_1 \quad b_2 \quad \cdots \quad b_{m-1} \quad b_m].$$

We leave it as Exercise 2.32 to show that the first column in $(\mathbf{I}_m - \mathbf{T})^{-1}$ is

$$(2.28) \quad \mathbf{n}_1 = \begin{bmatrix} 1 \\ s_1 \\ s_1 s_2 \\ \vdots \\ s_1 s_2 \cdots s_{i-1} \\ \vdots \\ s_1 s_2 \cdots s_{m-2} \\ s_1 s_2 \cdots s_{m-1} \frac{1}{1-s_m} \end{bmatrix}.$$

From formula (2.27), we obtain the net reproduction number

$$(2.29) \quad R_0 = \sum_{i=1}^{m-1} b_i \pi_i + b_m \pi_m \frac{1}{1-s_m},$$

where we have invented, for notational convenience, the notation

$$(2.30) \quad \pi_i = \begin{cases} 1 & \text{for } i = 1 \\ s_1 s_2 \cdots s_{i-1} & \text{for } i = 2, 3, \dots, m \end{cases}$$

for the probability that a newborn attains the i th age class. As in Example 2.11, the term $(1 - s_m)^{-1}$ is the expected amount of time spent in the m th class. \square

Example 2.18. Consider a population that is structured by a juvenile class x_1 and two different adult classes x_2 and x_3 with the life cycle graph in Figure 2.3. A juvenile matures into an adult of class $i = 2$ with probability $s_{21} \leq 1$ and into an adult of class $i = 3$ with probability $s_{31} \leq 1$. Adults of class $i = 2$ are semelparous and do not survive a unit of time for a second reproductive episode. Adults of class $i = 3$ are iteroparous and have post-reproductive survival probability s_{33} , where $0 < s_{33} < 1$. If the unit of time is the juvenile time to maturation, the fertility and transition matrices are

$$\mathbf{F} = \begin{bmatrix} 0 & f_{12} & f_{13} \\ 0 & 0 & 0 \\ 0 & 0 & 0 \end{bmatrix} \text{ and } \mathbf{T} = \begin{bmatrix} 0 & 0 & 0 \\ \tau_{21} & 0 & 0 \\ \tau_{31} & 0 & \tau_{33} \end{bmatrix},$$

where $f_{1i} > 0$ is the per capita number of newborns per i -class adult. The projection matrix

$$\mathbf{P} = \begin{bmatrix} 0 & f_{12} & f_{13} \\ \tau_{21} & 0 & 0 \\ \tau_{31} & 0 & \tau_{33} \end{bmatrix}$$

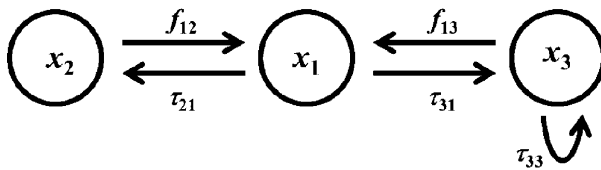


Figure 2.3. A structured population with 1 juvenile and 2 adult classes, one of which is semelparous and the other of which is iteroparous.

is irreducible, as can be seen by an inspection of the life cycle graph or by Theorem 2.8(a) from the positivity of the matrix

$$\begin{aligned}
 (\mathbf{I}_m + \mathbf{P})^{m-1} &= \left[\begin{array}{ccc} 1 & f_{12} & f_{13} \\ \tau_{21} & 1 & 0 \\ \tau_{31} & 0 & 1 + \tau_{33} \end{array} \right]^2 \\
 &= \left[\begin{array}{ccc} \tau_{21}f_{12} + \tau_{31}f_{13} + 1 & 2f_{12} & 2f_{13} + \tau_{33}f_{13} \\ 2\tau_{21} & \tau_{21}f_{12} + 1 & \tau_{21}f_{13} \\ 2\tau_{31} + \tau_{31}\tau_{33} & \tau_{31}f_{12} & \tau_{33}^2 + 2\tau_{33} + \tau_{31}f_{13} + 1 \end{array} \right].
 \end{aligned}$$

\mathbf{P} is also primitive since it has a positive diagonal entry (part (i) in Theorem 2.8(c)).

To calculate R_0 , we note that there is only one newborn class (only the first row of \mathbf{F} is a nonzero row), and we can therefore take advantage of the formula (2.27) with

$$\mathbf{f}_1^T = [\ 0 \quad f_{12} \quad f_{13} \].$$

The first column of $(\mathbf{I}_m - \mathbf{T})^{-1}$ is

$$\mathbf{n}_1 = \left[\begin{array}{c} 1 \\ \tau_{21} \\ \tau_{31} \frac{1}{1-\tau_{33}} \end{array} \right],$$

and therefore by (2.27), we have

$$R_0 = \mathbf{f}_1 \mathbf{n}_1 = f_{12}\tau_{21} + f_{13}\tau_{31} \frac{1}{1-\tau_{33}}.$$

This formula shows R_0 is the lifetime *expected number of newborns produced per newborn, summing newborns expected to be produced by adults of classes $i = 2$ and 3* . By Theorem 2.15 (note that $\rho(\mathbf{T}) = s_{33} < 1$),

the population decays to extinction if $R_0 < 1$ and grows exponentially if $R_0 > 1$. \square

In the previous examples, there is only one newborn class, which considerably simplifies the calculation of R_0 . In general, the analytic tractability of calculating R_0 is related to the number of newborn classes. In principle, a model could contain any number of newborn classes, although in most population models there is only a small number k of newborn classes. Mathematically, this means $m - k$ rows of zeros (i.e., all entries equal 0) in the fertility matrix \mathbf{F} . If, without any loss in modeling or mathematical generality, we assume all newborn classes are listed first in the vector \mathbf{x} , then the fertility matrix has the form

$$(2.31) \quad \mathbf{F} = \begin{bmatrix} f_{11} & f_{12} & \cdots & f_{1m} \\ \vdots & \vdots & & \vdots \\ f_{k1} & f_{k2} & \cdots & f_{km} \\ 0 & 0 & & 0 \\ \vdots & \vdots & & \vdots \\ 0 & 0 & \cdots & 0 \end{bmatrix}.$$

It follows that the next generation matrix also has $m - k$ zero rows (i.e., has this block matrix form):

$$(2.32) \quad \mathbf{F}(\mathbf{I}_m - \mathbf{T})^{-1} = \begin{bmatrix} \mathbf{N} & * \\ \mathbf{0}_{(m-k) \times k} & \mathbf{0}_{(m-k) \times (m-k)} \end{bmatrix},$$

where \mathbf{N} is a $k \times k$ nonnegative matrix, $\mathbf{0}_{i \times j}$ is the $i \times j$ matrix of zeros, and the asterisk denotes an unneeded submatrix block. The eigenvalues of the next generation matrix are those of the diagonal blocks (Exercise 2.26) and hence consist of 0 (with multiplicity $m - k$) and the eigenvalues of \mathbf{N} . Thus, R_0 is the dominant eigenvalue of the matrix \mathbf{N} , which if k is smaller than m , is what makes the calculation of R_0 potentially more tractable than the calculation of r_0 .

The next example involves a model with more than one newborn class, namely $k = 2$.

Example 2.19. Consider a population that is structured into two juvenile classes x_1 and x_2 and a class x_3 of adults with the life cycle graph in Figure 2.4. Using the maturation period as the unit of time and assuming adults produce both types of juveniles (with fertility rates $f_{12}, f_{13} > 0$) and are iteroparous with post-reproduction survival rate τ_{33} , $0 < \tau_{33} < 1$,

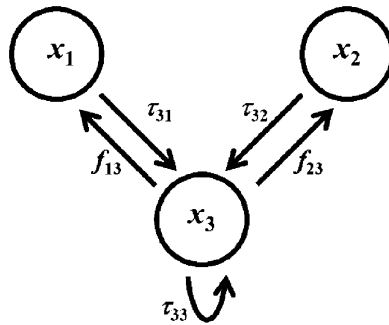


Figure 2.4. A structured population with 2 juvenile classes and 1 class of iteroparous adults who produce both types of juvenile offspring.

we have the fertility and transition matrices

$$\mathbf{F} = \begin{bmatrix} 0 & 0 & f_{13} \\ 0 & 0 & f_{23} \\ 0 & 0 & 0 \end{bmatrix} \text{ and } \mathbf{T} = \begin{bmatrix} 0 & 0 & 0 \\ 0 & 0 & 0 \\ \tau_{31} & \tau_{32} & \tau_{33} \end{bmatrix},$$

where τ_{31} and τ_{32} are the juvenile survival rates. The projection matrix

$$\mathbf{P} = \begin{bmatrix} 0 & 0 & f_{13} \\ 0 & 0 & f_{23} \\ \tau_{31} & \tau_{32} & \tau_{33} \end{bmatrix}$$

is irreducible, as can be seen by an inspection of the life cycle graph or by Theorem 2.8(a) from the positivity of the matrix

$$\begin{aligned} (\mathbf{I}_m + \mathbf{P})^{m-1} &= \begin{bmatrix} 1 & 0 & f_{13} \\ 0 & 1 & f_{23} \\ \tau_{31} & \tau_{32} & 1 + \tau_{33} \end{bmatrix}^2 \\ &= \begin{bmatrix} 1 + f_{13}\tau_{31} & f_{13}\tau_{32} & f_{13}(1 + \tau_{33}) \\ f_{23}\tau_{31} & 1 + f_{23}\tau_{32} & f_{23}(1 + \tau_{33}) \\ \tau_{31}(1 + \tau_{33}) & \tau_{32}(1 + \tau_{33}) & \tau_{33}^2 + f_{13}\tau_{31} + f_{23}\tau_{32} \end{bmatrix}. \end{aligned}$$

\mathbf{P} is also primitive since it has a positive diagonal entry τ_{33} (part (i) in Theorem 2.8(c)). The next generation matrix

$$\begin{aligned}\mathbf{F}(\mathbf{I}_m - \mathbf{T})^{-1} &= \left[\begin{array}{ccc} 0 & 0 & f_{13} \\ 0 & 0 & f_{23} \\ 0 & 0 & 0 \end{array} \right] \left(\left[\begin{array}{ccc} 1 & 0 & 0 \\ 0 & 1 & 0 \\ 0 & 0 & 1 \end{array} \right] - \left[\begin{array}{ccc} 0 & 0 & 0 \\ 0 & 0 & 0 \\ \tau_{31} & \tau_{32} & \tau_{33} \end{array} \right] \right)^{-1} \\ &= \left[\begin{array}{ccc} f_{13}\tau_{31} \frac{1}{1-\tau_{33}} & f_{13}\tau_{32} \frac{1}{1-\tau_{33}} & f_{13} \frac{1}{1-\tau_{33}} \\ f_{23}\tau_{31} \frac{1}{1-\tau_{33}} & f_{23}\tau_{32} \frac{1}{1-\tau_{33}} & f_{23} \frac{1}{1-\tau_{33}} \\ 0 & 0 & 0 \end{array} \right].\end{aligned}$$

This matrix is block diagonal, and its eigenvalues are 0 and those of the submatrix block

$$\mathbf{N} = \left[\begin{array}{cc} f_{13}\tau_{31} \frac{1}{1-\tau_{33}} & f_{13}\tau_{32} \frac{1}{1-\tau_{33}} \\ f_{23}\tau_{31} \frac{1}{1-\tau_{33}} & f_{23}\tau_{32} \frac{1}{1-\tau_{33}} \end{array} \right]$$

(cf. Exercise 2.26). The eigenvalues of \mathbf{N} are 0 and

$$R_0 = f_{13}\tau_{31} \frac{1}{1-\tau_{33}} + f_{23}\tau_{32} \frac{1}{1-\tau_{33}}.$$

By Theorem 2.15 (note that $\rho(\mathbf{T}) = \tau_{33} < 1$), the population decays to extinction if $R_0 < 1$ and grows exponentially if $R_0 > 1$. \square

2.3.2. Interpretation of R_0 . In Chapter 1, we saw in the $m = 1$ dimensional case that R_0 is the number of newborns produced per newborn per life time. In this section, we consider the meaning of R_0 for models of dimension $m > 1$ in which there are $k \leq m$ newborn classes. We assume without loss of generality that the k newborn classes are listed first in the vector \mathbf{x} . This means fertility matrix \mathbf{F} has the form (2.31), and the next generation matrix has the form (2.32). Consider an initial generation consisting only of newborns

$$(2.33) \quad \mathbf{x}(0) = \begin{bmatrix} \mathbf{n}(0) \\ \mathbf{0}_{m-k} \end{bmatrix},$$

where $\mathbf{0}_k \neq \mathbf{n}(0) \in R_+^k$. From

$$\begin{aligned}\mathbf{F}(\mathbf{I}_m - \mathbf{T})^{-1} \mathbf{x}(0) &= \begin{bmatrix} \mathbf{N} & * \\ \mathbf{0}_{(m-k) \times k} & \mathbf{0}_{(m-k) \times (m-k)} \end{bmatrix} \begin{bmatrix} \mathbf{n}(0) \\ \mathbf{0}_{m-k} \end{bmatrix} \\ &= \begin{bmatrix} \mathbf{N}\mathbf{n}(0) \\ \mathbf{0}_{m-k} \end{bmatrix},\end{aligned}$$

we see that the next generation of newborns is $\mathbf{n}(0) = \mathbf{N}\mathbf{x}_k(0)$. This generation gives the next generation

$$\mathbf{F}(\mathbf{I}_m - \mathbf{T})^{-1} \begin{bmatrix} \mathbf{N}\mathbf{n}(0) \\ \mathbf{0}_{m-k} \end{bmatrix} = \begin{bmatrix} \mathbf{N}^2\mathbf{n}(0) \\ \mathbf{0}_{m-k} \end{bmatrix}.$$

The resulting sequence of generations

$$\begin{bmatrix} \mathbf{N}^i\mathbf{n}(0) \\ \mathbf{0}_{m-k} \end{bmatrix}, \quad i = 1, 2, 3, \dots$$

produces the sequence of generational newborn classes $\mathbf{n}(i) = \mathbf{N}^i\mathbf{n}(0)$. Since R_0 is the dominant eigenvalue of \mathbf{N} , we have that

$$\lim_{t \rightarrow \infty} \frac{\mathbf{n}(i)}{R_0^i} = \mathbf{w}^T \mathbf{n}(0) \mathbf{v}$$

(Theorem 2.7), where \mathbf{w} and \mathbf{v} are left and right (positive) eigenvectors of \mathbf{N} associated with R_0 . For large i , $\mathbf{n}(i) \approx \mathbf{w}^T \mathbf{x}(0) \mathbf{v} R_0^i$ and

$$\frac{\|\mathbf{n}(i+1)\|}{\|\mathbf{n}(i)\|} \approx R_0,$$

that is to say the total number of next generation newborns divided by the total number of previous generation newborns is asymptotically equal to R_0 . This gives us the interpretation of the reproduction number R_0 as the *average number of newborns produced per newborn per generation*.

Theorem 2.15 tells us that a population goes extinct if $R_0 < 1$ and survives if $R_0 > 1$. This interpretation of R_0 makes sense in that newborns (or newborn generations) do not replace themselves when $R_0 < 1$ but do more than replace themselves when $R_0 > 1$.

2.4. Sensitivity and Elasticity Analysis

A structured population whose dynamics are described by the linear matrix equation

$$\mathbf{x}(t+1) = \mathbf{P}\mathbf{x}(t)$$

with a nonnegative, irreducible projection matrix \mathbf{P} is predicted to go extinct if the dominant eigenvalue r_0 of \mathbf{P} is less than 1. To avoid extinction, at least one entry in the projection matrix would have to change so as to make r_0 greater than 1. This raises the question of which entry in $\mathbf{P} = [p_{ij}]$ is the most effective in changing r_0 . If we consider r_0 to be a function of a specific entry p_{ij} , one way to address this question is to

consider the derivative of r_0 with respect to p_{ij} , which we define to be the **sensitivity** of r_0 with respect to p_{ij} , that is

$$s_{ij} := \frac{dr_0}{dp_{ij}},$$

and then to compare these derivatives for all entries p_{ij} .

Let \mathbf{w}^T and \mathbf{v} denote left and right, positive eigenvectors associated with r_0 :

$$\mathbf{P}\mathbf{v} = r_0\mathbf{v} \quad \text{and} \quad \mathbf{w}^T\mathbf{P} = r_0\mathbf{w}^T.$$

We focus on a specific entry p_{ij} in the projection matrix and consider r_0 and its associated eigenvectors to be functions of p_{ij} by writing $r_0 = r_0(p_{ij})$, $\mathbf{w}^T = \mathbf{w}^T(p_{ij})$ and $\mathbf{v} = \mathbf{v}(p_{ij})$. Then we have

$$(2.34) \quad \mathbf{P}(p_{ij})\mathbf{v}(p_{ij}) = r_0(p_{ij})\mathbf{v}(p_{ij})$$

and

$$\mathbf{w}^T(p_{ij})\mathbf{P}(p_{ij}) = r_0(p_{ij})\mathbf{w}^T(p_{ij}).$$

A differentiation of (2.34) with respect to p_{ij} yields

$$\frac{d\mathbf{P}}{dp_{ij}}\mathbf{v} + \mathbf{P}\frac{d\mathbf{v}}{dp_{ij}} = \frac{dr_0}{dp_{ij}}\mathbf{v} + r_0\frac{d\mathbf{v}}{dp_{ij}}$$

or

$$(\mathbf{P} - r_0\mathbf{I}_m)\frac{d\mathbf{v}}{dp_{ij}} = \left(s_{ij}\mathbf{I}_m - \frac{d\mathbf{P}}{dp_{ij}}\right)\mathbf{v}$$

(where, for notational convenience, the symbols “ (p_{ij}) ” have been dropped). This equation tells us that $\mathbf{z} = d\mathbf{v}/dp_{ij}$ satisfies the algebraic equation

$$(2.35) \quad (\mathbf{P} - r_0\mathbf{I}_m)\mathbf{z} = \left(s_{ij}\mathbf{I}_m - \frac{d\mathbf{P}}{dp_{ij}}\right)\mathbf{v}.$$

Since r_0 is geometrically simple (cf. Theorem 2.5), the null space of $\mathbf{P} - r_0\mathbf{I}_m$ is spanned by \mathbf{v} , and the null space of the transpose of $\mathbf{P} - r_0\mathbf{I}_m$ is spanned by \mathbf{w}^T . From linear algebra, it follows that equation (2.35) has a solution only if the right side is orthogonal to \mathbf{w}^T :

$$\mathbf{w}^T\left(s_{ij}\mathbf{I}_m - \frac{d\mathbf{P}}{dp_{ij}}\right)\mathbf{v} = 0,$$

which gives us the formula

$$s_{ij} = \frac{1}{\mathbf{w}^T\mathbf{v}}\mathbf{w}^T\frac{d\mathbf{P}}{dp_{ij}}\mathbf{v}.$$

This formula for the sensitivity can be simplified by noting that the matrix $d\mathbf{P}/dp_{ij}$ consists entirely of zeros except in the ij th entry where there appears a 1. As a result

$$\mathbf{w}^T \frac{d\mathbf{P}}{dp_{ij}} \mathbf{v} = w_i v_j;$$

hence,

$$s_{ij} = \frac{w_i v_j}{\mathbf{w}^T \mathbf{v}}.$$

Placing all sensitivities into a matrix, we get the **sensitivity matrix**

$$\mathbf{S} := [s_{ij}] = \frac{1}{\mathbf{w}^T \mathbf{v}} [w_i v_j].$$

Since $[w_i v_j] = \mathbf{w} \mathbf{v}^T$, we obtain the following theorem.

Theorem 2.20. Assume $\mathbf{P} = [p_{ij}]$ is nonnegative and irreducible and that \mathbf{w}^T and \mathbf{v} are positive left and right eigenvectors associated with its dominant eigenvalue r_0 . Then the **sensitivity**

$$s_{ij} = \frac{dr_0}{dp_{ij}}$$

of r_0 with respect to an entry p_{ij} in the projection matrix is equal to

$$(2.36) \quad s_{ij} = \frac{w_i v_j}{\mathbf{w}^T \mathbf{v}},$$

and the **sensitivity matrix** $\mathbf{S} = [s_{ij}]$ can be written

$$(2.37) \quad \mathbf{S} = \frac{1}{\mathbf{w}^T \mathbf{v}} \mathbf{w} \mathbf{v}^T.$$

Remark 2.21. Note that S is a positive matrix, and therefore r_0 increases with an increase in any entry p_{ij} .

The sensitivity of r_0 with respect to p_{ij} gives an approximation to the new value of r_0 , namely $r_0(p_{ij} + \Delta p_{ij})$, when p_{ij} is additively perturbed to $p_{ij} + \Delta p_{ij}$. Specifically, from the definition of a derivative

$$\frac{r_0(p_{ij} + \Delta p_{ij}) - r_0(p_{ij})}{\Delta p_{ij}} \approx \frac{dr_0(p_{ij})}{dp_{ij}},$$

we obtain

$$(2.38) \quad r_0(p_{ij} + \Delta p_{ij}) \approx r_0(p_{ij}) + \frac{dr_0(p_{ij})}{dp_{ij}} \Delta p_{ij}.$$

Thus, sensitivities provided additive perturbation approximations to the population growth rate r_0 caused by small additive perturbations in projection matrix entries.

Example 2.22. Consider the juvenile-adult model in Example 2.11 with fertility and survival values given in the projection matrix

$$(2.39) \quad \mathbf{P} = \begin{bmatrix} 0 & 0.7 \\ 0.5 & 0.6 \end{bmatrix}.$$

The dominant eigenvalue is (rounded to 3 significant digits)

$$r_0 \approx 0.963 < 1,$$

and as a result, the population is predicted to go extinct. Associated positive left and right eigenvectors are (rounded to 3 significant digits)

$$\mathbf{w} \approx \begin{bmatrix} 0.342 & 0.658 \end{bmatrix} \quad \text{and} \quad \mathbf{v} \approx \begin{bmatrix} 0.421 \\ 0.579 \end{bmatrix}.$$

Using formula (2.37)

$$\mathbf{w}^T \mathbf{v} \approx \begin{bmatrix} 0.342 & 0.658 \end{bmatrix} \begin{bmatrix} 0.421 \\ 0.579 \end{bmatrix} \approx 0.525,$$

we obtain the sensitivity matrix (rounded to 3 significant digits)

$$\mathbf{S} \approx \frac{1}{0.525} \begin{bmatrix} 0.342 \\ 0.658 \end{bmatrix} \begin{bmatrix} 0.421 & 0.579 \end{bmatrix} \approx \begin{bmatrix} 0.274 & 0.377 \\ 0.528 & 0.726 \end{bmatrix}.$$

For example, recalling from Example 2.11 that s_1 and s_2 are the survival rates (or survival probabilities) of a juvenile and an adult, respectively, we see from the last row in the sensitivity matrix \mathbf{S} that $dr_0/ds_1 \approx 0.528$ is less than $dr_0/ds_2 \approx 0.727$. We conclude that while a small additive increase in either juvenile or adult survival will increase r_0 (both sensitivities are positive), a small additive increase to adult survival s_2 gives a greater additive increase to r_0 than does the same additive increase in juvenile survival s_1 .

For example, suppose juvenile survival $s_1 = 0.5$ is additively increased by the increment $\Delta s_1 = 0.2$. From (2.38), the additive effect on r_0 is

$$r_0(0.5 + 0.2) \approx 0.963 + 0.528(0.2) \approx 1.07.$$

If adult survival $s_2 = 0.6$ is additively increased by the same increment $\Delta s_2 = 0.2$, then the additive effect on r_0 is

$$r_0(0.6 + 0.2) \approx 0.963 + 0.726(0.2) \approx 1.11.$$

Notice that the formula provides a sensitivity of 0.274 for the p_{11} entry in \mathbf{P} , even though the model is designed so that this entry equals 0 (since the time unit is chosen to be the maturation period). If, for some reason, a change in the model (say in the maturation period) were to occur, this sensitivity would reflect the effect on r_0 of that entry. Otherwise, the entry is not relevant. \square

In Example 2.22, additively increasing adult fertility $f_1 = 0.7$ by the increment $\Delta f = 0.2$ has the effect of (additively) increasing r_0 to

$$r_0(0.7 + 0.2) \approx 0.963 + 0.377(0.2) \approx 1.04.$$

Adding the same perturbation increment 0.2 to the survival probabilities in Example 2.22 allows a ready comparison between which perturbation has the greater or lesser effect on r_0 . Adding the same numerical increment 0.2 to the fertility rate doesn't lend itself to direct comparison, since fertility and survival rates are different phenomena expressed in different units. Another way to compare perturbations of survival and fertility probabilities is to consider proportional (percentage) changes and ask what proportional (percentage) changes they cause in r_0 .

If p_{ij} is changed by an amount Δp_{ij} , then its percent change is $(\Delta p_{ij}/p_{ij}) \times 100$. If this causes a change Δr_0 in r_0 , then the percent change in r_0 is $(\Delta r_0/r_0) \times 100$. We can compare these two percent changes by calculating their ratio

$$\frac{(\Delta r_0/r_0) \times 100}{(\Delta p_{ij}/p_{ij}) \times 100} = \frac{p_{ij}}{r_0} \frac{\Delta r_0}{\Delta p_{ij}}.$$

For small changes in p_{ij} , this is approximately equal to

$$(2.40) \quad e_{ij} := \frac{p_{ij}}{r_0} \frac{dr_0}{dp_{ij}},$$

which is called the **elasticity** of r_0 to changes in p_{ij} . (It is sometimes called the **sensitivity index** of p_{ij} .) Notice that the second factor in the elasticity (2.40) with respect to p_{ij} is the sensitivity (2.36) with respect to p_{ij} . We gather elasticities with respect to all entries p_{ij} into the **elasticity matrix**

$$\mathbf{E} = \frac{1}{r_0} [p_{ij}s_{ij}],$$

which we can rewrite as the Hadamard product of the projection matrix \mathbf{P} and the sensitivity matrix \mathbf{S} :

$$(2.41) \quad \mathbf{E} = \frac{1}{r_0} \mathbf{P} \odot \mathbf{S}.$$

Example 2.23. For the juvenile-adult model with projection matrix

$$\mathbf{P} = \begin{bmatrix} 0 & 0.7 \\ 0.5 & 0.6 \end{bmatrix},$$

we have from the calculations in Example 2.22 and formula (2.41) the elasticity matrix

$$\begin{aligned} \mathbf{E} &\approx \frac{1}{0.963} \begin{bmatrix} 0 & 0.7 \\ 0.5 & 0.6 \end{bmatrix} \odot \begin{bmatrix} 0.274 & 0.377 \\ 0.528 & 0.726 \end{bmatrix} \\ &= \frac{1}{0.963} \begin{bmatrix} 0(0.274) & 0.7(0.377) \\ 0.5(0.528) & 0.6(0.726) \end{bmatrix} \\ &\approx \begin{bmatrix} 0 & 0.274 \\ 0.274 & 0.452 \end{bmatrix}. \end{aligned}$$

The elasticities of r_0 with respect to f and s_1 are equal (see Exercise 2.37). A $p\%$ change in either f or s_1 results in a $0.274 \times p\%$ change in r_0 . The elasticity with respect to s_2 , however, is larger: a $p\%$ change in s_2 results in a $0.452 \times p\%$ change in r_0 . \square

2.5. Applications

In this section are three applications of linear matrix models. The LPA model is an $m = 3$ dimensional extended Leslie model applied to a beetle population (a nonlinear version of which will appear in Chapter 3). An $m = 5$ dimensional matrix model based on the life cycle stages of the American bullfrog and an $m = 8$ dimensional model for a tropical shrub based on stem diameter complete the section. The reproduction number R_0 is calculated and some sensitivity analysis is performed for each application.

2.5.1. The LPA Model. The $m = 3$ dimensional LPA model with projection matrix

$$\mathbf{P} = \begin{bmatrix} 0 & 0 & b_3 \\ s_1 & 0 & 0 \\ 0 & s_2 & s_3 \end{bmatrix} \text{ with } b_3 > 0 \text{ and } 0 < s_1, s_2 \leq 1,$$

introduced in Example 2.13 has been extensively used to study the population dynamics of flour beetles (species from the genus *Tribolium*), which is a serious agricultural pest. In this model, the population is structured by three life cycle stages

$$\mathbf{x} = \begin{bmatrix} x_1 \\ x_2 \\ x_3 \end{bmatrix} = \begin{bmatrix} \text{Larvae} \\ \text{Pupae} \\ \text{Adults} \end{bmatrix},$$

and the time unit is two weeks. Parameter estimates from controlled laboratory experiments of *Tribolium castaneum* [41], [52] give the fertility and transition matrices

$$\mathbf{F} = \begin{bmatrix} 0 & 0 & 10.67 \\ 0 & 0 & 0 \\ 0 & 0 & 0 \end{bmatrix} \text{ and } \mathbf{T} = \begin{bmatrix} 0 & 0 & 0 \\ 0.8045 & 0 & 0 \\ 0 & 1 & 0.9924 \end{bmatrix}.$$

The dominant eigenvalue of $\mathbf{P} = \mathbf{F} + \mathbf{T}$ (rounded to 4 significant digits) is

$$r_0 \approx 2.437,$$

which, being larger than 1, predicts population growth. The stable stage distribution is given by the associated positive eigenvector (normalized so that $\|\mathbf{v}\| = 1$)

$$\mathbf{v} \approx \begin{bmatrix} 0.6418 \\ 0.2118 \\ 0.1463 \end{bmatrix}.$$

(All calculations in this example are rounded to 4 significant digits since the original data in \mathbf{F} and \mathbf{T} are recorded to 4 significant digits.) Thus, in the long run, the growing population is predicted to consist of 64.15% larvae, 21.18% pupae, and 14.66% adults.

We can calculate the reproduction number (the expected number of larvae produced per individual per lifetime) from formula (2.29) to be

$$R_0 = (1.067 \times 10)(0.8045)(1) \frac{1}{1 - 0.9924} \approx 1129$$

or from its definition as the dominant eigenvalue of $\mathbf{F}(\mathbf{I}_m - \mathbf{T})^{-1}$, which equals

$$\begin{aligned} & \left[\begin{array}{ccc} 0 & 0 & 10.67 \\ 0 & 0 & 0 \\ 0 & 0 & 0 \end{array} \right] \left[\begin{array}{ccc} 1 & 0 & 0 \\ -0.8045 & 1 & 0 \\ 0 & -1 & 1 - 0.9924 \end{array} \right]^{-1} \\ & \approx \left[\begin{array}{ccc} 1129. & 1404. & 1404. \\ 0 & 0 & 0 \\ 0 & 0 & 0 \end{array} \right]. \end{aligned}$$

A left eigenvector of $\mathbf{P} = \mathbf{F} + \mathbf{T}$ is

$$\mathbf{w} \approx \begin{bmatrix} 0.08754 \\ 0.2653 \\ 0.6471 \end{bmatrix},$$

from which, using \mathbf{v} and formulas (2.37) and (2.41), we can calculate the sensitivity and elasticity matrices

$$\begin{aligned} \mathbf{S} &= \begin{bmatrix} 0.2714 & 0.08957 & 0.06187 \\ 0.8226 & 0.2715 & 0.1875 \\ 2.006 & 0.6621 & 0.4573 \end{bmatrix} \quad \text{and} \\ \mathbf{E} &\approx \begin{bmatrix} 0 & 0 & 0.2709 \\ 0.2716 & 0 & 0 \\ 0 & 0.2717 & 0.1862 \end{bmatrix}. \end{aligned}$$

As an example, consider the sensitivities $s_{21} = 0.8226$ and $s_{32} = 0.6621$ of the larval and pupal survival rates $s_1 = 0.8045$ and $s_2 = 1$, respectively. A decrease in the larval rate by, say, 0.1 to $s_2 = 0.7045$ will result in a larger decrease in r_0 than the same decrease of the pupal rate to $s_2 = 0.9$. Specifically, the decrease in s_1 will result in

$$r_0 \approx 2.437 - 0.8226 \times 0.1 \approx 2.355,$$

whereas the decrease in s_2 will result in

$$r_0 \approx 2.437 - 0.6621 \times 0.1 \approx 2.371.$$

Both of these decreases are greater than a 0.1 decrease in the adult survival rate $s_3 = 0.9924$ to 0.8924 (whose smaller sensitivity is 0.4573), which gives

$$r_0 \approx 2.437 - 0.4573 \times 0.1 \approx 2.391.$$

To compare the effects on r_0 of changes in adult fertility $b_3 = 10.67$ with changes in survival rates, we consider proportional perturbations and the elasticities in **E**. Notice that the elasticities of adult fertility and the larval and pupal survival rates are quite similar and, consequently, proportional changes in these vital rates will result in similar proportional changes in r_0 . A smaller proportional effect will occur, however, with the same proportional perturbation in the adult survival rate since its elasticity is smaller. For example, if adult fertility is decreased by 10%, then r_0 will decrease by approximately $0.2709 \times 10\% \approx 2.709\%$ to

$$r_0 \approx 2.437 - 0.02709 \times 2.437 \approx 2.371.$$

A decrease in adult survival by 10% will result in a decrease of approximately $0.1862 \times 10\% = 1.862\%$ to

$$2.437 - 0.01862 \times 2.437 \approx 2.392.$$

Suppose we wish to eliminate the population (as a pest) by, for example, decreasing the larval survival rate s_1 so that $r_0 < 1$. The threshold value of s_1 for doing this is that value for which $r_0 = 1$. Since we do not have a convenient formula for r_0 (it is the root of the cubic characteristic polynomial of P), we invoke Theorem 2.15 and use R_0 instead. From (2.29), we can determine the value of s_1 for which $R_0 = 1$. Solving

$$R_0 = 10.67 \times s_1 \times 1 \times \frac{1}{1 - 0.9924} = 1$$

for $s_1 = 7.123 \times 10^{-4}$, we conclude that $s_1 < 7.123 \times 10^{-4}$ implies $r_0 < 1$.

In Chapter 3, we consider a nonlinear version of the LPA model that has been extensively used in experimental population dynamics involving beetle species.

2.5.2. A Bullfrog Model. The life cycle graph in Figure 2.5 has been used to study the population dynamics of the American bullfrog (*Rana catesbeiana*) [70]. This model structures frog populations by using the five classes indicated in the demographic vector

$$\mathbf{x} = \begin{bmatrix} x_1 \\ x_2 \\ x_3 \\ x_4 \\ x_5 \end{bmatrix} = \begin{bmatrix} \text{Egg \& small tadpole} \\ \text{1st year large tadpole} \\ \text{2nd year tadpole} \\ \text{Metamorph/juvenile} \\ \text{Adult} \end{bmatrix}$$

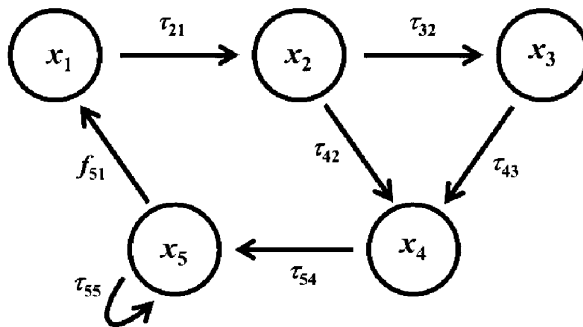


Figure 2.5. The life cycle diagram for the American bullfrog model.

and follows its dynamics on an annual timescale. Notice that an individual passes through a sequence of stages to reach the adult stage and that there are two possible paths: a fast track that skips stage x_3 and a slow track that includes it. The (nonnegative) fertility, transition, and population projection matrices associated with this graph are

$$\mathbf{F} = \begin{bmatrix} 0 & 0 & 0 & 0 & f_{15} \\ 0 & 0 & 0 & 0 & 0 \\ 0 & 0 & 0 & 0 & 0 \\ 0 & 0 & 0 & 0 & 0 \\ 0 & 0 & 0 & 0 & 0 \end{bmatrix}, \quad \mathbf{T} = \begin{bmatrix} 0 & 0 & 0 & 0 & 0 \\ \tau_{21} & 0 & 0 & 0 & 0 \\ 0 & \tau_{32} & 0 & 0 & 0 \\ 0 & \tau_{42} & \tau_{43} & 0 & 0 \\ 0 & 0 & 0 & \tau_{54} & \tau_{55} \end{bmatrix},$$

and $\mathbf{P} = \begin{bmatrix} 0 & 0 & 0 & 0 & f_{15} \\ \tau_{21} & 0 & 0 & 0 & 0 \\ 0 & \tau_{32} & 0 & 0 & 0 \\ 0 & \tau_{42} & \tau_{43} & 0 & 0 \\ 0 & 0 & 0 & \tau_{54} & \tau_{55} \end{bmatrix}$

with

$$f_{15} > 0, \quad 0 < \tau_{ij} \leq 1, \quad \text{and} \quad \tau_{55} < 1.$$

An inspection of the life cycle graph shows there is a path between every pair of classes, and as a result, \mathbf{P} is irreducible. Is \mathbf{P} primitive? Using a computer program to compute powers of \mathbf{P} , one will find that the first power that is positive is \mathbf{P}^6 ; hence, by Theorem 2.8(b), it follows that \mathbf{P} is primitive.

In order to determine conditions under which the population goes extinct ($r_0 < 1$) or grows ($r_0 > 1$), we can calculate the reproduction number R_0 and invoke Theorem 2.15. The reason this calculation is tractable is that all rows, except the first, in the fertility matrix \mathbf{F} consist entirely of zeros (because there is only one newborn class in the model). It follows that the same is true of the next generation matrix $\mathbf{F}(\mathbf{I}_5 - \mathbf{T})^{-1}$. Since the eigenvalues of this triangular matrix appear along its diagonal, we see that 0 is an eigenvalue of multiplicity four and that the dominant eigenvalue R_0 appears in the upper-left corner, which is the inner product of the first row of \mathbf{F} with the first column of $(\mathbf{I}_5 - \mathbf{T})^{-1} = [n_{ij}]$. Furthermore, since only the last entry f_{15} in the first row of \mathbf{F} is nonzero, it follows that this inner product is simply f_{15} times the last entry n_{51} in the first column of $(\mathbf{I}_5 - \mathbf{T})^{-1}$:

$$R_0 = [\begin{array}{ccccc} 0 & 0 & 0 & 0 & f_{15} \end{array}] \begin{bmatrix} n_{11} \\ n_{21} \\ n_{31} \\ n_{41} \\ n_{51} \end{bmatrix} = f_{15} n_{51}.$$

Using the cofactor method to calculate the entry n_{51} in the inverse $(\mathbf{I}_m - \mathbf{T})^{-1}$, we find that

$$\begin{aligned} n_{51} &= \frac{1}{\det(\mathbf{I}_5 - \mathbf{T})^{-1}} \det \begin{bmatrix} -\tau_{21} & 1 & 0 & 0 \\ 0 & -\tau_{32} & 1 & 0 \\ 0 & -\tau_{42} & -\tau_{43} & 1 \\ 0 & 0 & 0 & -\tau_{54} \end{bmatrix} \\ &= \frac{1}{1 - \tau_{55}} (\tau_{21}\tau_{42}\tau_{54} + \tau_{21}\tau_{32}\tau_{43}\tau_{54}) \end{aligned}$$

and that

$$(2.42) \quad R_0 = f_{15}\tau_{21}\tau_{42}\tau_{54} \frac{1}{1 - \tau_{55}} + f_{15}\tau_{21}\tau_{32}\tau_{43}\tau_{54} \frac{1}{1 - \tau_{55}}.$$

This formula implies that the net reproduction number is the sum of the lifetime expected numbers of offspring from individuals that follow the fast and slow life cycle paths. To see this, notice that $(1 - \tau_{55})^{-1}$ is the amount of time spent as an adult and $f_{15}(1 - \tau_{55})^{-1}$ is the expected amount of offspring, given survival to adulthood (the probabilities of which are $\tau_{21}\tau_{42}\tau_{54}$ and $\tau_{21}\tau_{32}\tau_{43}\tau_{54}$ for the fast and slow tracks, respectively). The population survives if $R_0 > 1$ and goes extinct if $R_0 < 1$.

As an example, parameter estimates are given in [70] for populations of bullfrogs in locations in suburban Victoria, British Columbia, Canada. With these estimates, the fertility and transition matrices are

$$\mathbf{F} = \begin{bmatrix} 0 & 0 & 0 & 0 & 2.08 \times 10^3 \\ 0 & 0 & 0 & 0 & 0 \\ 0 & 0 & 0 & 0 & 0 \\ 0 & 0 & 0 & 0 & 0 \\ 0 & 0 & 0 & 0 & 0 \end{bmatrix} \text{ and}$$

$$\mathbf{T} = \begin{bmatrix} 0 & 0 & 0 & 0 & 0 \\ 7.00 \times 10^{-2} & 0 & 0 & 0 & 0 \\ 0 & 7.80 \times 10^{-2} & 0 & 0 & 0 \\ 0 & 1.60 \times 10^{-2} & 2.00 \times 10^{-2} & 0 & 0 \\ 0 & 0 & 0 & 1.29 \times 10^{-1} & 3.18 \times 10^{-1} \end{bmatrix},$$

and the net reproduction number (2.42) is $R_0 \approx 4.84 \times 10^{-1} < 1$, which predicts that these populations are endangered. (We round answers to 3 significant digits throughout this example.)

We can use a linear algebraic computer program to calculate the dominant eigenvalue $r_0 \approx 8.55 \times 10^{-1}$ and associated eigenvectors

$$\mathbf{v} = \begin{bmatrix} 9.16 \times 10^{-1} \\ 7.51 \times 10^{-2} \\ 6.85 \times 10^{-3} \\ 1.57 \times 10^{-3} \\ 3.76 \times 10^{-4} \end{bmatrix} \text{ and } \mathbf{w} = \begin{bmatrix} 2.23 \times 10^{-4} \\ 2.72 \times 10^{-3} \\ 3.05 \times 10^{-3} \\ 1.30 \times 10^{-1} \\ 8.64 \times 10^{-1} \end{bmatrix}$$

of the population projection matrix $\mathbf{P} = \mathbf{F} + \mathbf{T}$. From these, we can calculate sensitivities and elasticities, but rather than calculate the entire 5×5 sensitivity and elasticity matrices, we calculate just those sensitivities s_{ij} and elasticities e_{ij} corresponding to the nonzero entries in the projection matrix $\mathbf{P} = [p_{ij}]$. These appear in Table 2.1, where we see that r_0 is most sensitive (with sensitivity 2.60) to additive perturbations of the transition rate τ_{21} of a first-year large tadpole. An increase of τ_{21} from

$$7.00 \times 10^{-2} \text{ to } 7.00 \times 10^{-2} + \Delta\tau_{21}$$

will result in an increase in r_0 from

$$8.55 \times 10^{-1} \text{ to approximately } 8.55 \times 10^{-1} + 2.60\Delta\tau_{21}.$$

For example, if $\Delta\tau_{21} = 2.00 \times 10^{-2}$, so that τ_{21} is increased from 7.00×10^{-2} to 9.00×10^{-2} , then r_0 will be increased to approximately

$$r_0 \approx 8.55 \times 10^{-1} + 2.60(2.00 \times 10^{-2}) = 9.07 \times 10^{-1}.$$

(As a check on this approximation, we can use a computer to calculate r_0 of the new $\mathbf{P} = \mathbf{F} + \mathbf{T}$ to be approximately 9.02×10^{-1} so that the error made using the sensitivity is an over estimate of only 0.55%.)

Table 2.1. The sensitivities and elasticities of r_0 to the nonzero entries in the bullfrog model with life cycle graph in Figure 5 with parameter values given in [70].

Entry	r_0 sensitivity	r_0 elasticity
$p_{15} = f_{15} = 2.08 \times 10^3$	8.75×10^{-5}	2.13×10^{-1}
$p_{21} = \tau_{21} = 7.00 \times 10^{-2}$	2.60	2.13×10^{-1}
$p_{32} = \tau_{32} = 7.80 \times 10^{-2}$	2.39×10^{-1}	2.18×10^{-2}
$p_{42} = \tau_{42} = 1.60 \times 10^{-2}$	1.02×10	1.91×10^{-1}
$p_{43} = \tau_{43} = 2.00 \times 10^{-2}$	9.32×10^{-1}	2.18×10^{-2}
$p_{54} = \tau_{54} = 1.29 \times 10^{-1}$	1.41	2.13×10^{-1}
$p_{55} = \tau_{55} = 3.18 \times 10^{-1}$	3.39×10^{-1}	1.26×10^{-1}

The column of elasticities in Table 2.1 allows a comparison of the proportional effects on r_0 from proportional changes from each of the model parameters. We find that *the largest elasticity is 2.13×10^{-1} , which occurs with respect to each of these three parameters: the birth rate f_{15} , the transitions rate τ_{21} to first-year large tadpole, and the transition from juvenile to adult τ_{54} .* A 10% increase in any of these parameters will increase r_0 by approximately

$$(2.13 \times 10^{-1}) 10\% = 2.13\%,$$

that is from 8.55×10^{-1} to

$$r_0 \approx 8.55 \times 10^{-1} (1.0213) = 8.73 \times 10^{-1}.$$

(As a check on this approximation, we can use a computer to calculate r_0 of the new $\mathbf{P} = \mathbf{F} + \mathbf{T}$ to be approximately 8.72×10^{-1} so that the error made using the elasticity is an over estimate of only 0.115%.) By contrast, a 10% change in $\tau_{32} = 7.80 \times 10^{-2}$ will increase r_0 by the smaller percentage of only $(2.18 \times 10^{-2}) 10\% = 0.218\%$.

2.5.3. A Tropical Shrub Model. In a study of tropical savanna plants, the (nonnegative) fertility and transition matrices (to 2 significant digits)

$$\mathbf{F} = \begin{bmatrix} 0 & 0 & 0.096 & 0.29 & 0.52 & 0.56 & 0.98 & 1.5 \\ 0 & 0 & 0 & 0 & 0 & 0 & 0 & 0 \\ 0 & 0 & 0 & 0 & 0 & 0 & 0 & 0 \\ 0 & 0 & 0 & 0 & 0 & 0 & 0 & 0 \\ 0 & 0 & 0 & 0 & 0 & 0 & 0 & 0 \\ 0 & 0 & 0 & 0 & 0 & 0 & 0 & 0 \\ 0 & 0 & 0 & 0 & 0 & 0 & 0 & 0 \\ 0 & 0 & 0 & 0 & 0 & 0 & 0 & 0 \end{bmatrix} \quad \text{and}$$

$$\mathbf{T} = \begin{bmatrix} 0.69 & 0.035 & 0 & 0 & 0 & 0 & 0 & 0 \\ 0.21 & 0.66 & 0 & 0.12 & 0.10 & 0 & 0.091 & 0.095 \\ 0 & 0.21 & 0.54 & 0.12 & 0.050 & 0.10 & 0 & 0 \\ 0 & 0.035 & 0.39 & 0.35 & 0.25 & 0 & 0 & 0 \\ 0 & 0 & 0.077 & 0.29 & 0.35 & 0.10 & 0 & 0 \\ 0 & 0 & 0 & 0 & 0.15 & 0.30 & 0 & 0.048 \\ 0 & 0 & 0 & 0 & 0.050 & 0.50 & 0.36 & 0.095 \\ 0 & 0 & 0 & 0 & 0 & 0 & 0.55 & 0.76 \end{bmatrix}$$

were used to study the dynamics of the evergreen shrub *Fabaceae Periandra mediterranea*[79].

Populations of this shrub are classified into eight size classes, $x_1, x_2, x_3, \dots, x_7$, and x_8 , based on stem diameters and the intervals 0–0.9mm, 1–1.9mm, 2–2.9mm, …, 6–6.9mm, and ≥ 7 mm, respectively. The unit of time is 1 year. Note that the two smallest size classes are nonreproductive. Also note that the model allows, each year, for stasis in stem diameter (diagonal entries in \mathbf{T}) or for either growth or shrinkage in stem diameter (entries above or below the diagonal in \mathbf{T}).

Using a computer to calculate powers of the population projection matrix $\mathbf{P} = \mathbf{F} + \mathbf{T}$, one finds that (to 2 significant digits)

$$(\mathbf{I}_m + \mathbf{P})^7 = \begin{bmatrix} 84 & 17 & 250 & 250 & 370 & 630 & 750 & 800 \\ 54 & 11 & 160 & 160 & 240 & 400 & 480 & 510 \\ 28 & 54 & 81 & 80 & 120 & 200 & 240 & 250 \\ 22 & 43 & 62 & 63 & 91 & 150 & 180 & 200 \\ 12 & 24 & 35 & 35 & 52 & 84 & 100 & 110 \\ 2.8 & 5.5 & 8.1 & 8.1 & 12 & 20 & 23 & 25 \\ 3.7 & 7.4 & 11 & 11 & 16 & 27 & 33 & 34 \\ 7.6 & 16 & 23 & 24 & 35 & 62 & 73 & 70 \end{bmatrix}$$

is positive and, by Theorem 2.8(a), that \mathbf{P} is irreducible. Another calculation shows that

$$\mathbf{P}^5 = \begin{bmatrix} 0.23 & 0.28 & 0.65 & 0.70 & 1.2 & 2.3 & 2.9 & 3.0 \\ 0.24 & 0.25 & 0.34 & 0.41 & 0.60 & 0.96 & 1.4 & 1.5 \\ 0.12 & 0.20 & 0.22 & 0.21 & 0.239 & 0.25 & 0.34 & 0.41 \\ 0.074 & 0.18 & 0.23 & 0.18 & 0.18 & 0.14 & 0.14 & 0.18 \\ 0.030 & 0.10 & 0.16 & 0.12 & 0.11 & 0.067 & 0.045 & 0.058 \\ 0.0028 & 0.016 & 0.039 & 0.033 & 0.038 & 0.042 & 0.039 & 0.040 \\ 0.0014 & 0.012 & 0.041 & 0.045 & 0.071 & 0.12 & 0.11 & 0.12 \\ 0.00015 & 0.036 & 0.025 & 0.046 & 0.14 & 0.39 & 0.46 & 0.45 \end{bmatrix}$$

is also positive and, by Theorem 2.8(b), that \mathbf{P} is primitive. Again using a computer, we find that the dominant eigenvalue and positive left and right eigenvectors are $r_0 \approx 1.1$ and

$$(2.43) \quad \mathbf{v} \approx \begin{bmatrix} 0.40 \\ 0.26 \\ 0.13 \\ 0.10 \\ 0.057 \\ 0.013 \\ 0.017 \\ 0.031 \end{bmatrix} \quad \text{and} \quad \mathbf{w} \approx \begin{bmatrix} 0.026 \\ 0.046 \\ 0.077 \\ 0.077 \\ 0.11 \\ 0.19 \\ 0.23 \\ 0.24 \end{bmatrix}.$$

Since $r_0 > 1$, this model predicts population growth (by approximately 10% per year), with a stable stem diameter size distribution given by \mathbf{v} . A computer can also easily calculate the next generation matrix

$$\mathbf{F}(\mathbf{I}_m - \mathbf{T})^{-1} \approx \begin{bmatrix} 5.0 & 7.4 & 10 & 9.2 & 12 & 19 & 21 & 22 \\ 0 & 0 & 0 & 0 & 0 & 0 & 0 & 0 \\ 0 & 0 & 0 & 0 & 0 & 0 & 0 & 0 \\ 0 & 0 & 0 & 0 & 0 & 0 & 0 & 0 \\ 0 & 0 & 0 & 0 & 0 & 0 & 0 & 0 \\ 0 & 0 & 0 & 0 & 0 & 0 & 0 & 0 \\ 0 & 0 & 0 & 0 & 0 & 0 & 0 & 0 \\ 0 & 0 & 0 & 0 & 0 & 0 & 0 & 0 \end{bmatrix}$$

whose dominant eigenvalue is $R_0 \approx 5.0$. Thus, on average, 5 new shrubs are produced per shrub per lifetime.

Formula (2.37), with \mathbf{v} and \mathbf{w} given by (2.43), yields the sensitivity matrix \mathbf{S} :

$$\begin{bmatrix} 0.17 & 0.11 & 0.056 & 0.044 & 0.024 & 0.0056 & 0.0074 & 0.013 \\ 0.31 & 0.20 & 0.107 & 0.079 & 0.044 & 0.010 & 0.014 & 0.024 \\ 0.50 & 0.33 & 0.17 & 0.13 & 0.073 & 0.017 & 0.022 & 0.040 \\ 0.50 & 0.33 & 0.17 & 0.13 & 0.073 & 0.017 & 0.022 & 0.039 \\ 0.74 & 0.48 & 0.24 & 0.19 & 0.11 & 0.024 & 0.033 & 0.058 \\ 1.3 & 0.82 & 0.42 & 0.33 & 0.18 & 0.042 & 0.056 & 0.099 \\ 1.5 & 0.97 & 0.50 & 0.39 & 0.22 & 0.050 & 0.070 & 0.12 \\ 1.6 & 1.0 & 0.52 & 0.41 & 0.23 & 0.052 & 0.070 & 0.12 \end{bmatrix}.$$

Formula (2.41) yields the elasticity matrix \mathbf{E} :

$$\begin{bmatrix} 0.11 & 0.0035 & 0.0050 & 0.012 & 0.012 & 0.0029 & 0.0068 & 0.019 \\ 0.060 & 0.12 & 0 & 0.0087 & 0.0041 & 0 & 0.0012 & 0.0021 \\ 0 & 0.063 & 0.084 & 0.014 & 0.0034 & 0.0016 & 0 & 0 \\ 0 & 0.011 & 0.0560 & 0.043 & 0.017 & 0 & 0 & 0 \\ 0 & 0 & 0.018 & 0.052 & 0.035 & 0.0023 & 0 & 0 \\ 0 & 0 & 0 & 0 & 0.026 & 0.012 & 0 & 0.0044 \\ 0 & 0 & 0 & 0 & 0.010 & 0.023 & 0.023 & 0.011 \\ 0 & 0 & 0 & 0 & 0 & 0 & 0.036 & 0.088 \end{bmatrix}.$$

We see that *the largest elasticities occur in the first two diagonal entries of E , which are the probabilities that the smallest and nonreproductive shrubs will survive and remain in the same stem diameter class.* Proportional changes in these two probabilities will have the greatest proportional effect on the population growth rate r_0 .

2.6. Concluding Remarks

The basic methodology for the derivation of discrete time matrix models for structured populations described in this chapter involves the formulation of fertility and transition matrices. The fertility matrix is used to predict, from the population distribution at one point in time, the distribution of newborn individuals at the next census time, while the transition matrix is used to predict the distribution of individuals who survive to the next census time. The sum of these matrices is the population projection matrix that predicts, by matrix multiplication, the population

distribution from one census time to the next. The Fundamental Theorem of Demography describes (amongst other things) a bifurcation phenomenon that focuses on population extinction versus survival. The extinction equilibrium loses stability as the dominant eigenvalue r_0 of the projection matrix and the population dies out (exponentially) if $r_0 < 1$ and grows exponentially without bound if $r_0 > 1$. Only if $r_0 = 1$ can long-term sustainable survival occur. The diagnostic quantity r_0 is a derived quantity from the entries appearing in the projection matrix for which, except in the lowest-dimensional cases, we cannot in general obtain algebraic formulas. For that reason, we studied how r_0 depends on projection matrices entries by means of sensitivity and elasticity analysis. Another diagnostic for these asymptotic alternatives—one that in general is more algebraically tractable than r_0 , namely the reproduction number R_0 —is also defined in this chapter.

The linear models and their analyses given in this chapter assume that the entries in the projection matrix remain fixed in time. In general, the entries involve various kinds of per capita (individual) vital rates and other biological processes, such as birth rates, survival probabilities, resource consumption rates, growth rates, and so on. These rates typically do not in fact remain constant in time, at least for long periods. They can change for any number of reasons. One important reason is the effect on such vital rates that (class specific) population densities can have, through interactions among individuals involving competition for resources, predation, etc. This is the topic of the following Chapter 3. Another reason is change due to natural selection, which we will consider in Chapter 5.

2.7. Exercises

Exercise 2.24. Provide a formal induction proof of the solution formula (2.14) for the linear matrix equation (2.3). Verify that the formula gives a solution by substituting it into both sides of the matrix equation to see that you get the same results.

Exercise 2.25. Suppose \mathbf{P} is diagonalizable and let \mathbf{v}_i and \mathbf{w}_i^T be m independent right and left eigenvectors associated with eigenvalues λ_i . (a) Show that $\mathbf{w}_j^T \mathbf{v}_i = \mathbf{0}_m$ for all $j \neq i$. (HINT: multiply $\mathbf{P}\mathbf{v}_i = \lambda_i \mathbf{v}_i$ on the left by \mathbf{w}_j^T and $\mathbf{w}_i^T \mathbf{P} = \lambda_i \mathbf{w}_i$ on the right by \mathbf{v}_i .) (b) Use (a) to obtain the formula (2.17).

Exercise 2.26. An upper block triangular matrix has the form

$$\mathbf{M} = \begin{bmatrix} \mathbf{M}_{11} & \mathbf{M}_{12} & \mathbf{M}_{13} & \cdots & \mathbf{M}_{1k} \\ \mathbf{0} & \mathbf{M}_{22} & \mathbf{M}_{23} & \cdots & \mathbf{M}_{2k} \\ \mathbf{0} & \mathbf{0} & \mathbf{M}_{33} & \cdots & \mathbf{M}_{3k} \\ \vdots & \vdots & \vdots & & \vdots \\ \mathbf{0} & \mathbf{0} & \mathbf{0} & \cdots & \mathbf{M}_{kk} \end{bmatrix},$$

where the diagonal blocks \mathbf{M}_{ii} are square matrices (not necessarily of the same size). Prove that the eigenvalues of \mathbf{M} are the eigenvalues of the blocks \mathbf{M}_{ii} .

Exercise 2.27. Show that the solution formula (2.18) is real valued even if \mathbf{P} has complex eigenvalues. (HINT: Complex roots occur in conjugate pairs. Show that the eigenvectors \mathbf{v} and \mathbf{w} and coefficients c_i corresponding to conjugate eigenvalue pairs are also conjugate pairs. Write λ_i in polar form and investigate the two terms in (2.18) arising from the two conjugate eigenvalues.)

Exercise 2.28. Show that an Usher projection matrix (2.10) is irreducible if and only if $b_m > 0$ and $\tau_{i+1,i} > 0$ for all i . Suppose \mathbf{P} is irreducible. Prove it is primitive if there exists at least one positive diagonal entry $\tau_{ii} > 0$.

Exercise 2.29. Calculate the eigenvalues of the semelparous Leslie matrix 2.23 and use them to prove that it is imprimitive.

Exercise 2.30. Use (2.16) and (2.3) to prove (2.14).

Exercise 2.31. Assuming $\rho(\mathbf{T}) < 1$ so that $(\mathbf{I}_m - \mathbf{T})^{-1}$ exists, prove (2.25).

Exercise 2.32. Prove that the first column of $(\mathbf{I}_m - \mathbf{T})^{-1}$ for the extended Leslie transition matrix \mathbf{T} is as given by (2.28). (HINT: Use the cofactor method to calculate a matrix inverse.)

Exercise 2.33. Use the cofactor method to calculate a matrix inverse to find the first column in $(\mathbf{I}_m - \mathbf{T})^{-1}$ for the Usher transition matrix (2.9). Then use your answer to derive the formula

$$R_0 = \sum_{i=1}^m f_i \prod_{j=1}^i \frac{\tau_{j,j-1}}{1 - \tau_{jj}}$$

for the reproduction number of the Usher projection matrix (2.10). In this formula, we have defined $\tau_{10} = 1$ for notational convenience.

Exercise 2.34. Calculate a formula for R_0 for the population projection matrix with these fertility and transition matrices:

- (a) \mathbf{F} given by (2.31) with $k = 1$ and $\mathbf{T} = \begin{bmatrix} \tau_{11} & \tau_{12} & \tau_{13} \\ \tau_{21} & \tau_{22} & \tau_{23} \\ \tau_{31} & \tau_{32} & \tau_{33} \end{bmatrix}$;
- (b) \mathbf{F} given by (2.31) with $k = 1$ and $\mathbf{T} = \begin{bmatrix} \tau_{11} & 0 & 0 & 0 \\ \tau_{21} & \tau_{22} & 0 & 0 \\ 0 & \tau_{32} & \tau_{33} & 0 \\ 0 & 0 & \tau_{43} & \tau_{44} \end{bmatrix}$;
- (c) \mathbf{F} given by (2.31) with $k = 1$ and $\mathbf{T} = \begin{bmatrix} 0 & 0 & 0 & 0 \\ \tau_{21} & 0 & 0 & 0 \\ \tau_{31} & \tau_{32} & 0 & 0 \\ \tau_{41} & \tau_{42} & \tau_{43} & 0 \end{bmatrix}$;
- (d) \mathbf{F} given by (2.31) with $k = 1$ and $\mathbf{T} = \begin{bmatrix} 0 & 0 & 0 & 0 \\ \tau_{21} & \tau_{22} & 0 & 0 \\ \tau_{31} & \tau_{32} & 0 & 0 \\ \tau_{41} & 0 & \tau_{43} & 0 \end{bmatrix}$;
- (e) $\mathbf{F} = \begin{bmatrix} 0 & 0 & f_{13} \\ 0 & 0 & f_{23} \\ 0 & 0 & 0 \end{bmatrix}$ and $\mathbf{T} = \begin{bmatrix} 0 & 0 & 0 \\ 0 & 0 & 0 \\ \tau_{31} & \tau_{32} & 0 \end{bmatrix}$;
- (f) $\mathbf{F} = \begin{bmatrix} 0 & 0 & f_{13} & f_{14} \\ 0 & 0 & 0 & f_{24} \\ 0 & 0 & 0 & 0 \\ 0 & 0 & 0 & 0 \end{bmatrix}$ and $\mathbf{T} = \begin{bmatrix} 0 & 0 & 0 & 0 \\ \tau_{21} & 0 & 0 & 0 \\ 0 & \tau_{32} & 0 & 0 \\ 0 & 0 & \tau_{43} & 0 \end{bmatrix}$.

Exercise 2.35. In Example 2.19, give interpretations of the individual terms

$$f_{13}\tau_{31}\frac{1}{1-\tau_{33}} \quad \text{and} \quad f_{23}\tau_{32}\frac{1}{1-\tau_{33}},$$

whose sum equals R_0 . Use your answer to provide another interpretation of R_0 .

Exercise 2.36. In Example 2.22, calculate the juvenile survival rate s_1 for which $r_0 = 1$. Then do the same for the adult survival rate s_2 .

Exercise 2.37. Consider the juvenile-adult model in Example 2.11 with projection matrix

$$\mathbf{P} = \begin{bmatrix} 0 & b_2 \\ s_1 & s_2 \end{bmatrix}.$$

- (a) Calculate the sensitivities of the reproduction number R_0 (given by formula (2.26)) with respect to juvenile and adult survival probabilities s_1 and s_2 . Under what conditions will R_0 be more sensitive to s_2 than to s_1 ? Calculate the elasticities of R_0 with respect to s_1 and s_2 and answer the same question.
- (b) Show that the elasticities of r_0 with respect to b_2 and s_1 in the juvenile-adult model with projection matrix are equal.

Exercise 2.38. The age structured Leslie model with fertility and transition matrices

$$\mathbf{F} = \begin{bmatrix} 0.01257 & 0.1002 & 0.3319 & 0.3319 \\ 0 & 0 & 0 & 0 \\ 0 & 0 & 0 & 0 \\ 0 & 0 & 0 & 0 \end{bmatrix} \text{ and}$$

$$\mathbf{T} = \begin{bmatrix} 0 & 0 & 0 & 0 \\ 0.1089 & 0 & 0 & 0 \\ 0 & 0.8680 & 0 & 0 \\ 0 & 0 & 0.8680 & 0.8680 \end{bmatrix}$$

has been used to model the population dynamics of the Northern Spotted Owl (*Strix occidentalis caurina*) [69]. The time unit is 1 year. Calculate r_0 and R_0 , the stable age distribution \mathbf{v} , and the sensitivity & elasticity matrices \mathbf{S} and \mathbf{E} .

Exercise 2.39. In [88], [112], a 13×13 Leslie matrix is used to model the dynamics of the endangered African elephant (*Loxodonta africana*) in Amboseli National Park, Kenya. The age class sizes used are of length 5 years, so the time unit in the matrix model is 5 years. The fertility matrix (2.4) and the transition matrix (2.5) have the entries in Table 2.2.

Table 2.2. Entries for the fertility and transition matrices.

i	1	2	3	4	5	6
b_i	0.000	0.014	0.550	0.925	1.040	1.053
$\tau_{i,i-1}$	NA	0.917	0.976	0.956	0.939	0.918
i	7	8	9	10	11	12
b_i	1.067	1.090	0.985	0.829	0.646	0.472
$\tau_{i,i-1}$	0.911	0.890	0.832	0.842	0.844	0.802
i	13					
b_i	0.099					
$\tau_{i,i-1}$	0.718					

Calculate r_0 and R_0 and the stable age distribution \mathbf{v} . Is the population growing or declining? Calculate and interpret the sensitivity & elasticity matrices \mathbf{S} and \mathbf{E} .

Exercise 2.40. A Seed Bank Model. Consider an annual plant that flowers in the spring of each year. Suppose that each spring a seed can either germinate, producing a new flowering plant for that season, or remain as a seed for another year. Suppose, however, that no seed can remain viable for more than 3 years. Let s_1 , s_2 , and s_3 ($0 < s_i < 1$) be the fraction of 1-, 2-, and 3-year-old seeds that germinate, respectively, and let $b_i > 0$ be the number of seeds produced by a plant from an i -year-old seed. Designate four classes: 1-, 2-, and 3-year-old seeds (at the beginning of spring) and flowering plants. Draw a life cycle graph and prove that the associated projection matrix is irreducible and primitive. Calculate the reproduction number R_0 .

Exercise 2.41. In a study of the effects that the infamous deep water horizon oil spill in 2010 had on the sperm whale population in the Gulf of Mexico, the authors in [2], [20] utilized a matrix model with demographic vector

$$\begin{bmatrix} x_1 \\ x_2 \\ x_3 \\ x_4 \\ x_5 \end{bmatrix} = \begin{bmatrix} \text{calves} \\ \text{juveniles} \\ \text{mature females} \\ \text{mothers} \\ \text{post breeding females} \end{bmatrix}$$

and projection matrix $\mathbf{P} = \mathbf{F} + \mathbf{T}$, where

$$\mathbf{F} = \begin{bmatrix} 0 & 0 & 0.1250 & 0 & 0 \\ 0 & 0 & 0 & 0 & 0 \\ 0 & 0 & 0 & 0 & 0 \\ 0 & 0 & 0 & 0 & 0 \\ 0 & 0 & 0 & 0 & 0 \end{bmatrix} \text{ and}$$

$$\mathbf{T} = \begin{bmatrix} 0.4778 & 0 & 0 & 0 & 0 \\ 0.4292 & 0.8339 & 0 & 0 & 0 \\ 0 & 0.1085 & 0.7249 & 0 & 0.4810 \\ 0 & 0 & 0.2528 & 0.4967 & 0 \\ 0 & 0 & 0 & 0.4810 & 0.4967 \end{bmatrix}.$$

The use of a computer program to carry out matrix calculations will be necessary for parts of this exercise.

- (a) Draw the associated life cycle graph.
- (b) Show that A is irreducible.
- (c) Show that A is primitive.
- (d) Calculate the dominant (Perron) eigenvalue $r_0 = \lambda_1$. Is the population growing or declining?
- (e) Calculate the positive eigenvector \mathbf{v}_1 associated with λ_1 that has norm $\|\mathbf{v}_1\| = 1$. In this normalized class distribution, the highest proportion of individuals and the lowest proportion of individuals are in which classes?
- (f) Calculate R_0 .
- (g) Calculate the sensitivity matrix. To which entry in A is r_0 most sensitive?
- (h) Calculate the elasticity matrix. To which entry in A is r_0 most elastic?

Chapter 3

Nonlinear Matrix Models for Structured Populations

In this chapter, we consider matrix models for structured populations in which the vital rates in the population project matrix are no longer necessarily fixed in time, but instead change over time because they are dependent on population density. Two fundamental goals in the study of such nonlinear matrix models, both biological and mathematical, involve the stability and instability of the **extinction equilibrium** and the existence and stability of **survival equilibria**, by which is meant equilibria lying in $R_+^m \setminus \{\mathbf{0}_m\}$. These questions are addressed in Sections 3.3 and 3.4, respectively, after the preliminary matters are dealt with in Section 3.1.

3.1. Modeling Methodology

In Example 2.11, we considered an $m = 2$ dimensional matrix model of a population structured into juvenile and adult classes

$$\mathbf{x} = \begin{bmatrix} x_1 \\ x_2 \end{bmatrix} = \begin{bmatrix} \text{juveniles} \\ \text{adults} \end{bmatrix}$$

with the fertility and transition matrices

$$\mathbf{F} = \begin{bmatrix} 0 & b_2 \\ 0 & 0 \end{bmatrix} \quad \text{and} \quad \mathbf{T} = \begin{bmatrix} 0 & 0 \\ s_1 & s_2 \end{bmatrix}$$

and the resulting population projection matrix

$$\mathbf{P} = \mathbf{F} + \mathbf{T} = \begin{bmatrix} 0 & b_2 \\ s_1 & s_2 \end{bmatrix}$$

whose entries are constants. If one or more of the three vital rates in this projection matrix do not remain constant over time but instead change when the density of the juvenile class and/or the adult class change, then the entries in the projection matrix become functions of \mathbf{x} . In this case, we have density-dependent fertility and transition matrices of the forms

$$\mathbf{F}(\mathbf{x}) = \begin{bmatrix} 0 & f_{12}(\mathbf{x}) \\ 0 & 0 \end{bmatrix} = \begin{bmatrix} 0 & f_{12}(x_1, x_2) \\ 0 & 0 \end{bmatrix} \quad \text{and}$$

$$\mathbf{T}(\mathbf{x}) = \begin{bmatrix} 0 & 0 \\ \tau_{21}(\mathbf{x}) & \tau_{22}(\mathbf{x}) \end{bmatrix} = \begin{bmatrix} 0 & 0 \\ \tau_{21}(x_1, x_2) & \tau_{22}(x_1, x_2) \end{bmatrix}.$$

The notation $f_{12}(\mathbf{x})$ and $\tau_{ij}(\mathbf{x})$ (or alternatively $f_{12}(x_1, x_2)$ and $\tau_{ij}(x_1, x_2)$) indicates a dependence of these vital rates on the class-specific densities x_1 and x_2 . This dependency can be caused, for example, by crowding and the resulting competition for resources (food, space, mates, etc.), which cause a decrease in the vital rate as x_1 and/or x_2 increase. Or, in contrast to such a negative effect, an increase in population density might cause instead an increase in a vital rate. Such a positive effect could be due, for example, to cooperation in the protection of offspring or in resource gathering. A negative density effect is mathematically described by a decreasing function of x_1 and/or x_2 in the modeling of a projection matrix entry, while a positive density effect results from use of an increasing function of x_1 and/or x_2 . Of course, a mixture of negative and positive effects are certainly possible in a model.

Density-dependent matrices $\mathbf{F}(\mathbf{x})$ and $\mathbf{T}(\mathbf{x})$ yield a density-dependent population projection matrix

$$(3.1) \quad \mathbf{P}(\mathbf{x}) = \begin{bmatrix} 0 & f_{12}(\mathbf{x}) \\ \tau_{21}(\mathbf{x}) & \tau_{22}(\mathbf{x}) \end{bmatrix}$$

with $\mathbf{x} = \text{col}(x_1, x_2)$ and the associated matrix equation

$$\mathbf{x}(t+1) = \mathbf{P}(\mathbf{x}(t))\mathbf{x}(t)$$

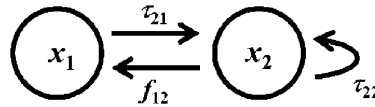


Figure 3.1. The life cycle graph associated with the juvenile-adult model projection matrix (3.1).

for the population dynamics. This matrix equation can alternatively be written less concisely as a system of two difference equations:

$$\begin{aligned} x_1(t+1) &= f_{12}(x_1(t), x_2(t)) x_2(t) \text{ and} \\ x_2(t+1) &= \tau_{21}(x_1(t), x_2(t)) x_1(t) + \tau_{22}(x_1(t), x_2(t)) x_2(t). \end{aligned}$$

The life cycle graph associated with the juvenile-adult model with projection matrix (3.1) is shown in Figure 3.1.

Example 3.1. A Nonlinear Juvenile-Adult Model. Consider

$$f_{12}(\mathbf{x}) = b_2 \frac{1}{1 + cx_2}$$

whereby adult per capita fertility decreases, from the inherent (density-free) fertility rate \$b_2\$, with increased adult population density \$x_2\$ (due, say, to competition for mates or food resources). In addition, assume juvenile survival \$s_1\$ is constant (density independent) and the population is semelparous, so that \$s_2 = 0\$. Then the (nonnegative and irreducible) population projection matrix (3.1) is

$$\mathbf{P}(\mathbf{x}) = \begin{bmatrix} 0 & b_2 \frac{1}{1 + cx_2} \\ s_1 & 0 \end{bmatrix}$$

with \$b_2, c > 0\$ and \$0 < s_1 \leq 1\$.

The resulting population model is

$$(3.2) \quad \begin{bmatrix} x_1(t+1) \\ x_2(t+1) \end{bmatrix} = \begin{bmatrix} 0 & b_2 \frac{1}{1 + cx_2(t)} \\ s_1 & 0 \end{bmatrix} \begin{bmatrix} x_1(t) \\ x_2(t) \end{bmatrix}.$$

□

The matrix model (3.2) is a special case of Ebenman's model

$$(3.3) \quad \begin{bmatrix} x_1(t+1) \\ x_2(t+1) \end{bmatrix} = \begin{bmatrix} 0 & b_2 \frac{1}{1+c_{21}x_1(t)+c_{22}x_2(t)} \\ s_1 \frac{1}{1+c_{11}x_1(t)+c_{12}x_2(t)} & 0 \end{bmatrix} \begin{bmatrix} x_1(t) \\ x_2(t) \end{bmatrix},$$

which has been used to study the consequences of resource competition between juveniles and adults [38], [66], [67].

As pointed out in the introduction to this chapter, basic questions of interest with regard to a nonlinear matrix equation concern the stability properties of the extinction equilibrium $\mathbf{x}_e = \mathbf{0}_m$ and the existence and stability of survival equilibria $\mathbf{x} \in R_+^m \setminus \{\mathbf{0}_m\}$. As an introduction to our study of these questions, we take a close look at the juvenile-adult model (3.2) for which answers are readily available. What we will find is that the asymptotic dynamics of this equation bear a strong similarity with the dynamics of discrete logistic equation (1.17).

Recall that the extinction equilibrium of the discrete logistic equation destabilizes as the inherent fertility rate increases through a critical value, with the result that stable positive equilibria are created (by a forward, stable bifurcation). In Example 3.2, we show that this same bifurcation phenomenon occurs in the juvenile-adult model (3.2), which motivates our goal of studying this bifurcation in general nonlinear matrix models in the following sections.

Example 3.2. For any initial condition $\mathbf{x}(0) = \text{col}(x_1(0), x_2(0)) \in R_+^2$, there corresponds a unique solution $\mathbf{x}(t) = \text{col}(x_1(t), x_2(t)) \in R_+^2$, $t \in Z_+$, of the juvenile-adult model (3.2). We first ask, Are there any equilibrium solutions? An equilibrium is a constant solution $\text{col}(x_1, x_2)$ that satisfies the nonlinear algebraic matrix equation

$$\begin{bmatrix} x_1 \\ x_2 \end{bmatrix} = \begin{bmatrix} 0 & b_2 \frac{1}{1+cx_2} \\ s_1 & 0 \end{bmatrix} \begin{bmatrix} x_1 \\ x_2 \end{bmatrix}.$$

A little bit of algebra shows that there are two solutions of this algebraic matrix equation:

$$\begin{bmatrix} x_1 \\ x_2 \end{bmatrix} = \begin{bmatrix} 0 \\ 0 \end{bmatrix} \quad \text{and} \quad \begin{bmatrix} \frac{b_2 s_1 - 1}{c s_1} \\ \frac{b_2 s_1 - 1}{c} \end{bmatrix},$$

the first of which is the extinction equilibrium and the second of which is a survival equilibrium if and only if $b_2 s_1 > 1$. What about nonequilibrium solutions?

It is left as Exercise 3.35 to verify that the solution with initial condition $\mathbf{x}(0) = \text{col}(x_1(0), x_2(0))$ is given by the (rather formidable) formulas

$$(3.4) \quad \begin{bmatrix} x_1(t) \\ x_2(t) \end{bmatrix} = \begin{cases} \begin{bmatrix} \frac{x_1(0)}{\frac{1}{(b_2 s_1)^i} + \frac{c s_1}{b_2 s_1 - 1} x_1(0)} \\ \frac{x_2(0)}{\frac{1}{(b_2 s_1)^i} + \frac{c}{b_2 s_1 - 1} x_2(0)} \end{bmatrix} & \text{for } t = 2i \text{ for } i \in \mathbb{Z}_+ \\ \begin{bmatrix} \frac{x_2(0)}{\frac{1}{b_2} \frac{1}{(b_2 s_1)^i} + \frac{c s_1}{b_2 s_1 - 1} x_2(0)} \\ \frac{x_1(0)}{\frac{1}{s_1} \frac{1}{(b_2 s_1)^i} + \frac{c}{b_2 s_1 - 1} x_1(0)} \end{bmatrix} & \text{for } t = 2i + 1 \text{ for } i \in \mathbb{Z}_+ \end{cases}$$

when $b_2 s_1 \neq 1$ and

$$\begin{bmatrix} x_1(t) \\ x_2(t) \end{bmatrix} = \begin{cases} \begin{bmatrix} \frac{b_2 x_1(0)}{i c x_1(0) + b_2} \\ \frac{x_2(0)}{i c x_2(0) + 1} \end{bmatrix} & \text{when } t = 2i \text{ for } i \in \mathbb{Z}_+ \\ \begin{bmatrix} \frac{b_2 x_2(0)}{(i+1) c x_2(0) + 1} \\ \frac{x_1(0)}{i c x_1(0) + b_2} \end{bmatrix} & \text{when } t = 2i + 1 \text{ for } i \in \mathbb{Z}_+ \end{cases}$$

when $b_2 s_1 = 1$. A careful investigation of these solution formulas shows, for all positive initial conditions $\text{col}(x_1(0), x_2(0)) \in \text{int}(\mathbb{R}_+^2)$, that

$$(3.5) \quad \lim_{t \rightarrow \infty} \begin{bmatrix} x_1(t) \\ x_2(t) \end{bmatrix} = \begin{cases} \begin{bmatrix} 0 \\ 0 \end{bmatrix} & \text{if } b_2 s_1 \leq 1 \\ \begin{bmatrix} \frac{b_2 s_1 - 1}{c s_1} \\ \frac{b_2 s_1 - 1}{c} \end{bmatrix} & \text{if } b_2 s_1 > 1 \end{cases}.$$

That is to say, solutions with positive initial conditions approach the extinction equilibrium (and the population goes extinct) if $b_2 s_1 \leq 1$ but approach the positive equilibrium (and the population survives) if $b_2 s_1 > 1$. \square

Adapting the jargon introduced in Chapter 1, we would say about the juvenile-adult model (3.2) that the extinction equilibrium is globally attracting on $\text{int}(\mathbb{R}_+^2)$ if $b_2 s_1 \leq 1$ and that the survival equilibrium is globally attracting on $\text{int}(\mathbb{R}_+^2)$ if $b_2 s_1 > 1$. These two alternatives are the same alternatives as we found for the discrete logistic equation (1.17) studied in Chapter 1. Namely, the extinction equilibrium is no longer

attracting after $b_2 s_1$ increases through 1, and as a result of this destabilization, a branch of stable survival (positive) equilibria bifurcates from the extinction equilibrium at $b_2 s_1 = 1$. This bifurcation phenomenon is a matrix model example of the basic bifurcation Theorems 1.12 and 1.17 in Section 1.2.1 for difference equations. One goal of the current chapter is to study this basic bifurcation phenomenon for general nonlinear matrix models of any dimension $m > 1$.

Following the modeling methodology in Section 2.1, we consider the nonlinear matrix model equations of the form

$$(3.6) \quad \mathbf{x}(t+1) = \mathbf{P}(\mathbf{x}(t)) \mathbf{x}(t),$$

where the projection matrix

$$(3.7) \quad \mathbf{P}(\mathbf{x}) = \mathbf{F}(\mathbf{x}) + \mathbf{T}(\mathbf{x}) = [p_{ij}(\mathbf{x})]$$

and the fertility and transition matrices

$$(3.8) \quad \mathbf{F}(\mathbf{x}) = [f_{ij}(\mathbf{x})] \quad \text{and} \quad \mathbf{T}(\mathbf{x}) = [\tau_{ij}(\mathbf{x})]$$

are allowed to be density-dependent.

In what follows, we will often describe population models by describing the projection matrix only, and it is to be understood that the dynamic model is the associated matrix difference equation (3.6). A matrix difference equation can also be written as a system of m (first order) difference equations

$$\begin{aligned} x_1(t+1) &= p_{11}(x_1(t), \dots, x_m(t)) x_1(t) + \\ &\quad \dots + p_{1m}(x_1(t), \dots, x_m(t)) x_m(t) \\ x_2(t+1) &= p_{21}(x_1(t), \dots, x_m(t)) x_1(t) + \\ &\quad \dots + p_{2m}(x_1(t), \dots, x_m(t)) x_m(t) \\ &\vdots \\ x_m(t+1) &= p_{m1}(x_1(t), \dots, x_m(t)) x_1(t) + \\ &\quad \dots + p_{mm}(x_1(t), \dots, x_m(t)) x_m(t), \end{aligned}$$

where x_i are the entries in \mathbf{x} and $p_{ij}(\mathbf{x}) = p_{ij}(x_1, \dots, x_m)$ are the entries in the projection matrix.

Before embarking on a study of the equilibria of equation (3.6), we need first to set some ground rules with regard to domains, ranges, and smoothness of the matrix entries as functions of \mathbf{x} .

Assumption 3.3. The entries in the fertility and transition matrices (3.8) of the population projection matrix (3.7) satisfy $f_{ij}, \tau_{ij} \in C^2(R^m : R_+)$ and $0 \leq \tau_{ij}(\mathbf{x}) \leq 1$, $\sum_{j=1}^m \tau_{ij}(\mathbf{x}) \leq 1$ for all $\mathbf{x} \in R_+^m$.

Note that Assumption 3.3 implies that all entries f_{ij} and τ_{ij} in the fertility and transition matrices are nonnegative-valued functions and, as a result, that the matrices $\mathbf{F}(\mathbf{x})$ and $\mathbf{T}(\mathbf{x})$ are nonnegative for all $\mathbf{x} \in R_+^m$.

Any initial condition $\mathbf{x}(0) \in R_+^m$ generates a unique sequence by iteration of the matrix equation (i.e., a unique solution of equation (3.6)). Assumption 3.3 implies the projection matrix $\mathbf{P}(\mathbf{x})$ is nonnegative for all $\mathbf{x} \in R_+^m$, which in turn implies the solution $\mathbf{x}(t) \in R_+^m$ for all $t \in Z_+$. (We say that R_+^m is **forward invariant**.)

Remark 3.4. Recalling Remark 1.3, we assume any mathematical expressions used for f_{ij}, τ_{ij} that are not defined or smooth outside of R_+ (e.g., in Ebenman's model in Example 3.1) are redefined outside of R_+ so as to satisfy Assumption 3.3. Given the (forward) invariant on R_+^m , any such redefinitions have no affect on the application of the matrix equation (3.6) to population dynamics.

The constraints in Assumption 3.3 on the ranges of the τ_{ij} are made because they are, in our models, survival fractions (or probabilities). The requirement that $\sum_{j=1}^m \tau_{ij}(\mathbf{x}) \leq 1$ implies that the fraction of individuals from any class i that survive a unit of time (and get dispersed throughout all classes) cannot exceed 1.

So that we can utilize results from Perron–Frobenius theory, we will also assume

Assumption 3.5. $\mathbf{P}(\mathbf{x})$ is irreducible for each $\mathbf{x} \in R_+^m$.

The matrix $\mathbf{P}(\mathbf{0}_m)$, which plays an important role in our following analysis, is called the **inherent** (or intrinsic or density-free) **projection matrix**. It models the population's (linear) dynamics when density effects are absent. The entries $f_{ij}(\mathbf{0}_m)$ and $\tau_{ij}(\mathbf{0}_m)$ in the **inherent fertility matrix** $\mathbf{F}(\mathbf{0}_m)$ and **inherent transition matrix** $\mathbf{T}(\mathbf{0}_m)$ are the **inherent fertility** and **transition rates**, respectively.

In building a density-dependent population model, one must specify the properties of, and decide upon mathematical expressions for, the

entries $f_{ij}(\mathbf{x})$ and $\tau_{ij}(\mathbf{x})$ in a way that accounts for how fertility and survival are affected by changes in population density. This can be done, as done in Section 1.2, by introducing factors that depend on the class densities and that modify the inherent rates:

$$f_{ij}(\mathbf{x}) = b_{ij}\beta_{ij}(\mathbf{x}) \quad \text{and} \quad \tau_{ij}(\mathbf{x}) = s_{ij}\sigma_{ij}(\mathbf{x}).$$

We assume the **density factors** $\beta_{ij}, \sigma_{ij} \in C^2(R^m : R_+)$ satisfy the normalizations

$$\beta_{ij}(\mathbf{0}_m) = \sigma_{ij}(\mathbf{0}_m) = 1,$$

so as to insure that the constants b_{ij} and s_{ij} have interpretations as the inherent (density-free) fertility and transition rates.

By Assumption 3.3, $\mathbf{P}(\mathbf{x})$ is a nonnegative matrix for all $\mathbf{x} \in R_+^m$. Together with Assumption 3.5 and Perron–Frobenius theory (cf. Theorem 2.5), we know that the spectral radius $\rho(\mathbf{P}(\mathbf{x}))$ of $\mathbf{P}(\mathbf{x})$ is a positive eigenvalue of $\mathbf{P}(\mathbf{x})$ that is greater than or equal to the absolute value of all other eigenvalues. We refer to this **dominant eigenvalue** as the population growth rate when the population has density distribution \mathbf{x} .

3.2. Equilibria and the Linearization Principle

An equilibrium of (3.6) is a solution $\mathbf{x} = \mathbf{x}_e \in R_+^m$ of the nonlinear algebraic equation

$$\mathbf{x} = \mathbf{P}(\mathbf{x})\mathbf{x}.$$

Clearly $\mathbf{x}_e = \mathbf{0}_m$ is an equilibrium (the extinction equilibrium). A **survival equilibrium** is a solution of this equation that lies in $R_+^m \setminus \{\mathbf{0}_m\}$, and **positive equilibrium** is a survival equilibrium that lies in $\text{int}(R_+^m)$.

Our first step is to extend stability definitions in Definition 1.8, when $m = 1$, to the higher-dimensional case $m \geq 1$. While any norm on R^m will work in these definitions, we use the norm

$$\|\mathbf{x}\| = \sum_{i=1}^m |x_i|,$$

which, in a population model, is the **total population size or density** associated with demographic vector $\mathbf{x} \in R_+^m$.

Definition 3.6. Assume $\mathbf{f} \in C(\Omega : \Omega)$, where $\Omega \subseteq R^m$ is an open set, and that $\mathbf{x}_e \in R^m$ is an equilibrium a difference equation

$$(3.9) \quad \mathbf{x}(t + 1) = \mathbf{f}(\mathbf{x}(t)),$$

that is to say \mathbf{x}_e solves the **equilibrium equation** $\mathbf{x} = \mathbf{f}(\mathbf{x})$.

- (a) \mathbf{x}_e is **locally stable** if for each $\varepsilon > 0$ there is a $\delta(\varepsilon) > 0$ such that for any initial condition $\mathbf{x}(0) \in \Omega$ satisfying $\|\mathbf{x}(0) - \mathbf{x}_e\| < \delta(\varepsilon)$ it follows that $\|\mathbf{x}(t) - \mathbf{x}_e\| < \varepsilon$ for all $t \in \mathbb{Z}_+$. If \mathbf{x}_e is not locally stable, we say it is **unstable**.
- (b) \mathbf{x}_e is **attracting** if there is a $\delta^* > 0$ such that for any initial condition $\mathbf{x}(0) \in \Omega$ satisfying $\|\mathbf{x}(0) - \mathbf{x}_e\| < \delta^*$ it follows that $\lim_{t \rightarrow +\infty} \|\mathbf{x}(t) - \mathbf{x}_e\| = 0$.
- (c) \mathbf{x}_e is **locally asymptotically stable** if it is both locally stable and attracting.

Remark 3.7. As in the case $m = 1$, when we say that an equilibrium x_e is stable, we always mean it is locally asymptotically stable.

Remark 3.8. If $\lim_{t \rightarrow +\infty} \|\mathbf{x}(t) - \mathbf{x}_e\| = 0$ for all initial conditions $\mathbf{x}(0)$ in a set $\Lambda \subseteq \Omega$, then we say x_e is **attracting** on Λ . If in addition x_e is locally asymptotically stable, then we say x_e is **globally asymptotically stable** on Λ .

The main method used for a study of the local asymptotic stability of an equilibrium is the Linearization Principle, the use of which requires the calculation of the **Jacobian** of $\mathbf{f}(\mathbf{x}) = \text{col}(f_i(\mathbf{x}))$, which is the $m \times m$ matrix

$$\mathbf{J}\mathbf{f}(\mathbf{x}) = \begin{bmatrix} \partial_{x_1} f_1(\mathbf{x}) & \partial_{x_2} f_1(\mathbf{x}) & \cdots & \partial_{x_m} f_1(\mathbf{x}) \\ \partial_{x_1} f_2(\mathbf{x}) & \partial_{x_2} f_2(\mathbf{x}) & \cdots & \partial_{x_m} f_2(\mathbf{x}) \\ \vdots & \vdots & & \vdots \\ \partial_{x_1} f_m(\mathbf{x}) & \partial_{x_2} f_m(\mathbf{x}) & \cdots & \partial_{x_m} f_m(\mathbf{x}) \end{bmatrix}$$

whose rows are the gradients of the entries $f_i(\mathbf{x})$. The spectral radius of $\mathbf{J}\mathbf{f}(\mathbf{x})$ is

$$\rho(\mathbf{J}\mathbf{f}(\mathbf{x})) = \max\{|\lambda_1|, |\lambda_2|, \dots, |\lambda_m|\},$$

where λ_i are the eigenvalues of $\mathbf{J}\mathbf{f}(\mathbf{x})$.

Theorem 3.9. The Linearization Principle[62]. Assume \mathbf{x}_e is an equilibrium of the difference equation (3.9) with $\mathbf{f} \in C^1(\Omega : \Omega)$ where $\Omega \subseteq \mathbb{R}^m$ is an open set containing \mathbf{x}_e . Then \mathbf{x}_e is locally asymptotically stable if $\rho(\mathbf{J}\mathbf{f}(\mathbf{x}_e)) < 1$ and is unstable if $\rho(\mathbf{J}\mathbf{f}(\mathbf{x}_e)) > 1$.

A proof of this theorem can be constructed by modifying the proof of Theorem 1.10 for the $m = 1$ case in Appendix A.2. (The reader might try their hand at this; or see [62].)

It is important to note, as we did in Chapter 1 when $m = 1$, that the Linearization Principle provides a sufficient, but not a necessary, condition for the local asymptotic stability of an equilibrium. This is because an application of Theorem 3.9 requires that $\rho(\mathbf{Jf}(\mathbf{x}_e)) \neq 1$ (in which case \mathbf{x}_e is said to be **hyperbolic**.)

Example 3.10. Consider the semelparous juvenile-adult model (3.2) for which

$$\mathbf{f}(\mathbf{x}) = \mathbf{P}(\mathbf{x})\mathbf{x} = \begin{bmatrix} 0 & b_2 \frac{1}{1+cx_2} \\ s_1 & 0 \end{bmatrix} \begin{bmatrix} x_1 \\ x_2 \end{bmatrix} = \begin{bmatrix} b_2 \frac{1}{1+cx_2} x_2 \\ s_1 x_1 \end{bmatrix}.$$

The Jacobian

$$\mathbf{Jf}(\mathbf{x}) = \begin{bmatrix} 0 & b_2 \frac{1}{(1+cx_2)^2} \\ s_1 & 0 \end{bmatrix}$$

evaluated at the extinction equilibrium is

$$(3.10) \quad \mathbf{Jf}(\mathbf{0}_2) = \begin{bmatrix} 0 & b_2 \\ s_1 & 0 \end{bmatrix}$$

and has eigenvalues $\pm\sqrt{b_2 s_1}$; hence, $r_0 = \rho(\mathbf{Jf}(\mathbf{0}_2)) = \sqrt{b_2 s_1}$. By the Linearization Principle (Theorem 3.9), we see that the extinction equilibrium is stable if $b_2 s_1 < 1$ and unstable if $b_2 s_1 > 1$. (Note that $\mathbf{Jf}(\mathbf{0}_2)$ is the same as the inherent projection matrix $\mathbf{P}(\mathbf{0}_2)$.)

For $b_2 s_1 > 1$, the Jacobian at the positive equilibrium

$$\mathbf{x}_e = \begin{bmatrix} \frac{1}{s_1} \frac{b_2 s_1 - 1}{c} \\ \frac{b_2 s_1 - 1}{c} \end{bmatrix}$$

is

$$\mathbf{Jf}(\mathbf{x}_e) = \begin{bmatrix} 0 & \frac{1}{s_1 b_2} \\ s_1 & 0 \end{bmatrix}$$

whose eigenvalues are $\pm 1/\sqrt{b_2 s_1}$. Thus, $\rho(\mathbf{Jf}(\mathbf{0}_m)) = 1/\sqrt{b_2 s_1} < 1$, and by the Linearization Principle, the positive equilibrium is stable. \square

The inherent projection matrix (3.10) of the juvenile-adult model (3.2) is a 2×2 Leslie matrix with inherent population growth rate $r_0 = \sqrt{b_2 s_1}$ and inherent reproduction number $R_0 = b_2 s_1$ (see Section 2.3). Note that $r_0 = \sqrt{R_0}$. *The destabilization of the extinction equilibrium of equation (3.2) occurs as r_0 , or equivalently R_0 , increases through 1.*

The Linearization Principle in Theorem 3.9 implies only the *local* stability of an equilibrium. However, by making use of the solution formulas (3.5) and the linearization analysis in Example 3.10, we find that when $b_2 s_1 < 1$, the extinction equilibrium of the juvenile-adult model (3.2) is both stable and attracting for all initial conditions $\mathbf{x}(0) \in R_+^2$ (that is to say, $\mathbf{x}_e = \mathbf{0}_2$ is *globally asymptotically stable on R_+^2*). And, in addition, we find that when $b_2 s_1 > 1$, the positive equilibrium is *globally asymptotically stable on $\text{int}(R_+^2)$* .

Example 3.10 shows that the juvenile-adult matrix model (3.2) undergoes a bifurcation directly analogous to what we saw for single difference equation models (1.11) in Chapter 1. Namely, upon destabilization of the extinction equilibrium, there occurs a forward bifurcation of stable positive (survival) equilibria. The main goal of the following several sections is to explore this basic bifurcation for general matrix models (3.6) of any dimension $m \geq 1$.

Remark 3.11. *The reader should carefully consider what it means to say that an equilibrium is unstable by considering the logical negation of the definition of local stability in Definition 3.6(a). Local stability means, roughly speaking, that solutions remain close to the equilibrium (as close as you want) if they initially start close enough to the equilibrium. However, instability does not mean that all initially nearby solutions fail to remain close to the equilibrium.*

A simple example that illustrates this remark is the (linear) matrix equation with projection matrix

$$P = \begin{bmatrix} 2 & 0 \\ 0 & \frac{1}{2} \end{bmatrix}$$

whose eigenvalues are $\lambda_1 = 2$ and $\lambda_2 = 1/2$. The equilibrium $\mathbf{x}_e = \mathbf{0}_2$ is unstable because $\lambda_1 > 1$. Nonetheless, there exist solutions whose initial conditions are arbitrarily close to $\mathbf{x}_e = \mathbf{0}$ that do not move or stay away from $\mathbf{x}_e = \mathbf{0}_2$; namely, the solutions

$$\mathbf{x}(t) = \begin{bmatrix} x_1(t) \\ x_2(t) \end{bmatrix} = \begin{bmatrix} 0 \\ x_2(0)\left(\frac{1}{2}\right)^t \end{bmatrix},$$

which approach $\mathbf{x}_e = \mathbf{0}_2$ as $t \rightarrow \infty$ for any $x_2(0) \neq 0$, even though $\mathbf{x}_e = \mathbf{0}_2$ is unstable.

A stronger concept of instability would require that all solutions, no matter how initially close to the equilibrium they might be, ultimately remain a finite distance away from an equilibrium. This leads to the notion of persistence [122].

Definition 3.12. We say the matrix equation (2.3) is (uniformly) **persistent** with respect to the extinction equilibrium $\mathbf{x}_e = \mathbf{0}_m$ if there exists a number $\eta > 0$ such that $\liminf_{t \rightarrow \infty} \|\mathbf{x}(t)\| \geq \eta$ for all initial conditions $\mathbf{x}(0) \in \text{int}(R_+^m)$.¹

As we have seen, when $s_1 b_2 > 1$, solutions of the juvenile-adult model (3.2) satisfy

$$\lim_{t \rightarrow \infty} \mathbf{x}(t) = \mathbf{x}_e = \begin{bmatrix} \frac{b_2 s_1 - 1}{c s_1} \\ \frac{b_2 s_1 - 1}{c} \end{bmatrix}$$

for all initial conditions $\mathbf{x}(0) \in \text{int}(R_+^2)$. From the formula (3.4) for \mathbf{x}_e , we have that

$$\liminf_{t \rightarrow \infty} \|\mathbf{x}(t) - \mathbf{0}_2\| = \|\mathbf{x}_e\| = \frac{b_2 s_1 - 1}{c s_1} + \frac{b_2 s_1 - 1}{c} = \eta > 0$$

for all initial conditions $\mathbf{x}(0) \in \text{int}(R_+^2)$ and conclude that this model is persistent with respect to $\mathbf{0}_2$.

All the facts we learned about the juvenile-adult model (3.2), as an example used to illustrate the stability notions in this section, were (with the exception of an application of the Linearization Principle) based on having available a solution formula for this special model. The availability of a solution formula for a nonlinear matrix model is, however, a very rare exception. To analyze the existence and stability properties of equilibria in the absence of solution formulas requires other methods, to which we turn our attention in the following sections.

3.3. The Extinction Equilibrium and Its Stability

A basic question concerning a biological population is whether or not it is threatened with extinction. From a modeling point of view, this question concerns the stability properties of the extinction equilibrium $\mathbf{x}_e = \mathbf{0}_m$. To apply the Linearization Principle of Theorem 3.9 to the extinction equilibrium $\mathbf{x}_e = \mathbf{0}_m$ of the matrix equation (3.6), we need to

¹The adjective “uniformly” indicates that η is independent of the initial condition $\mathbf{x}(0)$.

calculate the Jacobian of $\mathbf{f}(\mathbf{x}) = \mathbf{P}(\mathbf{x})\mathbf{x}$, evaluate the answer at $\mathbf{x}_e = \mathbf{0}_m$, and study the eigenvalues of the resulting matrix. It is left as Exercise 3.40 to show that this Jacobian equals the inherent projection matrix $\mathbf{P}(\mathbf{0}_m)$, that is to show that

$$\mathbf{J}_{\mathbf{x}}\mathbf{f}(\mathbf{0}_m) = \mathbf{P}(\mathbf{0}_m).$$

The Linearization Principle therefore directs our attention to the spectral radius

$$r_0 := \rho(\mathbf{P}(\mathbf{0}_m))$$

of the inherent projection matrix $\mathbf{P}(\mathbf{0}_m)$. We refer to r_0 as the **inherent (density-free) population growth rate**.

3.3.1. The Extinction Equilibrium and r_0 . An application of the Linearization Principle (Theorem 3.9) gives part (a) of the following theorem.

Theorem 3.13. *Assume the population projection matrix (3.7) satisfies Assumption 3.3.*

- (a) *The extinction equilibrium $\mathbf{x}_e = \mathbf{0}_m$ of the matrix model equation (3.6) is locally asymptotically stable if $r_0 < 1$ and unstable if $r_0 > 1$.*
- (b) *Assume further that Assumption 3.5 holds. If $r_0 > 1$, then (3.6) is persistent with respect to $\mathbf{x}_e = \mathbf{0}_m$.*

A proof of part (b) can be found in [92].

Example 3.14. For the juvenile-adult model in Example 3.10, the inherent projection matrix (3.10) has spectral radius (dominant eigenvalue)

$$r_0 = \max\left\{|\sqrt{b_2\tau_{12}}|, |-\sqrt{b_2\tau_{12}}|\right\} = \sqrt{b_2\tau_{12}}.$$

By Theorem 3.13, the extinction equilibrium is stable for $b_2\tau_{12} < 1$. For $b_2\tau_{12} > 1$, the extinction equilibrium is unstable and the model is persistent with respect to it. \square

In fact, the same conclusions reached in Example 3.14 are valid for the general semelparous juvenile-adult model with projection matrix

$$(3.11) \quad \mathbf{P}(\mathbf{x}) = \begin{bmatrix} 0 & b_2\beta(x_1, x_2) \\ s_1\sigma_1(x_1, x_2) & 0 \end{bmatrix}$$

since, by the normalizations (1.10) contained in Assumption 3.3, the inherent projection matrix is identical to that in the juvenile-adult model in Example 3.14.

Example 3.15. The population whose dynamics are described by the general juvenile-adult model with projection matrix (3.1) is iteroparous if the inherent adult survival probability is not zero (i.e., $s_2 \neq 0$). The inherent projection matrix

$$(3.12) \quad \mathbf{P}(\mathbf{0}_2) = \begin{bmatrix} 0 & b_2 \\ s_1 & s_2 \end{bmatrix}$$

has eigenvalues

$$\lambda_1 = \frac{1}{2}s_2 + \frac{1}{2}\sqrt{s_2^2 + 4b_2s_1} \text{ and } \lambda_2 = \frac{1}{2}s_2 - \frac{1}{2}\sqrt{s_2^2 + 4b_2s_1}.$$

A bit of algebra shows that $\lambda_1 > |\lambda_2|$; hence, the inherent population growth rate is $r_0 = \lambda_1$. By Theorem 3.13, the extinction equilibrium $\mathbf{x} = \mathbf{0}_2$ is stable if

$$r_0 = \frac{1}{2}s_2 + \frac{1}{2}\sqrt{s_2^2 + 4b_2s_1} < 1,$$

and the equation is persistent with respect to $\mathbf{x} = \mathbf{0}_2$ if

$$r_0 = \frac{1}{2}s_2 + \frac{1}{2}\sqrt{s_2^2 + 4b_2s_1} > 1.$$

□

3.3.2. The Extinction Equilibrium and R_0 . The 2×2 inherent projection matrix (3.12) in Example 3.15 is an extended Leslie matrix with reproduction number

$$R_0 = b_2 \frac{s_1}{1 - s_2},$$

which we call the inherent reproduction number for this matrix equation. It is not difficult to verify that the conclusions in Example 3.15 can be restated with the inherent population growth rate r_0 replaced by inherent reproduction number R_0 . (See Exercise 3.36.)

As pointed out in Chapter 2, for higher-dimensional linear models, a formula for r_0 is generally not available, while a formula for the reproduction number R_0 is often available. We can take advantage of this fact and apply it to the inherent projection matrix $\mathbf{P}(\mathbf{0}_m)$ associated with a nonlinear matrix model. For a matrix model with projection matrix

$\mathbf{P}(\mathbf{x}) = \mathbf{F}(\mathbf{x}) + \mathbf{T}(\mathbf{x})$, the Jacobian evaluated at the extinction equilibrium is the inherent projection matrix:

$$\mathbf{J}_{\mathbf{x}} \mathbf{P}(\mathbf{x}) \Big|_{\mathbf{x}_e = \mathbf{0}_m} = \mathbf{P}(\mathbf{0}_m) = \mathbf{F}(\mathbf{0}_m) + \mathbf{T}(\mathbf{0}_m).$$

Motivated by the definition of R_0 for linear matrix equations given in Section 2.3, we define the inherent reproduction number R_0 for a nonlinear matrix equation as follows.

Definition 3.16. Consider a nonlinear matrix model with projection matrix $\mathbf{P}(\mathbf{x}) = \mathbf{F}(\mathbf{x}) + \mathbf{T}(\mathbf{x})$ for which $\rho(\mathbf{T}(\mathbf{0}_m)) < 1$. The **inherent (or intrinsic) reproduction number**² is

$$R_0 := \rho(\mathbf{F}(\mathbf{0}_m)(\mathbf{I}_m - \mathbf{T}(\mathbf{0}_m))^{-1}).$$

Theorem 3.13 together with Theorem 2.15 yield the following result.

Theorem 3.17. *In addition to Assumptions 3.3 and 3.5, assume that $\rho(\mathbf{T}(\mathbf{0}_m)) < 1$. Then the conclusions of Theorem 3.13 hold with r_0 replaced by R_0 .*

Example 3.18. The general m -dimensional nonlinear Leslie model has fertility and transition matrices

$$\mathbf{F}(\mathbf{x}) = \begin{bmatrix} b_1\beta_1(\mathbf{x}) & b_2\beta_2(\mathbf{x}) & \cdots & b_{m-1}\beta_{m-1}(\mathbf{x}) & b_m\beta_m(\mathbf{x}) \\ 0 & 0 & \cdots & 0 & 0 \\ 0 & 0 & \cdots & 0 & 0 \\ \vdots & \vdots & & \vdots & \vdots \\ 0 & 0 & \cdots & 0 & 0 \end{bmatrix} \text{ and}$$

$$\mathbf{T}(\mathbf{x}) = \begin{bmatrix} 0 & 0 & \cdots & 0 & 0 \\ s_1\sigma_1(\mathbf{x}) & 0 & \cdots & 0 & 0 \\ 0 & s_2\sigma_2(\mathbf{x}) & \cdots & 0 & 0 \\ \vdots & \vdots & & \vdots & \vdots \\ 0 & 0 & \cdots & s_{m-1}\sigma_{m-1}(\mathbf{x}) & s_m\sigma_m(\mathbf{x}) \end{bmatrix},$$

²Over the years various other names for this quantity have been used, including reproductive value and reproduction rate.

where all $\beta_i(\mathbf{0}_m) = \sigma_i(\mathbf{0}_m) = 1$. Note that the eigenvalues of the inherent transition matrix³

$$\mathbf{T}(\mathbf{0}_m) = \begin{bmatrix} 0 & 0 & \cdots & 0 & 0 \\ s_1 & 0 & \cdots & 0 & 0 \\ 0 & s_2 & \cdots & 0 & 0 \\ \vdots & \vdots & & \vdots & \vdots \\ 0 & 0 & \cdots & s_{m-1} & s_m \end{bmatrix}$$

are s_m and 0 (with multiplicity $m - 1$). Hence, the requirement $\rho(\mathbf{T}(\mathbf{0}_m)) = s_m < 1$ is met. The inherent reproduction number R_0 is given by formulas (2.29)–(2.30), namely

$$R_0 = \sum_{i=1}^{m-1} b_i \pi_i + b_m \pi_m \frac{1}{1 - s_m}$$

where

$$\pi_i = \begin{cases} 1 & \text{for } i = 1 \\ s_1 s_2 \cdots s_{i-1} & \text{for } i = 2, 3, \dots, m \end{cases}.$$

By Theorem 3.17, the extinction equilibrium is stable if $R_0 < 1$. The extinction equilibrium is unstable, and the model is persistent with respect to it, if $R_0 > 1$. \square

Example 3.19. A nonlinear version of the matrix model whose life cycle graph appears in Figure 2.5, which was used to study the dynamics of the American bullfrog, has the projection matrix

$$\mathbf{P}(\mathbf{x}) = \begin{bmatrix} 0 & 0 & 0 & 0 & b_{15}\beta_{15}(\mathbf{x}) \\ s_{21}\sigma_{21}(\mathbf{x}) & 0 & 0 & 0 & 0 \\ 0 & s_{32}\sigma_{32}(\mathbf{x}) & 0 & 0 & 0 \\ 0 & s_{42}\sigma_{42}(\mathbf{x}) & s_{43}\sigma_{43}(\mathbf{x}) & 0 & 0 \\ 0 & 0 & 0 & s_{54}\sigma_{54}(\mathbf{x}) & s_{55}\sigma_{55}(\mathbf{x}) \end{bmatrix}$$

with $\beta_{15}(\mathbf{0}_m) = \sigma_{ij}(\mathbf{0}_m) = 1$.

Note that the eigenvalues of the inherent transition matrix (a triangular matrix)

$$\mathbf{T}(\mathbf{0}_m) = \begin{bmatrix} 0 & 0 & 0 & 0 & 0 \\ s_{21} & 0 & 0 & 0 & 0 \\ 0 & s_{32} & 0 & 0 & 0 \\ 0 & s_{42} & s_{43} & 0 & 0 \\ 0 & 0 & 0 & s_{54} & s_{55} \end{bmatrix}$$

³Recall that the eigenvalues of a triangular matrix appear along the diagonal.

are 0 (with multiplicity 4) and s_{55} ; hence, $\rho(\mathbf{T}(\mathbf{0}_m)) = s_{55} < 1$. The inherent reproduction number R_0 was calculated in Section 2.5.2 to be

$$R_0 = b_{15}s_{21}s_{42}s_{54} \frac{1}{1 - s_{55}} + b_{15}s_{21}s_{32}s_{43}s_{54} \frac{1}{1 - s_{55}},$$

which can be used in Theorem 3.17 to determine the stability properties of the extinction equilibrium.

For example, using the parameter estimates given in the application to the American bullfrog given in Section 2.5.2, we saw that $R_0 \approx 4.84 \times 10^{-1} < 1$. Thus, for any nonlinear version of this model with these particular parameter estimates, the extinction equilibrium is stable. \square

3.3.3. Global Stability of the Extinction Equilibrium. Recall that local asymptotic stability of an equilibrium does not necessarily mean that all solutions $\mathbf{x}(t)$ approach the equilibrium as $t \rightarrow \infty$, but only those whose initial condition $\mathbf{x}(0)$ is sufficiently close to the equilibrium. Thus, when $r_0 < 1$ (or $R_0 < 1$), Theorem 3.13 or Theorem 3.17 does not necessarily imply that all solutions of a matrix model will approach the extinction equilibrium $\mathbf{x}_e = \mathbf{0}_m$ as $t \rightarrow \infty$. (We saw this in Chapter 1 when we discussed the strong Allee effect.) The following theorem provides a criterion, one that can often be verified in applications by simple observations of the entries in the projection matrix, that is sufficient to guarantee the *global* asymptotic stability of $\mathbf{x}_e = \mathbf{0}_m$ (i.e., global extinction) when $r_0 < 1$.

Theorem 3.20. *Assume the population projection matrix (3.7) satisfies, in addition to Assumption 3.3, the inequality*

$$(3.13) \quad \mathbf{P}(\mathbf{x}) \leq \mathbf{P}(\mathbf{0}_m) \text{ for all } \mathbf{x} \in R_+^m.$$

Then the extinction equilibrium $\mathbf{x}_e = \mathbf{0}_m$ of the matrix model equation (3.6) is globally asymptotically stable on R_+^m if $r_0 < 1$. If in addition $\rho(\mathbf{T}(\mathbf{0}_m)) < 1$, then $\mathbf{x}_e = \mathbf{0}_m$ is globally asymptotically stable on R_+^m if $R_0 < 1$.

The inequality (3.13) means that all of the entries of $\mathbf{P}(\mathbf{x})$ satisfy $p_{ij}(\mathbf{x}) \leq p_{ij}(\mathbf{0}_m)$ for all $\mathbf{x} \in R_+^m$; that is to say, either the effect of population density on an entry p_{ij} is absent (i.e., $p_{ij}(\mathbf{x}) = p_{ij}(\mathbf{0}_m)$) or it decreases $p_{ij}(\mathbf{x})$ from the inherent (density-free) value $p_{ij}(\mathbf{0}_m)$. If all density effects are harmless or deleterious in this sense, then (3.13) holds, and the matrix model predicts global extinction for $r_0 < 1$.

Proof. We know by Assumption 3.3 that, for any initial condition $\mathbf{x}(0) \in \mathbb{R}_+^m$, the solution of the matrix equation (3.6) satisfies $\mathbf{x}(t) \in \mathbb{R}_+^m$ for all $t \in Z_+$. Therefore, by 3.13,

$$(3.14) \quad \mathbf{0}_m \leq \mathbf{x}(t+1) = \mathbf{P}(\mathbf{x}(t))\mathbf{x}(t) \leq \mathbf{P}(\mathbf{0}_m)\mathbf{x}(t)$$

for all $t \in Z_+$. Let $\mathbf{y}(t)$ be the solution of the linear matrix equation

$$(3.15) \quad \mathbf{y}(t+1) = \mathbf{P}(\mathbf{0}_m)\mathbf{y}(t)$$

with initial condition $\mathbf{y}(0) = \mathbf{x}(0)$. From (3.14), we see that

$$\mathbf{0}_m \leq \mathbf{x}(1) \leq \mathbf{P}(\mathbf{0}_m)\mathbf{x}(0) = \mathbf{P}(\mathbf{0}_m)\mathbf{y}(0) = \mathbf{y}(1)$$

and that if $\mathbf{x}(t) \leq \mathbf{y}(t)$ for any $t \in Z_+$, then

$$\mathbf{0}_m \leq \mathbf{x}(t+1) \leq \mathbf{P}(\mathbf{0}_m)\mathbf{x}(t) \leq \mathbf{P}(\mathbf{0}_m)\mathbf{y}(t) = \mathbf{y}(t+1).$$

It follows by induction that

$$(3.16) \quad \mathbf{0}_m \leq \mathbf{x}(t) \leq \mathbf{y}(t) \text{ for all } t \in Z_+.$$

Since $\mathbf{y}(t)$ satisfies the linear matrix equation (3.15) and since $r_0 = \rho(\mathbf{P}(\mathbf{0}_m))$, it follows by Theorem 2.7 that $\mathbf{y}(t) \rightarrow \mathbf{0}_m$ for all $\mathbf{y}(0) \in \mathbb{R}_+^m$ and, as a result of inequality (3.16), that $\mathbf{x}(t) \rightarrow \mathbf{0}_m$ for all initial conditions $\mathbf{x}(0) \in \mathbb{R}_+^m$. \square

One can often make use of the global stability test criterion (3.13) by simple observation of the entries $p_{ij}(\mathbf{x})$. For example, all entries in the projection matrix

$$\mathbf{P}(\mathbf{x}) = \begin{bmatrix} 0 & b_2 \frac{1}{1+c_{21}x_1+c_{22}x_2} \\ s_1 \frac{1}{1+c_{11}x_1+c_{12}x_2} & 0 \end{bmatrix}$$

from Ebenman's model (3.3) either are unaffected or are decreasing as functions of x_1 and x_2 . Thus, (3.13) holds, and the extinction equilibrium of this matrix equation model is *globally asymptotically stable* if $r_0 = \sqrt{b_2 s_1} < 1$.

3.4. Positive Equilibria: A Basic Bifurcation Theorem

Theorem 3.13 and its Theorem 3.17 show that the extinction equilibrium of a matrix model

$$(3.17) \quad \mathbf{x}(t+1) = \mathbf{P}(\mathbf{x}(t))\mathbf{x}(t)$$

destabilizes as the inherent population growth rate $r_0 = \rho(\mathbf{P}(\mathbf{0}_m))$, or the inherent reproduction number R_0 , increases through 1. In Chapter 1, we saw for the case $m = 1$ that, in general, this loss of stability results in the creation of a branch of positive equilibria that bifurcates from the extinction equilibrium at $r_0 = 1$ (equivalently $R_0 = 1$). This basic bifurcation result when $m = 1$ provides the existence of positive equilibria and relates their stability to the direction of bifurcation, at least in a neighborhood of bifurcation point $x = 0$ at $r_0 = 1$. Our goal in this section is to extend this basic bifurcation phenomenon to matrix model equations (3.17) of dimension $m > 1$.

We assume Assumptions 3.3 and 3.5 are in force. Let \mathbf{v} and \mathbf{w} be, respectively, right and left (positive) eigenvectors of the inherent projection matrix $\mathbf{P}(\mathbf{0}_m) = [p_{ij}(\mathbf{0}_m)]$ associated with the dominant eigenvalue $r_0 = \rho(\mathbf{P}(\mathbf{0}_m))$. When $r_0 = 1$, define the quantity

$$(3.18) \quad \kappa := -\mathbf{w}^T [\nabla_x^0 p_{ij} \cdot \mathbf{v}] \mathbf{v},$$

where

$$\nabla_x^0 p_{ij} = \begin{bmatrix} \partial_{x_1}^0 p_{ij} \\ \partial_{x_2}^0 p_{ij} \\ \vdots \\ \partial_{x_m}^0 p_{ij} \end{bmatrix} = \begin{bmatrix} \partial_{x_1} p_{ij}(\mathbf{x})|_{\mathbf{x}_e=\mathbf{0}} \\ \partial_{x_2} p_{ij}(\mathbf{x})|_{\mathbf{x}_e=\mathbf{0}} \\ \vdots \\ \partial_{x_m} p_{ij}(\mathbf{x})|_{\mathbf{x}_e=\mathbf{0}} \end{bmatrix}$$

is the gradient of the projection matrix entry $p_{ij}(\mathbf{x})$ evaluated at $\mathbf{x}_e = \mathbf{0}_m$ and $r_0 = 1$. Note that the superscript “0” denotes, as it always will, an evaluation of the expression at the bifurcation point $\mathbf{x}_e = 0, r_0 = 1$. We saw κ when $m = 1$ in Chapter 1 (formula (1.28) in Section 1.2.1).

The following basic bifurcation theorem provides existence and stability results for positive equilibria of a general matrix equation (3.17); it follows from Theorems 3.1 and 4.1 in [44].

Theorem 3.21. *Assume the projection matrix of the matrix equation (3.17) satisfies Assumptions 3.3 and 3.5.*

- (a) *If $\kappa \neq 0$, then for r_0 near 1 there exist equilibria \mathbf{x} near the extinction equilibria $\mathbf{0}_m$, and their Taylor expansion has the form*

$$\mathbf{x} = \frac{\mathbf{w}^T \mathbf{v}}{\kappa} \mathbf{v} (r_0 - 1) + O((r_0 - 1)^2).$$

It follows that if $\kappa > 0$, then the equilibria $\mathbf{x} \in \text{int}(R_+^m)$ are positive for $r_0 \gtrsim 1$, in which case the bifurcation is said to be

forward. If $\kappa < 0$, then the equilibria $\mathbf{x} \in \text{int}(R_+^m)$ are positive for $r_0 \gtrsim 1$, and the bifurcation is said to be **backward**.

- (b) Suppose $\mathbf{P}(\mathbf{0}_m)$ is primitive when $r_0 = 1$. Then $\kappa > 0$ implies that the positive equilibria for $r_0 \gtrsim 1$ are (locally asymptotically) stable. If $\kappa < 0$, then the positive equilibria for $r_0 \gtrsim 1$ are unstable.

When $\kappa > 0$ in Theorem 3.21(b), stable positive equilibria come into existence as r_0 increases through 1; we call this a **forward-stable bifurcation**. When $\kappa < 0$, we call the bifurcation **backward-unstable**. The adjectives “forward” and “backward” come from the geometric view of the bifurcation when equilibria are plotted as functions of the bifurcation parameter, which is denoted in the usual way along a horizontal axis oriented with increasing values to the right. Thus, the direction of bifurcation and the stability properties of the bifurcating positive equilibria are correlated, and we say that the **direction of bifurcation** determines stability.⁴ Moreover, Theorem 3.21 tells us that it is the sign of κ that determines the direction of bifurcation (and hence the stability properties of the positive equilibria).

The strength of Theorem 3.21 is its generality. To apply it involves only the determination of the sign of κ (one does not need to calculate it, but only determine its sign), and from this, one gets existence and stability results for positive equilibria. One thereby avoids having to prove the existence of solutions to the equilibrium equation $\mathbf{x} = \mathbf{P}(\mathbf{x})\mathbf{x}$ and perform a linearized stability analysis of them.

It is also important to note the shortcoming of the theorem, which is that it yields the existence and stability properties of positive equilibria only in a neighborhood of the bifurcation point (i.e., for r_0 near 1 and positive equilibria near the extinction equilibria). In population models, there can be (and usually are) positive equilibria outside a neighborhood of the bifurcation point (whose existence and stability properties have to be dealt with in other ways). For example, we see in Section 3.5.4 in Chapter 1 when $m = 1$ how hysteresis and backward bifurcations can lead to multiple attractor scenarios when equilibria outside a neighborhood of the bifurcation point are taken into account.

⁴Sometimes a forward bifurcation is said to be supercritical or to-the-right and a backward bifurcation is subcritical or to-the-left.

The inherent growth rate r_0 does not, in general, appear explicitly in a matrix equation. Instead it derives from the entries in the inherent projection matrix $\mathbf{P}(0_m)$ and hence is a function of some or all parameters appearing in the model. Given the lack of an explicit formula for r_0 in terms of these parameters, it can be a challenge to determine when r_0 passes through 1 when a selected model parameter of interest is manipulated. For a model with specific numerical values for the inherent parameters, this can be studied by numerical means with the aid of a computer. For a more general study of the bifurcation when r_0 passes through 1, we turn to the reproduction number R_0 , for which one often has an explicit formula, as we saw in Chapter 2. Combining Theorem 3.21 with Theorem 2.15, we have the following bifurcation result for a general matrix equation (3.17).

Theorem 3.22. *If $\rho(\mathbf{T}(0_m)) < 1$, then Theorem 3.21 holds with R_0 in place of r_0 .*

The sign of the diagnostic quantity κ determines the direction of bifurcation in Theorems 3.21 and 3.22. Since the eigenvectors \mathbf{w} and \mathbf{v} are positive vectors, we see from the formula (3.18) for κ that its sign depends on the partial derivatives $\partial_{x_k} p_{ij}(\mathbf{0})$ of the entries $p_{ij}(\mathbf{x})$ in the projection matrix with respect to the densities x_i in the population vector $\mathbf{x} = \text{col}(x_i)$ (evaluated at the bifurcation point $r_0 = 1$). These derivatives measure the effects that increases in low level densities have on the vital rates modeled by the entries $p_{ij}(\mathbf{x})$. One can often make use of this observation and apply the theorems by simply “eyeballing” the entries in the population projection matrix. Here is an example.

Corollary 3.23. *The bifurcation of positive equilibria in Theorem 3.21 (or in Theorem 3.22) is forward-stable if all $\partial_{x_k} p_{ij}(\mathbf{0}) \leq 0$ and at least one is negative.*

Example 3.24. The projection matrix $\mathbf{P}(\mathbf{x}) = \mathbf{F}(\mathbf{x}) + \mathbf{T}(\mathbf{x})$ with

$$\mathbf{F}(\mathbf{x}) = \begin{bmatrix} 0 & b \frac{1}{1+c_2 x_2} \\ 0 & 0 \end{bmatrix}, \quad \mathbf{T}(\mathbf{x}) = \begin{bmatrix} 0 & 0 \\ s_1 \frac{1}{1+c_1 x_1} & s_2 \end{bmatrix},$$

$$c_1, c_2 > 0, \quad b > 0, \quad \text{and} \quad 0 < s_1, s_2 < 1$$

defines the dynamics of a juvenile-adult population (the unit of time is the juvenile maturation period) in which the only effects of density are those of adults on their fertility rate and juveniles on their own survival

rate. Since $s_2 > 0$, we see by Theorem 2.12 that the inherent projection matrix

$$\mathbf{P}(\mathbf{0}_2) = \begin{bmatrix} 0 & b \\ s_1 & s_2 \end{bmatrix}$$

is primitive (unlike the semelparous models of Ebenman in Example 3.1), as is required in Theorems 3.21 and 3.22.

Since the only density factors $1/(1 + c_i x_i)$ in the projection matrix are (strictly) decreasing functions of $x_i \geq 0$, we conclude from Corollary (3.23) that $\kappa > 0$ and that a forward-stable bifurcation occurs at $r_0 = 1$ or equivalently $R_0 = 1$.

In this $m = 2$ dimensional example, formulas for both r_0 and R_0 , in terms of the three entries in $\mathbf{P}(\mathbf{0}_2)$, are readily available. From the quadratic characteristic polynomial $\lambda^2 - s_2\lambda - bs_1$ of $\mathbf{P}(\mathbf{0}_2)$, we obtain

$$r_0 = \frac{1}{2}s_2 + \frac{1}{2}\sqrt{s_2^2 + 4bs_1}.$$

The projection matrix $\mathbf{P}(\mathbf{0}_2)$ is a Leslie matrix for which (Chapter 1)

$$R_0 = b \frac{s_1}{1 - s_2}.$$

From either of these formulas, we can see how changes in any or all of the inherent rates b , s_1 , and s_2 in $\mathbf{P}(\mathbf{0}_2)$ can cause r_0 and R_0 to increase through 1 and, as a result, cause a forward-stable bifurcation of positive equilibria. For example, increasing the adult birth rate b through $b_0 = (1 - s_2)/s_1$ causes a forward-stable bifurcation. See Figures 3.2 and 3.3.

For more on this juvenile-adult model, see Exercise 3.41. □

We can use several kinds of graphs to visualize the bifurcation phenomenon in Theorem 3.21 geometrically. In Chapter 1, when $m = 1$, we drew **bifurcation diagrams** by plotting equilibria as a function of a selected bifurcation parameter. For models of higher dimension $m \geq 2$, equilibria are vectors, and we have to decide how to represent them in a similar bifurcation diagram. One way is to plot a selected component of the equilibrium vector and plot it against the bifurcation parameter. For example, for the juvenile-adult model in Example 3.24, we could plot either the juvenile or adult component of the equilibrium as a function of b . Another option is to plot the total population size $\|\mathbf{x}\| = \sum_{i=1}^m x_i$. See Figure 3.2.

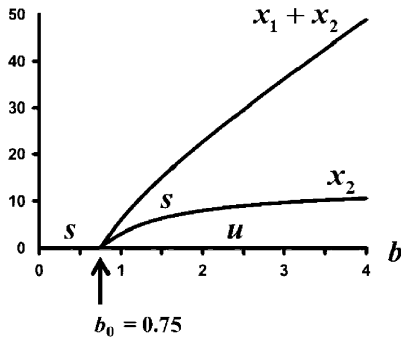


Figure 3.2. Shown are two bifurcation diagrams for the iteroparous juvenile-adult model in Example 3.24 using b as the bifurcation parameter. One plot shows the adult component x_2 of the positive equilibria, while the other plot shows the total population size $x_1 + x_2$. The extinction equilibrium destabilizes at $b_0 = (1 - s_2) / s_1$ where a forward-stable bifurcation occurs. Model parameter values used are $s_1 = 0.8$, $s_2 = 0.4$, $c_1 = 0.1$, and $c_2 = 0.01$, which yields $b_0 = 0.75$.

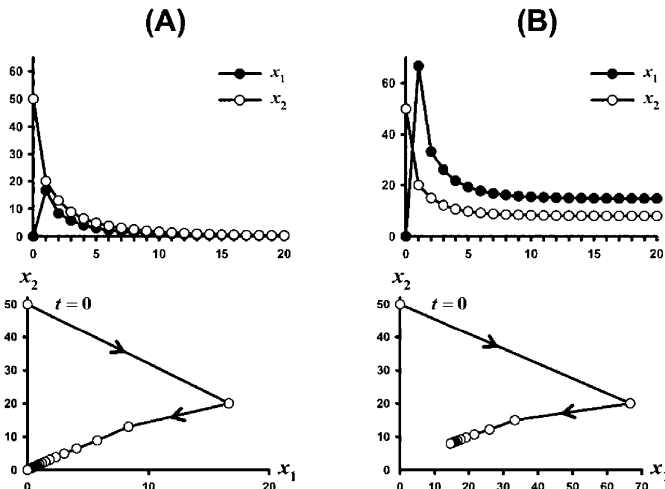


Figure 3.3. One sample solution of the iteroparous juvenile-adult model in Example 3.24, with initial conditions $\mathbf{x}(0) = \text{col}(0, 50)$ and the same parameter values as in Figure 3.2, is shown as time series and as an orbit in the (x_1, x_2) -plane in the plots in column (A) with $b = 0.5 < b_0 = 0.75$ and in column (B) with $b = 2 > b_0$. The population goes extinct in (A) and survives in (B), as predicted by Theorem 3.21.

We can also illustrate equilibria and their stability properties by **time series plots** of the components $x_i(t)$ of selected sample solutions $\mathbf{x}(t) = \text{col}(x_i(t))$. See Figure 3.3(A) for the juvenile-adult model in Example 3.24. For that example, and other $m = 2$ dimensional models, we can also plot selected **orbits** $\mathbf{x}(t) = \text{col}(x_1(t), x_2(t))$ in the **phase plane** (x_1, x_2) -plane, as in Figure 3.3.

Example 3.25. Nonlinear Leslie matrices with fertility and transitions matrices $\mathbf{F}(\mathbf{x})$ and $\mathbf{T}(\mathbf{x})$, as described in Example 3.18, have been widely used to model fish populations. For example, the matrix model with density dependence appearing in only the age-class specific fertility rates (called recruitment rates in fishery models)

$$\mathbf{F}(\mathbf{x}) = \begin{bmatrix} b_1\beta_1(\mathbf{x}) & b_2\beta_2(\mathbf{x}) & \cdots & b_{m-1}\beta_{m-1}(\mathbf{x}) & b_m\beta_m(\mathbf{x}) \\ 0 & 0 & \cdots & 0 & 0 \\ 0 & 0 & \cdots & 0 & 0 \\ \vdots & \vdots & & \vdots & \vdots \\ 0 & 0 & \cdots & 0 & 0 \end{bmatrix} \text{ and}$$

$$\mathbf{T}(\mathbf{x}) = \begin{bmatrix} 0 & 0 & \cdots & 0 & 0 \\ s_1 & 0 & \cdots & 0 & 0 \\ 0 & s_2 & \cdots & 0 & 0 \\ \vdots & \vdots & & \vdots & \vdots \\ 0 & 0 & \cdots & s_{m-1} & s_m \end{bmatrix}$$

with $b_i \geq 0$ and $0 < s_i < 1$ for all i and $b_m > 0$

is studied in [102] with fertility density factors of Ricker form

$$\beta_i(\mathbf{x}) = \exp(-c_i p_i), \quad c_i \geq 0,$$

where $p_i = \sum_{j=1}^m w_{ij} x_j$ is a weighted total population density with weights $w_{ij} \geq 0$ (but not all 0). The reason a weighted total population is used is that not all classes necessarily have the same effect on the fertilities of their own or other age classes. The use of such exponentially decreasing factors in fishery models is attributed to W. E. Ricker [117], [118].

Some density effects can be absent, but we assume not all are (otherwise the model is linear), that is we assume at least one $c_i > 0$. Then, because these exponential density effects are decreasing functions of x_i ,

we are assured $\kappa > 0$ and, by Corollary 3.23, that a forward-stable bifurcation of positive equilibria occurs as r_0 , or equivalently

$$R_0 = \sum_{i=1}^{m-1} b_i \pi_i + b_m \pi_m \frac{1}{1 - s_m} \quad \text{and}$$

$$\pi_i = \begin{cases} 1 & \text{for } i = 1 \\ s_1 s_2 \cdots s_{i-1} & \text{for } i = 2, 3, \dots, m \end{cases},$$

increases through 1. \square

Historically, negative density effects, by which we mean a decrease in an entry in the projection matrix with an increase in population density (i.e., $\partial_{x_k} p_{ij}(\mathbf{0}_m) < 0$), are the most common density effect found in population models. This is because it is generally assumed that increased density leads to lower survival and fertility rates, through such things as competition for food, mates, nesting sites, and so on. However, as discussed in Chapter 1, positive density effects when population densities are low (which are called **Allee component effects**) have been documented in many biological populations. They can be the result of numerous mechanisms, including enhanced protection from predators, cooperative hunting or offspring rearing, ability to local mates, and many more [26]. A model that includes such a density effect would include one or more positive derivatives $\partial_{x_k} p_{ij}(\mathbf{0}_m) > 0$. In this case, as one can see from the formula (3.18), there is the possibility that $\kappa < 0$ and that, as a result, the bifurcation of positive equilibria at $r_0 = 1$ (or $R_0 = 1$) is backward-unstable. If, in the projection matrix of a model, both positive and negative effects at low densities are present and hence derivatives $\partial_{x_k} p_{ij}(\mathbf{0}_m)$ of different signs occur, then κ needs to be calculated in order to determine if it is positive or negative.

Consider the general juvenile-adult matrix model with fertility and transition matrices

$$(3.19) \quad \mathbf{F}(\mathbf{x}) = \begin{bmatrix} 0 & b\beta(\mathbf{x}) \\ 0 & 0 \end{bmatrix} \quad \text{and} \quad \mathbf{T}(\mathbf{x}) = \begin{bmatrix} 0 & 0 \\ s_1\sigma_1(\mathbf{x}) & s_2\sigma_2(\mathbf{x}) \end{bmatrix}$$

with $b > 0$, $0 < s_1, s_2 < 1$,

and $\mathbf{x} = \text{col}(x_1, x_2)$. The inherent projection matrix and inherent reproduction number are

$$\mathbf{P}(\mathbf{0}_2) = \begin{bmatrix} 0 & b \\ s_1 & s_2 \end{bmatrix}$$

and

$$(3.20) \quad R_0 = bs_1 \frac{1}{1 - s_2}$$

(see Example 3.15). When $R_0 = 1$, the matrix $\mathbf{P}(\mathbf{0}_2)$ has right and left eigenvectors

$$\mathbf{v}^0 = \begin{bmatrix} 1 - s_2 \\ s_1 \end{bmatrix} \quad \text{and} \quad \mathbf{w}^0 = \begin{bmatrix} s_1 \\ 1 \end{bmatrix},$$

respectively. The direction of the bifurcation of positive equilibria that occurs when the extinction equilibrium destabilizes as R_0 increases through 1 is determined by the sign of κ . The matrix

$$\begin{aligned} [\nabla_{\mathbf{x}}^0 p_{ij} \cdot \mathbf{v}^0] &= \begin{bmatrix} 0 & \frac{1-s_2}{s_1} \nabla_{\mathbf{x}}^0 \beta \cdot \mathbf{v}^0 \\ \nabla_{\mathbf{x}}^0 \sigma_1 \cdot \mathbf{v}^0 & \nabla_{\mathbf{x}}^0 \sigma_2 \cdot \mathbf{v}^0 \end{bmatrix} \\ &= \begin{bmatrix} 0 & \frac{1-s_2}{s_1} ((1-s_2) \partial_{x_1}^2 \beta + s_1 \partial_{x_2}^2 \beta) \\ (1-s_2) \partial_{x_1}^2 \sigma_1 + s_1 \partial_{x_2}^2 \sigma_1 & (1-s_2) \partial_{x_1}^2 \sigma_2 + s_1 \partial_{x_2}^2 \sigma_2 \end{bmatrix} \end{aligned}$$

appears in the formula (3.18) for κ , and a calculation shows

$$(3.21) \quad \begin{aligned} \kappa &= s_1 (1 - s_2)^2 (-\partial_{x_1}^0 \beta) + s_1^2 (1 - s_2) (-\partial_{x_2}^0 \beta) \\ &\quad + (1 - s_2)^2 (-\partial_1^0 \sigma_{x_1}) + s_1 (1 - s_2) (-\partial_2^0 \sigma_{x_1}) \\ &\quad + s_1 (1 - s_2) (-\partial_1^0 \sigma_{x_2}) + s_1^2 (-\partial_2^0 \sigma_{x_2}). \end{aligned}$$

As complicated as this formula is, we see that it is a linear combination (with positive coefficients) of all the derivatives $-\partial_{x_i} \beta_j(\mathbf{x})$ and $-\partial_{x_i} \sigma_j(\mathbf{x})$ appearing in the model, evaluated at $\mathbf{x}_e = \mathbf{0}_2$. If derivatives of mixed signs occur, then the direction of bifurcation is determined by the sign of this linear combination. Here is an example.

Example 3.26. In the juvenile-adult model with projection matrix (3.19), the term $b\beta(\mathbf{x})$ is the per capita density of newborns produced during a unit of time that survive to the next census. Write the inherent per adult fertility rate (per unit time) as $b = b_m s$ where b_m is its maximal possible newborn production if all newborns were to survive to the next census time and where s is the fraction that do in fact survive. Assume, in addition, that the production of newborns is a decreasing function of adult density, modeled by

$$b_m \frac{1}{1 + cx_2}, \quad c > 0,$$

but that newborn survival is an increasing function of adult density (because adults provide, as a group, protection from predators), modeled by

$$s \frac{1 + ax_2}{1 + sax_2}, \quad 0 < s < 1, \quad a > 0.$$

Note that this latter assumption implies newborn survival probability is s when $x_2 = 0$ and tends to 1 as adult density x_2 increases without bound. The coefficient a measures the strength of the adult protection of newborns, at low density, in the sense that

$$\left. \frac{d}{dx_2} \left(s \frac{1 + ax_2}{1 + sax_2} \right) \right|_{x_2=0} = as(1-s),$$

which means a larger value of $a > 0$ yields a faster increase in newborn survival when adults density increasing. We call a the *Allee coefficient*.

These assumptions lead to

$$b = b_m s \quad \text{and} \quad \beta(\mathbf{x}) = \frac{1}{1 + cx_2} \frac{1 + ax_2}{1 + sax_2}$$

in the projection matrix (3.19). Here,

$$b_m, c, a > 0 \quad \text{and} \quad 0 < s < 1.$$

Assuming no density dependence in the juvenile or adult survival rates, we have the fertility and transition matrices

$$(3.22) \quad \mathbf{F}(\mathbf{x}) = \begin{bmatrix} 0 & b_m s \frac{1}{1+cx_2} \frac{1+ax_2}{1+sax_2} \\ 0 & 0 \end{bmatrix} \quad \text{and} \quad \mathbf{T}(\mathbf{x}) = \begin{bmatrix} 0 & 0 \\ s_1 & s_2 \end{bmatrix}.$$

We know that the extinction equilibrium destabilizes as

$$(3.23) \quad R_0 = b_m s \frac{s_1}{1 - s_2}$$

increases through 1 and that a bifurcation of positive equilibria occurs as a result. But is the bifurcation forward-stable or backward-unstable?

From formula (3.21), we have

$$\kappa = -s_1^2 (1 - s_2) \partial_{x_2}^0 \beta,$$

and a calculation shows

$$\kappa = ss_1^2 b_m (1 - s_2) (c - (1 - s) a).$$

The sign of κ is the same as that of the factor $c - (1 - s) a$. We conclude by Theorem 3.22 that the bifurcation at $R_0 = 1$ is

- backward-unstable if $\frac{a}{c} > \frac{1}{1-s}$;
- forward-stable if $\frac{a}{c} < \frac{1}{1-s}$.

In other words, if the Allee coefficient a is small relative to the negative density effects on the fertility, as measured by c , then the bifurcation is forward-stable.

On the other hand, if the Allee coefficient a is large enough relative to c , then the bifurcation is backward-unstable. In this case, the

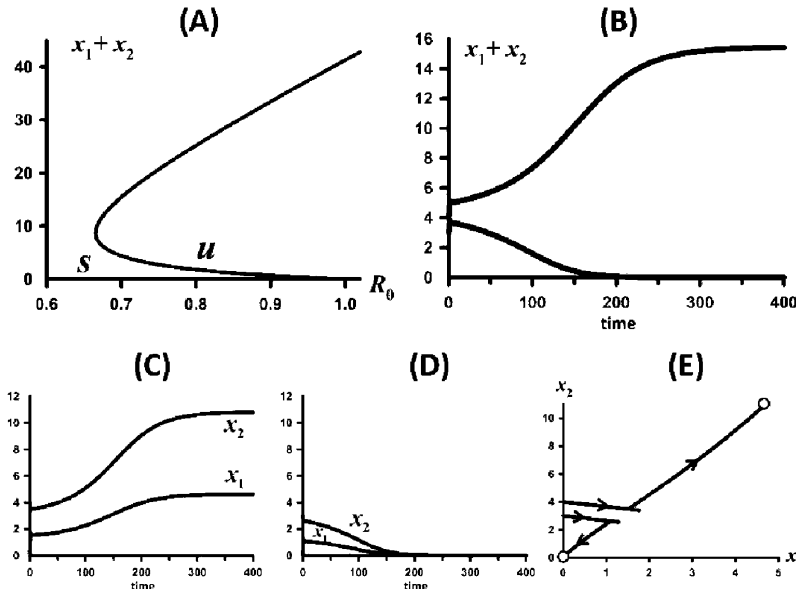


Figure 3.4. These plots illustrate a backward bifurcation, and the resulting strong Allee effect, that can occur in the juvenile-adult model in Example 3.26. Plot (A) shows the (backward) bifurcation diagram by plotting total population size at equilibrium as a function of R_0 when $s = 0.20$, $s_1 = 0.35$, and $s_2 = 0.85$. Plot (B) shows the time series of total population size $x_1(t) + x_2(t)$ for two sample solutions when $R_0 = 0.70$ (i.e., $b_m = 1.5$). Model coefficients are $c = 0.10$ and $a = 0.45$, and the initial conditions are $\text{col}(x_1(0), x_2(0)) = \text{col}(0, 4)$ and $\text{col}(0, 3)$. The first leads to survival and the second to extinction, which is the signature of a strong Allee effect. The two plots (C) and (D) show the time series of the individual juvenile and adult classes for the two solutions shown in (B). Plot (E) shows the orbits of these two solutions in the phase plane.

expectation is that a strong Allee effect occurs and that for $R_0 < 1$ there exist stable positive equilibria outside the neighborhood of the bifurcation point. That this does occur in this model is illustrated by sample numerical simulation examples shown in Figure 3.4. \square

It is important to remember that the bifurcation Theorem 3.21 and Theorem 3.22 are local bifurcation results; that is to say, they imply the existence and stability properties of positive equilibria only in a neighborhood of the bifurcation point (i.e., for r_0 and R_0 near 1 and positive equilibria near the extinction equilibria). The strength of these results is their generality, making them applicable to a most (if not the vast majority) of models used in population dynamic modeling. They do not, however, account for positive equilibria and parameter values outside a neighborhood of the bifurcation point.

3.5. Secondary Bifurcations

The existence and stability properties of positive equilibria outside a neighborhood of the bifurcation point must be ascertained by methods other than the local bifurcation results in Theorem 3.21 and Theorem 3.22. For the $m = 1$ dimensional case, we saw in Chapter 1 that the stability properties of the bifurcating positive equilibria might not persist outside a neighborhood of the bifurcation point. For example, we saw in Figure 1.5 that the positive equilibria from forward-stable bifurcation of the Ricker equation destabilize as $r_0 = R_0 = b_0$ increases and results in a bewildering sequence of bifurcations that involve periodic cycles and ultimately “chaos.” On the other hand, we saw that the positive equilibria of the discrete logistic equation remain stable for all $b_0 = r_0 = R_0$. Also, in Chapter 1, we saw unstable positive equilibria from a backward-unstable bifurcation become stable at a tipping point (tangent bifurcation) that creates a strong Allee effect; see Figure 1.3. Therefore, it is reasonable to expect that such phenomena can also occur in matrix models of dimension $m > 1$.

These examples, in the $m = 1$ case, show that the nature of the dynamics, outside of a neighborhood of the “primary” bifurcation point $\mathbf{x}_e = \mathbf{0}_m$ at $r_0 = 1$, is highly dependent on special features of the model equation under consideration and that general results concerning the existence and stability of equilibria (or of other attractors, such as periodic cycles) will not be possible without more restrictive assumptions

on the model's nonlinearities than those required for Theorem 3.21 and Theorem 3.22.⁵

Consider the case of a forward-stable bifurcation as the extinction equilibrium destabilizes when r_0 or R_0 increases through 1. The resulting positive equilibria for $r_0 > 1$, which are stable for $r_0 \lesssim 1$, might destabilize for larger values of r_0 , say as r_0 increases through a number $r_0^* > 1$. That is to say, the positive equilibria are stable for $r_0 < r_0^*$ and unstable for $r_0 \gtrsim r_0^*$. By the Linearization Principle this occurs if the Jacobian associated with the matrix model, when evaluated at the positive equilibria, has an eigenvalue λ that leaves the unit circle in the complex plane (i.e., $|\lambda| < 1$ for $r_0 < r_0^*$ and $|\lambda| > 1$ for $r_0 \gtrsim r_0^*$). Recall that eigenvalues, being roots of the characteristic polynomial, are either real or come in complex conjugate pairs.

An eigenvalue can leave the unit complex circle in one of three ways: λ can leave the unit complex circle through $+1$, -1 , or a complex number $\alpha + i\beta$, $\beta \neq 0$ with $\alpha^2 + \beta^2 = 1$. In the latter case, the eigenvalue's complex conjugate also leaves the complex unit circle. Each of these three cases results in a different kind of bifurcation. In the $+1$ case, the bifurcation involves equilibria, while in the -1 case, it involves 2-cycles. In the complex case, the bifurcation involves a more complicated attractor (to be described as follows). In this section, we informally describe and give examples that illustrate the basic kinds of bifurcations that typically occur in these cases. We do not attempt a complete list of all possibilities, since that is beyond the scope of this book (and is unnecessary for our applications to population dynamics). More rigorous mathematical theorems concerning these bifurcations (which can be found in [62], [63] and in many other advanced books on bifurcation theory) involve the calculation of diagnostic quantities that determine the nature of the bifurcation (its direction, the stability properties of the attractors involved, etc.), some of which are straightforward, but others of which can be difficult or even intractable to use in applications. A common practice in the latter case is to utilize numerical simulations to determine the detailed nature of a bifurcation, which will be our approach in this section.

Our focus will remain on **local bifurcations**, by which we mean those that occur in a neighborhood of a bifurcation point and can be

⁵An exception is that, in general, the bifurcating branch of positive equilibria has been shown to have a global extent [28], [31].

studied by means of linearization procedures. Other types of bifurcations for which this is not possible, called global bifurcations, can mathematically occur in nonlinear models but have not played a significant role (to date) in structured population dynamics. For this reason, we do not discuss them here.

We saw in Chapter 1, by means of the famous Ricker difference equation (Example 1.15), that bifurcations to new types of attractors can also occur when nonequilibrium attractors, such as periodic cycles, destabilize. The bifurcation diagram in Figure 1.5 associated with the Ricker equation is an iconic example of what is possible for a nonlinear model as r_0 increases: repeated bifurcations occur as attractors destabilize and new ones appear, ultimately resulting in very complicated attractors and dynamics. Of course, such a so-called route-to-chaos does not always occur, as the discrete logistic equation (which has no secondary bifurcations at all) shows; see the bifurcation diagram for the discrete logistic equation in Figure 1.3(A). Of course we would expect (and will see in following examples and applications) the same breadth of dynamic and bifurcation possibilities for nonlinear matrix models of dimension $m > 1$ as well.

Before we have a look at bifurcations in nonlinear matrix models, we pause for a moment to look at $m = 2$ dimensional *linear* matrix equations $\mathbf{x}(t + 1) = \mathbf{P}\mathbf{x}(t)$ where \mathbf{P} is a 2×2 matrix with eigenvalues λ_1 and λ_2 , which we assume are different ($\lambda_1 \neq \lambda_2$). This will offer some insight into the three basic bifurcations for nonlinear matrix equations to be discussed as follows.

If \mathbf{v}_1 and \mathbf{v}_2 are eigenvectors associated with λ_1 and λ_2 , respectively, then they are independent because $\lambda_1 \neq \lambda_2$, and we can use them as a basis of \mathbb{R}^2 . For any initial condition $\mathbf{x}(0) \in \mathbb{R}^2$, we have $\mathbf{x}(0) = c_1\mathbf{v}_1 + c_2\mathbf{v}_2$ for scalar coordinates c_i , and by iteration of the linear matrix equation, we get the solution formula

$$(3.24) \quad \mathbf{x}(t) = c_1\lambda_1^t\mathbf{v}_1 + c_2\lambda_2^t\mathbf{v}_2.$$

Consider the following scenario. We start with both eigenvalues satisfying $|\lambda_i| < 1$ (i.e., they lie inside the unit disk in the complex plane) and then continuously change λ_1 so that eventually $|\lambda_1| > 1$, all the while keeping $\lambda_1 \neq \lambda_2$. To do this, λ_1 must cross the boundary of the unit disk (i.e., at some point $|\lambda_1| = 1$). We distinguish three possibilities when this

occurs: (i) $\lambda_1 = 1$, (ii) $\lambda_1 = -1$, and (iii) $\lambda_1 = e^{i\theta}$ and $\lambda_2 = e^{-i\theta}$ for some polar angle $0 < \theta < \pi$.

In case (i), we find that $\mathbf{x}(t) - c_1 \mathbf{v}_1 = c_2 \lambda_2^t \mathbf{v}_2 \rightarrow 0$ as $t \rightarrow \infty$ (since $|\lambda_2| < 1$). Note that $c_1 \mathbf{v}_1$ is an equilibrium. This is because it is $\mathbf{0}_2$ if $c_1 = 0$ and it is an eigenvector of \mathbf{P} associated with eigenvalue +1 if $c_1 \neq 0$. We conclude in this case that all solutions approach an equilibrium.

In case (ii), we find that $\mathbf{x}(t) - c_1 (-1)^t \mathbf{v}_1 = c_2 \lambda_2^t \mathbf{v}_2 \rightarrow 0$ as $t \rightarrow \infty$. Note that $(-1)^t \mathbf{v}_1$ is a solution of the matrix equation (as an exercise, the reader should check this) which is periodic with period 2. We conclude in this case that all solutions approach a 2-cycle.

Case (iii) is more complicated. The eigenvalues and their eigenvectors are complex conjugates, as are the coordinates c_i . Thus, the solution formula (3.24) becomes $\mathbf{x}(t) = 2 \operatorname{Re}(c_1 e^{i\theta t} \mathbf{v}_1)$ which, if we write

$$c_1 = a + bi, \quad e^{i\theta t} = \cos \theta t + i \sin \theta t, \quad \text{and} \quad \mathbf{v}_1 = \begin{bmatrix} u_1 + iv_1 \\ u_2 + iv_2 \end{bmatrix}$$

(where a, b and u_i, v_i are real), becomes

$$(3.25) \quad \mathbf{x}(t) = \begin{bmatrix} (au_1 - bv_1) \cos \theta t - (av_1 + bu_1) \sin \theta t \\ (au_2 - bv_2) \cos \theta t - (av_2 + bu_2) \sin \theta t \end{bmatrix}.$$

The solution $\mathbf{x}(t)$ is periodic with period $p \in \mathbb{Z}_+$ if and only if $\mathbf{x}(t+p) = \mathbf{x}(t)$ for all $t \in \mathbb{Z}_+$, which occurs if and only if $\cos \theta(t+p) = \cos \theta t$ and $\sin \theta(t+p) = \sin \theta t$ or, in other words, $\theta p = 2\pi q$ for some integer $q \in \mathbb{Z}_+$. The solution in this case is a p -cycle if and only if θ is “rationally related to 2π ,” by which is meant $2\pi/\theta$ is a rational number. Otherwise, the solution is a bounded and oscillatory, but not necessarily periodic. There is a sophisticated theory of such kinds of oscillatory or “almost periodic” functions, but it goes beyond the level of this book. For our purposes, suffice it to say that the solutions in this case are either periodic or nonperiodic but bounded and oscillatory. Another fruitful way to view these solutions in this case is to plot their orbits in the (x_1, x_2) -plane. From analytic geometry, the plot of the solution (3.25) in this “phase-plane” lies on an ellipse centered at the origin, which is called an **invariant loop**.

In summary, for a two-dimensional linear matrix equation, under the scenario previously described, the asymptotic dynamics involves equilibria when $\lambda_1 = 1$, 2-cycles when $\lambda_1 = -1$, and invariant loops of either periodic or nonperiodic oscillatory solutions when $\lambda_1 = e^{i\theta}$.

These three cases and their associated dynamics play a role in bifurcations appearing in nonlinear matrix equations as well. In the sections that follow we give descriptions of these three basic types of bifurcations, but we will not delve into technical details (for which one can refer to any number of textbooks treating bifurcation theory; e.g., [63], [62], [132]).

3.5.1. +1 Bifurcations and Equilibria. The bifurcation caused by the destabilization of the extinction equilibrium $\mathbf{x}_e = \mathbf{0}_m$, as described in Theorem 3.21 for the general matrix equation (3.17), is an example of a **+1 bifurcation**. This type of bifurcation occurs when an equilibrium \mathbf{x}_e destabilizes because an eigenvalue of the Jacobian leaves the unit circle in the complex plane by passing through +1.

The bifurcation in Theorem 3.21 is a special type of +1 bifurcation called a **transcritical bifurcation** because two different branches of equilibria intersect at the bifurcation point, specifically the branch of extinction equilibria and a branch of nonextinction equilibria. A transcritical bifurcation is characterized by the existence, *in a neighborhood of a bifurcation point*, of two equilibria for r_0 on each side of the critical value $r_0 = r_0^*$ (i.e., there are two equilibria for $r_0 \lesssim r_0^*$ and two equilibria for $r_0 \gtrsim r_0^*$). Moreover, an **exchange of stability** between the two branches typically occurs (but not always, as we will see in Section 3.6). While Theorem 3.21 implies that a transcritical bifurcation involving the extinction equilibrium generally occurs in nonlinear matrix models, transcritical bifurcations involving two branches of positive equilibria are not as commonly found in population models.

A different type of +1 bifurcation is exemplified by the $m = 1$ dimensional model equations in Examples 1.16 and 1.21 that exhibit strong Allee and hysteresis effects. There is a loss (or gain) of stability between the upper and lower branches of parabolic-shaped tipping points in the bifurcation diagrams, seen in Figures 1.3(C) and 1.4, because the eigenvalue of the Jacobian is passing through +1. Such tipping points can also occur in $m > 1$ dimensional matrix equations. Here is an example.

Example 3.27. Consider the juvenile-adult matrix model in Example 3.26 with coefficients

$$s = 0.20, \quad s_1 = 0.35, \quad s_2 = 0.85, \quad c = 0.10, \quad \text{and} \quad a = 0.45$$

used in Figure 3.4. From the formula (3.23) for the inherent net reproduction number, we replace sb_m by

$$sb_m = \frac{1 - s_2}{s_1} R_0$$

in the projection matrix (3.22) to obtain

$$\mathbf{P}(\mathbf{x}) = \begin{bmatrix} 0 & 0.42857R_0 \frac{1}{1+0.10x_2} \frac{1+0.45x_2}{1+0.20(0.45)x_2} \\ 0.35 & 0.85 \end{bmatrix}.$$

In this example, we can solve the equilibrium equations

$$\begin{aligned} x_1 &= 0.42857R_0 \frac{1}{1 + 0.10x_2} \frac{1 + 0.45x_2}{1 + 0.20(0.45)x_2} x_2 \quad \text{and} \\ x_2 &= 0.35x_1 + 0.85x_2 \end{aligned}$$

for equilibria $\text{col}(x_1, x_2) \neq \text{col}(0, 0)$ as follows. Solve the second equation for $x_1 = 0.43x_2$ and place the answer into the first equation. This gives an equation for x_2 alone, which after a cancellation of a common factor of x_2 from both sides and the clearing of fractions, results in a quadratic polynomial in x_2 . The quadratic formula yields two positive solutions

$$(3.26) \quad x_2 = 25R_0 - 10.56 \pm 25\sqrt{R_0^2 - 0.67R_0 + 0.49 \times 10^{-3}}$$

and hence two positive equilibria $\text{col}(0.43x_2, x_2)$ provided R_0 lies in the interval $0.67 < R_0 < 1$. (The solution with the plus sign is also positive

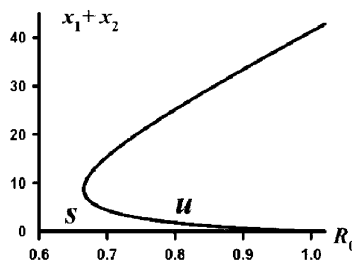


Figure 3.5. The bifurcation diagram for the juvenile-adult model in Example 3.27. The total population size at equilibrium is plotted against the inherent reproduction number R_0 , which shows a backward-unstable bifurcation at $R_0 = 1$ and a +1 bifurcation (tipping point) at $R_0 = 0.67$.

for $R_0 \geq 1$.) The tipping point is located at $R_0 = 0.67$, where the two equilibria coalesce at $\text{col}(x_1, x_2) = \text{col}(2.66, 6.19)$. A calculation shows that the Jacobian evaluated at this equilibrium when $R_0 = 0.67$ is

$$\begin{bmatrix} 0 & 0.43 \\ 0.35 & 0.85 \end{bmatrix}$$

whose eigenvalues are $+1$ and -0.15 . This illustrates that the tipping point is a $+1$ bifurcation. See Figure 3.5. \square

Suppose the eigenvalues of the Jacobian evaluated at an equilibrium are all real numbers. If all eigenvalues have absolute value less than 1 (and hence the equilibrium is stable), then the equilibrium is called a **stable node**. If at least one eigenvalue has absolute value greater than 1 (and hence the equilibrium is unstable), then the equilibrium is called a **saddle node**. If a $+1$ bifurcation occurs because an equilibrium changes from a saddle to a node, or vice versa, then the bifurcation is called a **saddle-node bifurcation**. The bifurcation at the tipping point $R_0 = 0.67$ in Example 3.27 is a saddle-node bifurcation. In Exercise 3.43, it is shown that the equilibria on the “upper” branch are stable, at least near the tipping point; also see Section 3.5.4.

$+1$ bifurcations involve branches of equilibria (and typically an exchange or loss of stability between branches). There are other types of $+1$ bifurcations besides the transcritical and saddle-node bifurcations. If you restrict attention to a neighborhood of the bifurcation point, then a transcritical bifurcation is characterized by the changing number of equilibria from 2 to 1 to 2 when passing through the bifurcation point. For a saddle-node bifurcation, the equilibrium count changes from 0 to 2 or vice versa. Another type of $+1$ bifurcation, called a pitchfork bifurcation, is associated with an equilibrium count change from 1 to 3 (or vice versa). We will confine our attention in this book to transcritical and saddle-node bifurcations, which are the most common $+1$ bifurcations in structured population models.

3.5.2. -1 Bifurcations and 2-cycles. When an equilibrium destabilizes because one (but not more than one) eigenvalue of the Jacobian evaluated at the equilibrium leaves the unit circle in the complex plane through -1 , the result in general is the creation of 2-cycles (periodic solutions of period 2). This bifurcation is called a **period-doubling bifurcation** (or a flip bifurcation).

We saw an example of a period-doubling bifurcation in the $m = 1$ dimensional Ricker equation (see Figure 1.5). The following example illustrates a -1 bifurcation in a higher-dimensional matrix model that results in a period-doubling bifurcation (and a route-to-chaos similar to that seen in the Ricker equation).

Example 3.28. The $m = 2$ projection matrix

$$\mathbf{P}(\mathbf{x}) = \begin{bmatrix} 0 & be^{-c(x_1+x_2)} \\ s_1 & s_2 \end{bmatrix}$$

is an example of the general juvenile-adult projection matrix (3.19) in which adult fertility is negatively affected by increases in total population size $x_1 + x_2$. Figure 3.6 shows a bifurcation diagram for this matrix model with parameter values

$$c = 1, \quad s_1 = \frac{1}{2}, \quad \text{and} \quad s_2 = \frac{1}{4},$$

plotting total population size attractors against the inherent reproduction number

$$R_0 = b \frac{s_1}{1 - s_2} = \frac{2}{3}b.$$

The bifurcation diagram indicates a forward-stable bifurcation of positive equilibria at $R_0 = 1$ (which we know follows from Theorem 3.17 since the only density-dependent term in $\mathbf{P}(\mathbf{x})$ is strictly decreasing in x_1 and x_2). The diagram also shows a loss of equilibrium stability, roughly $R_0 \approx 3$, at which point there is a period-doubling bifurcation to 2-cycles. We can verify this loss of stability by means of the Linearization Principle as follows.

From the projection matrix

$$(3.27) \quad \mathbf{P}(\mathbf{x}) = \begin{bmatrix} 0 & \frac{3}{2}R_0 e^{-(x_1+x_2)} \\ \frac{1}{2} & \frac{1}{4} \end{bmatrix},$$

we obtain the equilibrium equations

$$\begin{aligned} x_1 &= \frac{3}{2}R_0 e^{-(x_1+x_2)}x_2 \quad \text{and} \\ x_2 &= \frac{1}{2}x_1 + \frac{1}{4}x_2 \end{aligned}$$

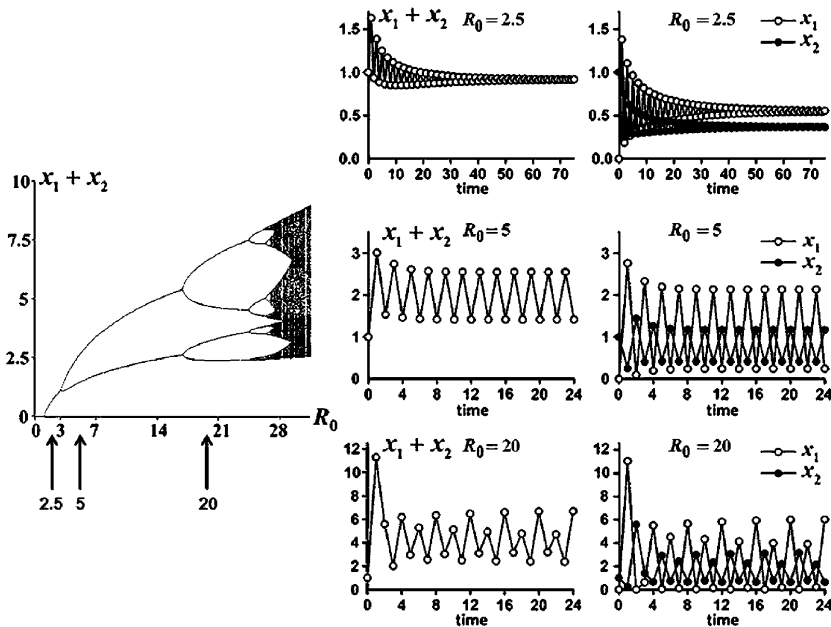


Figure 3.6. The bifurcation diagram, plotting total population size against R_0 , for the juvenile-adult model in Example 3.28 shows a -1 bifurcation at $R_0 = 3$ and a period-doubling cascade to chaos as R_0 increases. The displayed time series show sample solutions at three selected R_0 values, namely 2.5, 5, and 20. At $R_0 = 2.5$, the solution approaches an equilibrium; at $R_0 = 5$, the solution approaches a 2-cycle; and at $R_0 = 20$, the solution approaches a 4-cycle. These different attractors are those predicted by the bifurcation diagram.

whose solutions (other than the extinction equilibrium) are, provided $R_0 > 1$,

$$\begin{bmatrix} x_1 \\ x_2 \end{bmatrix} = \begin{bmatrix} \frac{3}{5} \ln R_0 \\ \frac{2}{5} \ln R_0 \end{bmatrix}.$$

The Jacobian matrix

$$(3.28) \quad J(\mathbf{x}) = \begin{bmatrix} -\frac{3}{2}R_0x_2e^{-(x_1+x_2)} & \frac{3}{2}R_0(1-x_2)e^{-(x_1+x_2)} \\ \frac{1}{2} & \frac{1}{4} \end{bmatrix}$$

evaluated at this positive equilibrium is

$$\begin{bmatrix} -\frac{3}{5} \ln R_0 & \frac{3}{2} - \frac{3}{5} \ln R_0 \\ \frac{1}{2} & \frac{1}{4} \end{bmatrix}.$$

It is left as Exercise 3.44 to show two things about the two eigenvalues of this matrix. First, both eigenvalues satisfy $|\lambda| < 1$ for

$$1 < R_0 < R_0^* = \exp\left(\frac{10}{9}\right) \approx 3;$$

hence, the positive equilibrium is stable for these R_0 values. Second, as R_0 increases through R_0^* , one of the eigenvalues decreases through -1 while the other satisfies $|\lambda| < 1$ (at least for R_0 not too large); hence, the positive equilibrium loses stability in a -1 bifurcation as R_0 increases through R_0^* . \square

As pointed out in Section 1.2.3 for $m = 1$ dimension difference equations, the existence and stability of 2-cycles of a matrix equation for any dimension $m \geq 1$ can be investigated by studying the equilibria of a composite of the matrix equation. Thus, for 2-cycles, setting

$$\mathbf{f}(\mathbf{x}) = \mathbf{P}(\mathbf{x})\mathbf{x},$$

we study the equilibria of the equation

$$\mathbf{x}(t+1) = \mathbf{f}^{(2)}(\mathbf{x}(t)),$$

where

$$\mathbf{f}^{(2)}(\mathbf{x}) = \mathbf{P}(\mathbf{P}(\mathbf{x})\mathbf{x})\mathbf{P}(\mathbf{x})\mathbf{x}.$$

This idea can be extended to p -cycles of any period. Applying the Linearization Principle to equilibria of the composite equation and using a chain rule for Jacobians (see Exercise 3.45), we have the following Linearization Principle for p -cycles.

Theorem 3.29. The Linearization Principle for cycles. *Assume $\mathbf{x}_i \in \Omega$ (for $i = 0, 1, \dots, p-1$) is a p -cycle of the difference equation $\mathbf{x}(t+1) = \mathbf{f}(\mathbf{x}(t))$ with $\mathbf{f} \in C^1(\Omega : \Omega)$ where $\Omega \subseteq \mathbb{R}^m$ is an open set. Then the p -cycle is locally asymptotically stable if $\rho(\mathbf{J}\mathbf{f}^{(p)}(\mathbf{x}_0)) < 1$ and is unstable if $\rho(\mathbf{J}\mathbf{f}^{(p)}(\mathbf{x}_1)) > 1$, where*

$$\mathbf{J}\mathbf{f}^{(p)}(\mathbf{x}_0) = \mathbf{J}\mathbf{f}(\mathbf{x}_{p-1})\mathbf{J}\mathbf{f}(\mathbf{x}_{p-2}) \cdots \mathbf{J}\mathbf{f}(\mathbf{x}_1)\mathbf{J}\mathbf{f}(\mathbf{x}_0).$$

To illustrate the application of this theorem, we return to the juvenile-adult model in Example 3.28.

Example 3.30. For the projection matrix (3.27) in Example 3.28, we found that the positive equilibrium destabilizes at $R_0 = R_0^*$, where $R_0^* = \exp(10/9) \approx 3$ where a -1 bifurcation occurs. The bifurcation diagram in Figure 3.6 indicates that the result is a period-doubling bifurcation to 2-cycles. Our goal in this example is to calculate analytically the 2-cycle and verify its stability, using Theorem 3.29, when $R_0 = 10$. We seek a fixed point of the composite of $\mathbf{f}(\mathbf{x}) = \mathbf{P}(\mathbf{x})\mathbf{x}$ with the projection matrix

$$\mathbf{P}(\mathbf{x}) = \begin{bmatrix} 0 & 15e^{-(x_1+x_2)} \\ \frac{1}{2} & \frac{1}{4} \end{bmatrix};$$

that is to say, fixed point

$$\mathbf{x}_0 = \begin{bmatrix} x_1 \\ x_2 \end{bmatrix}$$

of the composite $\mathbf{f}^{(2)}(\mathbf{x})$ for which $\mathbf{x}_1 = \mathbf{f}(\mathbf{x}_0) \neq \mathbf{x}_0$. Matrix multiplications give

$$\begin{aligned} \mathbf{x}_1 &= \mathbf{P}(\mathbf{x}_0)\mathbf{x}_0 = \begin{bmatrix} 15e^{-(x_1+x_2)}x_2 \\ \frac{1}{2}x_1 + \frac{1}{4}x_2 \end{bmatrix} \quad \text{and} \\ \mathbf{P}(\mathbf{x}_1)\mathbf{x}_1 &= \begin{bmatrix} \frac{15}{4}\exp\left(-\frac{1}{2}x_1 - \frac{1}{4}x_2 - 15e^{-(x_1+x_2)}x_2\right)(2x_1 + x_2) \\ \frac{1}{16}(2x_1 + x_2 + 120e^{-(x_1+x_2)}x_2) \end{bmatrix}. \end{aligned}$$

A fixed point $\mathbf{x}_0 = \mathbf{f}^{(2)}(\mathbf{x}_0)$ satisfies

$$\begin{bmatrix} x_1 \\ x_2 \end{bmatrix} = \begin{bmatrix} \frac{15}{4}\exp\left(-\frac{1}{2}x_1 - \frac{1}{4}x_2 - 15e^{-(x_1+x_2)}x_2\right)(2x_1 + x_2) \\ \frac{1}{16}(2x_1 + x_2 + 120e^{-(x_1+x_2)}x_2) \end{bmatrix},$$

which, by equating components, is equivalent to two algebraic equations for x_1 and x_2 . These highly nonlinear equations are not solvable explicitly, so we turn to the help of a computer equation solver. There are three solutions (rounded to 3 decimals):

$$\begin{bmatrix} 0 \\ 0 \end{bmatrix}, \quad \mathbf{x}_e \approx \begin{bmatrix} 1.382 \\ 0.921 \end{bmatrix}, \quad \text{and} \quad \mathbf{x}_0 \approx \begin{bmatrix} 3.652 \\ 0.553 \end{bmatrix}.$$

The first two are equilibria. The extinction equilibrium is unstable because $R_0 > 1$, and the positive equilibrium is, according to the analysis in Example 3.28, also unstable because $R_0 > R_0^*$. The third is the first term of the 2-cycle

$$\mathbf{x}_0 \approx \begin{bmatrix} 3.652 \\ 0.553 \end{bmatrix} \quad \text{and} \quad \mathbf{x}_1 = \mathbf{f}(\mathbf{x}_0) \approx \begin{bmatrix} 0.124 \\ 1.964 \end{bmatrix}.$$

To investigate the stability of this 2-cycle, we use the Jacobian (3.28) (with $R_0 = 10$) to calculate the product

$$\mathbf{J}\mathbf{f}^{(2)}(\mathbf{x}_0) = \mathbf{J}\mathbf{f}(\mathbf{x}_1)\mathbf{J}\mathbf{f}(\mathbf{x}_0) \approx \begin{bmatrix} -0.444 & -0.813 \\ 0.063 & 0.113 \end{bmatrix}$$

whose eigenvalues (to three decimals) are -0.003 and -0.328 . Thus,

$$\rho(\mathbf{J}\mathbf{f}^{(2)}(\mathbf{x}_0)) = 0.328 < 1,$$

and by Theorem 3.29, the 2-cycle is stable. \square

3.5.3. Neimark–Sacker Bifurcations. The third and final basic bifurcation caused by the destabilizing of an equilibrium that we will consider is the Neimark–Sacker bifurcation. This bifurcation is associated with the case when a complex eigenvalue leaves the unit circle in the complex plane at a complex number $e^{i\theta}$, $0 < \theta < \pi$. We saw in the previous preliminary discussion (preceding the discussion of +1 bifurcations) that when this occurs in a linear matrix equation, the result is an invariant loop in phase space and time series that are either periodic or complex nonperiodic oscillations. The Neimark–Sacker theorem [62], [132] guarantees the creation of such an invariant loop when an equilibrium destabilizes in this way for nonlinear matrix equations as well. As with +1 and -1 bifurcations, there are technical conditions that are required for the implementation of this theorem and that are needed to determine the direction of bifurcation and whether or not the invariant loop is attracting. (For example, the complex eigenvalues must not leave the unit circle at any of the first 4 roots of unity [i.e., $e^{ik\theta} \neq 1$ for $k = 1, 2, 3, 4$].) We will not concern ourselves with these technicalities in this book, but instead we will simply associate this kind of bifurcation with invariant loops and more complicated oscillatory time series and utilize computer simulations for their study. Here is an example.

Example 3.31. In the juvenile-adult model appearing in Example 3.28, adult fertility was negatively affected by increases in the total population size $x_1 + x_2$. Consider a modification of that same model that assumes adult fertility is affected by only increased adult population density x_2 (and juvenile population density x_1 plays no role). Figure 3.7 shows the bifurcation diagram of the matrix model with the resulting projection matrix

$$\mathbf{P}(\mathbf{x}) = \begin{bmatrix} 0 & \frac{3}{2}R_0e^{-cx_2} \\ s_1 & s_2 \end{bmatrix}$$

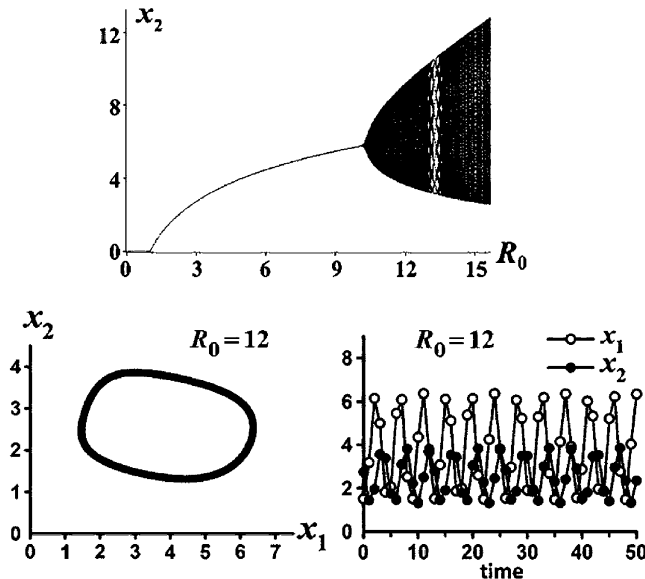


Figure 3.7. The bifurcation diagram for the juvenile-adult model in Example 3.31 shows a Neimark–Sacker bifurcation to an invariant loop at $R_0 = \exp(7/3) \approx 10.31$. The lower-left phase planes plot shows the invariant loop when $R_0 = 12$. The time series of a sample solution on the loop is displayed in the lower-right plot.

and the same parameters

$$c = 1, \quad s_1 = \frac{1}{2}, \quad \text{and} \quad s_2 = \frac{1}{4}$$

used in Example 3.28. The bifurcation from the extinction equilibrium at $R_0 = 1$ is forward-stable (the only density term in the projection matrix is a decreasing function of x_2). The bifurcation diagram in Figure 3.7 suggests that the destabilization of the bifurcating positive equilibria (at a value of R_0 slightly larger than 10) results in a Neimark–Sacker bifurcation to an invariant loop, rather than a -1 bifurcation to 2-cycles as in Example 3.28.

By solving the equilibrium equations

$$\begin{aligned} x_2 &= \frac{3}{2}R_0 e^{-cx_2}x_2 \quad \text{and} \\ x_2 &= \frac{1}{2}x_1 + \frac{1}{4}x_2, \end{aligned}$$

we obtain the positive equilibrium

$$\begin{bmatrix} x_1 \\ x_2 \end{bmatrix} = \begin{bmatrix} \frac{3}{2} \ln R_0 \\ \ln R_0 \end{bmatrix}$$

for $R_0 > 1$. The Jacobian

$$J = \begin{bmatrix} 0 & \frac{3}{2}R_0(1-x_2)e^{-x_2} \\ \frac{1}{2} & \frac{1}{4} \end{bmatrix}$$

evaluated at the positive equilibrium

$$\begin{bmatrix} 0 & \frac{3}{2}(1-\ln R_0) \\ \frac{1}{2} & \frac{1}{4} \end{bmatrix}$$

has eigenvalues

$$\lambda_1 = \frac{1}{8} + \frac{1}{8}\sqrt{49 - 48\ln R_0} \quad \text{and} \quad \lambda_2 = \frac{1}{8} - \frac{1}{8}\sqrt{49 - 48\ln R_0}.$$

It is left as an exercise for the reader to show, using the Linearization Principle, that the equilibrium loses stability as R_0 increases through $\exp(7/3)$ and that when $R_0 = \exp(7/3) \approx 10.31$, the eigenvalues are equal to $e^{\pm i\theta}$, where $\theta = \arctan 3\sqrt{7}$. This analysis corroborates, together with the bifurcation shown in Figure 3.7, that a Neimark–Sacker bifurcation of an invariant loop occurs. \square

3.5.4. Backward Bifurcations and Strong Allee Effects. In Chapter 1, we saw that one consequence of a backward-unstable bifurcation in $m = 1$ dimensional population models is a strong Allee effect (see Theorem 1.20). That is to say, one consequence of a backward-unstable bifurcation is a scenario in which there exists two stable equilibria, one of which is the extinction equilibrium and the other of which is a positive (survival) equilibrium. In such a scenario, the long-term fate of the modeled population—its (deterministic) extinction or survival—is initial-condition dependent. The fact that strong Allee effects can result from backward bifurcations for models of dimension $m \geq 2$ is illustrated by the juvenile-adult model in Examples 3.26 and 3.27. Figure 3.4 shows sample solutions that display the initial-condition dependent survival that defines a strong Allee effect (cf. Definition 1.18).

As pointed out in Definition 1.18, a strong Allee effect does not necessarily involve a survival equilibrium but can involve a positive attractor of any type (e.g., a periodic cycle or a chaotic attractor). The next example illustrates this possibility.

Example 3.32. If we replace the negative density factor on adult fertility used in the juvenile-adult model in Examples 3.26 and 3.27 (namely, the discrete logistic factor $1/(1 + cx_2)$) by the Ricker factor $\exp(-cx_2)$, then we get a matrix model with projection matrix

$$(3.29) \quad \mathbf{P}(\mathbf{x}) = \begin{bmatrix} 0 & b_m s e^{-cx_2} \frac{1+ax_2}{1+sax_2} \\ s_1 & s_2 \end{bmatrix}$$

in place of (3.22). It is left as Exercise 3.46 to show that the formula for R_0 remains unchanged as

$$R_0 = b_m s \frac{s_1}{1 - s_2}$$

and that an application of Theorem 3.17 leads to the same conclusions as in Example 3.26, namely that the bifurcation is

- backward-unstable if $\frac{a}{c} > \frac{1}{1-s}$;
- forward-stable if $\frac{a}{c} < \frac{1}{1-s}$.

With $s = 0.02$, $c = 1$, $s_1 = 0.9$, and $s_2 = 0.02$, Figure 3.8 shows the bifurcation diagrams for three values of the Allee coefficient a . In all three cases, there is a Neimark–Sacker bifurcation of the positive equilibria, leading to a cascade of complex attractors. For the smallest Allee coefficient $a = 1$, the bifurcation is forward-stable. Since a strong Allee effect does not occur, this is a weak Allee effect. For the two larger values of $a = 5$ and 15 , a backward-unstable bifurcation occurs, resulting in a strong Allee effect for an interval of $R_0 < 1$. From the middle plot in

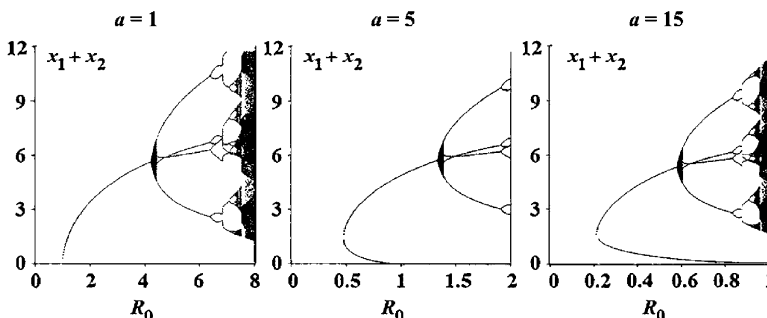


Figure 3.8. The bifurcation diagrams for the model in Example 3.32 for three values of the Allee coefficient a with coefficients $s = 0.02$, $c = 1$, $s_1 = 0.9$, and $s_2 = 0.02$ in the projection matrix (3.29).

Figure 3.8 when $a = 5$, we observe that the strong Allee effect involves only survival equilibria. On the other hand, for $a = 15$, we see from the rightmost plot that the survival attractor is not an equilibrium for $0.59 \lesssim R_0 < 1$. \square

3.6. Imprimitive Projection Matrices

As seen in Section 3.5, the asymptotic dynamics associated with nonlinear matrix equations

$$\mathbf{x}(t+1) = \mathbf{P}(\mathbf{x}(t))\mathbf{x}(t)$$

can be quite different from one equation to another depending on the details of the nonlinearities appearing in the equations. However, one feature they all have in common (under quite general conditions) is the basic bifurcation of positive equilibria that occurs upon destabilization of the extinction equilibria, as given by the basic bifurcation result contained in Theorem 3.21 and 3.13. This bifurcation result is of fundamental biological significance as well, since it deals with the basic question of extinction versus survival of a population.

Notice that part (b) of Theorem 3.21 that concerns the stability of the bifurcating branch of positive equilibria requires the primitivity of the inherent projection matrix $\mathbf{P}(\mathbf{0}_m)$. As we will see, there are applications in which this is not true. This raises the question, In what way does the lack of primitivity affect the basic bifurcation when $\mathbf{0}_m$ destabilizes? Theorem 3.21(a) guarantees that positive equilibria bifurcate from $\mathbf{0}_m$, that the direction of bifurcation is determined by κ , and that backward bifurcating equilibria are unstable. *However, it is no longer true in general that forward bifurcating equilibria are stable.*

We illustrate this assertion by means of an example that has a forward bifurcation of *unstable* positive equilibria. The matrix model with projection matrix

$$(3.30) \quad \mathbf{P}(\mathbf{x}) = \begin{bmatrix} 0 & b_2 \frac{1}{1+2x_1+x_2} \\ \frac{1}{2} \frac{1}{1+x_1} & 0 \end{bmatrix}$$

is a special case of Ebenman's semelparous juvenile-adult model (3.3). The inherent projection matrix

$$\mathbf{P}(\mathbf{0}_2) = \begin{bmatrix} 0 & b_2 \\ \frac{1}{2} & 0 \end{bmatrix}$$

has eigenvalues $\pm\sqrt{R_0}$, where $R_0 = b_2/2$ is the inherent reproduction number. The dominant eigenvalue $r_0 = \sqrt{R_0}$ is not strictly dominant, since the other eigenvalue $-\sqrt{R_0}$ has the same absolute value, which implies $\mathbf{P}(\mathbf{0}_2)$ is not primitive. As R_0 increases through 1, the extinction equilibrium destabilizes. Our goal is to show that, as a result of this destabilization, positive equilibria bifurcate from the extinction equilibrium for $R_0 \gtrsim 1$ (the bifurcation is forward) but that they are unstable.

Equilibria are solutions of the equilibrium equation

$$\begin{bmatrix} x_1 \\ x_2 \end{bmatrix} = \begin{bmatrix} 0 & \frac{2R_0}{1+2x_1+x_2} \\ \frac{1}{2}\frac{1}{1+x_1} & 0 \end{bmatrix} \begin{bmatrix} x_1 \\ x_2 \end{bmatrix},$$

which is equivalent to the system of two algebraic equations

$$\begin{aligned} x_1 &= 2R_0 \frac{1}{1+2x_1+x_2} x_2 \quad \text{and} \\ x_2 &= \frac{1}{2} \frac{1}{1+x_1} x_1. \end{aligned}$$

Substituting x_2 from the second equation into the first equation, we obtain the quadratic equation

$$(1 - R_0) + \frac{7}{2}x_1 + 2x_1^2 = 0$$

for x_1 . This equation has a positive solution $x_1 > 0$ if and only if $R_0 > 1$ that, by the quadratic formula, is

$$x_1 = \frac{1}{8} (\sqrt{32R_0 + 17} - 7).$$

From the second equilibrium equation, we get

$$x_2 = \frac{1}{2} \frac{\sqrt{32R_0 + 17} - 7}{\sqrt{32R_0 + 17} + 1},$$

and we conclude that there exists a positive (and only one positive) equilibrium

$$(3.31) \quad \begin{bmatrix} x_1 \\ x_2 \end{bmatrix} = \begin{bmatrix} \frac{1}{8} (\sqrt{32R_0 + 17} - 7) \\ \frac{1}{2} \frac{\sqrt{32R_0 + 17} - 7}{\sqrt{32R_0 + 17} + 1} \end{bmatrix}$$

if and only if $R_0 > 1$. This shows that a forward bifurcation of positive equilibria occurs at $R_0 = 1$ in this example. Are these positive equilibria stable or unstable?

In principle, we can answer this question using the Linearization Principle by substituting the formula for the positive equilibria into the Jacobian

$$(3.32) \quad \mathbf{J}(\mathbf{x}) = \begin{bmatrix} -4R_0 \frac{x_2}{(2x_1+x_2+1)^2} & 2R_0 \frac{2x_1+1}{(2x_1+x_2+1)^2} \\ \frac{1}{2(x_1+1)^2} & 0 \end{bmatrix}$$

and by calculating the eigenvalues of the resulting matrix using the quadratic formula on its characteristic equation. Given the complexity of the formula (3.31) for the equilibria, to do this by hand is tedious and, even with the aid of a computer algebra program, leads to rather intractable formulas for the eigenvalues. However, treating them as functions of R_0 , we can use a computer algebra program to calculate the first few terms in the Taylor expansion of the eigenvalues, centered at $R_0 = 1$:

$$\begin{aligned} \lambda_1(R_0) &= 1 - \frac{1}{2}(R_0 - 1) + O((R_0 - 1)^2) \quad \text{and} \\ \lambda_2(R_0) &= -1 - \frac{1}{14}(R_0 - 1) + O((R_0 - 1)^2). \end{aligned}$$

From these expansions, we see for $R_0 \gtrsim 1$ that $0 < \lambda_1(R_0) < 1$ and $\lambda_2(R_0) < -1$. It follows, from the second inequality, that the positive equilibria are unstable for $R_0 \gtrsim 1$.

This matrix model shows that *a forward bifurcation of positive equilibria at $R_0 = 1$ is not necessarily stable when the inherent projection matrix is imprimitive*. We can also gain some initial insight into matrix models with imprimitive inherent projection matrices by noting two facts about this example.

First, as R_0 increases through 1, both eigenvalues $\pm\sqrt{R_0}$ leave the unit circle in the complex plane simultaneously: one through +1 and the other through -1. This suggests the bifurcation involves both equilibria and 2-cycles (see Section 3.5). Thus, in addition to the forward bifurcating positive equilibria, we suspect 2-cycles also play some kind of role in this example.

The second fact is the observation that the imprimitive projection matrix (3.30) holds the boundary of R_+^2 invariant. What this means is that $\mathbf{x}(0) \in \partial R_+^2$ implies $\mathbf{x}(t) \in \partial R_+^2$ for all $t \in Z_+$. (Note $\mathbf{x} \in \partial R_+^2$ means that $x_1 = 0$, $x_2 = 0$, or both.) To see this, consider an

initial condition

$$\mathbf{x}(0) = \begin{bmatrix} x_1(0) \\ 0 \end{bmatrix} \in \partial R_+^2$$

where $x_2(0) > 0$. Then using the projection matrix (3.30), we calculate

$$\begin{aligned} \mathbf{x}(1) &= \begin{bmatrix} x_1(1) \\ x_2(1) \end{bmatrix} = \begin{bmatrix} 0 \\ \frac{1}{2} \frac{1}{1+x_1(0)} x_1(0) \end{bmatrix} \in \partial R_+^2 \quad \text{and} \\ \mathbf{x}(2) &= \begin{bmatrix} x_1(2) \\ x_2(2) \end{bmatrix} = \begin{bmatrix} 0 \\ 2R_0 \frac{1}{1+x_2(1)} x_2(1) \end{bmatrix} \in \partial R_+^2, \end{aligned}$$

and we conclude by induction that such an initial condition generates a solution all of whose terms

$$(3.33) \quad \begin{bmatrix} x_1(0) \\ 0 \end{bmatrix}, \quad \begin{bmatrix} 0 \\ * \end{bmatrix}, \quad \begin{bmatrix} * \\ 0 \end{bmatrix}, \quad \begin{bmatrix} 0 \\ * \end{bmatrix}, \quad \begin{bmatrix} * \\ 0 \end{bmatrix}, \dots$$

lie on the boundary ∂R_+^2 . Notice that this solution implies that the adult and juvenile classes never overlap (i.e., that the generations are alternately synchronized so as to be temporally separated). For this reason, such a solution is called a **synchronous solution**. Similarly, it is easy to see that an initial condition $x_1(0) = 0$ where $x_2(0) > 0$ also produces a synchronous solution.

These two facts lead us to suspect that **synchronous 2-cycles** play a role in the matrix model with projection matrix (3.30). Consider first the possible existence of synchronous 2-cycles. We look for a solution for which

$$\mathbf{x}(0) = \begin{bmatrix} x_1(0) \\ 0 \end{bmatrix} \in \partial R_+^2, \quad x_1(0) > 0$$

and $\mathbf{x}(0) = \mathbf{x}(2)$. (Note that $\mathbf{x}(0) \neq \mathbf{x}(1)$ is guaranteed by (3.33).) A calculation shows $\mathbf{x}(0) = \mathbf{x}(2)$ occurs if and only if

$$\begin{bmatrix} x_1(0) \\ 0 \end{bmatrix} = \begin{bmatrix} \left(R_0 \frac{1}{1+\frac{3}{2}x_1(0)}\right) x_1(0) \\ 0 \end{bmatrix},$$

and we have a positive 2-cycle if and only if

$$x_1(0) = \frac{2}{3} (R_0 - 1) > 0.$$

Thus, for $R_0 > 1$, there exists a (unique) synchronous 2-cycle consisting of the two vectors

$$(3.34) \quad \mathbf{x}_1 = \begin{bmatrix} \frac{2}{3}(R_0 - 1) \\ 0 \end{bmatrix} \quad \text{and} \quad \mathbf{x}_2 = \begin{bmatrix} 0 \\ \frac{R_0 - 1}{2R_0 + 1} \end{bmatrix}$$

on the boundary of \mathbb{R}_+^2 .

We conclude that two bifurcations occur in this example as R_0 increases through 1: a forward bifurcation of positive equilibria and a forward bifurcation of synchronous 2-cycles.

We have already seen that the positive equilibria are unstable for $R_0 \gtrapprox 1$. But what about the 2-cycles? We can answer this question by using the Linearization Principle for cycles in Theorem 3.29. We evaluate the Jacobian (3.32) at the cycle points (3.34) and then calculate the product

$$\mathbf{Jf}^{(2)}(\mathbf{x}_0) = \mathbf{Jf}(\mathbf{x}_1)\mathbf{Jf}(\mathbf{x}_0) = \begin{bmatrix} \frac{1}{R_0} & -\frac{8}{3}(R_0 - 1)\frac{2R_0 + 1}{4R_0 - 1} \\ 0 & 3\frac{R_0}{4R_0 - 1} \end{bmatrix}.$$

The eigenvalues of this triangular matrix appear along the diagonal:

$$\lambda_1 = \frac{1}{R_0} \quad \text{and} \quad \lambda_2 = 3\frac{R_0}{4R_0 - 1}.$$

Clearly, for $R_0 > 1$, we have $0 < \lambda_1 < 1$. A little algebra shows that $0 < \lambda_2 < 1$, and as a result, the 2-cycle is stable.

In summary, *in the $m = 2$ dimensional model with projection matrix (3.30), there occurs two simultaneously forward bifurcations at $R_0 = 1$: one of unstable positive equilibria and another of stable synchronous 2-cycles.*

This double bifurcation is not peculiar to this example but in fact always occurs in the $m = 2$ dimensional, imprimitive Leslie model with projection matrix (3.11) of the form

$$(3.35) \quad \mathbf{P}(\mathbf{x}) = \begin{bmatrix} 0 & b_2\beta(\mathbf{x}) \\ s_1\sigma(\mathbf{x}) & 0 \end{bmatrix}$$

with $b_2 > 0$, $0 < s_1 < 1$, and

$$\beta(\mathbf{0}_2) = \sigma(\mathbf{0}_2) = 1.$$

(The life cycle graph appears in Figure 3.9.) However, it is not always the case that the bifurcating 2-cycles are stable and the positive equilibria

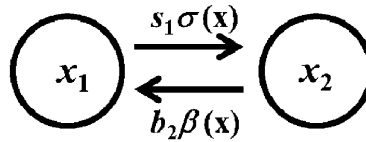


Figure 3.9. The life cycle graph associated with the semelparous juvenile-adult model with projection matrix (3.35).

are unstable. Sometimes the reverse is true, although it never occurs that both are stable or both are unstable; see Theorem 3.33.

Define the quantities

$$c_w := -\partial_{x_1}^0 \sigma - s_1 \partial_{x_2}^0 \beta, \quad c_b := -\partial_{x_1}^0 \beta - s_1 \partial_{x_2}^0 \sigma,$$

$$\kappa_+ = c_w + c_b, \quad \text{and} \quad \kappa_- = c_w - c_b.$$

(Recall that the superscript “0” denotes evaluation at $\mathbf{x}_e = \mathbf{0}_2$ and $R_0 = b_2 s_1 = 1$.)

Theorem 3.33. [29], [34] Assume $\sigma, \beta \in C^2(R^2 : R_+)$ and that $0 \leq s_1\sigma(\mathbf{x}) \leq 1$ for $\mathbf{x} \in R_+$ in the semelparous juvenile-adult model with projection matrix (3.35). The extinction equilibrium is stable for $R_0 = b_2 s_1 < 1$ and unstable for $R_0 > 1$.

- (a) If $\kappa_+ \neq 0$, then positive equilibria bifurcate from the extinction equilibrium $\mathbf{x}_e = \mathbf{0}_2$ at $R_0 = 1$. If $\kappa_+ < 0$, then the bifurcation is backward and unstable. If $\kappa_+ > 0$, then the bifurcation is forward, and it is stable if $\kappa_- > 0$ and unstable if $\kappa_- < 0$.
- (b) If $c_w \neq 0$, then synchronous 2-cycles bifurcate from the extinction equilibrium $\mathbf{x}_e = \mathbf{0}_2$ at $R_0 = 1$. If $c_w < 0$, then the bifurcation is backward and unstable. If $c_w > 0$, then the bifurcation is forward, and it is stable if $\kappa_- < 0$ and unstable if $\kappa_- > 0$.

Notice the following features of the bifurcation at $R_0 = 1$ in Theorem 3.33. First, backward bifurcations are unstable for both positive equilibria and synchronous 2-cycles. Second, the direction of bifurcation of the equilibria and that of the 2-cycles occur independently (i.e., one can be forward and one backward, both backward, or both forward). Third, when both bifurcations are forward, then either the positive equilibria are stable and the synchronous 2-cycles are unstable or vice versa

(never are both stable or both unstable), a situation we refer to as a **dynamic dichotomy**. Which of the two bifurcating entities in this dichotomy is stable is determined by the sign of κ_- . This is illustrated in the following example.

Example 3.34. From the projection matrix for the Ebenman's semelparous juvenile-adult model (3.3)

$$(3.36) \quad \mathbf{P}(\mathbf{x}) = \begin{bmatrix} 0 & b_2 \frac{1}{1+c_{21}x_1+c_{22}x_2} \\ s_1 \frac{1}{1+c_{11}x_1+c_{12}x_2} & 0 \end{bmatrix}$$

with $b_2 > 0$, $0 < s_1 \leq 1$, and

$c_{ij} \geq 0$ and not all equal to 0,

we have

$$\beta(x_1, x_2) = \frac{1}{1 + c_{21}x_1 + c_{22}x_2} \quad \text{and} \quad \sigma(x_1, x_2) = \frac{1}{1 + c_{11}x_1 + c_{12}x_2},$$

from which we obtain

$$c_w = c_{11} + s_1 c_{22}, \quad c_b = c_{21} + s_1 c_{12}, \quad \text{and} \\ \kappa_+ = c_{11} + s_1 c_{22} + c_{21} + s_1 c_{12}.$$

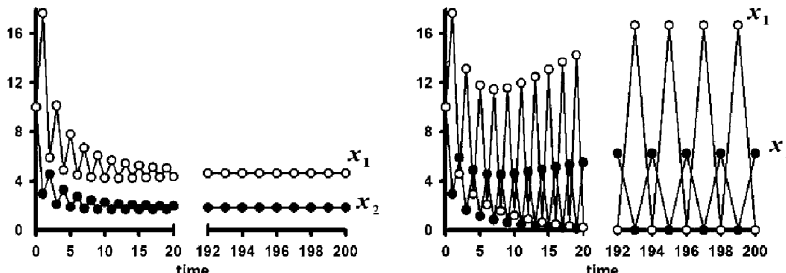


Figure 3.10. Two sample solutions of the semelparous juvenile-adult model with projection matrix (3.36), with initial conditions $x_1(0) = x_{21}(0) = 10$ and parameters $b_2 = 3$ and $s_1 = 0.5$ ($R_0 = 1.5$), illustrate the dynamic dichotomy in Example 3.34 when the bifurcation at $R_0 = 1$ of both positive equilibria and synchronous 2-cycles are forward. (A) $c_{11} = c_{22} = 0.5$ and $c_{12} = c_{21} = 0.2$ imply that $\kappa_- = 0.45 > 0$ and that the positive equilibrium is stable. (B) $c_{11} = c_{22} = 0.2$ and $c_{12} = c_{21} = 0.5$ imply that $\kappa_- = -0.45 < 0$ and that the synchronous 2-cycle is stable.

Since both κ_+ and c_w are positive, Theorem 3.33 implies both positive equilibria and synchronous 2-cycles forward bifurcate at $R_0 = b_2 s_1 = 1$. Which is stable and which is unstable is determined by the sign of

$$\kappa_- = c_{11} + s_1 c_{22} - (c_{21} + s_1 c_{12}).$$

If $\kappa_- > 0$, then the bifurcating positive equilibria are stable and the synchronous 2-cycles are unstable. This situation can be interpreted as occurring when the competition within the adult and juvenile classes (among themselves), as measured by $c_w = c_{11} + s_1 c_{22}$, is stronger than the competition between juveniles and adults, as measured by $c_b = c_{21} + s_1 c_{12}$. In this case, the stable positive equilibria implies that ultimately both juveniles and adults will be present at any given time.

On the other hand, if the competition between the two classes is stronger than the competition within the classes ($\kappa_- < 0$), then the synchronous 2-cycles are stable, which means that in the long run, juveniles and adults will never occur at the same time and the generations will be temporally separated. See Figure 3.10 for an example of both cases.

Note that by Theorem 3.20, the extinction equilibrium is globally asymptotically stable when $R_0 < 1$. \square

Theorem 3.33 and Example 3.34 concern an imprimitive Leslie model of the lowest dimension $m = 2$. Nonetheless, it serves to illustrate some of the complications that arise in the imprimitive case. The dynamic complications that can arise increase significantly with increased dimension m , and a thorough understanding of the possibilities is lacking for dimensions $m > 3$, except for a few specialized types of projection matrices.

For example, imprimitive Leslie models (of which the semelparous juvenile-adult is the lowest-dimensional case) have been studied by several authors [11], [34], [42], [47], [48], [56], [58], [59], motivated primarily by studies of semelparous species, such as the famous periodical cicadas (see Section 3.7.3). Nonetheless, a complete understanding of the dynamics has not been attained even for this special case.

One basic fact that is known is that, in addition to the bifurcation at $R_0 = 1$ of positive equilibria, there occurs a bifurcation of synchronous m -cycles in which exactly one age class is present at all times; these

so-called year-class cycles have the form

$$(3.37) \quad \begin{bmatrix} x_1(0) \\ 0 \\ 0 \\ \vdots \\ 0 \end{bmatrix}, \quad \begin{bmatrix} 0 \\ * \\ 0 \\ \vdots \\ 0 \end{bmatrix}, \quad \begin{bmatrix} 0 \\ 0 \\ * \\ \vdots \\ 0 \end{bmatrix}, \quad \dots, \quad \begin{bmatrix} 0 \\ 0 \\ 0 \\ \vdots \\ * \end{bmatrix}, \quad \begin{bmatrix} * \\ 0 \\ 0 \\ \vdots \\ 0 \end{bmatrix}, \quad \dots$$

(the asterisks represent positive numbers). However, other synchronous cycles that contain at all times exactly two (or three or more) age classes can also arise by bifurcation at $R_0 = 1$. To determine which of these many synchronous cycles occur and are stable is a difficult analytic task. In fact, it can turn out that all the bifurcating synchronous cycles and positive equilibria are unstable and that the bifurcating attractor is a more complicated entity. An example appears in Section 3.7.3.

For a special class of imprimitive projection matrices for which a general bifurcation theorem and dynamic dichotomy result has been rigorously established, see [127].

3.7. Applications

The following applications were chosen not only because they have been used in ecological studies of specific biological species but because they illustrate the mathematical features centered around the basic bifurcation at $R_0 = 1$ that we studied in this chapter.

The first two applications have primitive inherent projection matrices: the first featuring a forward-stable bifurcation (with secondary bifurcations) and the second a backward-unstable bifurcation with an associated strong Allee effect. The third application has an imprimitive inherent projection matrix and features a dynamic dichotomy between positive equilibria and synchronous cycles.

3.7.1. Flour Beetles. The LPA model in Example 2.13 is a general model for an insect with a larva-pupa-adult life cycle. A nonlinear

version of this model, with projection matrix

$$(3.38) \quad \mathbf{P}(\mathbf{x}) = \begin{bmatrix} 0 & 0 & b_3\beta(\mathbf{x}) \\ s_1 & 0 & 0 \\ 0 & s_2\sigma_2(\mathbf{x}) & s_3\sigma_3(\mathbf{x}) \end{bmatrix}$$

with $b_3 > 0$, $0 < s_i \leq 1$, and

$$\beta(\mathbf{0}_3) = \sigma_i(\mathbf{0}_3) = 1,$$

(see the life cycle graph in Figure 3.11) has been extensively used in experimental studies of flour beetle species (*Tribolium* sp.) [25], [114]. In those studies, the density factors account for cannibalism between life cycle stages, specifically cannibalism of eggs and pupae by larvae and adults. They take the form of Ricker-type exponential factors according to the following derivation [41].

Suppose the probability that an individual encounters a cannibal during a short interval of time from t to $t + \Delta t$ is approximately proportional to the elapsed time $\Delta t \approx 0$ (i.e., equals $c\Delta t$ for a constant $c > 0$). The probability the individual escapes cannibalism by that cannibal is $1 - c\Delta t$. If there are x cannibals and encounters with them are independent, then the probability the individual escapes cannibalism is approximately $(1 - c\Delta t)^x$. Consider the interval from t to $t + 1$ in the matrix model (the unit of time is two weeks for *Tribolium* studies). If we divide this interval into q subintervals of length $\Delta t = 1/q$, where q is a large

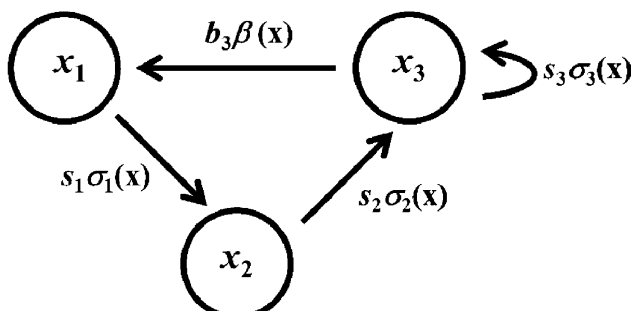


Figure 3.11. The life cycle graph associated with the nonlinear LPA model with projection matrix (3.38).

positive integer, and if the encounters on each subinterval are independent events, then the probability of an individual escaping cannibalism from time t to $t+1$ is approximately $\left((1 - c\Delta t)^x\right)^q$. We get the probability an individual escapes cannibalism from x cannibals during the interval t to $t+1$ by letting $q \rightarrow \infty$:

$$\begin{aligned} \lim_{q \rightarrow \infty} \left(\left(1 - c \frac{1}{q}\right)^x \right)^q &= \lim_{q \rightarrow \infty} \left(\left(1 - c \frac{1}{q}\right)^q \right)^x \\ &= \lim_{q \rightarrow \infty} \left(\left(1 - \frac{1}{q/c}\right)^{q/c} \right)^{cx} \\ &= \lim_{n \rightarrow \infty} \left(\left(1 - \frac{1}{n}\right)^n \right)^{cx} \\ &= \left(\lim_{n \rightarrow \infty} \left(1 - \frac{1}{n}\right)^n \right)^{cx} \\ &= (e^{-1})^{cx}, \end{aligned}$$

where $n = q/c$. Thus, the probability an individual escapes cannibalism (i.e., the per capita cannibalism survival rate) from x cannibals is e^{-cx} . This leads to the projection matrix

$$(3.39) \quad \mathbf{P}(\mathbf{x}) = \begin{bmatrix} 0 & 0 & b_3 \exp(-c_1 x_1 - c_2 x_3) \\ 1 - \mu_1 & 0 & 0 \\ 0 & (1 - \mu_2) \exp(-c_3 x_3) & 1 - \mu_3 \end{bmatrix},$$

where the coefficients c_1 and c_2 measure the loss of eggs due to cannibalism by larvae and adults, respectively, and c_3 measures the loss of pupae due to cannibalism by adults. Here, we have replaced the inherent survival probabilities s_i by $1 - \mu_i$, where μ_i is the probability of not surviving a unit of time (mortality rate), in order to align our notation with that commonly used for this model.

The inherent projection matrix

$$\mathbf{P}(\mathbf{0}_3) = \begin{bmatrix} 0 & 0 & b_3 \\ 1 - \mu_1 & 0 & 0 \\ 0 & 1 - \mu_2 & 1 - \mu_3 \end{bmatrix}$$

is primitive with inherent net reproduction number

$$R_0 = b_3 (1 - \mu_1) (1 - \mu_2) \frac{1}{\mu_3}$$

(see equations (2.29) and (2.30)).

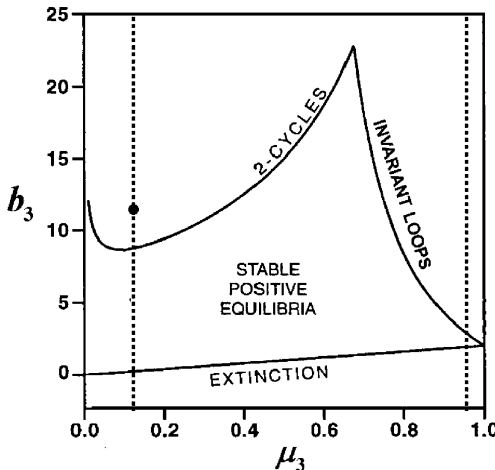


Figure 3.12. This map shows the bifurcation locations and type using b_3 and μ_3 as parameters (with the remaining parameters given by (3.40)). The vertical dashed lines correspond to the bifurcation diagrams in Figures 3.13 and 3.14. The vertical dashed line at $\mu = 0.1108$ corresponds to the experimental data reported in [50], and the solid black circle is the b_3 estimated for that experiment. The model therefore predicts a 2-cycle oscillation, which in fact was observed (see Figure 3.13). The other vertical dashed line located at $\mu = 0.96$ corresponds to the bifurcation diagram in Figure 3.14.

By Theorem 3.20, the extinction equilibrium is globally asymptotically stable for $R_0 < 1$. The extinction equilibrium destabilizes as R_0 increases through 1, and since all density factors have negative derivatives at $\mathbf{x}_e = \mathbf{0}_3$, the bifurcation of positive equilibria is forward and stable (see Corollary 3.23).

Thus, the nonlinear LPA model with projection matrix (3.39) predicts a forward bifurcation of positive equilibria that are stable at least for $R_0 \gtrapprox 1$.

Lacking formulas for the positive equilibria, it is difficult to ascertain analytically whether secondary bifurcations occur for larger values of R_0 .

Numerical simulations suggest that both -1 (period doubling) and Neimark–Sacker (invariant loop) bifurcations are possible, depending on the values of the model's parameters, as R_0 is increased.

Using data obtained from their (replicated and controlled) experiments with *Tribolium castaneum* Herbst, the authors in [50] obtained (maximum likelihood) estimates

$$(3.40) \quad \begin{aligned} b_3 &= 11.6772, & \mu_1 &= 0.5129, & \mu_2 &= 0, & \mu_3 &= 0.1108, \\ c_1 &= 0.0093, & c_2 &= 0.0110, & \text{and } c_3 &= 0.0178 \end{aligned}$$

for the parameters, and they located bifurcation points when using either b_3 or μ_3 as a bifurcation parameter as shown in Figure 3.12. Two sample bifurcation diagrams, obtained by varying b_3 along the two vertical dashed lines in Figure 3.12, are displayed in Figures 3.13 and 3.14.

The bifurcation diagram in Figure 3.13 corresponds to $\mu_3 = 0.1108$ and shows a forward-stable bifurcation of positive equilibria (at $b_3 =$

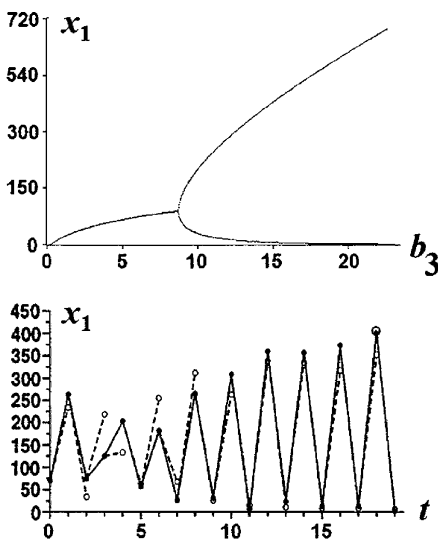


Figure 3.13. The upper plot is the bifurcation diagram associated with the LPA model (3.39) using b_3 as the bifurcation parameter. The remaining parameter values are given in (3.40). The lower plot shows the time series of larval data (solid circles) taken from one replicate of the experiment reported in [50] in which $b_3 = 11.6772$. The open circles are the one step model predictions from each data point.

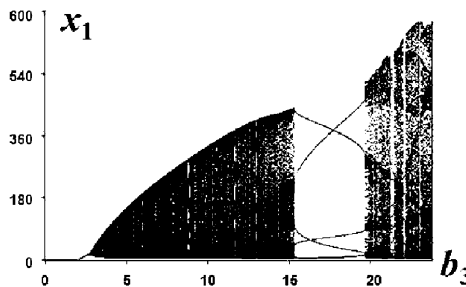


Figure 3.14. The bifurcation diagram associated with the vertical dashed line in Figure 3.12 located at $\mu_3 = 0.96$ shows a forward-stable bifurcation of positive equilibria at $b_3 = 1.9708$ followed (rather soon) by a Neimark–Sacker bifurcation of invariant loops. Further increases in b_3 result in a cascade of complicated bifurcations and chaos.

0.2275 where $R_0 = 1$) followed by a period-doubling bifurcation to stable 2-cycles. Also shown is a plot of the larval time series data from one of the replicated experiments reported in [50], which clearly displays a 2-cycle oscillation as predicted by the bifurcation diagram at $b_3 = 11.6772$. Dashed lines connect the data points (solid circles) to the model-predicted larval population size based on that data point (open circles), which gives a sense of how accurate the model predictions are. A thorough statistical analysis of the prediction accuracy is given in [50].

The bifurcation diagram in Figure 3.14 corresponds to the vertical dashed line at $\mu_3 = 0.96$ on the map in Figure 3.12. As indicated on the map, this diagram shows a forward-stable bifurcation of positive equilibria followed by a Neimark–Sacker (invariant loop) bifurcation. This diagram also indicates that other complicated attractors are present as b_3 is increased (including cycles and “chaotic” attractors), which was the motivation for over a decade of carefully designed and implemented experiments (replicated and controlled) to demonstrate that *Tribolium* populations would indeed behave in the laboratory in the model-predicted ways [23], [52], [87], [41], [54].

This successful project of matching models to data shows how matrix models can accurately and quantitatively predict (not just fit) the dynamics of a biological population. In addition to serving as the first unequivocal demonstration of chaotic dynamics in a biological population

(albeit in a laboratory setting), this project successfully demonstrated, by means of replicated and controlled experiments, the existence of many other dynamic phenomena (some unexpectedly) predicted by the model [24], [40], [41], [51], [53], [74], [75], [76], [77], [78].

3.7.2. Cannibalism and Climate Change. Cannibalism has been documented to occur in a wide diversity of animals, across many taxa, including vertebrates, invertebrates, and protozoans [65], [115]. There can be many causes of cannibalism, such as overcrowding and stress, but poor food quality and lack of adequate food constitute the most important reasons for its occurrence [61]. Changes in climate can cause food resource availability to decrease for individuals in a species, who then resort to cannibalism as a way to cope. For example, cannibalism in some marine birds, lobsters, and polar bears has recently been correlated to increased ocean temperatures that have affected their primary food sources. In this section, we look at a model inspired by one studied in [43] and consider circumstances under which a population that would go extinct because of reduced food resource availability but can survive if it engages in cannibalism.

While cannibalism occurs in many forms, a common form is the cannibalization of juveniles by adults. For example, the model in [43] was motivated by rigorously documented cannibalism of eggs by adults in colonies of glaucous-winged gulls (*Larus glaucescens*) that is correlated with the loss of marine food resources with increasing mean sea temperatures (particularly during El Niño years) [72]. The model is an $m = 2$ dimension matrix model with

$$\mathbf{x} = \begin{bmatrix} x_1 \\ x_2 \end{bmatrix},$$

where x_1 and x_2 are juvenile and adult densities, respectively, and with a projection matrix of the form (3.19)

$$(3.41) \quad \mathbf{P}(\mathbf{x}) = \begin{bmatrix} 0 & b\beta(\mathbf{x}) \\ s_1\sigma_1(\mathbf{x}) & s_2\sigma_2(\mathbf{x}) \end{bmatrix}$$

with $b > 0$, $0 < s_1, s_2 < 1$, and

$$\beta(\mathbf{0}_2) = \sigma_1(\mathbf{0}_2) = \sigma_2(\mathbf{0}_2) = 1.$$

The parameters b , s_1 , and s_2 are the inherent adult fertility rate, juvenile survival probability, and adult survival probability, respectively. The inherent projection matrix

$$\mathbf{P}(\mathbf{0}_2) = \begin{bmatrix} 0 & b \\ s_1 & s_2 \end{bmatrix}$$

is nonnegative and primitive, and the reproduction number is

$$R_0 = bs_1 \frac{1}{1 - s_2}.$$

(See (3.20) and Example 3.15.) Theorem 3.17 implies that the extinction equilibrium loses stability as R_0 increases through 1 and that the resulting bifurcation of positive equilibria is forward-stable if $\kappa > 0$ and backward-unstable if $\kappa < 0$, where κ is given by formula (3.21), namely

$$(3.42) \quad \begin{aligned} \kappa = & s_1(1 - s_2)^2(-\partial_{x_1}^0 \beta) + s_1^2(1 - s_2)(-\partial_{x_2}^0 \beta) \\ & + (1 - s_2)^2(-\partial_1^0 \sigma_{x_1}) + s_1(1 - s_2)(-\partial_2^0 \sigma_{x_1}) \\ & + s_1(1 - s_2)(-\partial_1^0 \sigma_{x_2}) + s_1^2(-\partial_2^0 \sigma_{x_2}). \end{aligned}$$

In this application, we are interested in the latter case and its potential for a strong Allee effect. If this can occur because of positive effects on some survival rates due to cannibalism, then the population can survive if $R_0 < 1$ when it would go extinct in the absence of cannibalism.

The trade-offs on which we will focus are: a negative correlation between cannibalistic activity and environmental resource foraging (if one goes up the other goes down); and the negative effect on juvenile survival of cannibalism versus the positive effect the cannibalistic resource has on adult survival (when environmental resource availability decreases).

The model derivation entails specifying submodels for the nonlinear density factors $\sigma_i(\mathbf{x})$ and $\beta(\mathbf{x})$, which describe the effects and trade-offs present when adults x_2 cannibalize juveniles x_1 . We deal with each of the three density terms in turn. While we wish to focus on as small a number of mechanisms as possible in this low-dimensional model, capturing the key relevant ones will still result in a somewhat complicated projection matrix $\mathbf{P}(\mathbf{x})$.

The Juvenile Survival Density Factor σ_1 . Let p denote the probability an individual juvenile is cannibalized in the presence of x_2 adults. We assume p depends on the amount of environmental resource available, which we denote by $\rho > 0$, as well as the number of juveniles and adults

present. Therefore, we write $p = p(\rho, \mathbf{x})$. To apply our analysis in this chapter (specifically, for Assumption 3.3 to hold), this mathematical expression needs to be twice continuously differentiable in x_1 and x_2 and have a range in the interval $0 \leq p(\rho, \mathbf{x}) < 1$. Furthermore, $p(\rho, \mathbf{x})$ should be increasing in x_2 and decreasing in ρ and x_1 . The reason for the first condition is obvious: as the number of adult cannibals increases, the probability of being cannibalized increases. The reason $p(\rho, \mathbf{x})$ should be decreasing in ρ is because we assume that cannibalism activity increases when environmental availability decreases. Finally, that $p(\rho, \mathbf{x})$ should be decreasing in x_1 is a familiar assumption in ecology called the *predator saturation effect* (or in this case, the cannibal saturation effect), which states that an individual's probability of being a victim goes down in the presence of a higher number of potential victims. Then

$$\sigma_1(\mathbf{x}) = 1 - p(\rho, \mathbf{x})$$

in the projection matrix (3.41).

An example mathematical expression that satisfies these assumptions, based on the use of rational functions, is

$$(3.43) \quad p(\rho, \mathbf{x}) = \frac{1}{1 + \rho} \frac{1}{1 + c_1 x_1} \frac{v x_2}{1 + v x_2},$$

where $c_1 \geq 0$ measures the strength of the cannibalism saturation effect and $v \geq 0$, which we call the cannibalism coefficient, measures the aggressiveness of an individual adult cannibal.

The Adult Survival Density Factor σ_2 . In our model, we assume that the benefit an adult receives from cannibalistic resources is increased survival probability. Therefore, we take an adult's survival σ_2 to be an increasing function $\sigma_2 = \sigma_2(w)$ of the total number of juvenile cannibalized by the adult, which we denote by w . The function $\sigma_2(w)$ must be designed so that not only $\sigma_2(0) = 1$ but $s_3 \sigma_2(w) \leq 1$ for all $w \geq 0$. As an example, we use

$$(3.44) \quad \sigma_2(w) = \frac{1 + c_3 w}{1 + \alpha c_3 w}, \quad c_3 > 0, \quad s_2 < \alpha < 1.$$

The total number of juveniles cannibalized by all adults x_2 is $p(\rho, \mathbf{x}) x_1$; hence, the amount taken by an individual adult is

$$w = \frac{p(\rho, \mathbf{x})}{x_2} x_1,$$

which with (3.43) is

$$(3.45) \quad w(\rho, \mathbf{x}) = \frac{1}{1+\rho} \frac{1}{1+c_1 x_1} \frac{v}{1+v x_2} x_1.$$

The Adult Fertility Density Factor β . We assume the only effect of density is the usual negative effect of adult density, as for example with

$$(3.46) \quad \beta(\mathbf{x}) = \frac{1}{1+c_2 x_2}, \quad c > 0.$$

The Inherent (Density-Free) Parameters. We assume the per-adult inherent fertility rate b is proportional to the environmental resource availability ρ with a constant of proportionality that is a decreasing function of cannibalistic activity. That is to say, there is a trade-off between environmental resource gathering and cannibalistic activity. As an example,

$$b = b_0 \frac{1}{1+v} \rho.$$

Finally, we take inherent juvenile and adult survival probabilities s_1 and s_2 to be independent of ρ and v .

Using the example submodels (3.43), (3.45), (3.44), and (3.46), we obtain the projection matrix

$$\mathbf{P}(\mathbf{x}) = \begin{bmatrix} 0 & b_0 \frac{1}{1+v} \rho \beta(\mathbf{x}) \\ s_1(1-p(\rho, \mathbf{x})) & s_2 \sigma_2(w(\rho, \mathbf{x})) \end{bmatrix}$$

and the reproduction number

$$R_0(\rho) = b_0 \frac{1}{1+v} \rho \frac{s_1}{1-s_2}.$$

From this formula, we can put $R_0(\rho)$ explicitly into $\mathbf{P}(\mathbf{x})$ and obtain

$$(3.47) \quad \mathbf{P}(\mathbf{x}) = \begin{bmatrix} 0 & R_0(\rho) \frac{1-s_2}{s_1} \beta(\mathbf{x}) \\ s_1(1-p(\rho, \mathbf{x})) & s_2 \sigma_2(w(\rho, \mathbf{x})) \end{bmatrix}.$$

Despite the complexity of this model, we know (as pointed out previously) from Theorem 3.17 that the extinction equilibrium loses stability as $R_0(\rho)$ increases through 1 and that whether the resulting bifurcation of positive equilibria is forward and stable or backward and unstable is determined by the sign of κ . Since not all partial derivatives of the entries in $\mathbf{P}(\mathbf{x})$ have the same sign (when evaluated at the bifurcation point

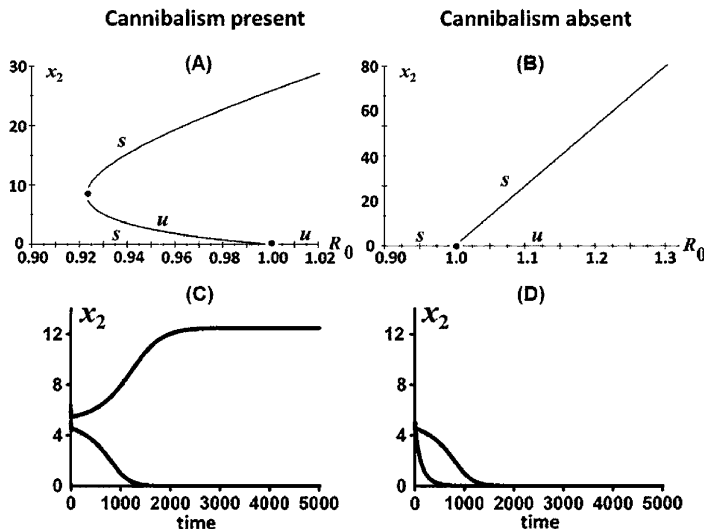


Figure 3.15. Shown are bifurcation diagrams and sample time series solutions for the matrix model with projection matrix (3.47) with coefficients $s_1 = 0.5$, $s_2 = 0.9$, $c_1 = c_2 = 0.01$, $c_3 = 100$, $\rho = 1$, and $\alpha = 0.95$. (A) and (B), respectively, show the bifurcation diagrams with cannibalism present ($v = 0.01$) and absent ($v = 0$). When cannibalism is present, the bifurcation is backward-unstable ($\kappa(1) = -4.74 \times 10^{-1} < 0$); when it is absent, the bifurcation is forward-stable ($\kappa(1) = 2.50 \times 10^{-4} > 0$). (C) and (D) show time series of two sample orbits when $R_0 = 0.923 < 1$ with initial conditions $\mathbf{x}(0) = \text{col}(0, 5)$ and $\text{col}(0, 6)$. In (C), cannibalism is present, and the first solution goes extinct while the second does not, indicating the occurrence of a strong Allee effect and initial-condition dependent survival. In (D), on the other hand, cannibalism is absent, and both solutions go extinct.

$R_0(\rho) = 1$ and $\mathbf{x}_e = \mathbf{0}_2$), we cannot use Corollary 3.23 and must resort to the calculation of $\kappa(\rho)$ by the formula in (3.42).

After some calculus, followed by some algebraic manipulations, we find that

$$\kappa(\rho) = s_1(1 - s_2) \frac{v}{1 + \rho} \left(1 + \frac{1 + \rho}{v} s_1 c_2 - (1 - \alpha) c_3 \right),$$

and the sign of $\kappa(\rho)$ is the same as the sign of the bracketed expression. We conclude the following:

The bifurcation at $R_0(\rho) = 1$ in the cannibalism model with projection matrix (3.47) is

- (3.48) (a) *forward and stable if $(1 - \alpha)c_3 < 1 + \frac{1+\rho}{v}s_1c_2$;*
 (b) *backward and unstable if $(1 - \alpha)c_3 > 1 + \frac{1+\rho}{v}s_1c_2$.*

To interpret this result, we note that

$$(1 - \alpha)c_3 = \left. \frac{d\sigma_2(w)}{dw} \right|_{w=0}$$

measures how quickly the adult survival rate increases due to (a low level) of juvenile cannibalization. Thus, if cannibalism is sufficiently beneficial in this sense (i.e., if $(1 - \alpha)c_3$ is large enough so that the inequality in (3.48)(b) is met), then the bifurcation is backward-unstable.

This result, based on the general bifurcation results in Section 3.4, accounts only for the dynamics of the model near the bifurcation point $R_0 = 1$. However, as pointed out in Section 3.5.4, a backward bifurcation in population models is usually associated with a strong Allee effect, and while we will not attempt to prove this rigorously, we can show by numerical simulations that this does occur in this model.

Figure 3.15 shows sample bifurcation diagrams when cannibalism is present and absent. In graph (A), cannibalism is present ($v > 0$), and the bifurcation is backward-unstable ($\kappa(\rho) < 0$); in (B), cannibalism is absent ($v = 0$), and the bifurcation is forward-stable ($\kappa(\rho) > 0$). This cannibalism-induced backward bifurcation creates a strong Allee effect and initial-condition dependent survival when $R_0(\rho) \lesssim 1$, as illustrated in graph (C) showing two sample solution time series when $R_0(\rho) = 0.923$, one of which survives and the other of which goes extinct. When cannibalism is absent, however, the same initial conditions lead to solutions that both go extinct when $R_0(\rho) = 0.923$.

The cannibalism model with projection matrix (3.47) predicts that a cannibalistic population can survive when environmental resources drop so low that $R_0(\rho) < 1$ and a noncannibalistic population would go extinct.

This survival capability in a deteriorated environment comes, however, with two important caveats:

- The population density cannot initially be (or at some point in time drop) so low that it is in the basin of attraction of the extinction equilibria.
- Environmental resource availability must not decrease so low that $R_0(\rho)$ falls below the tipping point in the bifurcation diagram (approximately 0.92 in Figure 3.15), because then the population would experience a sudden collapse to extinction.

3.7.3. Periodical Insects. Periodical insects have a life cycle that entails development over a fixed number of years followed by a short reproductive stage in which all adults appear synchronously after which individuals die. The result is that the population consists of isolated yearly classes (cohorts) that do not overlap. Examples include many species of beetles, flies, wasps, moths, and butterflies whose life cycles range from 1 to 5 years [73]. The most famous examples, however, are the periodical cicadas whose life cycles are 13 years for some species (*Magicicada tredecim*, *M. tredecassini*, and *M. tredecula*) and 17 years for others (*M. septendecim*, *M. cassini*, and *M. septendecula*).⁶

In a seminal study of periodic insect dynamics, Bulmer [11] utilizes a nonlinear semelparous Leslie model with projection matrix

$$(3.49) \quad \mathbf{P}(\mathbf{x}) = \begin{bmatrix} 0 & 0 & \cdots & 0 & b_m \beta(\mathbf{x}) \\ s_1 \sigma_1(\mathbf{x}) & 0 & \cdots & 0 & 0 \\ 0 & s_2 \sigma_2(\mathbf{x}) & \cdots & 0 & 0 \\ \vdots & \vdots & & \vdots & \vdots \\ 0 & 0 & \cdots & s_{m-1} \sigma_{m-1}(\mathbf{x}) & 0 \end{bmatrix}$$

with $b_m > 1$, $0 < s_i < 1$, and

$$\beta(\mathbf{0}_m) = \sigma_i(\mathbf{0}_m) = 1$$

and a time unit of one year. In this age-structured model, individuals are juveniles for $m - 1$ years and emerge in the m th year as reproducing adults. Because of the 0 in the lower-right corner, adults do not survive an additional breeding year; hence, the population is semelparous. The

⁶There are, however, thousands of other cicada species that are not periodical.

inherent projection matrix

$$(3.50) \quad P(\mathbf{0}_m) = \begin{bmatrix} 0 & 0 & \cdots & 0 & b_m \\ s_1 & 0 & \cdots & 0 & 0 \\ 0 & s_2 & \cdots & 0 & 0 \\ \vdots & \vdots & & \vdots & \vdots \\ 0 & 0 & \cdots & s_{m-1} & 0 \end{bmatrix}$$

is *imprimitive* (Example 2.13). To see this, we note that its m eigenvalues

$$(3.51) \quad \lambda_i = \sqrt[m]{R_0} u_i$$

are the m th roots of the inherent net reproduction number

$$R_0 = b_m s_1 s_2 \cdots s_{m-1},$$

where $u_i = \exp(2\pi i/m)$, $i = 1, 2, \dots, m$, are the m th roots of unity. (See Exercise 3.47.) Thus, the dominant eigenvalue $r_0 = \lambda_1 = \sqrt[m]{R_0}$ is not strictly dominant (since all eigenvalues have the same absolute value).

By Theorem 3.20, the extinction equilibrium is globally asymptotically stable for $R_0 < 1$.

From the results described in Section 3.6, we know that upon destabilization of the extinction equilibrium, when R_0 increases through 1, there come into existence both positive equilibria and synchronous cycles. In a population at a positive equilibrium, individuals from all age classes are present at all times, whereas in a population in single-class synchronous cycle (3.37), the age classes are synchronized so as to never overlap and interact. It is the latter situation, in which adults emerge only once every m years, that is the mathematical representation of the periodical insect life cycle. So, in a modeling study of periodic insects, a main goal is to determine the circumstances under which there exist stable single-year synchronous cycles (3.37).

The main conclusion in Bulmer's study [11] is that strong competition among the different age classes is the main mechanism that promotes synchronous cycles and a periodical life cycle. Following Bulmer, we model interclass and intraclass competition by using Ricker-type exponential factors

$$\beta(\mathbf{x}) = \exp\left(-\sum_{j=1}^m c_{mj} x_j\right) \quad \text{and} \quad \sigma_i(\mathbf{x}) = \exp\left(-\sum_{j=1}^m c_{ij} x_j\right)$$

in the projection matrix (3.49). The coefficients $c_{ii} > 0$ measure the intensity of competition among individuals in the i th age class (intraclass competition), while $c_{ij} \geq 0$ for $i \neq j$ measure the effect of competition on the survival of an i -class individual from individuals in the j -class (interclass competition). For insects whose maturation takes $m = 2$ years (such as most species of periodical moths [73]), Theorem 3.33 provides criteria for stable synchronous 2-cycles. It is left as Exercise 3.47 to show that the formulas for the diagnostic quantities in Theorem 3.33 are the same as in Example 3.34:

$$\begin{aligned} c_w &= c_{11} + s_1 c_{22} > 0, & c_b &= c_{21} + s_1 c_{12} \geq 0, \\ \kappa_+ &= c_{11} + s_1 c_{22} + c_{21} + s_1 c_{12} > 0, & \text{and} \\ \kappa_- &= c_{11} + s_1 c_{22} - (c_{21} + s_1 c_{12}). \end{aligned}$$

This establishes the same conclusions for this semelparous Leslie model with $m = 2$ obtained in Example 3.34:

There is a dynamic dichotomy between the forward bifurcating positive equilibria and synchronous 2-cycles as R_0 increases through 1. The synchronous 2-cycles are stable (and the positive equilibria unstable) if $\kappa_- < 0$, which means between age class competition is more significant than within age class competition. It follows that sufficiently intense interclass competition will produce periodical life cycle dynamics.

This is the same conclusion reached by Bulmer [11] in his study of this $m = 2$ dimensional case.

While the $m = 2$ dimensional semelparous Leslie model is appropriate for the many species of periodical insects (including many moths and butterflies as listed in [73]) that synchronously emerge every 2 years, there are periodical insects whose emergence period is longer. Examples include May beetles (*Melolontha* sp.), whose periods range from 3 to 6 years, and the famous periodical cicadas (*Magicicada* sp.) with emergence periods of 13 and 17 years. While it is known that positive equilibria and single-year, synchronous m -cycles bifurcate at $R_0 = 1$ for a nonlinear matrix model with a projection matrix (3.49) of any dimensions $m \geq 2$, a dynamic dichotomy between them does not necessarily hold when $m \geq 3$ as it does when $m = 2$ [42]. Other types of attractors can also arise by bifurcation at $R_0 = 1$ when $m \geq 3$. To illustrate this, we

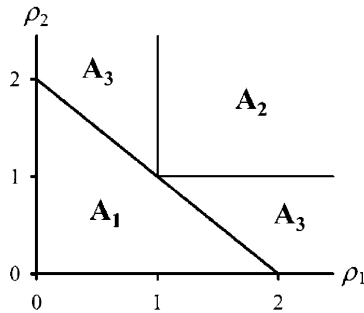


Figure 3.16. The parameter map that determines the nature of the bifurcation at $R_0 = 1$ for the $m = 3$ dimension semelparous Leslie model with projection matrix (3.49). Region A_1 : $\rho_1 + \rho_2 < 2$. Region A_2 : $\rho_1 > 1$ and $\rho_2 > 1$. Region A_3 : $\rho_1 + \rho_2 < 2$ and either $\rho_1 < 1$ or $\rho_2 < 1$ (but not both).

take a brief look at the case $m = 3$, for which the bifurcation at $R_0 = 1$ is fairly well understood [30].

Consider the projection matrix (3.49) with $m = 3$ and density factors (3.52)

$$\beta(\mathbf{x}) = \exp\left(-\sum_{j=1}^3 c_{3j}x_j\right) \quad \text{and} \quad \sigma_i(\mathbf{x}) = \exp\left(-\sum_{j=1}^3 c_{ij}x_j\right) \quad \text{for } i = 1 \text{ and } 2,$$

where the coefficients $c_{ij} \geq 0$ measure competitive intensity. It is shown in [30] that the bifurcation of positive equilibria and the bifurcation of single-year, synchronous 3-cycles are both forward and that their stability properties (at least for $R_0 \gtrapprox 1$) are determined by the two ratios

$$\rho_1 := \frac{c_{21} + s_1 c_{32} + s_1 s_2 c_{13}}{c_{11} + s_1 c_{22} + s_1 s_2 c_{33}} \quad \text{and} \quad \rho_2 := \frac{c_{31} + s_1 c_{12} + s_1 s_2 c_{23}}{c_{11} + s_1 c_{22} + s_1 s_2 c_{33}}.$$

The denominator is a measure of intraclass competition in the population, since it involves only the competition coefficients c_{ii} (at least one of which we assume is positive). The numerators are measures of interclass competition in the population. The numerators in ρ_1 (respectively ρ_2) involve coefficients that measure competition effects that each age class has on the age class one year older (respectively younger).

We locate which region A_i in the positive quadrant of the (ρ_1, ρ_2) -plane, as shown in Figure 3.16, the point (ρ_1, ρ_2) lies. The bifurcating

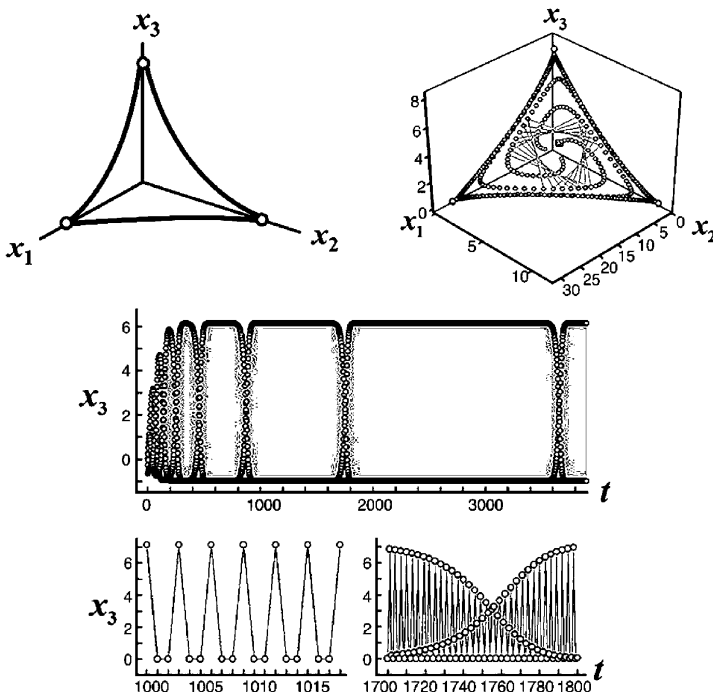


Figure 3.17. Graphs obtained from the $m = 3$ dimensional semelparous Leslie model with projection matrix (3.49) and density factors (3.52) [30]. Inherent parameter values are $b_2 = 4$, $s_1 = 0.5$, and $s_2 = 0.75$; hence, $R_0 = 1.5$. The competition coefficients

are given in the matrix $[c_{ij}] = \begin{bmatrix} 0.01 & 0 & 0 \\ 0.03 & 0.01 & 0 \\ 0.01 & 0.02 & 0.01 \end{bmatrix}$. The point

$(\rho_1, \rho_2) = (2.133, 0.5333)$ lies in region A_3 in Figure 3.16. The upper-left graph shows the bifurcating invariant loop containing the single-year, synchronous 3-cycle shown by open circles. The upper-right graph shows the orbit of a typical solution (with initial conditions $(x_1(0), x_2(0), x_3(0)) = (1, 1, 1)$). Note that it spirals outward and approaches the invariant loop. The middle graph shows the time series of the adult component $x_3(t)$ of this solution. The bottom-left graph shows a sample close-up of the synchronous 3-cycle oscillation of $x_3(t)$ that occurs during the recurring episodes. The bottom-right graph shows a close-up of a typical transition phase between 3-cycle episodes, which results in a phase shift of the oscillation. Reproduced from Fig. 5 in [30] with permission.

positive equilibria are stable if $(\rho_1, \rho_2) \in A_1$ and are unstable if $(\rho_1, \rho_2) \in A_2 \cup A_3$. The bifurcating single-year, synchronous 3-cycles are unstable if $(\rho_1, \rho_2) \in A_1 \cup A_3$ and are stable if $(\rho_1, \rho_2) \in A_2$.

Thus, if we restrict (ρ_1, ρ_2) to lie in $A_1 \cup A_2$, the dynamic dichotomy between the equilibria and the synchronous 3-cycles holds. We interpret $(\rho_1, \rho_2) \in A_1$ as weak interclass competition since neither ρ_1 nor ρ_2 can be large, and we interpret (ρ_1, ρ_2) outside of A_1 as strong interclass competition. With this interpretation, we conclude once again, provided $(\rho_1, \rho_2) \notin A_3$, that strong interclass competition results in a periodical life cycle.

But what about $(\rho_1, \rho_2) \in A_3$? In this case, *both* the positive equilibria and synchronous 3-cycles are unstable. It is shown in [30] that an invariant loop of the form shown in the upper-left graph of Figure 3.17 also forward bifurcates at $R_0 = 1$. This triangular shaped loop lies entirely on the boundary ∂R_+^3 of the positive octant R_+^3 (which means that at all of its points, there is at least one missing age class). The bifurcating synchronous 3-cycle is in the loop, as shown by the open circles in Figure 3.16. The connecting sides of the loop are invariant (that is to say, if an initial point lies on a side, then the solution remains on the loop for all time). Furthermore, for $(\rho_1, \rho_2) \in A_3$, the loop is the attractor of solutions in R_+^3 . To see how solutions approaching this loop behave, the time series plots of the adult class x_3 of a sample solution is also shown in Figure 3.17.

Note that the adult class shows recurring episodes of emergence with period 3 of increasing duration. These episodes are separated by a transition phase that, it turns out, shifts the 3-cycle pattern to a new phase. (Since the solution recurrently visits the three phases of the 3-cycle, the loop is called a **cycle chain**.) So, although solutions do not approach the single-year, synchronous 3-cycle, they nonetheless show a synchronous, 3-cycle emergence pattern over longer and longer lasting episodes as time goes on. In this sense, the model predicts a periodical life cycle of period 3 in region A_3 as well as in region A_2 . In summary,

For the $m = 3$ dimensional semelparous Leslie model with density factors (3.52), the bifurcation at $R_0 = 1$ produces a dynamic dichotomy between positive equilibria (with overlapping generations) versus synchronized 3-cycles of nonoverlapping generations, with the

latter dynamic occurring if interclass competition intensity is sufficiently high.

Other casual mechanisms for a periodical life cycle have also been investigated using semelparous Leslie models. For example, the role of predation on the emerging adults can be a contributing factor. See Exercise 3.49.

The existence of bifurcating cycle chains in this model serves to illustrate the complexity of the dynamics that can occur in higher-dimensional models with imprimitive projection matrices. In fact, there are other dynamic patterns possible in this $m = 3$ dimensional model that we will not look at here. See [30], [42], [47], [48], [56], [59], [58], [89], [90], [91], [93], [127], [128] for more studies and applications of models with imprimitive inherent projection matrices.

3.8. Concluding Remarks

In this chapter, the matrix modeling methodology for the dynamics of a structured population developed in Chapter 2 is extended to include density effects (i.e., to include the effects that population densities can have on class-specific vital rates). This makes the entries in the projection matrix $\mathbf{P} = \mathbf{P}(\mathbf{x})$ dependent on the population state variable \mathbf{x} with the result that the matrix equation is nonlinear.

The main biological focus of this chapter, as it is in Chapter 1 for the $m = 1$ case, is on the question of the population's extinction versus survival. Mathematically, this focus is on the stability or instability of the extinction equilibrium. The main theorems of the chapter show that, under general conditions, the bifurcation of positive (survival) equilibria that occurs when the extinction equilibrium destabilizes is not vertical, as it is for linear equations, but is either forward or backward. Moreover, when the inherent projection matrix is primitive, the stability of the bifurcating positive equilibria is correlated with the direction of bifurcation.

For example, when r_0 (or R_0) is used as the bifurcation parameter, a forward bifurcation produces stable positive equilibria, while a backward bifurcation produces unstable positive equilibria. This general result is, however, limited to a neighborhood of the bifurcation point

$r_0 = 1$ (or $R_0 = 1$) and $\mathbf{x}_e = \mathbf{0}_m$; outside this neighborhood, other bifurcations can occur as the positive equilibria change their stability properties to form other equilibria, periodic cycles, or invariant loops.

Of particular interest, is the occurrence of a strong Allee effect as a consequence of a backward-unstable bifurcation. A strong Allee effect is a scenario in which multiple stable attractors exists, one of which is the extinction equilibrium and another of which is a survival attractor. This general state of affairs requires the technical assumption that the inherent projection matrix is $\mathbf{P}(\mathbf{0}_m)$ primitive. When this technical assumption is dropped, other more complicated bifurcations can occur in the neighborhood of the bifurcation point. This is illustrated in Sections 3.6 and 3.7.3 by the simultaneous bifurcation of synchronous cycles and positive equilibria.

3.9. Exercises

Exercise 3.35. Verify that (3.4) is a solution of the juvenile-adult model (3.2) when $b_2 s_1 \neq 1$.

Exercise 3.36. Use the formulas for r_0 and R_0 for the juvenile-adult model in Example 3.15 to corroborate Theorem 2.15.

Exercise 3.37. Calculate R_0 and apply Theorem 3.22 to the matrix equation with these fertility and transition matrices (all coefficients are positive):

$$(a) \quad \mathbf{F}(\mathbf{x}) = \begin{bmatrix} 0 & b_2 \exp(-c_1 x_1 - c_2 x_2) \\ 0 & 0 \end{bmatrix} \text{ and } \mathbf{T}(\mathbf{x}) = \begin{bmatrix} 0 & 0 \\ s_1 & s_2 \end{bmatrix};$$

$$(b) \quad \mathbf{F}(\mathbf{x}) = \begin{bmatrix} 0 & b_2 \frac{1+x_2}{1+c x_2^2} \\ 0 & 0 \end{bmatrix} \text{ and } \mathbf{T}(\mathbf{x}) = \begin{bmatrix} 0 & 0 \\ s_1 & s_2 \end{bmatrix};$$

$$(c) \quad \mathbf{F}(\mathbf{x}) = \begin{bmatrix} 0 & 0 & b_2 \exp(-c_1 x_1 - c_2 x_3) \\ 0 & 0 & 0 \\ 0 & 0 & 0 \end{bmatrix} \text{ and}$$

$$\mathbf{T}(\mathbf{x}) = \begin{bmatrix} 0 & 0 & 0 \\ s_{12} & 0 & 0 \\ 0 & s_{32} \exp(-c_3 x_3) & s_{33} \end{bmatrix};$$

$$(d) \quad \mathbf{F}(\mathbf{x}) = \begin{bmatrix} 0 & 0 & b_3 \frac{e^{-c_1 x_4}}{1+c_1 x_3 + c_2 x_4} & b_4 \frac{e^{-c_1 x_4}}{1+c_1 x_3 + c_2 x_4} \\ 0 & 0 & 0 & 0 \\ 0 & 0 & 0 & 0 \\ 0 & 0 & 0 & 0 \end{bmatrix} \text{ and}$$

$$\mathbf{T}(\mathbf{x}) = \begin{bmatrix} s_{11} & 0 & 0 & 0 \\ s_{21} & 0 & 0 & 0 \\ 0 & s_3 e^{-c_5 x_2} & 0 & 0 \\ 0 & 0 & s_4 e^{-c_6 x_3} & s_4 e^{-c_7 x_4} \end{bmatrix}.$$

Exercise 3.38. Prove Theorem 3.9) by adapting the proof of Theorem 1.10 given in Appendix A.2.

Exercise 3.39. Verify that

$$\begin{bmatrix} x_1(t) \\ x_2(t) \end{bmatrix} = \begin{cases} \begin{bmatrix} \frac{b_2 x_1(0)}{icx_1(0)+b_2} \\ \frac{x_2(0)}{icx_2(0)+1} \end{bmatrix} & \text{when } t = 2i \text{ for } i \in \mathbb{Z}_+ \\ \begin{bmatrix} \frac{b_2 x_2(0)}{(i+1)c x_2(0)+1} \\ \frac{x_1(0)}{icx_1(0)+b_2} \end{bmatrix} & \text{when } t = 2i+1 \text{ for } i \in \mathbb{Z}_+ \end{cases}$$

is a formula for the solution of the semelparous juvenile-adult model (3.2) when $b_2 s_1 = 1$ and use it to show that the extinction equilibrium is globally asymptotically stable.

Exercise 3.40. Prove that the Jacobian of $\mathbf{P}(\mathbf{x})\mathbf{x}$ evaluated at $\mathbf{x}_e = \mathbf{0}_m$ is the inherent projection matrix $\mathbf{P}(\mathbf{0}_m)$.

Exercise 3.41. Find a formula for the positive equilibrium of the iteroparous juvenile-adult model in Example 3.24 when $b > b_0$. Use the formula to perform a stability analysis and show that the positive equilibria are locally asymptotically stable for all values of $b > b_0$. (Theorem 3.21 guarantees stability only for $b \gtrsim b_0$.)

Exercise 3.42. Suppose in the nonlinear Leslie matrix in Example 3.25 that all the density factors are identical (i.e., $\beta_i(\mathbf{x}) = \exp(-cp)$ and $p = \sum_{j=1}^m w_j x_j$). (This is the case studied in [102].) We saw in Example 3.25 that the general bifurcation theory shows there exist positive equilibria for $R_0 \gtrsim 1$.

- (a) Show that there exists a unique positive equilibrium for every $R_0 > 1$ by finding an algebraic formula for the positive equilibria.

- (b) Based on what we learned about the Ricker difference equation in Chapter 1, we should not be surprised if the bifurcating positive equilibria that are stable for $R_0 \lesssim 1$ might lose stability as R_0 increases. Here is an example to confirm this. Consider the $m = 2$ dimension case with just two age classes and take parameter values $b_1 = 1$, $b_2 = 20$, $s_1 = 0.1$, and $s_2 = 0.05$. Show $R_0 > 1$ and calculate the positive equilibrium $\mathbf{x} = \text{col}(x_1, x_2)$. Use the Linearization Principle to show that this positive equilibrium is unstable.

Exercise 3.43. Show that for $R_0 \gtrsim 0.67$, the positive equilibrium of the juvenile-adult model in Example 3.27 obtained from the larger root x_2 (using the plus sign in (3.26)) is stable and that the positive equilibrium obtained from the smaller root x_2 (using the minus sign in (3.26)) is unstable. (HINT: Find first degree Taylor polynomial approximations to the eigenvalues $\lambda = \lambda(R_0)$ of the Jacobian evaluated at the positive equilibria, using first degree Taylor polynomial approximations of the roots $x_2 = x_2(R_0) \approx x_2(0.67) + \partial_{R_0}(0.67)(R_0 - 0.67)$ centered at $R_0 = 0.67$.)

Exercise 3.44. In Example 3.28, prove the assertions concerning the eigenvalues as a function of R_0 .

Exercise 3.45. Prove that $\mathbf{Jf}^{(2)}(\mathbf{x}) = \mathbf{Jf}(\mathbf{x}_1)\mathbf{Jf}(\mathbf{x})$, where $\mathbf{x}_1 = \mathbf{f}(\mathbf{x})$. Then by induction, prove that

$$\mathbf{Jf}^{(p)}(\mathbf{x}) = \mathbf{Jf}(\mathbf{x}_{p-1})\mathbf{Jf}(\mathbf{x}_{p-2}) \cdots \mathbf{Jf}(\mathbf{x}_1)\mathbf{Jf}(\mathbf{x}),$$

where $\mathbf{x}_i = \mathbf{f}^{(i)}(\mathbf{x})$ and $p \geq 3$ is an integer (that is, $\mathbf{f}^{(1)}(\mathbf{x})$ is the same as $\mathbf{f}(\mathbf{x})$).

Exercise 3.46. In Example 3.32, verify the formula for R_0 and the forward and backward bifurcation inequalities.

Exercise 3.47. Prove that the eigenvalues of the semelparous Leslie matrix (3.50) are given by (3.51).

Exercise 3.48. Consider the $m = 2$ dimensional juvenile-adult model with fertility and transition matrices

$$\mathbf{F} = \begin{bmatrix} 0 & be^\mu \frac{1}{1+c_2 x_2} \\ 0 & 0 \end{bmatrix} \quad \text{and} \quad \mathbf{T} = \begin{bmatrix} 0 & 0 \\ s_1 & s_2 e^{-\mu} \end{bmatrix}.$$

Here, $\mu > 0$ represents the effort put into gathering food resources, and the birth rate be^μ is an (exponentially) increasing function of this effort.

This effort in resource gathering results, however, in a decreased adult survival, a trade-off expressed in the entry $s_2 e^{-\mu}$.

- (a) Calculate the inherent reproduction number and consider it as a function of μ .
- (b) Assume $R_0 < 1$ when $\mu = 0$ and show, in this case when no effort is expended in resource gathering, that the extinction equilibrium is globally asymptotically stable (and hence the population goes extinct).
- (c) When $R_0 < 1$ when $\mu = 0$, use Theorem 3.22 to show that there exists a unique value $\mu_0 > 0$ at which a forward and stable bifurcation of positive equilibria occurs as μ increases through μ_0 .
- (d) Extend the result in (c) by solving the equilibrium equations and performing a stability analysis by using the Linearization Principle.

Exercise 3.49. In his modeling study of periodical insects, Bulmer [11] also considers the effect that predation on the emerging adults has. He does this by introducing another factor into the fertility density term $\beta(\mathbf{x})$ in the projection matrix (3.49). The factor is taken to be an increasing function of adult density x_m in order to model the so-called **predator saturation effect**. This effect assumes that a population of predators can consume only so many emerging adults and that if only few adults emerge, nearly all will be eaten and reproduction will be low, but if more adults merge, then more will survive predation and reproduction will be greater. The factor Bulmer uses is $1 - \exp(-px_m)$, $p > 0$, and in the $m = 2$ dimensional case, this leads to the projection matrix (3.49) with

$$\begin{aligned}\beta(\mathbf{x}) &= \exp(-c_{21}x_1 - c_{22}x_2)(1 - \exp(-px_2)) \quad \text{and} \\ \sigma_1(\mathbf{x}) &= \exp(-c_{11}x_1 - c_{12}x_2).\end{aligned}$$

- (a) Use Theorem 3.33 to determine conditions on p and on the competition coefficients c_{ij} under which the bifurcations of both the positive equilibria and synchronous 2-cycles are forward (and hence the dynamic dichotomy described in Theorem 3.33 holds). Does the conclusion that sufficiently strong interclass competition causes the synchronous 2-cycles to be stable still hold?

- (b) Assume when predation is absent ($p = 0$) that, in the dynamic dichotomy of Theorem 3.33, the bifurcation of positive equilibria is forward and stable. Show that under this circumstance, it is possible for predation to reverse the stability alternative in the dichotomy (i.e., that there are values of $p > 0$ for which the synchronous 2-cycles are stable). This shows that, under the right circumstances, predation can be the cause of a periodical life cycle.

Exercise 3.50. The stability of the extinction equilibrium and the bifurcation of positive equilibria upon its destabilization are related to the inherent population growth rate r_0 in Theorems 3.13 and 3.21 and to the inherent reproduction rate R_0 in Theorems 3.22 and 3.17. In general, neither of these two quantities appear explicitly in a matrix model, but they are quantities derived from the parameters in the model equations. One can instead relate the stability and bifurcation results in these theorems to a parameter, call it μ , that does appear explicitly in the model equations by asking, When does a change in μ cause r_0 to increase through 1? Since r_0 depends on μ , we write $r_0(\mu)$.

Suppose there exists a value μ_0 for which $r(\mu_0) = 1$ (equivalently $R_0(\mu_0) = 1$). Use (2.36) and the chain rule to show that

$$\frac{dr_0(\mu_0)}{d\mu} = \frac{1}{\mathbf{w}^T \mathbf{v}} \mathbf{w}^T \frac{d\mathbf{P}(\mu_0)}{d\mu} \mathbf{v}.$$

It follows that if $dr_0(\mu_0)/d\mu > 0$ (or $dr_0(\mu_0)/d\mu < 0$), then $r_0(\mu)$ increases through 1 as μ increases (respectively decreases) through μ_0 and the extinction equilibrium destabilization and positive equilibria bifurcation results of Theorems 3.13 and 3.21 apply.

This relates these stability and bifurcation results to the signs of the derivatives $d p_{ij}(\mu_0)/d\mu$ of the entries p_{ij} in the projection matrix. As an example, if all entries $p_{ij}(\mu)$ that depend on μ are (strictly) increasing functions of μ (at least when $\mu = \mu_0$), then one knows immediately that the destabilization of the extinction equilibrium and a forward-stable bifurcation of positive equilibria occur as μ increases through μ_0 .

Chapter 4

Disease and Epidemic Models

In a structured population model designed to study the spread of a disease through a population, individuals are classified according to a selection of disease-related categories: susceptible, infected, infectious, recovered, quarantined, vaccinated, and so on. Because of the obvious interest and importance of understanding epidemics, there is a huge (and continually growing) amount of literature in which models for innumerable kinds of diseases are derived and analyzed. Almost all of these models structure a population (in some cases the pathogen causing the disease as well) into a finite number of discrete categories. Tracking these subpopulations in continuous time results in models based on differential equations. On the other hand, there is substantial literature on models in discrete time disease as well. This chapter contains a brief introduction to the discrete time modeling of diseases and the dynamics of epidemics, treating the subject in the spirit of and using the analytic methods in Chapters 2 and 3. A good reference for both differential- and difference-equation-based epidemic models is [9].

4.1. Preliminaries

For the populations models considered in Chapters 2 and 3, a basic concern is with the extinction or survival of the population (or mathematically, the stability of the extinction equilibrium $\mathbf{x}_e = \mathbf{0}$). For a model

structured by classes related to a disease, the main concern is generally not with the extinction of the population, but instead with the extinction of the infected classes within the population. For this reason, we begin our model building by applying the basic discrete time modeling methodology to the infected classes, which we place in a vector $\mathbf{x}_1 \in R_+^m$. The remaining classes we denote by $\mathbf{x}_2 \in R_+^n$. For example, in the lowest-dimensional case, $\mathbf{x}_1 = [x_1]$ is the (scalar) class of infected (and infectious) individuals, and $\mathbf{x}_2 = [x_2]$ is the (scalar) class of noninfected, but susceptible individuals (and in these one-dimensional cases, we as usual drop the bracket notation). With these epidemic class distinctions, we can write a general epidemic model in the form

$$(4.1) \quad \begin{aligned} (a) \quad & \mathbf{x}_1(t+1) = \mathbf{f}_1(\mathbf{x}_1(t), \mathbf{x}_2(t)) \\ (b) \quad & \mathbf{x}_2(t+1) = \mathbf{f}_2(\mathbf{x}_1(t), \mathbf{x}_2(t)). \end{aligned}$$

We assume that infections only occur by transmission from infected individuals so that $\mathbf{0}_m = \mathbf{f}_1(\mathbf{0}_m, \mathbf{x}_2)$. We also assume that in the absence of the disease, the population has a stable equilibrium, that is to say the **disease-free equation**

$$(4.2) \quad \mathbf{x}_2(t+1) = \mathbf{f}_2(\mathbf{0}_m, \mathbf{x}_2(t))$$

has a (locally asymptotically) stable equilibrium. These requirements are part of our general assumptions on

$$\mathbf{f}(\mathbf{x}) := \text{col}(\mathbf{f}_1(\mathbf{x}_1, \mathbf{x}_2), \mathbf{f}_2(\mathbf{x}_1, \mathbf{x}_2))$$

for the model equations (4.1) and are summarized as follows.

Assumption 4.1. $\mathbf{f} \in C^2(R^{m+n} : R_+^{m+n})$. Furthermore, $\mathbf{0}_m = \mathbf{f}_1(\mathbf{0}_m, \mathbf{x}_2)$ for all $\mathbf{x}_2 \in R_+^n$, and there exists $\mathbf{x}_{2e} \in R_+^n$, $\mathbf{x}_{2e} \neq \mathbf{0}_n$ such that $\mathbf{x}_{2e} = \mathbf{f}_2(\mathbf{0}_m, \mathbf{x}_{2e})$ and $\rho(\mathbf{J}_{\mathbf{x}_2} \mathbf{f}_2(\mathbf{0}_m, \mathbf{x}_{2e})) < 1$, where $\mathbf{J}_{\mathbf{x}_2} \mathbf{f}_2$ is the $n \times n$ Jacobian of $\mathbf{f}_2(\mathbf{x}_1, \mathbf{x}_2)$ with respect to \mathbf{x}_2 .

Under Assumption 4.1, the system of equations (4.1) has the **disease-free equilibrium**

$$(4.3) \quad \mathbf{x}_e = \begin{bmatrix} \mathbf{0}_m \\ \mathbf{x}_{2e} \end{bmatrix} \in \partial R_+^{m+n}.$$

Example 4.2. A Susceptible-Infected (SI) Model. Consider a population of susceptibles x_2 whose dynamics are governed, in the absence

of the disease, by the equation

$$(4.4) \quad x_2(t+1) = b_0 \frac{1}{1 + cx_2(t)} x_2(t) + \sigma_S x_2(t)$$

$$\text{with } b_0, c > 0 \text{ and } 0 < \sigma_S < 1$$

(as in Section 1.2). In the presence of the disease, we let φ be the fraction of susceptibles x_2 who do not become infected (per unit time). This fraction (called the **escape probability**) depends, of course, on the number of infected individuals x_1 , so we write $\varphi = \varphi(x_1)$. Then the fraction of surviving susceptibles that remain susceptible at $t + 1$ is $\sigma_S \varphi(x_1)$, and the equation for the susceptibles x_2 becomes

$$x_2(t+1) = b_0 \frac{1}{1 + cx_2(t)} x_2(t) + \sigma_S \varphi(x_1(t)) x_2(t).$$

The fraction of susceptibles that become infected (per unit time), and hence move into the infected class, is $(1 - \varphi(x_1)) \sigma_S$; thus, the infected class is given by (the newly infected plus the surviving infected)

$$x_1(t+1) = (1 - \varphi(x_1(t))) \sigma_S x_2(t) + \sigma_I x_1(t),$$

where σ_I is the survival probability of infected individuals.

We assume the **escape function** $\varphi(x_1)$ is a decreasing function of x_1 (i.e., $\partial_{x_1} \varphi(x) < 0$ for $x \geq 0$) that equals 1 at $x_1 = 0$ (no infection occurs when no infected individuals are present) and approaches 0 as $x_1 \rightarrow \infty$ (the probability of escaping infection drops to 0 as the class of infected individuals increases without bound).

The equations for this susceptible-infected model (or SI model) are

$$(4.5) \quad \begin{aligned} (a) \quad x_1(t+1) &= (1 - \varphi(x_1(t))) \sigma_S x_2(t) + \sigma_I x_1(t) \quad \text{and} \\ (b) \quad x_2(t+1) &= b_0 \frac{1}{1 + cx_2(t)} x_2(t) + \varphi(x_1(t)) \sigma_S x_2(t) \end{aligned}$$

and have the form (4.1) with

$$\mathbf{f}_1(\mathbf{x}_1, \mathbf{x}_2) = (1 - \varphi(x_1)) \sigma_S x_2 + \sigma_I x_1 \quad \text{and}$$

$$\mathbf{f}_2(\mathbf{x}_1, \mathbf{x}_2) = b_0 \frac{1}{1 + cx_2} x_2 + \varphi(x_1) \sigma_S x_2.$$

(We drop the bracket notation for one-dimensional vectors.) It is

straightforward to show that Assumption 4.1 is satisfied by the equilibrium

$$x_{2e} = \frac{1}{c} \left(b \frac{1}{1 - \sigma_S} - 1 \right), \quad b \frac{1}{1 - \sigma_S} > 1$$

(which by Theorem 1.26, is in fact globally asymptotically stable on $\text{int}(R_+)$). The disease-free equilibrium of the SI model is

$$\mathbf{x}_e = \begin{bmatrix} \mathbf{0} \\ x_{2e} \end{bmatrix} = \begin{bmatrix} \mathbf{0} \\ \frac{1}{c} \left(b \frac{1}{1 - \sigma_S} - 1 \right) \end{bmatrix}, \quad b \frac{1}{1 - \sigma_S} > 1.$$

□

A cycle graph associated with the SI model in example 4.2 appears in Figure 4.1. Note that in this elementary model, it is assumed that newborns are susceptible (i.e., none are born infected), infected individuals do not reproduce, and there is no recovery from the disease.

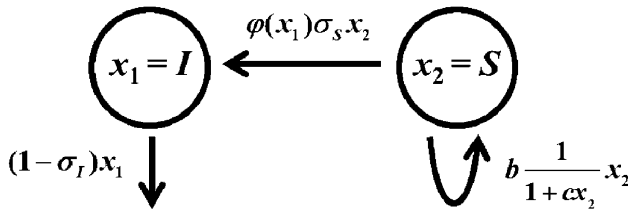


Figure 4.1. A cycle graph for the SI model (4.5).

Remark 4.3. *A remark about notation: In epidemic models, it is common to denote the state variables by (usually uppercase) letters suggestive of their disease-related definitions, such as I for infected, S for susceptible, R for recovered, and so on. With this notation, a common way of writing the basic SI model (4.5) is*

$$\begin{aligned} S(t+1) &= b \frac{1}{1 + cS(t)} S(t) + \varphi(I(t)) \sigma_S S(t) \\ I(t+1) &= (1 - \varphi(I(t))) \sigma_S S(t) + \sigma_I I(t). \end{aligned}$$

While we will occasionally adopt this suggestive notation, we will for the most part keep the state variable notation x_i so as to be notationally consistent with the notation in earlier chapters on structured population dynamics.

4.2. Disease-Free Equilibria and R_0

If the disease-free equilibrium

$$\mathbf{x}_e = \begin{bmatrix} \mathbf{0}_m \\ \mathbf{x}_{2e} \end{bmatrix}$$

is (locally asymptotically) stable, then $\mathbf{x}(0)$ near \mathbf{x}_e implies

$$\lim_{t \rightarrow \infty} \mathbf{x}_1(t) = \mathbf{0}_m,$$

that is to say when the susceptible population is at or near its equilibrium, then an infection will ultimately disappear after an invasion by a small population of infected individuals. To attain this desirable result, so as to avoid the disease remaining in the population (i.e., becoming endemic), we are interested in conditions under which the disease-free equilibrium is stable. Towards this end, we apply the Linearization Principle by calculating the Jacobian matrix associated with the model equations (4.1) evaluated at the disease-free equilibrium:

$$\mathbf{J}_x \mathbf{f}(\mathbf{x}_e) := \mathbf{J}_x \mathbf{f}(\mathbf{x})|_{\mathbf{x}=\mathbf{x}_e}.$$

By Assumption 4.1, we obtain a block diagonal matrix

$$\mathbf{J}_x \mathbf{f}(\mathbf{x}_e) = \begin{bmatrix} \mathbf{J}_{x_1} \mathbf{f}_1(\mathbf{0}, \mathbf{x}_{2e}) & \mathbf{0}_{m \times n} \\ \mathbf{J}_{x_2} \mathbf{f}_2(\mathbf{0}, \mathbf{x}_{2e}) & \mathbf{J}_{x_2} \mathbf{f}_2(\mathbf{0}, \mathbf{x}_{2e}) \end{bmatrix},$$

where $\mathbf{J}_{x_i} \mathbf{f}_j(\mathbf{x}_0, \mathbf{x}_1)$ is the Jacobian of \mathbf{f}_j with respect to x_i and evaluated at the disease-free equilibrium (4.3)

$$\mathbf{J}_{x_i} \mathbf{f}_j(\mathbf{0}, \mathbf{x}_1^*) := \mathbf{J}_{x_i} \mathbf{f}_j(\mathbf{x}_0, \mathbf{x}_1)|_{(\mathbf{x}_0, \mathbf{x}_1)=(\mathbf{0}, \mathbf{x}_1^*)}.$$

The eigenvalues of $\mathbf{J}_x \mathbf{f}(\mathbf{x}_e)$ consist of the eigenvalues of the diagonal blocks $\mathbf{J}_{x_1} \mathbf{f}_1(\mathbf{0}, \mathbf{x}_{2e})$ and $\mathbf{J}_{x_2} \mathbf{f}_2(\mathbf{0}, \mathbf{x}_{2e})$. Since $\rho(\mathbf{J}_{x_2} \mathbf{f}_2(\mathbf{0}_m, \mathbf{x}_{2e})) < 1$ by Assumption 4.1, the eigenvalues of the diagonal block $\mathbf{J}_{x_2} \mathbf{f}_2(\mathbf{0}_m, \mathbf{x}_{2e})$ all lie within the unit circle of the complex plane, and as a result, the stability of the disease-free equilibrium is determined, according to the Linearization Principle, by the eigenvalues of the remaining diagonal block $\mathbf{J}_{x_1} \mathbf{f}_1(\mathbf{0}, \mathbf{x}_{2e})$. In particular, if $\rho(\mathbf{J}_{x_1} \mathbf{f}_1(\mathbf{0}, \mathbf{x}_{2e})) < 1$, then the disease-free equilibrium is (locally asymptotically) stable.

The term $\mathbf{f}_1(\mathbf{x}_1, \mathbf{x}_2)$ in equation (4.5)(a) describes the dynamics of the infected classes in the vector \mathbf{x}_1 . We model it by adding newly infected individuals to the surviving infected individuals to get

$$\mathbf{f}_1(\mathbf{x}_1, \mathbf{x}_2) = \mathbf{n}(\mathbf{x}_1, \mathbf{x}_2) + \mathbf{s}(\mathbf{x}_1, \mathbf{x}_2).$$

Then we can write the Jacobian as

$$\mathbf{J}_{\mathbf{x}_1} \mathbf{f}_1(\mathbf{0}, \mathbf{x}_{2e}) = \mathbf{F}(\mathbf{0}, \mathbf{x}_{2e}) + \mathbf{T}(\mathbf{0}, \mathbf{x}_{2e}),$$

where we use the notation

$$(4.6) \quad \begin{aligned} \mathbf{F}(\mathbf{0}, \mathbf{x}_{2e}) &:= \mathbf{J}_{\mathbf{x}_1} \mathbf{n}(\mathbf{0}, \mathbf{x}_{2e}) \\ \mathbf{T}(\mathbf{0}, \mathbf{x}_{2e}) &:= \mathbf{J}_{\mathbf{x}_1} \mathbf{s}(\mathbf{0}, \mathbf{x}_{2e}), \end{aligned}$$

which is directly analogous to that used in the calculation of R_0 in Section 3.3. (In this analog, $\mathbf{F}(\mathbf{0}, \mathbf{x}_{2e})$ is associated with newly infected individuals rather than with newborns.) As in Chapter 3, we can equivalently determine the stability of the disease-free equilibrium using

$$(4.7) \quad R_0 = \rho \left(\mathbf{F}(\mathbf{0}_m, \mathbf{x}_{2e})(\mathbf{I} - \mathbf{T}(\mathbf{0}_m, \mathbf{x}_{2e}))^{-1} \right)$$

instead of $\rho(\mathbf{J}_{\mathbf{x}_1} \mathbf{f}_1(\mathbf{0}, \mathbf{x}_{2e}))$. The entries in $\mathbf{F}(\mathbf{0}, \mathbf{x}_{2e})$ and $\mathbf{T}(\mathbf{0}, \mathbf{x}_{2e})$ are, respectively, per capita rates of new infections and survival with class transitions; therefore, in a properly formulated model, these two matrices will satisfy the assumptions needed for us to apply Theorem 2.15 and Theorem 3.17. We can assign an interpretation of the reproduction number R_0 as the **average number of new infections** (*called secondary infections*) **per infectious individual** over the time spent infectious (see Section 2.3.2).

Theorem 4.4. *Assume Assumption 4.1 and that $\mathbf{F}(\mathbf{0}, \mathbf{x}_{2e})$ and $\mathbf{T}(\mathbf{0}, \mathbf{x}_{2e})$ defined by (4.6) satisfy (2.2) in Chapter 2 with $\rho(\mathbf{T}(\mathbf{0}, \mathbf{x}_{2e})) < 1$. Then the disease-free equilibrium is (locally asymptotically) stable if $R_0 < 1$ and unstable if $R_0 > 1$, where the reproduction number R_0 is defined by (4.7).*

4.3. Examples

In this section, we illustrate further the methodology of building disease models and the use of Theorem 4.4 to study stability properties of disease-free equilibria.

4.3.1. The Susceptible-Infected (SI) Model. As seen in Example 4.2, the SI model described by equations (4.5) has a (unique) disease-free equilibrium

$$(4.8) \quad \mathbf{x}_e = \begin{bmatrix} \mathbf{0} \\ x_{2e} \end{bmatrix} = \begin{bmatrix} \mathbf{0} \\ \frac{1}{c} \left(b \frac{1}{1-\sigma_S} - 1 \right) \end{bmatrix}, \quad b \frac{1}{1-\sigma_S} > 1$$

for which Assumption 4.1 holds. From equation (4.5)(a), we identify

$$\mathbf{n}(\mathbf{x}_1, \mathbf{x}_2) = (1 - \varphi(x_1)) \sigma_S x_2 \quad \text{and} \quad \mathbf{s}(\mathbf{x}_1, \mathbf{x}_2) = \sigma_I x_1$$

and calculate, using formulas (4.6),

$$\mathbf{F}(\mathbf{0}, \mathbf{x}_{2e}) = -\partial_{x_1} \varphi(0) \sigma_S x_{2e} > 0 \quad \text{and} \quad \mathbf{T}(\mathbf{0}, \mathbf{x}_{2e}) = \sigma_I < 1$$

from which, together with formula (4.7), we obtain

$$R_0 = -\partial_{x_1} \varphi(0) \sigma_S x_{2e} \frac{1}{1 - \sigma_I} > 0.$$

Notice that among the factors that make up R_0 are $-\varphi'(0) > 0$, which is called the **force of infection**, and

$$\frac{1}{1 - \sigma_I} = 1 + \sigma_I + \sigma_I^2 + \cdots = \sum_{j=0}^{\infty} \sigma_I^j,$$

which is the **expected time an individual remains infected**.

The elementary SI model in Example 4.2 and Section 4.3.1 assumes the escape function depends only on the number x_1 of infected individuals alone. Another modeling assumption is that φ also depends on the number of susceptibles. For example, consider the following derivation of an escape function for the SI model.

Assume, in a small interval of time Δt , that a susceptible individual comes into contact with at most one other individual and that contact with any individual in the population is equally likely with any other. Assume the probability a contact with another individual occurs is proportional to Δt and write it as $\pi \Delta t$, where $\pi > 0$ is the constant of proportionality. If a contact occurs, then the probability it is with an infected individual equals the fraction of infected individuals in the population (i.e., equals x_1/p , where

$$p = x_1 + x_2$$

is the total population size). With this notation, we have that the probability a susceptible individual contacts an infected individual during a

time interval of length Δt equals

$$\frac{x_1}{p} \pi \Delta t.$$

Will the contact result in an infection? If the probability of infection from a contact with an infected individual is i , then the probability the susceptible individual becomes infected during the time interval Δt is approximately

$$c_i \frac{x_1}{p} \Delta t,$$

where $c_i := i\pi$. It follows that the probability a susceptible escapes infection during the interval Δt is equal to

$$1 - c_i \frac{x_1}{p} \Delta t.$$

In order to avoid infection from t to $t + 1$, an individual must avoid infection a total of $1/\Delta t$ times. The probability that this occurs is

$$\left(1 - c_i \frac{x_1}{p} \Delta t\right)^{\frac{1}{\Delta t}}.$$

Letting $\Delta t \rightarrow 0$, we have from calculus that

$$\varphi(\mathbf{x}) := \lim_{\Delta t \rightarrow 0} \left(1 - c_i \frac{x_1}{p} \Delta t\right)^{\frac{1}{\Delta t}} = \exp\left(-c_i \frac{x_1}{p}\right)$$

is the probability that a susceptible escapes infection from time t to $t + 1$.

The equations for the SI model in Example 4.2 with the escape function

$$\varphi(\mathbf{x}) = \exp\left(-c_i \frac{x_1}{p}\right)$$

are

$$(4.9) \quad \begin{aligned} x_1(t+1) &= \left(1 - \exp\left(-c_i \frac{x_1(t)}{p(t)}\right)\right) \sigma_S x_2(t) + \sigma_I x_1(t) \quad \text{and} \\ x_2(t+1) &= b \frac{1}{1+c x_2(t)} x_2(t) + \exp\left(-c_i \frac{x_1(t)}{p(t)}\right) \sigma_S x_2(t). \end{aligned}$$

From

$$\mathbf{n}(\mathbf{x}_1, \mathbf{x}_2) = \left(1 - \exp\left(-c_i \frac{x_1}{x_1 + x_2}\right)\right) \sigma_S x_2 \quad \text{and} \quad \mathbf{s}(\mathbf{x}_1, \mathbf{x}_2) = \sigma_I x_1,$$

we see, using formulas (4.6), that

$$\mathbf{F}(\mathbf{0}, \mathbf{x}_{2e}) = c_i \sigma_S > 0 \quad \text{and} \quad \mathbf{T}(\mathbf{0}, \mathbf{x}_{2e}) = \sigma_I < 1$$

from which, by formula (4.7), we obtain

$$(4.10) \quad R_0 = c_i \sigma_S \frac{1}{1 - \sigma_I}.$$

By Theorem 4.4, the disease-free equilibrium (4.8) of (4.9) is (locally asymptotically) stable if $R_0 < 1$ and is unstable if $R_0 > 1$, where R_0 is given by formula (4.10).

4.3.2. A Susceptible-Infected-Recovered (SIR) Model. The SI model (4.5) in Example 4.2 and Section 4.3.1 is very basic in that it structures the population into only two disease related classes: infected and susceptible individuals. More sophisticated models include any number of other disease related classes, such as individuals who are recovered and immune from the disease, exposed but not yet infectious, exposed but quarantined, immune by vaccination, and so on. In this section, we consider a basic example that includes three classes: infected, susceptible, and recovered individuals.

In this model, $\mathbf{x}_1 = [x_1]$ and $\mathbf{x}_2 = \text{col}(x_2, x_3)$, where the numbers in the classes of infected (and infectious), susceptible, and recovered individuals are denoted by x_1 , x_2 , and x_3 , respectively. We assume an infected individual can recover from the infection. Individuals in the recovered class are neither infected nor susceptible to infection and hence have acquired immunity. We allow in the model, however, for the possibility that immunity is not permanent, and there is a probability that a recovered individual will again become infected. The cycle diagram appears in Figure 4.2.

For the dynamics of x_1 , we use the escape function similar to that in the SI model developed in Section 4.3.1:

$$\varphi(\mathbf{x}) = \exp\left(-c_i \frac{x_1}{p}\right),$$

where now the total population size is

$$p = x_1 + x_2 + x_3.$$

Then the equation for the infected class x_1 is

$$x_1(t+1) = \left(1 - \exp\left(-c_i \frac{x_1(t)}{p(t)}\right)\right) \sigma_S x_2(t) + \sigma_I (1 - \rho_I) x_1(t),$$

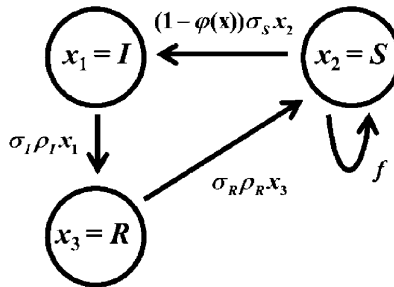


Figure 4.2. A cycle graph for the SIR model (4.11). Only transitions among classes are indicated (removals by deaths are not indicated).

where:

- ρ_I is the probability an infected individual recovers from the disease (per unit time); hence, $1 - \rho_I$ is the probability a (surviving) infected individual remains infected;
- $\mathbf{n}(\mathbf{x}_1, \mathbf{x}_2) = \left(1 - \exp\left(-c_i \frac{x_1}{p}\right)\right) \sigma_S x_2$;
- $\mathbf{s}(\mathbf{x}_1, \mathbf{x}_2) = \sigma_I (1 - \rho_I) x_1$.

For the susceptible class x_2 , we have an equation similar to that in the SI model in Section 4.3.1 except with an added input of new susceptibles from the recovered class x_3 . Thus,

$$x_2(t+1) = b \frac{1}{1 + cx_2(t)} x_2(t) + \exp\left(-c_i \frac{x_1(t)}{p(t)}\right) \sigma_S x_2(t) + \sigma_R \rho_R x_3(t),$$

where ρ_R is the probability a surviving recovered individual becomes again susceptible (hence, $1 - \rho_R$ is the probability it remains immune) and σ_R is the survival rate of recovered individuals.

Finally, the recovered individuals at time $t + 1$ equals the newly recovered individuals $\sigma_I \rho_I x_1(t)$ from the infected class plus the surviving recovered individuals from time t :

$$x_3(t+1) = \sigma_I \rho_I x_1(t) + \sigma_R (1 - \rho_R) x_3(t).$$

In summary, the equations for this SIR model are

$$(4.11) \quad \begin{aligned} (a) \quad x_1(t+1) &= \left(1 - \exp\left(-c_i \frac{x_1(t)}{p(t)}\right)\right) \sigma_S x_2(t) \\ &\quad + \sigma_I (1 - \rho_I) x_1(t); \\ (b) \quad x_2(t+1) &= b \frac{1}{1+c(x_2(t)+x_3(t))} (x_2(t) + x_3(t)) \\ &\quad + \exp\left(-c_i \frac{x_1(t)}{p(t)}\right) \sigma_S x_2(t) + \sigma_R \rho_R x_3(t); \\ (c) \quad x_3(t+1) &= \sigma_I \rho_I x_1(t) + \sigma_R (1 - \rho_R) x_3(t). \end{aligned}$$

If $\rho_R = 0$, then the model assumes **permanent immunity** after recovery from the disease. If $\rho_R > 0$, then immunity is only partial. A cycle graph for this model is shown in Figure 4.2.

In Exercise 4.12, the reader is asked to show that the disease-free equilibrium

$$\mathbf{x}_{2e} = \begin{bmatrix} x_{2e} \\ x_{3e} \end{bmatrix} = \begin{bmatrix} \frac{1}{c} \left(\frac{b}{1-\sigma_S} - 1 \right) \\ 0 \end{bmatrix}, \quad \frac{b}{1-\sigma_S} > 1$$

of the disease-free equilibrium equations

$$\begin{aligned} x_2(t+1) &= b \frac{1}{1+c(x_2(t)+x_3(t))} (x_2(t) + x_3(t)) \\ &\quad + \exp\left(-c_i \frac{x_1(t)}{p(t)}\right) \sigma_S x_2(t) + \sigma_R \rho_R x_3(t) \quad \text{and} \\ x_3(t+1) &= \sigma_I \rho_I x_1(t) + \sigma_R (1 - \rho_R) x_3(t) \end{aligned}$$

(obtained by setting x_1 equal to 0 in the SIR model equations (4.11)) satisfies Assumption 4.1. From equation (4.11)(a) and formulas (4.6), we have that

$$\mathbf{F}(\mathbf{0}, \mathbf{x}_{2e}) = c_i \sigma_S > 0 \quad \text{and} \quad \mathbf{T}(\mathbf{0}, \mathbf{x}_{2e}) = \sigma_I (1 - \rho_I) < 1;$$

from formula (4.7), we have that

$$(4.12) \quad R_0 = c_i \sigma_S \frac{1}{1 - \sigma_I (1 - \rho_I)}.$$

We conclude that the disease-free equilibrium \mathbf{x}_{2e} of the SIR model (4.11) is (locally asymptotically) stable if $R_0 < 1$ and is unstable if $R_0 > 1$, where R_0 is given by the formula (4.12).

Remark 4.5. If we use the notation S , I , and R for the classes of susceptible, infectious, and recovered individuals, respectively, then the SIR model equations (4.11) are

$$\begin{aligned} S(t+1) &= b \frac{1}{1+c(S(t)+R(t))} (S(t) + R(t)) \\ &\quad + \exp\left(-c_i \frac{I(t)}{p(t)}\right) \sigma_S S(t) + \sigma_R \rho_R R(t), \\ I(t+1) &= \left(1 - \exp\left(-c_i \frac{I(t)}{p(t)}\right)\right) \sigma_S S(t) + \sigma_I (1 - \rho_I) I(t), \quad \text{and} \\ R(t+1) &= \sigma_I \rho_I I(t) + \sigma_R (1 - \rho_R) R(t). \end{aligned}$$

4.3.3. An SAIR Model. In the SI and SIR models in Sections 4.3.1 and 4.3.2, there is only one infectious class ($m = 1$). This implies that the matrices needed are 1×1 , and as a result, the calculation of the next generation map and R_0 is relatively simple. In this section, we extend the SIR to include $m = 2$ infectious classes. This will require us to deal with 2×2 matrices in the calculation of R_0 .

In the vector $\mathbf{x}_1 = \text{col}(x_1, x_2)$ of infected individuals, let

- x_1 = infectious but asymptomatic individuals;
- x_2 = infectious but symptomatic individuals.

In the vector $\mathbf{x}_2 = \text{col}(x_3, x_4)$ of noninfected individuals, let

- x_3 = susceptible individuals;
- x_4 = recovered and nonsusceptible individuals.

We assume all newly infected individuals are at first asymptomatic but have probability ρ_A of becoming symptomatic after a unit time.

Let φ_1 and φ_2 be the probabilities that a susceptible individual escapes infection by an asymptomatic individual or by a symptomatic individual, respectively. Then $\varphi_1 \varphi_2$ is the probability of escaping infection altogether, and $1 - \varphi_1 \varphi_2$ is the probability of becoming infected (per unit time). We assume φ_i is a decreasing function of the fraction x_i/p . Specifically, following the derivation in Section 4.3.1, we take

$$\varphi_i\left(\frac{x_i}{p}\right) = \exp\left(-c_i \frac{x_i}{p}\right),$$

where

$$p = x_1 + x_2 + x_3 + x_4$$

is the total population size. Then the escape function is

$$\varphi_1\left(\frac{x_1}{p}\right)\varphi_2\left(\frac{x_2}{p}\right) = \exp\left(-\frac{c_1x_1 + c_2x_2}{p}\right),$$

and we obtain the following extension of the SIR model in Section 4.3.2:

$$(4.13) \quad \begin{aligned} (a) \quad x_1(t+1) &= \left(1 - \exp\left(-\frac{c_1x_1(t) + c_2x_2(t)}{p(t)}\right)\right)\sigma_S x_3(t) \\ &\quad + \sigma_A(1 - \rho_A)x_1(t); \\ (b) \quad x_2(t+1) &= \sigma_A\rho_A x_1(t) + \sigma_I(1 - \rho_I)x_2(t); \\ (c) \quad x_3(t+1) &= b \frac{1}{1+c(x_3(t)+x_4(t))}(x_3(t) + x_4(t)) \\ &\quad + \exp\left(-\frac{c_1x_1(t) + c_2x_2(t)}{p(t)}\right)\sigma_S x_3(t) \\ &\quad + \sigma_R\rho_R x_4(t); \\ (d) \quad x_4(t+1) &= \sigma_I\rho_I x_2(t) + \sigma_R(1 - \rho_R)x_4(t). \end{aligned}$$

In this case, σ_S , σ_A , σ_I , and σ_R are the survival probabilities of susceptible, asymptomatic, symptomatic, and recovered classes, respectively. The coefficients ρ_A , ρ_I , and ρ_R are, respectively, the fractions of asymptomatic individuals that become symptomatic, symptomatic individuals that recover, and recovered individuals that lose immunity and become again susceptible. The cycle graph for the SAIR model (4.13) appears in Figure 4.3.

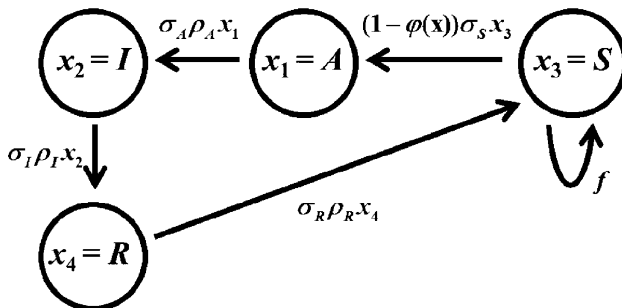


Figure 4.3. A cycle graph for the SAIR model (4.13). Only transitions among classes are indicated (removals by deaths are not indicated).

The disease-free equation (4.2) can be written as the two difference equations

$$\begin{aligned}x_3(t+1) &= b \frac{1}{1+c(x_3(t)+x_4(t))} (x_3(t) + x_4(t)) \\&\quad + \sigma_S x_3(t) + \sigma_R \rho_R x_4(t) \quad \text{and} \\x_4(t+1) &= \sigma_R (1 - \rho_R) x_4(t),\end{aligned}$$

which are mathematically the same as the SIR model of Section 4.3.2 with x_3 and x_4 substituted in place of x_2 and x_3 , respectively. By Exercise 4.12, these equations have a (locally asymptotically) stable equilibrium

$$\mathbf{x}_{2e} = \begin{bmatrix} x_{3e} \\ x_{4e} \end{bmatrix} = \begin{bmatrix} \frac{1}{c} \left(\frac{b}{1-\sigma_S} - 1 \right) \\ 0 \end{bmatrix}, \quad \frac{b}{1-\sigma_S} > 1$$

that satisfies Assumption 4.1. Thus, the SAIR model (4.13) has the disease-free equilibrium

$$(4.14) \quad \mathbf{x}_e = \begin{bmatrix} x_{1e} \\ x_{2e} \\ x_{3e} \\ x_{4e} \end{bmatrix} = \begin{bmatrix} 0 \\ 0 \\ \frac{1}{c} \left(\frac{b}{1-\sigma_S} - 1 \right) \\ 0 \end{bmatrix}, \quad \frac{b}{1-\sigma_S} > 1.$$

To apply Theorem 4.4, we need to calculate R_0 .

The equations (4.13) have the form of the general epidemic model (4.1) with

$$\mathbf{x}_1 = \text{col}(x_1, x_2), \quad \mathbf{x}_2 = \text{col}(x_3, x_4)$$

and

$$(4.15) \quad \begin{aligned}\mathbf{f}_1(\mathbf{x}_1, \mathbf{x}_2) &= \begin{bmatrix} \left(1 - \exp\left(-\frac{c_1 x_1 + c_2 x_2}{x_1 + x_2 + x_3 + x_4}\right)\right) \sigma_S x_3 + \sigma_A (1 - \rho_A) x_1 \\ \sigma_A \rho_A x_1 + \sigma_I (1 - \rho_I) x_2 \end{bmatrix} \\ \mathbf{f}_2(\mathbf{x}_1, \mathbf{x}_2) &= \mathbf{n}(\mathbf{x}_1, \mathbf{x}_2) + \mathbf{s}(\mathbf{x}_1, \mathbf{x}_2),\end{aligned}$$

where

$$(4.16) \quad \begin{aligned}\mathbf{n}(\mathbf{x}_1, \mathbf{x}_2) &= \begin{bmatrix} \left(1 - \exp\left(-\frac{c_1 x_1 + c_2 x_2}{x_1 + x_2 + x_3 + x_4}\right)\right) \sigma_S x_3 \\ 0 \end{bmatrix} \quad \text{and} \\ \mathbf{s}(\mathbf{x}_1, \mathbf{x}_2) &= \begin{bmatrix} \sigma_A (1 - \rho_A) x_1 \\ \sigma_A \rho_A x_1 + \sigma_I (1 - \rho_I) x_2 \end{bmatrix}.\end{aligned}$$

Notice the zero component in $\mathbf{n}(\mathbf{x}_1, \mathbf{x}_2)$, which is the result of the assumption that all newly infected individuals are asymptomatic and

hence lie in the x_1 class. From formulas (4.6), we get the Jacobians

$$\mathbf{F}(\mathbf{0}, \mathbf{x}_{2e}) = \begin{bmatrix} c_1\sigma_S & c_2\sigma_S \\ 0 & 0 \end{bmatrix} \quad \text{and}$$

$$\mathbf{T}(\mathbf{0}, \mathbf{x}_{2e}) = \begin{bmatrix} \sigma_A(1-\rho_A) & 0 \\ \sigma_A\rho_A & \sigma_I(1-\rho_I) \end{bmatrix}.$$

Notice that $\mathbf{F}(\mathbf{0}, \mathbf{x}_{2e})$ has a row of zeros, which produces in a row of zeros in the next generation matrix $\mathbf{F}(\mathbf{0}_2, \mathbf{x}_{2e})(\mathbf{I} - \mathbf{T}(\mathbf{0}_2, \mathbf{x}_{2e}))^{-1}$, which is

$$\begin{bmatrix} \sigma_S c_1 & \sigma_S c_2 \\ 0 & 0 \end{bmatrix} \left[\begin{array}{cc} 1 - \sigma_A(1 - \rho_A) & 0 \\ -\sigma_A \rho_A & 1 - \sigma_I(1 - \rho_I) \end{array} \right]^{-1}$$

$$= \begin{bmatrix} \frac{\sigma_S c_1}{1 - \sigma_A(1 - \rho_A)} + \frac{\sigma_S c_2 \rho_A}{(1 - \sigma_A(1 - \rho_A))(1 - \sigma_I(1 - \rho_I))} & \frac{\sigma_S c_2}{1 - \sigma_I(1 - \rho_I)} \\ 0 & 0 \end{bmatrix}$$

and whose dominant eigenvalue therefore appears in the upper-left corner as

$$(4.17) \quad R_0 = \sigma_S c_1 \frac{1}{1 - \sigma_A(1 - \rho_A)} + \sigma_S c_2 \frac{\rho_A}{(1 - \sigma_A(1 - \rho_A))(1 - \sigma_I(1 - \rho_I))}.$$

From Theorem 4.4, we conclude that the disease-free equilibrium (4.14) of the SAIR model (4.13) is (locally asymptotically) stable if $R_0 < 1$ and unstable if $R_0 > 1$, where R_0 is given by the formula (4.17).

Remark 4.6. If we use the notation S , A , I , and R for the classes of susceptible, infectious asymptomatic, infectious symptomatic, and recovered individuals (x_3 , x_1 , x_2 , and x_4), respectively, then the SAIR model equations (4.13) are

$$\begin{aligned} S(t+1) &= b \frac{1}{1+c(S(t)+R(t))} (S(t) + R(t)) \\ &\quad + \exp\left(-\frac{c_1 I(t) + c_2 A(t)}{p(t)}\right) \sigma_S S(t) \\ &\quad + \sigma_R \rho_R R(t), \\ A(t+1) &= \left(1 - \exp\left(-\frac{c_1 I(t) + c_2 A(t)}{p(t)}\right)\right) \sigma_S S(t) + \sigma_A(1 - \rho_A) A(t), \\ I(t+1) &= \sigma_A \rho_A A(t) + \sigma_I(1 - \rho_I) I(t), \quad \text{and} \\ R(t+1) &= \sigma_I \rho_I I(t) + \sigma_R(1 - \rho_R) R(t). \end{aligned}$$

In this notation, the state variables are listed in the order of disease progression.

In the SAIR model of Section 4.3.3, asymptomatic individuals do not recover without first becoming symptomatic. An alternative would allow that asymptomatic individuals can recover without becoming

symptomatic; see Exercise 4.13. Another extension is to allow newly infected susceptibles to be either asymptomatic or symptomatic; see Exercise 4.14.

4.4. Endemic Equilibria: A Basic Bifurcation Theorem

Theorem 4.4 (and the examples in Section 4.2) focuses on the stability of a disease-free equilibrium. This desirable outcome, when a low-level infection ultimately dies out and a persistent epidemic is avoided, occurs in general when $R_0 < 1$. In this section, we consider the existence and stability of endemic equilibria (i.e., equilibria $\mathbf{x} = \text{col}(\mathbf{x}_1, \mathbf{x}_2) \in R^{m+n}$, $\mathbf{x}_1 \neq \mathbf{0}_m$) of the model equations (4.1):

$$(4.18) \quad \begin{aligned} (a) \quad \mathbf{x}_1(t+1) &= \mathbf{f}_1(\mathbf{x}_1(t), \mathbf{x}_2(t)); \\ (b) \quad \mathbf{x}_2(t+1) &= \mathbf{f}_2(\mathbf{x}_1(t), \mathbf{x}_2(t)). \end{aligned}$$

The existence and stability of such an equilibrium would imply that the disease does not ultimately die out and would be endemic in the population.

Theorem 4.4 provides conditions under which a disease-free equilibrium

$$(4.19) \quad \mathbf{x}_e = \begin{bmatrix} \mathbf{0}_m \\ \mathbf{x}_{2e} \end{bmatrix} \in \partial R^{m+n}$$

loses stability as R_0 (defined by (4.7)) increases through 1. Based on the analogous situation with general population dynamic models in Chapter 3, we suspect that this destabilization will result in a (transcritical) bifurcation of endemic equilibria from the disease-free equilibrium and that their stability will be related to the direction of bifurcation. This bifurcation is the subject of Theorem 4.7.

Recall that a diagnostic quantity called κ was key to determining the properties of the bifurcation at $R_0 = 1$ in the general Theorem 3.21 given for population models. The same is true for the bifurcation at $R_0 = 1$ for general disease models. To define this quantity, we start by identifying the entries $p_{ij}(\mathbf{x}_1, \mathbf{x}_2)$ of the Jacobian matrix

$$\mathbf{J}_{\mathbf{x}_1}^0 \mathbf{f}_1(\mathbf{x}_1, \mathbf{x}_2) = [p_{ij}(\mathbf{x}_1, \mathbf{x}_2)].$$

Then we define

$$(4.20) \quad \kappa := -\mathbf{w}^T [\kappa_{ij}] \mathbf{v},$$

where

$$(4.21) \quad \kappa_{ij} := \nabla_{\mathbf{x}_1}^0 p_{ij} \cdot \mathbf{v} + \nabla_{\mathbf{x}_2}^0 p_{ij} \cdot (\mathbf{I} - \mathbf{J}_{\mathbf{x}_2}^0 \mathbf{f}_2(\mathbf{0}_m, \mathbf{x}_{2e}))^{-1} \mathbf{J}_{\mathbf{x}_1}^0 \mathbf{f}_2(\mathbf{0}_m, \mathbf{x}_{2e}) \mathbf{v}$$

and \mathbf{w}^T and \mathbf{v} are positive left and right eigenvectors of $\mathbf{J}_{\mathbf{x}_1}^0 \mathbf{f}_1(\mathbf{0}_m, \mathbf{x}_{2e})$ associated with the eigenvalue 1. (A superscript “0” now denotes evaluation at the disease-free equilibrium $\mathbf{x} = \text{col}(\mathbf{0}_m, \mathbf{x}_{2e})$ when $R_0 = 1$.)

Theorem 4.7. [64] As in Theorem 4.4, assume Assumption 4.1 and that $\mathbf{F}(\mathbf{0}, \mathbf{x}_{2e})$ and $\mathbf{T}(\mathbf{0}, \mathbf{x}_{2e})$ (defined by (4.6)) satisfy (2.2) in Chapter 3. Assume, in addition, that $\rho[\mathbf{T}(\mathbf{0}_m, \mathbf{x}_{2e})] < 1$ and $\kappa \neq 0$.

- (a) Then endemic equilibria of equation (4.18) bifurcate from the disease-free equilibrium (4.19) at $R_0 = 1$. Their bifurcation is forward if $\kappa > 0$ and backward if $\kappa < 0$.
- (b) If $\mathbf{J}_{\mathbf{x}_1}^0 \mathbf{f}_1(\mathbf{x}_1, \mathbf{x}_2)$ is primitive, then $\kappa > 0$ implies the forward bifurcation is stable, and $\kappa < 0$ implies the backward bifurcation is unstable.

While the technical details of the proof of this theorem are beyond the level of this book, the basic idea behind the proof is straightforward. Solving the equilibrium equation $\mathbf{x}_2 = \mathbf{f}_2(\mathbf{x}_1, \mathbf{x}_2)$ associated with equation (4.18)(b) for \mathbf{x}_2 as a function of \mathbf{x}_1 (by means of the Implicit Function Theorem in Appendix A.1) and substituting the answer into the equilibrium equation associated with equation (4.18)(a), we get a matrix equation for \mathbf{x}_1 , to which we apply the bifurcation Theorems 3.21 and 3.22.

Example 4.8. In Section 4.3.1, we saw that the disease-free equilibrium

$$\mathbf{x}_e = \begin{bmatrix} 0 \\ x_{2e} \end{bmatrix},$$

$$x_{2e} = \frac{1}{c} \left(\frac{b}{1 - \sigma_S} - 1 \right), \quad \frac{b}{1 - \sigma_S} > 1,$$

of the SI model

$$(4.22) \quad \begin{aligned} x_1(t+1) &= \left(1 - \exp \left(-c_i \frac{x_1(t)}{x_1(t) + x_2(t)} \right) \right) \sigma_S x_2(t) + \sigma_I x_1(t) \\ x_2(t+1) &= b \frac{1}{1 + c x_2(t)} x_2(t) + \exp \left(-c_i \frac{x_1(t)}{x_1(t) + x_2(t)} \right) \sigma_S x_2(t) \end{aligned}$$

loses stability as

$$R_0 = c_i \sigma_S \frac{1}{1 - \sigma_I}$$

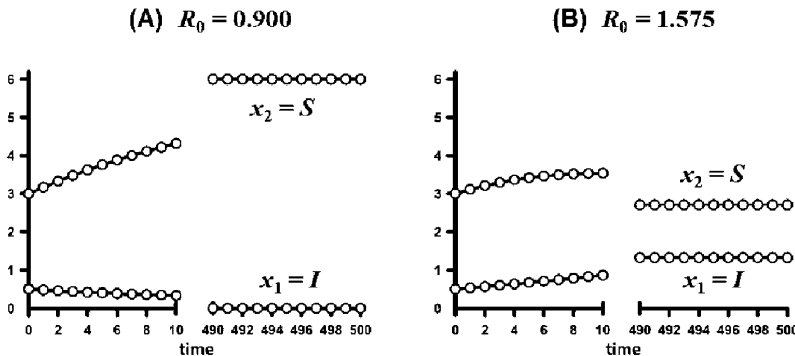


Figure 4.4. Sample solutions of the SI model equations (4.22) with parameter values $\sigma_S = 0.9$, $\sigma_I = 0.8$, $b = 1$, and $c = 1.5$ and initial conditions $x_1(0) = 0.5$ and $x_2(0) = 3$. (A) With force of infection $c_i = 0.2$, the reproduction number $R_0 < 1$, and the disease-free equilibrium $\mathbf{x}_e = \text{col}(0, 6)$ is stable. (B) With force of infection $c_i = 0.35$, the reproduction number $R_0 > 1$, and the disease-free equilibrium $\mathbf{x}_e = \text{col}(0, 6)$ is unstable. In this case, we see that the solution approaches an endemic equilibrium $\mathbf{x}_e = \text{col}(1.321, 2.707)$.

increases through 1. To apply Theorem 4.7, we need to calculate κ from formulas (4.20)–(4.8).

In this example, $m = n = 1$, and the vectors and matrices in these formulas are all scalars, so we drop the bracket notation. In one-dimensional cases such as this, it is always the case that $\mathbf{v} = \mathbf{w} = 1$. From $\mathbf{J}_{\mathbf{x}_1}^0 \mathbf{f}_1(\mathbf{x}_1, \mathbf{x}_2) = p_{11}(\mathbf{x}_1, \mathbf{x}_2)$, where

$$p_{11}(\mathbf{x}_1, \mathbf{x}_2) = \frac{1 - \exp\left(-c_i \frac{\mathbf{x}_1}{\mathbf{x}_1 + \mathbf{x}_2}\right)}{\mathbf{x}_1} \sigma_S \mathbf{x}_2 + \sigma_I,$$

we calculate

$$\begin{aligned} \nabla_{\mathbf{x}_1}^0 p_{11} &= \lim_{\mathbf{x}_1 \rightarrow 0} \frac{\partial p_{11}(\mathbf{x}_1, \mathbf{x}_2^*)}{\partial \mathbf{x}_1} = -\frac{1}{2} \sigma_S c_i \frac{c_i + 2}{\mathbf{x}_2^*} \quad \text{and} \\ \nabla_{\mathbf{x}_2}^0 p_{11} &= \lim_{\mathbf{x}_1 \rightarrow 0} \frac{\partial p_{11}(\mathbf{x}_1, \mathbf{x}_2^*)}{\partial \mathbf{x}_2} = 0 \end{aligned}$$

so that

$$\kappa = \frac{1}{2} \sigma_S c_i \frac{c_i + 2}{\mathbf{x}_2^*} > 0.$$

It follows that a forward-stable bifurcation of endemic equilibria occurs at $R_0 = 1$.

See Figure 4.4 for simulation examples that illustrate this bifurcation result. \square

Example 4.9. Consider the SAIR model (4.13) in Example 4.3.3. We saw there that the disease-free equilibrium (4.14)

$$\mathbf{x}_e = \begin{bmatrix} 0 \\ 0 \\ x_{3e} \\ 0 \end{bmatrix},$$

$$x_{3e} = \frac{1}{c} \left(\frac{b}{1 - \sigma_S} - 1 \right), \quad \frac{b}{1 - \sigma_S} - 1 > 0,$$

destabilizes as R_0 , given by formula (4.17), increases through 1. To determine whether the resulting bifurcation of endemic equilibria is forward (hence stable) or backward (hence unstable) by an application of Theorem 4.7, we calculate the sign of κ given by formulas (4.20)–(4.8). Some lengthy calculations show that from the components

$$p_{11} = \frac{1 - \exp\left(-\frac{c_1 x_1 + c_2 x_2}{p}\right)}{c_1 x_1 + c_2 x_2} \sigma_S x_3 c_1 + \sigma_A (1 - \rho_A),$$

$$p_{12} = \frac{1 - \exp\left(-\frac{c_1 x_1 + c_2 x_2}{p}\right)}{c_1 x_1 + c_2 x_2} \sigma_S x_3 c_2,$$

$$p_{21} = \sigma_A \rho_A, \quad \text{and}$$

$$p_{22} = \sigma_I (1 - \rho_I)$$

of the 2×2 Jacobian matrix $\mathbf{J}_{\mathbf{x}_1}^0 \mathbf{f}_1(\mathbf{x}_1, \mathbf{x}_2) = [p_{ij}(\mathbf{x}_1, \mathbf{x}_2)]$, we obtain the gradients

$$\nabla_{\mathbf{x}_1}^0 p_{11} = -\frac{1}{2} \sigma_S \frac{c_1}{x_3} \begin{bmatrix} c_1 + 2 \\ c_2 + 2 \end{bmatrix}, \quad \nabla_{\mathbf{x}_2}^0 p_{11} = -\sigma_S \frac{c_1}{x_3} \begin{bmatrix} 0 \\ 1 \end{bmatrix},$$

$$\nabla_{\mathbf{x}_1}^0 p_{12} = -\frac{1}{2} \sigma_S \frac{c_2}{x_3} \begin{bmatrix} c_1 + 2 \\ c_2 + 2 \end{bmatrix}, \quad \nabla_{\mathbf{x}_2}^0 p_{12} = -\sigma_S \frac{c_2}{x_3} \begin{bmatrix} 0 \\ 1 \end{bmatrix},$$

$$\nabla_{\mathbf{x}_1}^0 p_{21} = \nabla_{\mathbf{x}_2}^0 p_{21} = \mathbf{0}, \quad \text{and}$$

$$\nabla_{\mathbf{x}_1}^0 p_{22} = \nabla_{\mathbf{x}_2}^0 p_{22} = \mathbf{0}$$

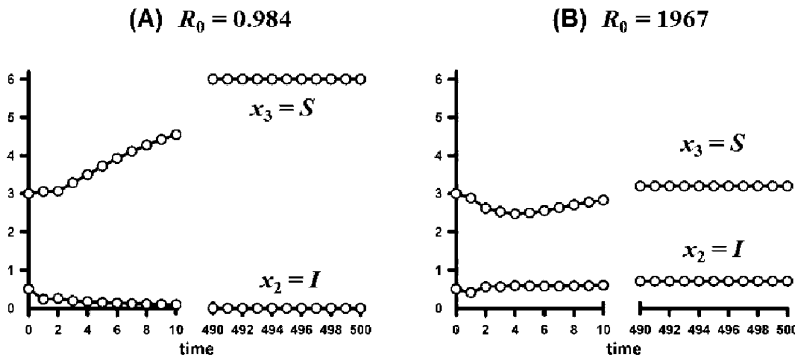


Figure 4.5. Time series plots of the $x_1(t)$ and $x_3(t)$ components of sample solutions of the SAIR model equations (4.13) with parameter values $\sigma_S = 0.9$, $\sigma_A = 0.95$, $\sigma_I = 0.8$, $\sigma_R = 0.5$, $\rho_A = 0.9$, $\rho_I = 0.9$, $\rho_R = 0.5$, $b = 1$, and $c = 1.5$ and initial conditions $x_1(0) = 0.5$, $x_2(0) = 0$, $x_3(0) = 2$, and $x_4(0) = 0$. (A) With forces of infection $c_1 = c_2 = 0.5$, the reproduction number satisfies $R_0 < 1$, and the disease-free equilibrium $\mathbf{x}_e = \text{col}(0, 0, 6, 0)$ is stable. (B) With forces of infection $c_1 = c_2 = 1$, the reproduction number satisfies $R_0 > 1$, and the disease-free equilibrium $\mathbf{x}_e = \text{col}(0, 6)$ is unstable. In this case, we see that the solution approaches an endemic equilibrium $\mathbf{x}_e = \text{col}(0.707, 0.657, 3.197, 0.861)$.

to be used in formula (4.8). Finally from (4.15), we calculate the 2×2 Jacobian matrices

$$\begin{aligned} J_{x_1}^0 \mathbf{f}_2(\mathbf{0}_m, \mathbf{x}_{2e}) &= \begin{bmatrix} -\sigma_S c_1 & -\sigma_S c_2 \\ 0 & 0 \end{bmatrix} \quad \text{and} \\ J_{x_2}^0 \mathbf{f}_2(\mathbf{0}_m, 0) &= \begin{bmatrix} 0 & 0 \\ 0 & 0 \end{bmatrix}. \end{aligned}$$

These ingredients in (4.8) give us the matrix

$$[\kappa_{ij}] = \frac{1}{2} \sigma_S \frac{(c_1 + 2)v_1 + (c_2 + 2)v_2}{x_{3e}} \begin{bmatrix} -c_1 & -c_2 \\ 0 & 0 \end{bmatrix}.$$

Since this 2×2 matrix has no positive entries, it follows that $\kappa = -\mathbf{w}^T [\kappa_{ij}] \mathbf{v} > 0$.

By Theorem 4.7, a forward bifurcation of (locally asymptotically) stable endemic equilibria bifurcate

from the disease-free equilibrium as R_0 increases through 1.

See Figure 4.5 for simulation examples that illustrate this bifurcation result. \square

4.5. Applications

The two applications in this section illustrate the disease modeling methodology and analysis studied in this chapter. The first application considers a vaccination program in the basic SI and SIR models and the notion of **herd immunity**. The second application concerns a model of a specific disease, namely malaria.

4.5.1. Vaccinations and Herd Immunity. An infection that invades a susceptible population at a low level will not succeed in establishing itself permanently in the population if the disease-free equilibrium is (locally asymptotically) stable (i.e., if $R_0 < 1$). However, if $R_0 > 1$, then one can consider implementing procedures designed to reduce R_0 with the goal of attaining $R_0 < 1$ and a stable disease-free equilibrium. These include vaccination programs, quarantine protocols, cleaning and sterilization procedures, pathogen vector control (such as insecticides), social behavior modification (such as masking and social distancing), and so on. In this section, we look at the use of vaccination programs to reduce R_0 in the basic SI and SIR models introduced in this chapter.

4.5.1.1. SI Model. In Section 4.3.1, we saw that SI model

$$(4.23) \quad \begin{aligned} x_1(t+1) &= \left(1 - \exp\left(-c_i \frac{x_1(t)}{p(t)}\right)\right) \sigma_S x_2(t) + \sigma_I x_1(t) \\ x_2(t+1) &= b \frac{1}{1+c x_2(t)} x_2(t) + \exp\left(-c_i \frac{x_1(t)}{p(t)}\right) \sigma_S x_2(t) \end{aligned}$$

has the disease-free equilibrium

$$\mathbf{x}_e = \left[\begin{array}{c} 0 \\ \frac{1}{c} \left(\frac{b}{1-\sigma_S} - 1 \right) \end{array} \right], \quad \frac{b}{1-\sigma_S} > 1,$$

and that the reproduction number is

$$R_0 = c_i \sigma_S \frac{1}{1 - \sigma_I}.$$

Assume that $R_0 > 1$ so that (by Theorem 4.4) the disease-free equilibrium is unstable. (By Theorem 4.7, there are stable endemic equilibria, at least for $R_0 \gtrapprox 1$.)

Assume that a vaccination program is put in place and succeeds in accomplishing the following: at any given time t , a fraction v of the susceptibles $x_2(t)$ are vaccinated (during the interval t to $t + 1$) and become immune to the disease at time $t + 1$. Thus, $(1 - v)x_2(t)$ susceptibles remain at time $t + 1$ (if they survive). This assumption replaces the survival probability σ_S in the model equations (4.23) by $(1 - v)\sigma_S$, which now become

$$\begin{aligned} x_1(t+1) &= \left(1 - \exp\left(-c_i \frac{x_1(t)}{p(t)}\right)\right)(1-v)\sigma_S x_2(t) + \sigma_I x_1(t) \quad \text{and} \\ x_2(t+1) &= b \frac{1}{1+c x_2(t)} x_2(t) + \exp\left(-c_i \frac{x_1(t)}{p(t)}\right)(1-v)\sigma_S x_2(t), \end{aligned}$$

and the disease-free equilibrium becomes

$$\mathbf{x}_e = \left[\begin{array}{c} 0 \\ \frac{1}{c} \left(\frac{b}{1-(1-v)\sigma_S} - 1 \right) \end{array} \right], \quad \frac{b}{1-(1-v)\sigma_S} > 1.$$

We could recalculate R_0 for this vaccination model, but it is easier simply to note that the calculations are the same as those in Section 4.3.2 with σ_S replaced by $(1 - v)\sigma_S$. Consequently, we can use formula (4.12) to obtain the reproduction number

$$R_0(v) = c_i(1 - v)\sigma_S \frac{1}{1 - \sigma_I},$$

which is now a function of the vaccination fraction v . Note that

$$(4.24) \quad R_0(v) = (1 - v)R_0(0),$$

where

$$(4.25) \quad R_0(0) = c_i\sigma_S \frac{1}{1 - \sigma_I} > 1$$

is the reproduction number in the absence of the vaccination program. The question is this, If the fraction v is sufficiently high (close to 1), will an epidemic be avoided? And if so, what is the vaccination threshold?

From formula (4.25), we find that $R_0(v) < 1$, and the disease-free equilibrium is stable if the vaccination fraction satisfies

$$v > v_0 := 1 - \frac{1}{R_0(0)}.$$

If this threshold for the fraction of vaccinated individuals is met, it is said that the population has **herd immunity**. Note that the vaccination threshold v_0 can be calculated by this formula from a knowledge of $R_0 = R_0(0)$ in the absence of the vaccination program. See Table 4.1 for examples.

Table 4.1. (Data from Wikipedia: https://en.wikipedia.org/wiki/Basic_reproduction_number. Text is available under the Creative Commons Attribution-ShareAlike License 4.0, additional terms may apply.)

Disease	Estimated R_0	Estimated $v_0 = 1 - \frac{1}{R_0}$	Estimated % Needed for Herd Immunity
Measles	12 – 18	$\frac{11}{12} – \frac{17}{18}$	92 – 94%
Chickenpox	10 – 12	$\frac{10}{9} – \frac{11}{12}$	90 – 92%
Mumps	10 – 12	$\frac{10}{9} – \frac{12}{12}$	90 – 92%
Rubella	6 – 7	$\frac{6}{5} – \frac{7}{6}$	83 – 86%
Polio	5 – 7	$\frac{5}{4} – \frac{6}{7}$	80 – 86%
Covid-19 (variants)	3 – 8	$\frac{2}{3} – \frac{7}{8}$	67 – 88%
Pertussis	5 – 6	$\frac{4}{5} – \frac{5}{6}$	80 – 83%
Smallpox	3.5 – 6	$\frac{5}{7} – \frac{5}{6}$	71 – 83%
Covid-19 (wild type)	2.4 – 3.4	$\frac{7}{12} – \frac{12}{17}$	58 – 71%
HIV/AIDS	2 – 5	$\frac{1}{2} – \frac{4}{5}$	50 – 80%
SARS	2 – 4	$\frac{1}{2} – \frac{3}{4}$	50 – 75%
Common cold	2 – 3	$\frac{1}{2} – \frac{2}{3}$	50 – 67%
Diphtheria	1.7 – 4.3	$\frac{7}{17} – \frac{33}{43}$	41 – 77%
Ebola	1.4 – 1.8	$\frac{2}{7} – \frac{4}{9}$	29 – 44%
Influenza	1.2 – 1.4	$\frac{1}{6} – \frac{2}{7}$	17 – 29%

4.5.1.2. *SIR Model.* Consider the SIR model in Section 4.3.2 but with permanent acquired immunity (i.e., with $\rho_R = 0$):

$$(4.26) \quad \begin{aligned} (a) \quad x_1(t+1) &= \left(1 - \exp\left(-c_i \frac{x_1(t)}{p(t)}\right)\right) \sigma_S x_2(t) \\ &\quad + \sigma_I (1 - \rho_I) x_1(t); \\ (b) \quad x_2(t+1) &= b \frac{1}{1 + c_i(x_2(t) + x_3(t))} (x_2(t) + x_3(t)) \\ &\quad + \exp\left(-c_i \frac{x_1(t)}{p(t)}\right) \sigma_S x_2(t); \\ (c) \quad x_3(t+1) &= \sigma_I \rho_I x_1(t) + \sigma_R x_3(t). \end{aligned}$$

In Section 4.3.2, it is shown that this model has the disease-free equilibrium

$$\mathbf{x}_e = \begin{bmatrix} x_{1e} \\ x_{2e} \\ x_{3e} \end{bmatrix} = \begin{bmatrix} 0 \\ \frac{1}{c_i} \left(\frac{b}{1 - \sigma_S} - 1 \right) \\ 0 \end{bmatrix}, \quad \frac{b}{1 - \sigma_S} > 1,$$

and that

$$R_0 = c_i \sigma_S \frac{1}{1 - \sigma_I (1 - \rho_I)}.$$

If we assume, as in the SI model in Section 4.5.1.1, that a fraction v of susceptibles becomes immune to the disease by implementation of a vaccination program, then we have the modified SIR model equations

$$(4.27) \quad \begin{aligned} (a) \quad x_1(t+1) &= \left(1 - \exp\left(-c_i \frac{x_1(t)}{p(t)}\right)\right) (1 - v) \sigma_S x_2(t) \\ &\quad + \sigma_I (1 - \rho_I) x_1(t); \\ (b) \quad x_2(t+1) &= b \frac{1}{1 + c_i(x_2(t) + x_3(t))} (x_2(t) + x_3(t)) \\ &\quad + \exp\left(-c_i \frac{x_1(t)}{p(t)}\right) (1 - v) \sigma_S x_2(t); \\ (c) \quad x_3(t+1) &= \sigma_I \rho_I x_1(t) + v \sigma_S x_2(t) + \sigma_R x_3(t). \end{aligned}$$

Note that the vaccinated individuals $v x_2$ are placed in the recovered class x_3 (if they survive). The recovered class in this model consists of individuals who have immunity by one of two means: those $\rho_I x_1$ with acquired immunity (i.e., who had and recovered from the disease) and those $v x_2$ who have been vaccinated.

It is left as Exercise 4.16 to show that the disease-free equilibrium is

$$(4.28) \quad \mathbf{x}_e = \frac{1}{c} \frac{1}{1 - (1 - v) \sigma_S} \left(b - (1 - \sigma_R) \frac{1 - (1 - v) \sigma_S}{1 - \sigma_R + v \sigma_S} \right) \begin{bmatrix} 0 \\ 1 \\ v \frac{\sigma_S}{1 - \sigma_R} \end{bmatrix}.$$

To calculate the reproduction number, we identify from equation (4.27)(a) that

$$\mathbf{f}_1(\mathbf{x}_1, \mathbf{x}_2) = \mathbf{n}(\mathbf{x}_1, \mathbf{x}_2) + \mathbf{s}(\mathbf{x}_1, \mathbf{x}_2),$$

where

$$\mathbf{n}(\mathbf{x}_1, \mathbf{x}_2) = \left(1 - \exp\left(-c_i \frac{x_1}{x_1 + x_2 + x_3}\right)\right)(1-v)\sigma_S x_2.$$

From formulas (4.6), we get the 1×1 Jacobian matrices

$$\begin{aligned}\mathbf{F}(0, \mathbf{x}_{2e}) &= c_i \frac{1 - \sigma_R}{1 - \sigma_R + v\sigma_S} (1-v)\sigma_S \quad \text{and} \\ \mathbf{T}(0, \mathbf{x}_{2e}) &= \sigma_I (1 - \rho_I),\end{aligned}$$

and from formula (4.7),

$$R_0(v) = c_i \frac{1 - \sigma_R}{1 - \sigma_R + v\sigma_S} (1-v)\sigma_S \frac{1}{1 - \sigma_I(1 - \rho_I)}.$$

Here we have indicated that the reproduction number $R_0(v)$ depends on the fraction v of the population that is vaccinated. Note that

$$R_0(v) = \frac{1 - \sigma_R}{1 - \sigma_R + v\sigma_S} (1-v) R_0(0),$$

where

$$R_0(0) = c_i \sigma_S \frac{1}{1 - \sigma_I(1 - \rho_I)}$$

is the reproduction number if the population is unvaccinated.

Suppose the disease-free equilibrium is unstable if the population is unvaccinated (i.e., suppose $R_0(0) > 1$). Can the disease-free equilibrium be stabilized (and an epidemic avoided) by vaccination? And if so, what level of vaccination will suffice? The answer is that the vaccination fraction will accomplish this if $R_0(v) < 1$, which occurs when

$$(4.29) \quad v > v_0 := \frac{(1 - \sigma_R)}{\sigma_S + R_0(0)(1 - \sigma_R)} (R_0(0) - 1).$$

We conclude from this model the following. Suppose the unvaccinated population is threatened with an epidemic because $R_0(0) > 1$, and therefore, the disease-free equilibrium is unstable. The vaccinated population can avoid an epidemic (i.e., $R_0(v) < 1$ will be satisfied) provided the vaccination fraction v exceeds the threshold v_0 given by formula (4.29).

If we rewrite the vaccination threshold as

$$v_0 := \frac{1}{1 + \frac{\sigma_S}{1 - \sigma_R} \frac{1}{R_0(0)}} \left(1 - \frac{1}{R_0(0)}\right),$$

then since

$$\frac{1}{1 + \frac{\sigma_S}{1 - \sigma_R} \frac{1}{R_0(0)}} < 1,$$

we see that the threshold $v > v_0$ is met if

$$v > 1 - \frac{1}{R_0(0)}.$$

Thus, the criterion for herd immunity in the SI model is sufficient, but not necessary, to attain herd immunity in the SIR model.

4.5.2. A Malaria Model. The examples in this chapter have not focussed on any specific disease but instead on low-dimensional general models. This is done in order to emphasize the modeling methodology, analytic techniques, and concepts. We close this chapter with a model that is focused on a specific disease, namely malaria. It is a discrete time analog of the ordinary differential equation model studied in [17], [18], [19]. We will direct our attention here solely to the formulation of the model equations and the calculation of R_0 for this rather complicated model.

Mosquitoes are considered the most deadly animal in the world to humans [86]. Malaria is the most lethal of many mosquito-borne diseases, which also include dengue, zika, yellow fever, West Nile virus, chikungunya, and equine encephalitis. Malaria is caused by one of several species of protozoan parasites from the genus *Plasmodium*. The parasite is transmitted to a human by the bite of an infected female mosquito of the genus *Anopheles*. After passing through developmental life cycle stages in the human liver, the parasite is transmitted (in the form of gametocytes) back to a mosquito when it bites an infected human. After the parasite passes through more life stages in the mosquito, the mosquito becomes infectious and capable of repeating the cycle by biting a susceptible human. Thus, the disease is spread in humans not by direct contact with the pathogen but by contact with an infected mosquito, which is called a vector for the disease. So our model will account for the dynamics and interactions of both human and mosquito populations.

Because of the latency periods associated with the developmental stages of the parasite, we structure both populations into three classes: susceptibles S , exposed E (infected but not infectious), and infectious I . Humans can recover from malaria, but recovered individuals still have low levels of parasites and can infect mosquitoes. After some time, recovered individuals revert to the susceptible class. Mosquitoes, on the other hand, remain infectious for life. For these reasons, we create a recovered class R for humans but not for mosquitoes. The model for the human population is called an SEIR model, and that for the mosquito population is called an SEI model. A common notational procedure is to list the model equations for these classes in the order of passage for individuals and refer to them as SEIR and SIR models, respectively. However, in keeping with our notation for the calculation of R_0 , in which *infected classes are listed first*, we write the state variables in the order

$$\mathbf{x} = \begin{bmatrix} x_1 \\ x_2 \\ x_3 \\ x_4 \\ x_5 \\ x_6 \\ x_7 \end{bmatrix} = \begin{bmatrix} E_h \\ E_m \\ I_h \\ I_m \\ S_h \\ S_m \\ R \end{bmatrix},$$

where a subscript h indicates humans and a subscript m indicates mosquitoes. Using the same modeling methodology used throughout this chapter, we construct the following equations for the components of $\mathbf{x} = \mathbf{x}(t)$ (see graph in Figure 4.6):

$$(4.30) \quad \begin{aligned} E_h(t+1) &= (1 - \varphi_h(\mathbf{x}(t))) \sigma_{Sh} S_h(t) \\ &\quad + (1 - v_{Eh}) \sigma_{Eh} E_h(t), \\ E_m(t+1) &= (1 - \varphi_m(\mathbf{x}(t))) \sigma_{Sm} S_m(t) \\ &\quad + (1 - v_{Em}) \sigma_{Em} E_m(t) \\ I_h(t+1) &= v_{Eh} \sigma_{Eh} E_h(t) + (1 - v_{Ih}) \sigma_{Ih} I_h(t), \\ I_m(t+1) &= v_{Em} \sigma_{Em} E_m(t) + \sigma_{Im} I_m(t), \\ S_h(t+1) &= b_h \frac{1}{1+c_h p_h(t)} p_h(t) + v_{Rh} \sigma_{Rh} R_h(t) \\ &\quad + \varphi_h(\mathbf{x}(t)) \sigma_{Sh} S_h(t), \\ S_m(t+1) &= b_m \frac{1}{1+c_m p_m(t)} p_m(t) + \varphi_m(\mathbf{x}(t)) \sigma_{Sm} S_m(t), \text{ and} \\ R_h(t+1) &= v_{Ih} \sigma_{Ih} I_h(t) + (1 - v_{Rh}) \sigma_{Rh} R_h(t). \end{aligned}$$

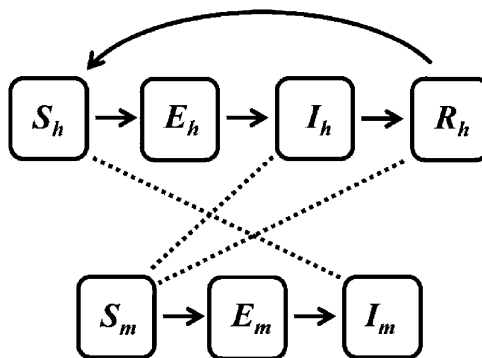


Figure 4.6. The flow diagram for the malaria model (4.30). The dashed lines indicate interactions between humans (top row) and mosquitoes (bottom row).

The time unit is one day. The σ coefficients denote survival probabilities for the class indicated by their subscripts in (4.30), and the v denote the probability of a transition between classes as indicated their subscripts; see Table 4.2.

What remains for the specification of the model are the infection escape functions φ_h and φ_m . For this purpose, we again use decreasing exponential functions

$$\varphi_h = \exp\left(-\delta_h \frac{I_m}{p_m}\right) \quad \text{and} \quad \varphi_m = \exp\left(-\delta_m \frac{I_h}{p_h}\right),$$

where

$$p_h = S_h + E_h + I_h + R_h \quad \text{and} \quad p_m = S_m + E_m + I_m$$

are total population sizes of humans and mosquitoes, respectively. In this model, the coefficients δ_h and δ_m in the escape functions are related to the number of bites per human per mosquito per day, as given in [18], by

$$\begin{aligned} \delta_h &:= \beta_h(p_h, p_m) i_{hm} \quad \text{and} \\ \delta_m &:= \beta_m(p_h, p_m) i_{mh}, \end{aligned}$$

where

$$\begin{aligned}\beta_h(p_h, p_m) &:= \frac{\beta_m p_m \beta_h p_h}{\beta_m p_m + \beta_h p_h} \frac{1}{p_h} \quad \text{and} \\ \beta_m(p_h, p_m) &:= \frac{\beta_m p_m \beta_h p_h}{\beta_m p_m + \beta_h p_h} \frac{1}{p_m}.\end{aligned}$$

Thus,

$$\begin{aligned}\varphi_h(\mathbf{x}(t)) &= \exp\left(-\beta_h(p_h, p_m) i_{hm} \frac{I_m}{p_m}\right) \quad \text{and} \\ \varphi_m(\mathbf{x}(t)) &= \exp\left(-\beta_m(p_h, p_m) i_{mh} \frac{I_h}{p_h}\right)\end{aligned}$$

in (4.30). The interpretation of the coefficients in these expressions appear in Table 4.2.

Note that the disease-free equations for the susceptibles $S_h(t)$ and $S_m(t)$ (obtained by setting E_h, E_m, I_h, I_m , and R_h identically equal to 0) are the two, uncoupled one-dimensional difference equations

$$\begin{aligned}S_h(t+1) &= b_h \frac{1}{1+c_h S_h(t)} S_h(t) + \sigma_{Sh} S_h(t) \quad \text{and} \\ S_m(t+1) &= b_m \frac{1}{1+c_m S_m(t)} S_m(t) + \sigma_{Sm} S_m(t)\end{aligned}$$

Table 4.2. Parameters for the Malaria Model (4.30)

Survival Probabilities	Transition and Infection Probabilities
σ_{Sh} susceptible human	v_{Eh} exposed human becomes infectious
σ_{Sm} susceptible mosquito	v_{Em} exposed mosquito becomes infectious
σ_{Eh} exposed human	v_{Ih} infectious human recovers
σ_{Em} exposed mosquito	v_{Rh} recovered human becomes susceptible
σ_{Ih} infectious human	i_{mh} mosquito is infected by biting a human
σ_{Im} infectious mosquito	i_{hm} human is infected by a mosquito bite
σ_{Rh} recovered human	
Logistic Growth Coefficients	Biting Rates
b_h, b_m birth rates	β_h average bites a human receives per day
c_h, c_m density coefficients	β_m average bites a mosquito gives per day

for the human and mosquito populations. We can analyze both of these equations using the methods of Chapter 1 to find

$$\lim_{t \rightarrow \infty} S_h(t) = \begin{cases} 0 & \text{if } \frac{b_h}{1-\sigma_{Sh}} < 1 \\ S_{he} := \frac{1}{c_h} \left(\frac{b_h}{1-\sigma_{Sh}} - 1 \right) & \text{if } \frac{b_h}{1-\sigma_{Sh}} > 1 \end{cases} \quad \text{and}$$

$$\lim_{t \rightarrow \infty} S_m(t) = \begin{cases} 0 & \text{if } \frac{b_m}{1-\sigma_{Sm}} < 1 \\ S_{me} := \frac{1}{c_m} \left(\frac{b_m}{1-\sigma_{Sm}} - 1 \right) & \text{if } \frac{b_m}{1-\sigma_{Sm}} > 1 \end{cases}$$

for all positive initial conditions $S_h(0) > 0$ and $S_m(0) > 0$. We proceed under the assumption that both populations survive in the absence of the parasite, that is to say that

$$\frac{b_h}{1-\sigma_{Sh}} > 1 \quad \text{and} \quad \frac{b_m}{1-\sigma_{Sm}} > 1.$$

The model equations in (4.30) have the general epidemic model format (4.1) with

$$\mathbf{x} = \begin{bmatrix} \mathbf{x}_1 \\ \mathbf{x}_2 \end{bmatrix},$$

where

$$\mathbf{x}_1 = \begin{bmatrix} x_1 \\ x_2 \\ x_3 \\ x_4 \end{bmatrix} = \begin{bmatrix} E_h \\ E_m \\ I_h \\ I_m \end{bmatrix} \quad \text{and} \quad \mathbf{x}_2 = \begin{bmatrix} x_5 \\ x_6 \\ x_7 \end{bmatrix} = \begin{bmatrix} S_h \\ S_m \\ R_h \end{bmatrix},$$

with

$$\mathbf{f}_1(\mathbf{x}_1, \mathbf{x}_2) = \mathbf{n}(\mathbf{x}_1, \mathbf{x}_2) + \mathbf{s}(\mathbf{x}_1, \mathbf{x}_2) \quad \text{and}$$

$$\mathbf{f}_2(\mathbf{x}_1, \mathbf{x}_2) = \begin{bmatrix} b_h \frac{1}{1+c_h N_h} N_h + v_{Rh} \sigma_{Rh} R_h + \varphi_h(\mathbf{x}) \sigma_{Sh} S_h \\ b_m \frac{1}{1+c_m N_m} N_m + \varphi_m(\mathbf{x}) \sigma_{Sm} S_m \\ v_{Ih} \sigma_{Ih} I_h + (1 - v_{Rh}) \sigma_{Rh} R_h \end{bmatrix},$$

and with

$$\mathbf{n}(\mathbf{x}_1, \mathbf{x}_2) = \begin{bmatrix} (1 - \varphi_h(\mathbf{x})) \sigma_{Sh} S_h \\ (1 - \varphi_m(\mathbf{x})) \sigma_{Sm} S_m \\ 0 \\ 0 \end{bmatrix} \quad \text{and}$$

$$\mathbf{s}(\mathbf{x}_1, \mathbf{x}_2) = \begin{bmatrix} (1 - v_{Eh}) \sigma_{Eh} E_h \\ (1 - v_{Em}) \sigma_{Em} E_m \\ v_{Eh} \sigma_{Eh} E_h + (1 - v_{Ih}) \sigma_{Ih} I_h \\ v_{Em} \sigma_{Em} E_m + \sigma_{Im} I_m \end{bmatrix}.$$

This model has the disease-free equilibrium

$$\mathbf{x}_e = \begin{bmatrix} 0 \\ 0 \\ 0 \\ 0 \\ x_{5e} \\ x_{6e} \\ 0 \end{bmatrix} = \begin{bmatrix} 0 \\ 0 \\ 0 \\ 0 \\ S_{he} \\ S_{me} \\ 0 \end{bmatrix},$$

which by Theorem 4.4, destabilizes as R_0 increases through 1.

To calculate the reproduction number R_0 using the method in Section 4.2, we calculate (using formulas (4.6)) the Jacobian matrices

$$\mathbf{F}(\mathbf{0}_m, \mathbf{x}_{2e}) = \begin{bmatrix} 0 & 0 & 0 & \frac{S_{he}\beta_{hm}\sigma_{Sh}\beta_h(S_{he}, S_{me})}{S_{me}} \\ 0 & 0 & \frac{S_{me}\beta_{mh}\sigma_{Sm}\beta_m(S_{he}, S_{me})}{S_{he}} & 0 \\ 0 & 0 & 0 & 0 \\ 0 & 0 & 0 & 0 \end{bmatrix}$$

and

$$\mathbf{T}(\mathbf{0}_m, \mathbf{x}_{2e}) = \begin{bmatrix} (1 - v_{Eh}) \sigma_{Eh} & 0 & 0 & 0 \\ 0 & (1 - v_{Em}) \sigma_{Em} & 0 & 0 \\ v_{Eh} \sigma_{Eh} & 0 & (1 - v_{Ih}) \sigma_{Ih} & 0 \\ 0 & v_{Em} \sigma_{Em} & 0 & \sigma_{Im} \end{bmatrix}$$

and the next generation matrix

$$\mathbf{F}(\mathbf{0}_m, \mathbf{x}_{2e})(\mathbf{I} - \mathbf{T}(\mathbf{0}_m, \mathbf{x}_{2e}))^{-1} = \begin{pmatrix} \mathbf{N} & * \\ \mathbf{0}_{2 \times 2} & \mathbf{0}_{2 \times 2} \end{pmatrix},$$

where \mathbf{N} is the matrix

$$\begin{bmatrix} 0 & \frac{S_{he}}{S_{me}} \frac{\beta_{hm}\sigma_{Sh}\nu_{Em}\sigma_{Em}\beta_h(S_{he}, S_{me})}{(1-(1-\nu_{Em})\sigma_{Em})(1-\sigma_{Im})} \\ \frac{S_{me}}{S_{he}} \frac{\beta_{mh}\nu_{Sm}\sigma_{Eh}\sigma_{Eh}\beta_m(S_{he}, S_{me})}{(1-(1-\nu_{Eh})\sigma_{Eh})(1-(1-\nu_{Ih})\sigma_{Ih})} & 0 \end{bmatrix}$$

and the asterisk denotes an unneeded block submatrix. The eigenvalues of this next generation matrix are 0 (with multiplicity 2) and those of \mathbf{N} , which are $\pm\sqrt{R_{0h}R_{0m}}$, where

$$(4.31) \quad R_{0h} := \frac{\beta_{mh}\sigma_{Sh}\nu_{Eh}\sigma_{Eh}\beta_h(S_{he}, S_{me})}{(1-(1-\nu_{Eh})\sigma_{Eh})(1-(1-\nu_{Ih})\sigma_{Ih})} \quad \text{and} \\ R_{0m} := \frac{\beta_{hm}\sigma_{Sm}\nu_{Em}\sigma_{Em}\beta_m(S_{he}, S_{me})}{(1-(1-\nu_{Em})\sigma_{Em})(1-\sigma_{Im})}.$$

It follows that

$$(4.32) \quad R_0 = \sqrt{R_{0h}R_{0m}}.$$

Note that

$$R_{0h} = [\text{bites per human per unit time}] \\ \times [\text{probability of human-to-mosquito transmission}] \\ \times [\text{expected time a human is infectious}] \\ = \left[\begin{array}{c} \text{average number of mosquitoes infected} \\ \text{by humans per unit time} \end{array} \right] \\ \times [\text{expected time a human is infectious}] \\ = \left[\begin{array}{c} \text{average number of mosquitoes infected} \\ \text{by a human per lifetime} \end{array} \right],$$

and similarly, R_{0m} is the average number of humans infected by a mosquito per lifetime.

The reproduction number R_0 that determines the stability of the disease-free equilibrium in the malaria model (4.30) is the geometric mean (4.32) of the two averages R_{0h} and R_{0m} given by formulas (4.31).

More analysis of the continuous time version of the malaria model (4.30) can be found in [18], [19].

4.6. Concluding Remarks

In this chapter, we consider an important type of structured population model in which individuals are classified according to various disease-related stages. The focus was on the modeling methodology and the stability properties of a disease-free equilibrium (i.e., an equilibrium of a model in which there are no individuals infected with the pathogen). We describe a general procedure for calculating the famous quantity R_0 (the inherent reproduction number) associated with a specific disease-free equilibrium. The disease-free equilibrium destabilizes as R_0 increases through 1, and this destabilization results in the creation of endemic equilibrium (i.e., equilibria in which the infected class is not empty). This basic (transcritical) bifurcation is analogous to that for matrix models considered in Chapter 3 except that the bifurcation is not of survival equilibria from a population extinction equilibrium but of endemic equilibria from a disease-free equilibrium.

To protect the population from an epidemic, a focus is placed on attaining $R_0 < 1$. It should be remembered, however, that the stability analysis in Theorem 4.4 only guarantees the local stability for initial conditions near the disease-free equilibrium (i.e., for populations near the disease-free equilibrium that are invaded by a small number of diseased individuals). While this might indeed be appropriate for many cases, for other circumstances, $R_0 < 1$ might not guarantee the asymptotic elimination of the disease. A global analysis of the existence and stability of endemic equilibria is needed for such a conclusion.

4.7. Exercises

Exercise 4.10. Assume the disease-free equation in the SI model of Example 4.2 and Section 4.3.1 is the Ricker equation

$$x_1(t+1) = bx(t) \exp(-cx(t))$$

instead of the discrete logistic equation. Calculate R_0 and apply Theorems 4.4 and 4.7.

Exercise 4.11. Prove (4.24) still holds for the vaccination modified SI model (4.23) with a general escape function $\varphi(x_1/p)$ with $\varphi(0) = 1$ and $\varphi'(0) < 0$.

Exercise 4.12. Show that the disease-free equilibrium x_{2e} of the SAIR model in Section 4.3.3 satisfies Assumption 4.1.

Exercise 4.13. Consider an extension of the SAIR model in Example 4.3.3 in which asymptomatic individuals can also recover and move the recovered class x_4 with a certain probability. Modify the cycle graph in Figure 4.3 to include this possibility. Calculate R_0 and apply Theorems 4.4 and 4.7.

Exercise 4.14. Consider an extension of the SAIR model in Example 4.3.3 in which infected susceptibles can be either asymptomatic or symptomatic. Modify the cycle graph in Figure 4.3 to include this possibility. Calculate R_0 and apply Theorems 4.4 and 4.7.

Exercise 4.15. Consider an extension of the SAIR model in Example 4.3.3 that includes both added features in Exercises 4.13 and 4.14. Modify the cycle graph in Figure 4.3 to include this possibility. Calculate R_0 and apply Theorems 4.4 and 4.7.

Exercise 4.16. Derive the formula (4.28) for the disease-free equilibrium of the vaccination SIR model in Section 4.5.1.2. Also, check the formula by substitution into the disease-free equilibrium equations.

Chapter 5

Darwinian Dynamics

In the models considered in Chapters 1–4, the coefficients appearing in the equations remain constant in time. These coefficients describe various biological and environmental parameters that, except in extraordinary circumstances (such as in controlled laboratory experiments), will in fact not likely remain constant but suffer changes and fluctuations for any number of reasons. Changing physical and biological environments can change vital rates such as those associated with reproduction, survival, resource consumption, and growth rates, to name a few. The models in Chapters 1–4 can be adapted to take into account coefficients that are not constant in time, and to do so leads to new types of mathematical equations that present new challenges. For example, if the changes are due to regular periodic fluctuations in the environment (e.g., daily or seasonal variations), one can model the dynamics by using periodic coefficients in a model equation, resulting in a type of nonautonomous equation called a periodically forced equation. In other circumstances, the environment might shift from one state to another over time—a situation that could be modeled by equations with coefficients that asymptotically move from one set of values to another—resulting in what are called asymptotically autonomous equations. Yet another situation occurs when environmental fluctuations are random and the model coefficients become random variables, which leads to stochastic difference equations.

In this chapter, we consider the case when model coefficients change due to the Darwinian principles of natural selection. In Sections 5.1, 5.2, and 5.3, we study the modeling methodology of so-called **trait (strategy) driven evolution** [129]. The model equations are derived from a selected population model (as found in Chapters 1 and 3) and modified by prescribing how one or more coefficients in the model depend on a phenotypic trait that is subject to evolution, which is supplemented by an equation for the dynamics of the population's mean trait. These equations, which couple the population/ecological dynamics with the evolutionary dynamics, constitute a Darwinian version of the original population equation. We show in Sections 5.2 and 5.3 how the basic bifurcation phenomena of survival equilibria from a destabilized extinction equilibrium that occurs for nonevolutionary models (Chapter 3) also occurs for Darwinian evolutionary models. That is to say, our starting point is to consider the problem of extinction versus survival by studying the stability properties of extinction states (Section 5.2) and then the creation of survival (positive) equilibria by bifurcation when an extinction state destabilizes (Section 5.3).

The Darwinian models studied in Sections 5.1–5.3 track the evolutionary change of the mean trait as it occurs within a single population. Another means of evolutionary change is **invasion driven evolution** [129]. This evolutionary change occurs when a (reproductively separate) mutant population with a different mean trait displaces a resident population [129]. This concept leads to the notion of an ESS trait, which we briefly study in Section 5.4.

We conclude this chapter with several applications that not only illustrate these methods and results but address some fundamental biological questions that have interested researchers both historically and recently (Section 5.6).

5.1. Modeling Methodology

Return, for the moment, to the lowest-dimensional ($m = 1$) matrix equation (1.11) considered in Chapter 1:

$$(5.1) \quad x(t+1) = r(x(t))x(t)$$

with

$$(5.2) \quad r(x) := b_0\beta(x) + s_0\sigma(x)$$

and

$$\beta(0) = \sigma(0) = 1.$$

Recall that b_0 and s_0 are inherent (density-free) per capita fertility and survival rates, i.e., the fertility and survival rates of each individual in the population (all of whom in such models are considered identical) in the absence of interactions with other individuals in the population. We now want to consider the case when all individuals do not have the same inherent vital rates.

We assume that individuals differ with regard to some (phenotypic) trait that determines their vital rates b_0 and s_0 and that this trait is subject to the axioms of natural selection (variability, heritability, and differential fitness). This trait can be a physiological characteristic that affects the individual's ability to produce viable offspring and survive (for example, by affecting its ability to gather food resources, establish and defend territories, find mates, or resist diseases), a behavioral trait (for example, how aggressively it competes or cooperates with other individuals for resources and mates), a metabolic trait (for example, the ability to utilize certain food resources or a growth or maturation rate), etc. To begin, we consider a model in which there is only one such trait, which we denote by v , and assume $b_0 = b_0(v)$ and $s_0 = s_0(v)$.

When interactions among individuals occur, the density-dependent fertility and survival factors $\beta(x)$ and $\sigma(x)$ that affect an individual's fertility and survival depend not only on the individual's inherited trait v but can also depend on the traits of other individuals with whom it interacts. For example, if the trait is body size, then in a contentious competition for a resource, the competitive ability of an individual could depend on its size relative to that of its competitors. In the modeling methodology considered here, the comparison is made between the individual's trait v and that of the typical individual, by which we mean an individual whose trait equals the population's mean trait, denoted by u . Thus, we allow β and σ to depend on both v and u and write

$$(5.3) \quad r(x, v, u) := b_0(v)\beta(x, v, u) + s_0(v)\sigma(x, v, u) \quad \text{and}$$

$$\beta(0, v, u) \equiv \sigma(0, v, u) \equiv 1.$$

The latter normalization assumptions insure that $b_0(v)$ and $s_0(v)$ retain their interpretations as the inherent (density-free) fertility and survival rates. If $x = x(t)$ and $u = u(t)$ change over time and $x_v(t)$ denotes

the subpopulation of those individuals with trait v , then the population dynamics of this subpopulation are governed by the equation

$$(5.4) \quad x_v(t+1) = r(x(t), v, u(t)) x_v(t).$$

The method of Darwinian dynamics (evolutionary game theory) follows the dynamics of the entire population $x = x(t)$ with its mean trait $u = u(t)$, which are described by equation (5.4) with $v = u(t)$, that is to say the equation [129]

$$(5.5) \quad x(t+1) = r(x(t), v, u(t))|_{v=u(t)} x(t).$$

What is missing is a model for the dynamics of the mean trait $u(t)$.

In Appendix A.4, the reader will find a derivation of the equation

$$(5.6) \quad u(t+1) = u(t) + \theta \partial_v \ln r(x, v, u(t))|_{v=u(t)}$$

for the dynamics of the mean trait (for other derivations, see [3], [96], [97], [129]). This derivation assumes that evolution does not occur too rapidly (often referred to as first order dynamics) and that the trait is at all times symmetrically distributed about the mean.

The coefficient $\theta \geq 0$ is the variance of the traits around the mean and is constant in first order dynamics (see Appendix A.4); it is called the **speed of evolution**. Note that if $\theta = 0$ (i.e., if there is no trait variability within the population), then no evolution occurs (since in this case $u(t+1) = u(t)$, the mean trait remains fixed at its initial condition $u(0)$) and the model reduces to a nonevolutionary, one-dimensional population equation (5.5) of the type studied in Chapter 1.

The term $\ln r(x, v, u)$ appearing in the trait equation (5.6) is called the **fitness** of the population.¹ This equation for $u(t)$, which says that the change in the mean trait is proportional to the fitness gradient, goes by various names, including the canonical equation of evolution, Lande's equation, Fisher's equation (of additive genetic variance), or the breeder's equation.

In summary, once a modeler has chosen a population model (5.1)–(5.2) and how r in (5.3)—that is to say, the fitness $\ln r(x, v, u)$ of an individual with trait v when in a population with density x and mean trait

¹The somewhat clumsy notation in equations (5.5) and (5.6) is used so as to ensure that the derivative in the fitness gradient appearing in (5.6) is taken with respect to the individual trait v and not, mistakenly, with respect to the population mean trait u .

u —depends on v and u , then this methodology (called **Darwinian dynamics** or **evolutionary game theory**) produces the evolutionary version of the population model (5.5)–(5.6). These equations describe the (trait driven) evolution of the mean phenotypic as it is coupled with the population dynamics of the population.

An important part of building a Darwinian model are the details of how $r(x, v, u)$ (i.e., how the coefficients in the model equations) depend on an individual's trait v and/or on the population mean trait u . These details reflect the biological assumptions of interest to the modeler. Different assumptions can lead, of course, to very different dynamics and hence very different biological punch lines. Often simple assumptions that concern the monotonicity properties of a coefficient with respect to v and/or u or that a coefficient has a maximum or minimum at certain trait values are enough to permit an analysis of the model. This lends a level of generality to the analysis and conclusions. Other times, specific mathematical formulas for the coefficients (such as exponential functions, rational functions, or Gaussian distributions) are utilized. Here are some examples.

With regard to density-free coefficients (i.e., coefficients appearing in $r(0, v, u)$), it is natural to assume that they do not depend on u but can depend on v . The reason for this is that if population density has no effect on the coefficient, then neither will the population's mean trait u . The (per capita) inherent fertility rate b_0 in the general model equation (1.11) is a case in point, as is the (per capita) inherent survival rate s_0 . For example, in the discrete logistic equation (1.17)

$$x(t+1) = b_0 \frac{1}{1 + cx(t)} x(t)$$

for which

$$r(x) = b_0 \frac{1}{1 + cx},$$

we could assume $b_0 = b_0(v)$ is dependent on the trait v and then consider specific properties and/or a specific formula for $b_0(v)$. The mathematical properties of the function $b_0(v)$, as a function of the trait v , depend on the biological and ecological circumstances in which the modeler is interested. For example, one might assume that there exists a trait v at which the birth rate is maximal, a specific example of which is

$$b_0 \exp\left(-\frac{1}{2} \frac{(v - v_0)^2}{w}\right),$$

where v_0 is the trait at which the maximum birth rate b_0 is attained and $w > 0$ measures the width of the distribution of birth rates as a function of v . Note that no scale or reference point for measuring the trait v is prescribed, and therefore there is no loss in mathematical generality in assuming that the maximal birth rate occurs at trait $v_0 = 0$ and that $w = 1$:

$$(5.7) \quad b_0 \exp\left(-\frac{1}{2}v^2\right).$$

Another example is

$$b_0 \frac{1}{1 + v^2}.$$

Density-dependent coefficients might also depend on v and not u (the Darwinian LPA model utilized in [116] is an example). On the other hand, since such coefficients involve population density, they might rely on u as well as v . An example is the competition coefficient c in the discrete logistic for which we then write $c = c(v, u)$. When combined with $b_0(v)$, this classical equation then has per capita growth rate

$$r(x, v, u) = b_0(v) \frac{1}{1 + c(v, u)x}$$

from which we can build a Darwinian version of the logistic. The coefficient $c(v, u)$ accounts for the effect that competition has on an individual with trait v in its interaction with other individuals in the population, as represented by the most typical individual with trait u . One assumption often made is that this effect depends on how different the individual is from its competitor (i.e., on the trait difference $v - u$ [129]). Perhaps the simplest expression of this assumption is when $c(v, u)$ is a function of $v - u$, which we might write as $c(v - u)$ and assign suitable properties to the function $c(z)$ as a function of z . In this case, $c_0 = c(0)$ is the competitive intensity experienced by an individual that inherits the mean trait $v = u$. If we are interested in the case when competition becomes more severe as competitors become more similar (as Darwin points out is often the case [46]), then $c(z)$ would have a maximum of $c_0 > 0$ at $z = 0$. A specific example is

$$c(z) = c_0 \exp\left(-\frac{1}{2w}z^2\right), \quad c_0, w > 0.$$

A variation when c_0 depends on the population mean is

$$c(v, u) = c_0(u) \exp\left(-\frac{1}{2w}(v - u)^2\right), \quad w > 0,$$

which is a coefficient (with a normal distribution for $c_0(u)$) that is widely used in competition studies (see [129] and the many references cited therein). Other types of competition coefficients are of course possible when specific ecological scenarios are in mind. For example, monotonicity assumption can be appropriate when considering hierarchical competition effects. Consider a forest in which the competitive effect of sunlight is a function of tree height v (taller trees shade shorter trees). In this case, $c(v, u)$ decreases as a function of v (i.e., for taller trees v in a forest with mean tree height u). On the other hand, $c(v, u)$ increases as a function of u , as the competitive effect on a tree of height v increases as the mean tree height u increases. An example might be

$$c(v, u) = \varpi(v)v(u)$$

with $\varpi(v)$ and $v(u)$ being decreasing and increasing functions of their arguments, respectively;

$$c(v, u) = c_0 \exp(-c_1 v) \exp(c_2 u)$$

with all $c_i > 0$ is an example, which becomes an example of type

$$c(v - u) = c_0 \exp(-w(v - u))$$

when $c_1 = c_2 := w$.

Clearly, the choice of the submodels for the coefficients will determine the complexity of the resulting Darwinian model equations and of the technical details and formulas involved their analysis. Our goal will be to focus on the illustration of the theorems and analytic methodologies given in this chapter, and for that tutorial reason, we will restrict attention to simpler model coefficients in our choice of illustrative examples. In fact, we will mostly focus on inherent parameters of Gaussian form (5.7) and density coefficients of the form $c(v - u)$.

Example 5.1. For the discrete logistic equation (1.17) introduced in Example 1.4, the per capita population growth rate is

$$r(x) = b_0 \frac{1}{1 + cx}.$$

Consider a Darwinian version of this equation by replacing the fertility rate b_0 with

$$b_0 \exp\left(-\frac{1}{2}v^2\right).$$

That is to say, we assume fertility has a normal distribution with respect to the trait v . We have assumed that this distribution has mean

0 and standard deviation equal to 1, which is no loss in generality because we are free to choose any reference point and scale for v . The coefficient c describes the competitive effect of interactions among individuals, which we now want to consider as a function of an individual's inherited trait v and of the trait of the typical individual with the population mean trait u . A common assumption is that this intraspecific competition coefficient is a function of the difference $v - u$ (i.e., depends on how different the individual with trait v is from the typical individual with trait u). Thus, we replace c by a function $c(v - u)$ and arrive at

$$r(x, v, u) = b_0 \exp\left(-\frac{1}{2}v^2\right) \frac{1}{1 + c(v - u)x}.$$

Here $c(z)$ is a positive-valued, differentiable function of its argument $z \in \mathbb{R}^1$. If we set

$$c_0 := c(0) \quad \text{and} \quad c_1 := \partial_z c(0),$$

then the Darwinian equations (5.5) and (5.6) become

$$(5.8) \quad \begin{aligned} x(t+1) &= b_0 \exp\left(-\frac{1}{2}u^2(t)\right) \frac{1}{1+c_0x(t)} x(t) \quad \text{and} \\ u(t+1) &= u(t) + \theta\left(-u(t) - c_1 \frac{1}{1+c_0x(t)} x(t)\right). \end{aligned}$$

As another example, consider a similar Darwinian version of the Ricker equation (1.25) with

$$r(x, v, u) = b_0 e^{-v^2/2} e^{-c(v-u)x}.$$

Equations (5.5) and (5.6) become

$$(5.9) \quad \begin{aligned} x(t+1) &= b_0 \exp\left(-\frac{1}{2}u^2(t)\right) \exp(-c_0x(t)) x(t) \quad \text{and} \\ u(t+1) &= u(t) + \theta(-u(t) - c_1 x(t)) \end{aligned}$$

We return to this Darwinian Ricker model in Section 5.6.3. □

For an evolutionary version of the matrix model of the type studied in Chapters 2 and 3, that is

$$\mathbf{x}(t+1) = \mathbf{P}(\mathbf{x}(t)) \mathbf{x}(t),$$

the entries of the projection matrix $\mathbf{P}(\mathbf{x}) = [p_{ij}(\mathbf{x})]$, as per capita or individual rates (birth, survival, stage transition, etc.), are taken as functions of v and u , and we write $p_{ij} = p_{ij}(\mathbf{x}, v, u)$. The Darwinian dynamics for such a matrix model are described by the population and trait equations

$$(5.10) \quad \begin{aligned} \mathbf{x}(t+1) &= \mathbf{P}(\mathbf{x}(t), v, u(t))|_{v=u(t)} \mathbf{x}(t) \quad \text{and} \\ u(t+1) &= u(t) + \theta \partial_v \ln \rho(\mathbf{P}(\mathbf{x}(t), v, u(t)))|_{v=u(t)}, \end{aligned}$$

where **fitness** is $\ln \rho(\mathbf{P}(\mathbf{x}, v, u))$, which is the logarithm of the spectral radius of the projection matrix. The derivation of the trait equation for the matrix model is more complicated than that given in Appendix A.4 for the $m = 1$ dimensional model, and we will not give one here; see [3], [129]. Note that when $m = 1$, the matrix model (5.10) reduces to the model (5.5)–(5.6) since $\mathbf{P}(\mathbf{x}, v, u) = [r(x, v, u)]$ and $\rho(\mathbf{P}(\mathbf{x}, v, u)) = r(x, v, u)$.

Example 5.2. Consider a Darwinian version of the juvenile-adult model (3.1) with projection matrix

$$(5.11) \quad \mathbf{P}(\mathbf{x}, v, u) = \begin{bmatrix} 0 & b_0 \exp\left(-\frac{1}{2}v^2\right) \frac{1}{1+c(v-u)x_2} \\ s_1 & s_2 \end{bmatrix}.$$

In this example, an adult's inherent fertility is trait-dependent on its inherited trait v and has a normal distribution as a function of v . The fertility-dependent factor, describing decreasing fertility with increased adult density x_2 , has a trait-dependent, intraspecific competition coefficient $c(z)$, in the same manner as in Example 5.1. Juvenile and adult survival, s_1 and s_2 , are assumed to be density and trait independent.

The eigenvalues of $\mathbf{P}(\mathbf{x}, v, u)$ are the roots of its quadratic characteristic equation

$$\lambda^2 - s_2 \lambda - s_1 b_0 \exp\left(-\frac{1}{2}v^2\right) \frac{1}{1 + c(v-u)x_2} = 0.$$

The spectral radius (dominant eigenvalue) of $\mathbf{P}(\mathbf{x}, v, u)$ is

$$\rho(\mathbf{P}(\mathbf{x}, v, u)) = \frac{1}{2} \left(s_2 + \sqrt{s_2^2 + \frac{4s_1 b_0 \exp\left(-\frac{1}{2}v^2\right)}{1 + c(v-u)x_2}} \right).$$

A straightforward (if tedious) calculation gives

$$\begin{aligned} \partial_v \ln \rho(\mathbf{P}(\mathbf{x}, v, u))|_{v=u} &= \frac{u(1 + c_0 x_2) + c_1 x_2}{(1 + c_0 x_2)^2} \\ &\cdot \frac{-2s_1 b_0 \exp\left(-\frac{1}{2}u^2\right)}{\left(s_2 + \sqrt{s_2^2 + 4s_1 b_0 \exp\left(-\frac{1}{2}u^2\right) \frac{1}{1+c_0x_2}}\right) \sqrt{s_2^2 + 4s_1 b_0 \exp\left(-\frac{1}{2}u^2\right) \frac{1}{1+c_0x_2}}}, \end{aligned}$$

where

$$c_0 := c(0) \quad \text{and} \quad c_1 := \partial_z c(0).$$

From (5.10), we get the Darwinian equations

$$(5.12) \quad \begin{bmatrix} x_1(t+1) \\ x_2(t+1) \end{bmatrix} = \begin{bmatrix} 0 & \frac{b_0 \exp(-\frac{1}{2}u^2(t))}{1+c_0x_2(t)} \\ s_1 & s_2 \end{bmatrix} \begin{bmatrix} x_1(t) \\ x_2(t) \end{bmatrix} \quad \text{and}$$

$$u(t+1) = u(t) + \theta \partial_v \ln \rho(\mathbf{P}(\mathbf{x}(t), v, u(t)))|_{v=u(t)}$$

as an evolutionary version of this juvenile-adult model. \square

Example 5.2 illustrates that when $m \geq 2$, the equations (5.10) for the Darwinian matrix model are likely to be quite complicated. This is especially true for the trait equation since it is unlikely that an analytic formula will be available for the spectral radius of the projection matrix. Despite these difficulties, in Sections 5.2 and 5.3, we will be able to develop analytic methods to study the stability properties of extinction equilibria and the resulting bifurcation of survival equilibria (as in Chapter 3 for nonevolutionary models).

We begin with the domain and smoothness properties required of the entries in projection matrix $\mathbf{P}(\mathbf{x}, v, u) = [p_{ij}(\mathbf{x}, v, u)]$, which we will assume are enforced throughout this chapter.

Assumption 5.3. $p_{ij} \in C^2(R^m \times \Lambda \times \Lambda : R_+)$, where Λ is an open interval in R^1 . The projection matrix $\mathbf{P}(\mathbf{x}, v, u) = [p_{ij}(\mathbf{x}, v, u)]$ is irreducible for each $(\mathbf{x}, v, u) \in R_+^m \times \Lambda \times \Lambda$, and for all $u, v \in \Lambda$ and i, j , the entry $p_{ij}(\mathbf{0}_m, v, u)$ is independent of u , that is

$$(5.13) \quad \partial_u p_{ij}(\mathbf{0}_m, v, u) \equiv 0.$$

The equation (5.13) implies that the projection matrix $\mathbf{P}(\mathbf{0}_m, v, u)$, and hence its spectral radius $\rho(\mathbf{P}(\mathbf{x}, v, u))$, are independent of u . This in turn implies the inherent fitness $\ln \rho(\mathbf{P}(\mathbf{0}_m, v, u))$ is independent of u , that is

$$(5.14) \quad \partial_u \ln \rho(\mathbf{P}(\mathbf{0}_m, v, u)) \equiv 0 \text{ for all } v, u \in \Lambda.$$

As always, the first step in the analysis of a dynamic model is to deal with the existence of equilibrium solutions and then their local stability properties, as determined by the Linearization Principle. In population models, such as those in Chapters 1, 2, and 3, extinction equilibria play a fundamental role since they relate to the basic biological question of extinction versus survival. In this section, we consider extinction equilibria for the (single trait) Darwinian version of a nonlinear matrix model (5.10).

The equilibrium equations associated with (5.10) are

$$\begin{aligned}\mathbf{x} &= \mathbf{P}(\mathbf{x}, v, u)|_{v=u} \mathbf{x} \quad \text{and} \\ 0 &= \theta \partial_v \ln \rho(\mathbf{P}(\mathbf{x}, v, u))|_{v=u},\end{aligned}$$

which if evolution occurs (i.e., $\theta > 0$), are equivalent to

$$(5.15) \quad \begin{aligned}\mathbf{x} &= \mathbf{P}(\mathbf{x}, v, u)|_{v=u} \mathbf{x} \quad \text{and} \\ 0 &= \partial_v \rho(\mathbf{P}(\mathbf{x}, v, u))|_{v=u}.\end{aligned}$$

Definition 5.4. A **survival equilibrium** of the Darwinian model (5.10) is a pair

$$(5.16) \quad \left[\begin{array}{c} \mathbf{x} \\ u \end{array} \right] = \left[\begin{array}{c} \mathbf{x}_e \\ u_e \end{array} \right] \in R_+^m \times \Lambda$$

with $\mathbf{x}_e \neq \mathbf{0}_m$ that solves the equations (5.15). If $\mathbf{x}_e = \mathbf{0}_m$, then the equilibrium is called an **extinction equilibrium**. If $\mathbf{x}_e \in \text{int}(R_+^m)$, then it is called a **positive equilibrium**.

Since by assumption $\mathbf{P}(\mathbf{x}, v, u)|_{v=u}$ is nonnegative and irreducible, Perron–Frobenius theory implies that it has a simple, positive dominant eigenvalue with a positive eigenvector and that no other eigenvalue has a nonnegative eigenvector. It follows from the first equilibrium equation that 1 is an eigenvalue of $\mathbf{P}(\mathbf{x}_e, v, u_e)|_{v=u_e}$ associated with eigenvector $\mathbf{x}_e \in R_+^m$, and as a result, $\mathbf{x}_e \in \text{int}(R_+^m)$ is a positive equilibrium.

Example 5.5. The equilibrium equations associated with the Darwinian discrete logistic model (5.8) are (after a cancellation of θ)

$$\begin{aligned}x &= b_0 \exp\left(-\frac{1}{2}u^2\right) \frac{1}{1+c_0x} x \quad \text{and} \\ 0 &= -u + c_1 \frac{1}{1+c_0x} x\end{aligned}$$

from which we find, given any $b_0 > 0$, that there is only extinction equilibrium, namely

$$\left[\begin{array}{c} x \\ u \end{array} \right] = \left[\begin{array}{c} 0 \\ 0 \end{array} \right].$$

To find positive equilibria, we need to solve these algebraic equations for $x > 0$. After a cancellation of the factor x in the first equation, the equations for a positive equilibrium are

$$\begin{aligned}1 &= b_0 \exp\left(-\frac{1}{2}u^2\right) \frac{1}{1+c_0x} \quad \text{and} \\ 0 &= -u + c_1 \frac{1}{1+c_0x} x.\end{aligned}$$

Unfortunately, we cannot solve these equations analytically to obtain formulas for positive equilibria. (This is not unusual for Darwinian models.) However, we can argue that there exists a unique positive equilibrium for each $b_0 > 1$ (and that there are no positive equilibria for $b_0 \leq 1$) as follows. Solve the second equation for

$$u = c_1 \frac{1}{1 + c_0 x}$$

and substitute this into the first equation to obtain the equation

$$1 = b_0 e^{-\frac{1}{2} c_1^2 \left(\frac{1}{1+c_0 x} x \right)^2} \frac{1}{1 + c_0 x}$$

to be solved for $x > 0$. While we cannot do this analytically, we can easily solve for b_0 as a function of x and take the approach used in Chapter 1. The right side of the result equation

$$(5.17) \quad b_0 = (1 + c_0 x) \exp \left(\frac{1}{2} c_1^2 \left(\frac{1}{1 + c_0 x} x \right)^2 \right)$$

is easily shown to be a monotonically increasing function of $x \geq 0$ which equals 1 when $x = 0$ and approaches $+\infty$ as $x \rightarrow +\infty$. Thus, the range of this function is $1 \leq b_0 < +\infty$. From this, we see that for any $b_0 \leq 1$ there is no solution $x > 0$ of the equilibrium equation but that for each $b_0 > 1$ there is exactly one solution $x = x_e(b_0) > 0$. We conclude that for each $b_0 > 1$ there exists a unique positive equilibrium

$$\begin{bmatrix} x \\ u \end{bmatrix} = \begin{bmatrix} x_e(b_0) \\ c_1 \frac{1}{1 + c_0 x_e(b_0)} x_e(b_0) \end{bmatrix},$$

where $x = x_e(b_0)$ satisfies equation (5.17). \square

Example 5.6. The equilibrium equations associated with the Darwinian juvenile-adult model (5.12) are

$$\begin{bmatrix} x_1 \\ x_2 \end{bmatrix} = \begin{bmatrix} 0 & b_0 \exp(-\frac{1}{2} u^2) \frac{1}{1 + c_0 x_2} \\ s_1 & s_2 \end{bmatrix} \begin{bmatrix} x_1 \\ x_2 \end{bmatrix} \quad \text{and}$$

$$0 = 2u(1 + c_0 x_2) + c_1 x_2.$$

There exists an extinction equilibrium $\mathbf{x} = \mathbf{0}_2$ if and only if u is a root of the second equation with $x_2 = 0$ (i.e., $u = 0$). Thus, the only extinction equilibrium is $\text{col}(\mathbf{x}, u) = \text{col}(\mathbf{0}_2, 0)$.

It is not possible to calculate a formula for survival equilibria, but we can prove that there exists no survival equilibrium if $R_0 < 1$, where

$$R_0 = b_0 \frac{s_1}{1 - s_2},$$

and that there exist unique positive equilibrium for each $R_0 > 1$. We can do this as follows. If we solve the last two of the equilibrium equations

$$\begin{aligned} x_1 &= b_0 \exp\left(-\frac{1}{2}u^2\right) \frac{1}{1 + c_0 x_2} x_2, \\ x_2 &= s_1 x_1 + s_2 x_2, \quad \text{and} \\ 0 &= 2u(1 + c_0 x_2) + c_1 x_2 \end{aligned}$$

for

$$x_1 = \frac{1 - s_2}{s_1} x_2 \quad \text{and} \quad u = -\frac{c_1 x_2}{2(1 + c_0 x_2)},$$

respectively, and place these in the first equation, then the result is an equation for x_2 . After some algebraic manipulations, this equation is

$$1 + c_0 x_2 = R_0 \exp\left(-\frac{1}{2} \left(\frac{c_1 x_2}{2(1 + c_0 x_2)}\right)^2\right).$$

Note that the left side is an increasing (linear) function, while the right side is a decreasing function of $x_2 > 0$. Thus, we see geometrically that the graphs of these two positive functions will intersect (exactly once) at a value of $x_2 > 0$ if and only if the right side is larger than the left side when $x_2 = 0$ (i.e., if and only if $R_0 > 1$). \square

In this section, we have restricted our modeling efforts to a single trait subject to evolutionary change. To include multiple traits involves utilizing a vector of n mean traits $\mathbf{u} = \text{col}(u_i)$ and an extension of the trait equation to describe its dynamics. The equations take the form [129]

$$\begin{aligned} \mathbf{x}(t+1) &= \mathbf{P}(\mathbf{x}(t), \mathbf{v}, \mathbf{u}(t))|_{\mathbf{v}=\mathbf{u}(t)} \mathbf{x}(t) \quad \text{and} \\ \mathbf{u}(t+1) &= \mathbf{u}(t) + \Theta \partial_v \ln \rho(\mathbf{P}(\mathbf{x}(t), \mathbf{v}, \mathbf{u}(t)))|_{\mathbf{v}=\mathbf{u}(t)}, \end{aligned}$$

where Θ is an $n \times n$ variance/covariance matrix. While the theorems and results in the following sections can be extended to this case, we will restrict attention to the single variable $n = 1$ case.

5.2. Extinction Equilibria

Since $\mathbf{x} = \mathbf{0}_m$ clearly satisfies the first equilibrium equation in (5.15),

$$(5.18) \quad \begin{bmatrix} \mathbf{x} \\ u \end{bmatrix} = \begin{bmatrix} \mathbf{0}_m \\ u_c \end{bmatrix}$$

is an extinction equilibrium if and only if the trait component u_c satisfies the equation

$$0 = \partial_v \rho(\mathbf{P}(\mathbf{0}_m, v, u_c))|_{v=u_c}.$$

We refer to u_c as a **critical trait**.

Assuming the existence of a critical trait, we can study the stability properties of the associated extinction equilibrium by means of the Linearization Principle. The Jacobian associated with the Darwinian model (5.15) when evaluated at an extinction equilibrium is a block diagonal matrix

$$\begin{bmatrix} \mathbf{P}(\mathbf{0}_m, v, u_c)|_{v=u_c} & \mathbf{0}_m \\ * & 1 + \theta \partial_u (\partial_v \ln \rho(\mathbf{P}(\mathbf{0}_m, v, u))|_{v=u})|_{u=u_c} \end{bmatrix}$$

whose eigenvalues are the eigenvalues of the diagonal blocks (the asterisk denotes an unneeded $1 \times m$ matrix). Making use of (5.14), we have

$$\begin{aligned} \partial_u (\partial_v \ln \rho(\mathbf{P}(\mathbf{0}_m, v, u))|_{v=u}) &= \partial_v^2 \ln \rho(\mathbf{P}(\mathbf{0}_m, v, u))|_{v=u} \\ &\quad + \partial_u \partial_v \ln \rho(\mathbf{P}(\mathbf{0}_m, v, u))|_{v=u} \\ &= \partial_v^2 \ln \rho(\mathbf{P}(\mathbf{0}_m, v, u))|_{v=u} \\ &\quad + \partial_v \partial_u \ln \rho(\mathbf{P}(\mathbf{0}_m, v, u))|_{v=u} \\ &= \partial_v^2 \ln \rho(\mathbf{P}(\mathbf{0}_m, v, u))|_{v=u}, \end{aligned}$$

and the Jacobian becomes

$$\begin{bmatrix} \mathbf{P}(\mathbf{0}_m, v, u_c)|_{v=u_c} & \mathbf{0}_m \\ * & 1 + \theta \partial_v^2 \ln \rho(\mathbf{P}(\mathbf{0}_m, v, u_c))|_{v=u_c} \end{bmatrix}.$$

Define the **inherent population growth rate** (at a critical trait) to be

$$r_0 := \rho(\mathbf{P}(\mathbf{0}_m, v, u_c)|_{v=u_c}).$$

The Linearization Principle gives the following results.

Lemma 5.7. *Assume Assumption 5.3 holds, that $\theta > 0$, and that $u = u_c$ is a critical trait. Then the extinction equilibrium (5.18) of the Darwinian*

model (5.15) is (locally asymptotically) stable if these inequalities hold:

- (a) $\partial_v^2 \ln \rho(\mathbf{P}(\mathbf{0}_m, v, u_c))|_{v=u_c} < 0;$
- (b) $-2 < \theta \partial_v^2 \ln \rho(\mathbf{P}(\mathbf{0}_m, v, u_c))|_{v=u_c};$
- (c) $r_0 < 1.$

If any one of these three inequalities is reversed, the extinction equilibrium is unstable.

Let $\mathbf{x}(t) = \text{col}(\mathbf{x}(t), u(t)) \in R_+^m \times \Lambda$ be a solution of the Darwinian model (5.15). At any time t , the function of v

$$\ln \rho(\mathbf{P}(\mathbf{x}(t), v, u(t)))$$

is called the **adaptive landscape** associated with the model. Note that the trait equation in the Darwinian model (5.15) implies that the mean trait, at each time, moves in an uphill direction on the landscape at that time (note that the landscape is not in general fixed in time as $u(t)$ evolves). A critical trait u_c is, by its definition, a critical point $v = u_c$ (in the calculus sense) of the adaptive landscape $\ln \rho(\mathbf{P}(\mathbf{0}_m, v, u_c))$ at the extinction equilibrium. The necessary condition (a) in Lemma 5.7 for the stability of the associated extinction equilibrium implies that $v = u_c$ is located at a local maximum on this adaptive landscape. On the other hand, if the inequality (a) is reversed and u_c is located at a local minimum, then the extinction equilibrium is unstable. We return to adaptive landscapes in Section 5.4.

Assuming that inequality (a) holds, we can interpret the necessary condition (b) for stability in Lemma 5.7 as a constraint on the speed of evolution θ . If the speed of evolution is too fast, in the sense that (b) fails to hold, then the extinction equilibrium is unstable.

From Lemma 5.7, we obtain the following result concerning the stability of an extinction equilibrium as r_0 is increased through 1.

Theorem 5.8. *Assume Assumption 5.3 holds and that $\theta > 0$. If $u = u_c$ is a critical trait for which Lemma 5.7(a) and (b) hold when $r_0 = 1$, then the extinction equilibrium (5.18) associated with u_c loses stability as the inherent population growth rate $r_0 \approx 1$ increases through 1.*

Proof. We need only note that if (a) and (b) hold in Lemma 5.7 when $r_0 = 1$, then by continuity they hold for $r_0 \approx 1$. Thus by Lemma 5.7, the extinction equilibrium is stable for $r_0 < 1$ and unstable $r_0 > 1$. \square

Example 5.9. The Darwinian semelparous discrete logistic model (5.8) in Example 5.1,

$$\begin{aligned}x(t+1) &= b_0 \exp\left(-\frac{1}{2}u^2(t)\right) \frac{1}{1+c_0x(t)} x(t) \\ u(t+1) &= u(t) + \theta\left(-u(t) - c_1 \frac{1}{1+c_0x(t)} x(t)\right),\end{aligned}$$

is associated with the 1×1 projection matrix

$$(5.19) \quad \mathbf{P}(\mathbf{x}, v, u) = \left[b_0 \exp\left(-\frac{1}{2}v^2\right) \frac{1}{1+c(v-u)x} \right]$$

whose spectral radius is

$$\rho(\mathbf{P}(\mathbf{x}, v, u)) = b_0 \exp\left(-\frac{1}{2}v^2\right) \frac{1}{1+c(v-u)x}.$$

We saw in Example 5.5 that the only critical trait is $u_c = 0$ and that the associated extinction equilibrium is $\mathbf{x} = \text{col}(x, u) = \text{col}(0, 0)$ for all values of $b_0 > 0$. A calculation shows

$$r_0 = \rho(\mathbf{P}(\mathbf{0}_m, v, u_c)|_{v=u_c}) = b_0$$

and

$$\partial_v^2 \ln \rho(\mathbf{P}(\mathbf{0}_m, v, 0))|_{v=0} = -1 < 0.$$

Thus, (a) and (b) in Lemma 5.7 hold if $\theta < 2$ (i.e., the speed of evolution is not too fast), in which case the extinction equilibrium, by Theorem 5.8, loses stability as b_0 increases through 1. On the other hand, if $\theta > 2$, then the extinction equilibrium is unstable for all values of b_0 . \square

Example 5.10. In Example 5.2, we calculated the spectral radius

$$\rho(\mathbf{P}(\mathbf{x}, v, u)) = \frac{1}{2} \left(s_2 + \sqrt{s_2^2 + 4s_1 b_0 \exp\left(-\frac{1}{2}v^2\right) \frac{1}{1+c(v-u)x_2}} \right)$$

of the 2×2 projection matrix (5.11) and used it to construct the Darwinian juvenile-adult model (5.12). We saw in Example 5.6 that the only critical trait is $u_c = 0$, which yields the associated extinction equilibrium $\mathbf{x} = \text{col}(\mathbf{0}_2, 0)$ for all values of $b_0 > 0$ and

$$r_0 = \rho(\mathbf{P}(\mathbf{0}_m, v, 0)|_{v=0}) = \frac{1}{2} \left(s_2 + \sqrt{s_2^2 + 4s_1 b_0} \right).$$

In order to apply Theorem 5.8, we need to verify conditions (a) and (b) in Lemma 5.7, which involves a calculation of the second derivative

$$\partial_v^2 \ln \rho(\mathbf{P}(\mathbf{0}_m, v, 0))|_{v=0}$$

when $r_0 = 1$, that is to say when

$$b_0 = \frac{1 - s_2}{s_1}.$$

The result is

$$\partial_v^2 \ln \rho(\mathbf{P}(\mathbf{0}_m, v, 0))|_{v=0} = -\frac{1}{2 - s_2} < 0,$$

which shows (a) in Lemma 5.7 holds. Inequality (b) in Lemma 5.7 holds if

$$\theta < 2(2 - s_2),$$

and under this condition, we conclude from Theorem 5.8 that the extinction equilibrium of the Darwinian juvenile-adult model (5.12) loses stability as r_0 increases through 1 (or equivalently, as b_0 increases through $(1 - s_2)/s_1$). On the other hand, if $\theta > 2(2 - s_2)$, then the extinction equilibrium is unstable for all values of r_0 . \square

The tedious details in dealing with the first and second derivatives of the spectral radius $\ln \rho(\mathbf{P}(\mathbf{x}, v, u))$ in making use of Theorem 5.8 can be simplified by using R_0 , a topic we take up in Section 5.5.

5.3. A Basic Bifurcation Theorem

We saw in Chapters 1 and 3 how the destabilization of the extinction equilibrium (or a disease-free equilibrium in Chapter 4) gives rise to positive equilibria (or endemic equilibria in Chapter 4) through a transcritical bifurcation. It is natural to expect the same is true for Darwinian models (5.10).

If (similar to (3.18) for nonevolutionary matrix models) we define

$$(5.20) \quad \kappa := -\mathbf{w}^T [\nabla_{\mathbf{x}}^0 p_{ij} \cdot \mathbf{v}] \mathbf{v},$$

where the superscript “0” now means evaluation at the bifurcation point $\text{col}(\mathbf{x}, u) = \text{col}(\mathbf{0}_m, u_c)$ when $r_0 = 1$ and \mathbf{w}^T and \mathbf{v} are left and right positive eigenvectors of $\mathbf{P}(\mathbf{0}_m, v, u_c)|_{v=u_c}$ associated with eigenvalue 1, then Theorem 5.11 follows from Theorem 3.2 in [37].

Theorem 5.11. *Assume Assumption 5.3, that $\theta > 0$, and that $u = u_c$ is a critical trait for which $\kappa \neq 0$.*

(a) *Equilibria of the Darwinian model (5.10) of the form*

$$\mathbf{x}_e = \frac{\mathbf{w}^T \mathbf{v}}{\kappa} (r_0 - 1) \mathbf{v} + O((r_0 - 1)^2)$$

$$u_e = u_c + O(r_0 - 1).$$

bifurcate from the extinction equilibrium $\text{col}(\mathbf{x}, u) = \text{col}(\mathbf{0}_m, u_c)$ for $r_0 \approx 1$.

(b) *Assume $\mathbf{P}(\mathbf{0}_m, v, u_c)|_{v=u_c}$ is primitive. If (a) and (b) in Lemma 5.7 hold when $r_0 = 1$, then $\kappa > 0$ implies that the bifurcating equilibria are positive for $r_0 \gtrapprox 1$ and are (locally asymptotically) stable, in which case we say the bifurcation is forward and stable. If $\kappa < 0$, then the bifurcating equilibria are positive for $r_0 \lesssim 1$ and are unstable, in which case we say the bifurcation is backward and unstable.*

The following corollary is an immediate consequence of the definition (5.20) of κ and the positivity of the vectors \mathbf{w} and \mathbf{v} .

Corollary 5.12. *Assume the conditions in Theorem 5.11 hold. If all partial derivatives $\partial_{x_k}^0 p_{ij}$ are nonpositive and at least one is negative, then the bifurcation of positive equilibria at $r_0 = 1$ is forward and stable.*

Example 5.13. We saw in Example 5.9 that (a) and (b) in Lemma 5.7 hold at $r_0 = 1$ for the Darwinian semelparous discrete logistic model (5.8) when $\theta < 2$. Since the single entry in the 1×1 projection matrix (5.19) is a (strictly) decreasing function of $x > 0$, we conclude from Corollary 5.12 that when $\theta < 2$, there occurs a forward-stable bifurcation of positive equilibria as $r_0 = b_0$ increases through 1. \square

The Darwinian juvenile-adult model (5.12) in Example 5.10 provides an application to a structured population model.

Example 5.14. We saw in Example 5.10 that (a) and (b) in Lemma 5.7 hold at $r_0 = 1$ when $\theta < 2(2 - s_2)$. We note that the projection matrix is primitive if $s_2 > 0$. Since the only density-dependent entry in the projection matrix (5.11) of the Darwinian juvenile-adult model (5.12) is a (strictly) decreasing function of $x_2 > 0$, we conclude from Corollary 5.12 that there occurs a forward-stable bifurcation of positive equilibria as

$$r_0 = \frac{1}{2} \left(s_2 + \sqrt{s_2^2 + 4s_1 b_0} \right)$$

increases through 1 (or as b_0 increases through $(1 - s_2)/s_1$). \square

Models with a nonlinear term that increases with increases in low-level population density (i.e., that have an Allee component) can have backward-unstable bifurcations. Here is an example.

Example 5.15. Suppose we modify the discrete logistic by including an Allee component effect that acts on newborn survival. Specifically, we use the Allee factor (1.14) with $q = 1$ and obtain the population growth rate

$$r(x) = b \frac{1}{1+cx} s \frac{1+ax}{1+sax}$$

with $b, c, a > 0$ and $0 < s < 1$.

A Darwinian version of the model results from assuming that fertility

$$b = b_0 e^{-v^2/2}$$

depends on the phenotypic trait and that the competition and Allee coefficients $c = c(v - u)$ and $a = a(v - u)$ depend on the trait difference to the population mean. This gives

$$r(x, v, u) = sb_0 \exp\left(-\frac{1}{2}v^2\right) \frac{1}{1+c(v-u)x} \frac{1+a(v-u)x}{1+s a(v-u)x}.$$

In this example, we assume the competition and Allee coefficients $c(z)$ and $a(z)$ have global maxima at $z = 0$ so that

$$\partial_z c(0) = \partial_z a(0) = 0.$$

Biologically these assumptions mean that the maximum density effect c_0 on the fertility of an individual with trait v caused by intraspecific competition occurs when $v = u$ (i.e., the individual is like most other individuals as represented by the mean) and that the optimal benefit of the Allee component a_0 , due say to communal protection of newborns, is provided to a newborn with the most common trait u in the population.

With these assumptions in the general Darwinian model (5.10), we obtain the equations

$$(5.21) \quad \begin{aligned} x(t+1) &= sb_0 \exp\left(-\frac{1}{2}u^2(t)\right) \frac{1}{1+c_0x(t)} \frac{1+a_0x(t)}{1+s a_0x(t)} x(t) \quad \text{and} \\ u(t+1) &= (1-\theta)u(t). \end{aligned}$$

The only extinction equilibrium is $\text{col}(x, u) = \text{col}(0, 0)$. To invoke Theorem 5.11, we need to ensure conditions (a) and (b) in Lemma 5.7 hold

when $r_0 = 1$, namely that

- (a) $\partial_v^2 \ln r(0, v, 0)|_{v=0} < 0$;
- (b) $-2 < \theta \partial_v^2 \ln r(0, v, 0)|_{v=0}$.

A calculation shows

$$r_0 = sb_0$$

and

$$\partial_v^2 \ln r(0, v, 0)|_{v=0} = -1$$

when $r_0 = 1$; hence, (a) holds. Condition (b) holds if $\theta < 2$ (i.e., if the speed of evolution is not too fast). Under this condition, the extinction equilibrium loses stability as $r_0 = sb_0$ increases through 1 (Theorem 5.8), resulting in a bifurcation of positive equilibrium from the extinction equilibrium (Theorem 5.11(a)).

To determine the direction of bifurcation (and hence the stability of the bifurcating positive equilibria), we calculate κ from formula (5.20) (noting that $\mathbf{v} = \mathbf{w} = 1$ in an $m = 1$ dimensional case):

$$\kappa := -\partial_x r(0, v, 0)|_{v=0} = sb_0(c_0 - (1-s)a_0).$$

By Theorem 5.11(b), we see that the bifurcation is

- forward and stable if $\frac{a_0}{c_0} < \frac{1}{1-s}$;
- backward and unstable if $\frac{a_0}{c_0} > \frac{1}{1-s}$.

If the Allee component effect a_0 on newborn survival is sufficiently large compared to the strength of the negative feedback effect c_0 on fertility, then the bifurcation is backward and unstable. In the opposite case, the bifurcation is forward and stable. \square

We saw in Section 3.5.4 that backward bifurcations in population models generally give rise to a strong Allee effect (i.e., to an interval of r_0 values less than 1 for which there exist a stable positive equilibrium in addition to the stable extinction equilibrium). We might expect to see this multi-attractor scenario for Darwinian models as well, although there are currently no general theorems to support this (as there are for nonevolutionary models [33]). The simulations shown in Figure 5.1 suggests that a strong Allee effect can occur in the model (5.21).

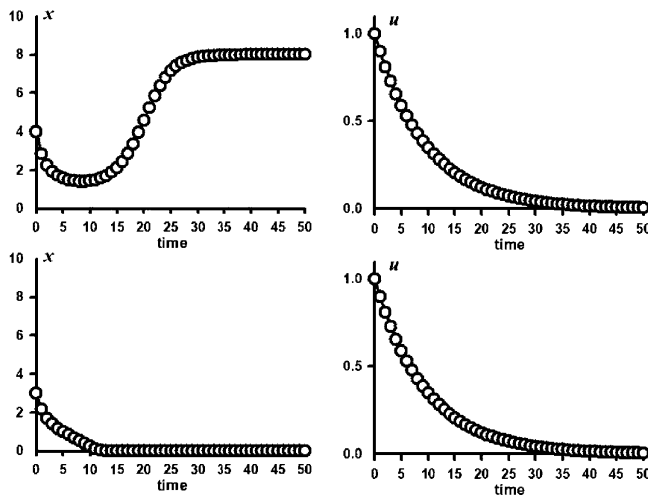


Figure 5.1. Two solutions of Equations (5.21) with $b_0 = 2$, $s = 0.1$, $c_0 = 0.1$, $a_0 = 10$, and $\theta = 0.1$ illustrate a strong Allee effect. **First row:** The solution with initial condition $\text{col}(x(0), u(0)) = (4, 1)$ approaches the positive equilibrium $\text{col}(8, 0)$. **Second row:** The solution with initial condition $\text{col}(x(0), u(0)) = (3, 1)$ approaches the extinction equilibrium.

5.4. The ESS Maximum Principle

The Darwinian model equations (5.1) and (5.2) concern trait-driven (or strategy-driven) evolution. The model tracks the evolution of the mean trait within a population. Invasion-driven evolution, on the other hand, concerns evolutionary change caused by the invasion of mutant populations displacing a resident population [129]. However, if the resident population is immune to invasion by mutant populations, then its trait is said to be an ESS, which stands for **evolutionarily stable strategy** (strategy is synonymous with trait). Here, the invading species is reproductively isolated from the resident species (i.e., members of the resident species do not have mutant offspring and vice versa).²

One way to approach this problem is to begin with a Darwinian model (5.10) that has a stable equilibrium $\text{col}(\mathbf{x}_e, u_e)$ and couple it to

²This is the case with an asexually reproducing population in which a genetic mutation has occurred. It is also the central notion of allopatric speciation of sexually reproducing species, in which two subpopulations are geographically separated for enough time to become, by natural selection, reproductively isolated and are then reunited.

a Darwinian model for the invading mutant population (which presumably would be a similar model to that of the resident since it models a mutant population). The resulting high-dimensional, coupled system has an equilibrium with the resident population at $\text{col}(\mathbf{x}_e, u_e)$ and the invading population at an extinction equilibrium, which if globally attracting, would imply that the mutant invasion would fail. Another approach is to make use of the following theorem.

Theorem 5.16. The ESS Maximum Principle [129]. *The trait component u_e associated with an equilibrium $\text{col}(\mathbf{x}_e, u_e)$ of the Darwinian equations (5.10) is an ESS if and only if*

- (a) *$\text{col}(\mathbf{x}_e, u_e)$ is a stable equilibrium of the Darwinian equations (5.10), and*
- (b) *the adaptive landscape $\ln \rho(\mathbf{P}(\mathbf{x}_e, v, u_e))$ has a global maximum at $v = u_e$.*

As an example, consider the Darwinian semelparous discrete logistic model (5.8) with a competition coefficient

$$(5.22) \quad c(v - u) = c_0 \exp\left(-\frac{1}{2w}(v - u)^2\right).$$

This models the situation when the maximum competition intensity is experienced individuals whose trait v equals the population mean trait u . The Darwinian model equations (5.8) become

$$(5.23) \quad \begin{aligned} x(t+1) &= b_0 \exp\left(-\frac{1}{2}u^2(t)\right) \frac{1}{1+c_0x(t)} x(t) \quad \text{and} \\ u(t+1) &= (1-\theta)u(t). \end{aligned}$$

In Example 5.13, we saw that Corollary 5.12 implies that when $\theta < 2$, the extinction equilibrium loses stability as b_0 increases through 1, at which a forward-stable bifurcation of positive equilibria occurs for $b_0 \gtrapprox 1$.

We can prove more in this example by solving the equilibrium equations

$$\begin{aligned} x &= b_0 \exp\left(-\frac{1}{2}u^2\right) \frac{1}{1+c_0x} x \quad \text{and} \\ u &= (1-\theta)u \end{aligned}$$

explicitly for the positive equilibria

$$(5.24) \quad \mathbf{x}_e = \begin{bmatrix} x_e \\ u_e \end{bmatrix} = \begin{bmatrix} \frac{b_0-1}{c_0} \\ 0 \end{bmatrix} \quad \text{for all } b_0 > 1,$$

which exist (and are unique). The Jacobian associated with (5.23), when evaluated at a positive equilibrium, is

$$\begin{bmatrix} \frac{1}{b_0} & 0 \\ 0 & 1 - \theta \end{bmatrix}.$$

When $\theta < 2$, the eigenvalues $\lambda_1 = 1/b_0$ and $\lambda_2 = 1 - \theta$ satisfy $|\lambda_i| < 1$, and by the Linearization Principle, the positive equilibria are (locally asymptotically) stable for all $b_0 > 1$.

But is the trait component $u_e = 0$ associated with these stable equilibria an ESS? The answer is “not necessarily.” This is because adaptive landscape at a positive equilibrium

$$\begin{aligned} \ln \rho(\mathbf{P}(\mathbf{x}_e, v, 0)) &= \ln \left(b_0 \exp\left(-\frac{1}{2}v^2\right) \frac{1}{1 + c(v) \frac{b_0 - 1}{c_0}} \right) \\ &= \ln b_0 - \frac{1}{2}v^2 - \ln \left(1 + (b_0 - 1) \exp\left(-\frac{v^2}{2w}\right) \right) \end{aligned}$$

does not necessarily have a global maximum at $v = 0$.

To see this, we first note that this function of v approaches $-\infty$ as $v \rightarrow \pm\infty$; hence, its global maximum occurs at a finite critical point, which is a root of the derivative

$$\partial_v \ln \rho(\mathbf{P}(\mathbf{x}_e, v, 0)) = v \frac{-w + (1-w)(b_0 - 1) \exp\left(-\frac{v^2}{2w}\right)}{w \left((b_0 - 1) \exp\left(-\frac{v^2}{2w}\right) + 1 \right)}.$$

Clearly $v = 0$ is a critical point. If it is the only critical point, then the global maximum of the adaptive landscape must occur there, and $v = 0$ is an ESS.

However, other critical points are possible on the adaptive landscape. Two other critical points are found from the roots of the numerator, namely

$$v_{\pm} = \pm 2w \ln \left(\frac{(b_0 - 1)(1 - w)}{w} \right) \neq 0$$

provided

$$\frac{(b_0 - 1)(1 - w)}{w} > 1,$$

that is to say provided

$$w < 1 \quad \text{and} \quad b_0 > \frac{1}{1 - w}.$$

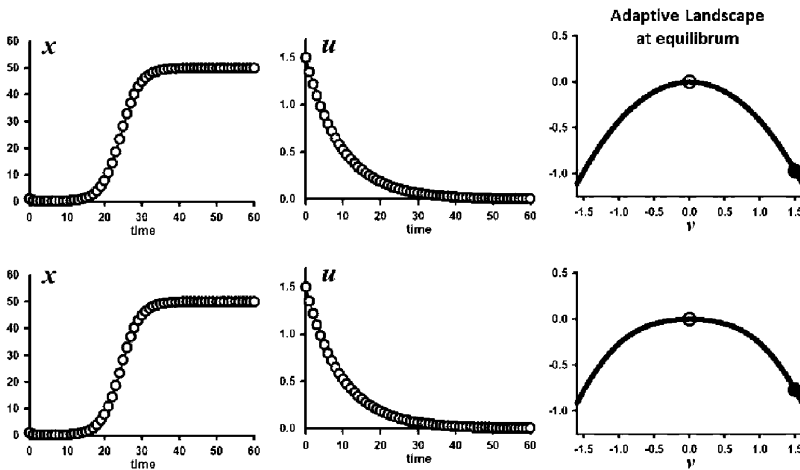


Figure 5.2. These two rows of plots illustrate the two possibilities found for the Darwinian model (5.23) when the trait component $u_e = 0$ of the positive equilibrium (5.24) is an ESS. Shown are the time series of the x and u components of the solution of equations (5.23) with initial condition $\mathbf{x}(0) = \text{col}(1, 1.5)$, parameter values $\theta = 1/10$, $b_0 = 3/2$, and $c_0 = 1/100$, and equilibrium $\mathbf{x}_e = \text{col}(50, 0)$ given by formula (5.24). **First row:** $w = 2$. **Second row:** $w = 1/2$ (in which case $b_0 < (1-w)^{-1} = 2$). The solid circle on the adaptive landscapes indicates the location of the initial condition $u(0) = 1.5$. The open circle indicates that of the equilibrium trait component $u_e = 0$, which is located at the global maximum of the landscape.

In this case, a calculation shows

$$\partial_v^2 \ln \rho(\mathbf{P}(\mathbf{x}_e, v, 0))|_{v=0} = \frac{1-w}{wb_0} \left(b_0 - \frac{1}{1-w} \right) > 0,$$

and as a result, $v = 0$ is a local minimum. This means that the global maximum of the adaptive landscape occurs at $v = v_{\pm}$ and that $v = 0$ is not an ESS.

In summary, for $\theta < 2$:

- If the width w of the distribution (5.22) of the trait difference dependent competition coefficient is sufficiently large, specifically if $w > 1$, then the trait $u = 0$

associated with the stable positive equilibrium (5.24) is an ESS for all $b_0 > 1$.

- On the other hand, if the width $w < 1$, then $u = 0$ is an ESS only for inherent birth rates b_0 small enough, namely $b_0 < (1 - w)^{-1}$, and is not an ESS for larger b_0 .

What happens when the speed of evolution is too fast (i.e., if $\theta > 2$)? In this case, the population goes extinct for all $b_0 > 1$ (despite the fact that the extinction equilibrium is unstable!). This is a case of so-called **evolutionary suicide**. See Exercise 5.29.

See Figure 5.2 for examples when $u = 0$ is an ESS trait for the Darwinian logistic equation (5.23). Figure 5.3 shows an example when $u = 0$ is not an ESS and also how $u = 0$ ends up at a minimum on the adaptive landscape despite the fact that the trait equation in Darwinian models requires $u(t)$ to move uphill on the adaptive landscape. This occurs because the adaptive landscape does not remain constant over time.

A method utilizing Darwinian dynamic models that is widely used to study evolutionary processes, called Adaptive Dynamics, applies under some severe restrictions. It assumes that only equilibrium dynamics occur and that the timescale on which the population dynamics equilibrate is virtually instantaneous compared to the timescale for the evolutionary dynamics of the mean trait. The method then utilizes a method called quasi-equilibration or quasi-steady-state approximation to study the trait-driven dynamics of a Darwinian model.³ Roughly speaking, it is assumed that the population remains near an equilibria (in a so-called quasi-equilibrium state), which reduces the dimension of the model to just the trait equation with the population held fixed at the quasi-equilibrium. The equilibrium of the resulting trait equation is then returned to the population equation, held fixed, to get a new quasi-equilibrium state for the population, and the process is repeated until the sequence of quasi-equilibrium traits converge. The accuracy of this method to describe trait-driven evolution defined by the Darwinian equations is not always guaranteed but can be rigorously justified using what is called singular perturbation theory (topics beyond the scope of

³This classical method was originally developed for the study of thermodynamics in physics.

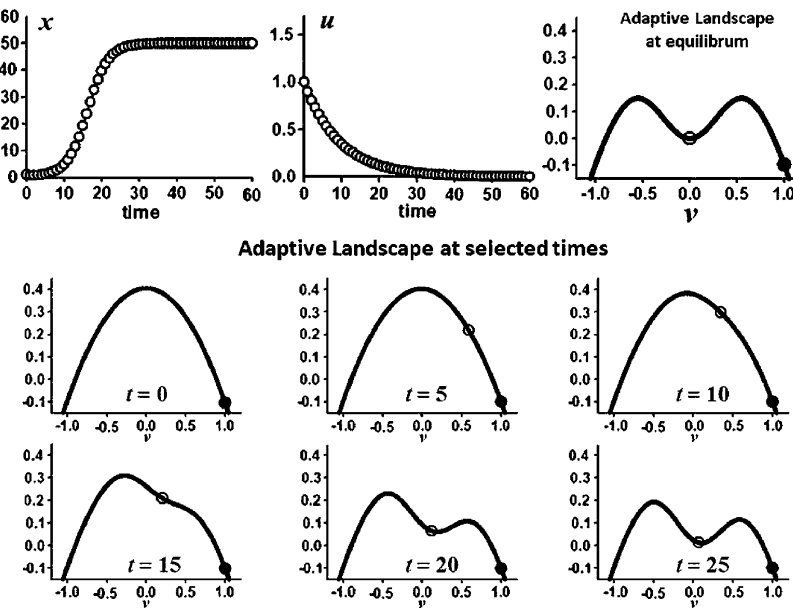


Figure 5.3. These graphs illustrate a case found for the Darwinian model (5.23) when the trait component $u_e = 0$ of the positive equilibrium (5.24) is not an ESS. **First row:** Shown are the time series of the x and u components of the solution of equations (5.23) with initial condition $\mathbf{x}(0) = \text{col}(1, 1)$ and parameter values $\theta = 0.1$, $b_0 = 1.5$, $c_0 = 0.01$, and $w = 0.1$. In this case, $w < 1$ and $b_0 > b_c = 10/9$. These graphs show that the solution approaches the equilibrium $\mathbf{x}_e = \text{col}(50, 0)$ given by formula (5.24). The open circle on the adaptive landscape at equilibrium indicates the location of the equilibrium trait $u_e = 0$, and the solid circle indicates that of the initial condition $u(0) = 1$. Note that the open circle is not located at the global maximum of the landscape, but at a local minimum. **Second and third rows:** The evolving landscape is shown at selected times in order to illustrate how the trait $u(t)$ (indicated by the open circles) manages to end up at a minimum as $t \rightarrow +\infty$, all the while moving uphill on the landscape.

this book). Using this method for trait-driven evolution, Adaptive Dynamics then analyzes mutant- or invasion-driven dynamics by studying the adaptive landscape. This method is generally applied to differential equation models but could in principle be applied to difference equation models. See [57] for an introduction to this method. The webpage <https://www.mv.helsinki.fi/home/kisdi/addyn.htm> con-

tains many references to papers and review articles on Adaptive Dynamics. Also see [1] and the cited references for further commentary and discussion.

5.5. R_0 for Darwinian Models

Suppose we additively decompose the projection matrix in equation (5.10), as in Chapters 2 and 3, into a fertility and transition matrix

$$\mathbf{P}(\mathbf{x}, v, u) = \mathbf{F}(\mathbf{x}, v, u) + \mathbf{T}(\mathbf{x}, v, u),$$

where the entries in the fertility matrix

$$\mathbf{F}(\mathbf{x}, v, u) = [f_{ij}(\mathbf{x}, v, u)]$$

and transition matrix

$$\mathbf{T}(\mathbf{x}, v, u) = [\tau_{ij}(\mathbf{x}, v, u)].$$

Assumption 5.17. $f_{ij}, \tau_{ij} \in C^2(R^m \times \Lambda \times \Lambda : R_+)$, where Λ is an open interval in R^1 . For all $(\mathbf{x}, v, u) \in R_+^m \times \Lambda \times \Lambda$, the inequalities $0 \leq \tau_{ij}(\mathbf{x}, v, u) \leq 1$ and $\sum_{j=1}^m \tau_{ij}(\mathbf{x}, v, u) \leq 1$ hold, and the density-free terms $f_{ij}(\mathbf{0}_m, v, u)$ and $\tau_{ij}(\mathbf{0}_m, v, u)$ satisfy

$$(5.25) \quad \partial_u f_{ij}(\mathbf{0}_m, v, u) \equiv \partial_u \tau_{ij}(\mathbf{0}_m, v, u) \equiv 0$$

for all $u, v \in \Lambda$. The projection matrix $\mathbf{P}(\mathbf{x}, v, u)$ is irreducible for each $(\mathbf{x}, v, u) \in R_+^m \times \Lambda \times \Lambda$.

If we assume Assumption 5.17, then the projection matrix $\mathbf{P}(\mathbf{x}, v, u)$ satisfies Assumption 5.3 that was necessary for the results in the previous sections.

The analysis of the Darwinian matrix model (5.10) in Sections 5.2 and 5.3 utilizes the spectral radius of the inherent projection matrix

$$\mathbf{P}(\mathbf{0}_m, v, u)|_{v=u} = \mathbf{F}(\mathbf{0}_m, v, u)|_{v=u} + \mathbf{T}(\mathbf{0}_m, v, u)|_{v=u}.$$

As for nonevolutionary matrix models in Chapter 3, we can instead use the often more analytically tractable reproduction number R_0 for the analysis. From the next generation matrix

$$\mathbf{F}(\mathbf{x}, v, u)(\mathbf{I} - \mathbf{T}(\mathbf{x}, v, u))^{-1},$$

we define the reproduction number

$$r_0(\mathbf{x}, v, u) := \rho(\mathbf{F}(\mathbf{x}, v, u)(\mathbf{I} - \mathbf{T}(\mathbf{x}, v, u))^{-1}).$$

For notational simplification, we introduce the notation

$$\begin{aligned} r_0(\mathbf{0}_m, v, u) &:= \rho(\mathbf{P}(\mathbf{0}_m, v, u)) \quad \text{and} \\ R_0(\mathbf{0}_m, v, u) &:= \rho\left(\mathbf{F}(\mathbf{0}_m, v, u)(\mathbf{I} - \mathbf{T}(\mathbf{0}_m, v, u))^{-1}\right). \end{aligned}$$

Note that the bifurcation parameter in Sections 5.2 and 5.3 is $r_0 = r_0(\mathbf{0}_m, v, u_c)|_{v=u_c}$, where u_c is a critical trait.

In order to locate the bifurcation point from the theorems in Sections 5.2 and 5.3, we need to locate a critical trait $u = u_c$ such that

$$(5.26) \quad \begin{aligned} r_0(\mathbf{0}_m, v, u_c)|_{v=u_c} &= 1, \\ \partial_v r_0(\mathbf{0}_m, v, u_c)|_{v=u_c} &= 0, \quad \text{and} \\ \partial_v^2 r_0(\mathbf{0}_m, v, u_c)|_{v=u_c} &< 0. \end{aligned}$$

To do this using R_0 in place of r_0 , we utilize the following theorem.

Theorem 5.18. [32] Assume Assumption 5.17, $\theta > 0$, and

$$\rho\left(\mathbf{T}(\mathbf{0}_m, v, u_e)|_{v=u_e}\right) < 1.$$

(a) Then for any $u \in U$,

$$(5.27) \quad r_0(0, v, u)|_{v=u} = 1 \text{ if and only if } R_0(0, v, u)|_{v=u} = 1.$$

(b) If (5.27) holds for $u \in U$, then there exists a constant $k > 0$ such that

$$\partial_v R_0(0, v, u)|_{v=u} = k \partial_v r_0(0, v, u)|_{v=u}.$$

As a result,

$$(5.28) \quad \partial_v r_0(0, v, u)|_{v=u} = 0 \text{ if and only if } \partial_v R_0(0, v, u)|_{v=u} = 0.$$

(c) If (5.27) and (5.28) hold for $u \in U$, then

$$\partial_v^2 R_0(0, v, u)|_{v=u} = k \partial_v^2 r_0(0, v, u)|_{v=u}.$$

As a result,

$$(5.29) \quad \partial_v^2 r_0(0, v, u)|_{v=u} < 0 \text{ if and only if } \partial_v^2 R_0(0, v, u)|_{v=u} < 0.$$

It also follows that (5.29) remains valid if “ $<$ ” is replaced by “ $>$ ” or “ $=$ ”.

Based on Theorem 5.18, we see that finding trait $u = u_c$ that satisfies (5.26) is equivalent to finding a trait that satisfies

$$\begin{aligned} R_0(\mathbf{0}_m, v, u_c)|_{v=u_c} &= 1, \\ \partial_v R_0(\mathbf{0}_m, v, u_c)|_{v=u_c} &= 0, \quad \text{and} \\ \partial_v^2 R_0(\mathbf{0}_m, v, u_c)|_{v=u_c} &< 0. \end{aligned}$$

As a result, we have the following theorem.

Theorem 5.19. *Under the added assumption that*

$$\rho(T(\mathbf{0}_m, v, u_c)|_{v=u_c}) < 1,$$

Theorem 5.8, Theorem 5.11, and Corollary 5.12 hold with

$$r_0 := \rho(P(\mathbf{0}_m, v, u_c)|_{v=u_c})$$

replaced by

$$R_0 := R_0(\mathbf{0}_m, v, u_c)|_{v=u_c}.$$

A higher-dimensional Leslie matrix is a basic example for which no analytic formula is, in general, available for the dominant eigenvalue r_0 but for which a formula is available for R_0 (Chapter 2).

Example 5.20. Consider an m -dimensional nonlinear Leslie model with fertility and transition matrices

$$\mathbf{F}(\mathbf{x}) = \begin{bmatrix} 0 & b_2\beta_2(\mathbf{x}) & \cdots & b_{m-1}\beta_{m-1}(\mathbf{x}) & b_m\beta_m(\mathbf{x}) \\ 0 & 0 & \cdots & 0 & 0 \\ 0 & 0 & \cdots & 0 & 0 \\ \vdots & \vdots & & \vdots & \vdots \\ 0 & 0 & \cdots & 0 & 0 \end{bmatrix} \quad \text{and}$$

$$\mathbf{T}(\mathbf{x}) = \begin{bmatrix} 0 & 0 & \cdots & 0 & 0 \\ s_1 & 0 & \cdots & 0 & 0 \\ 0 & s_2 & \cdots & 0 & 0 \\ \vdots & \vdots & & \vdots & \vdots \\ 0 & 0 & \cdots & s_{m-1} & 0 \end{bmatrix} \quad \text{with } 0 < s_i < 1,$$

where $b_i > 0$ and all $\beta_i(\mathbf{0}_m) = 1$ (cf. Example 3.18). The associated matrix equation models the dynamics of a population structured into a juvenile class x_1 and $m - 1$ adult age classes x_i for $i = 2, \dots, m - 1$ with the time unit equal to the juvenile maturation period. Density affects fertility only, and individuals do not survive more than m time units.

Assume that an individual's age class fertility rates $b_i\beta_i(\mathbf{x})$ are dependent on its inherited trait v . Specifically, assume the density-free fertility rates have a Gauss-like distribution centered at $v = 0$

$$b_i(v) = b_{i,0}e^{-v^2/2w_i}, \quad w_i > 0 \text{ (not all equal to 0)},$$

where $b_{i,0} > 0$ is the maximal birth rate for i -class individuals. We leave the density factors $\beta_i(\mathbf{x}, v, u)$ general except that

$$\beta_i(\mathbf{0}_m, v, u) \equiv 1$$

so that Assumption 5.3 holds.

There is no analytic formula available for the dominant eigenvalue $r_0(\mathbf{x}, v, u)$ of the projection matrix $\mathbf{P}(\mathbf{x}, v, u) = \mathbf{F}(\mathbf{x}, v, u) + \mathbf{T}(\mathbf{x}, v, u)$, but there is a formula for $R_0(\mathbf{x}, v, u)$, namely

$$R_0(\mathbf{x}, v, u) = \sum_{i=1}^m \pi_i b_{i,0} e^{-v^2/2w_i} \beta_i(\mathbf{x}, v, u),$$

where

$$\pi_i = \begin{cases} 1 & \text{for } i = 1 \\ s_1 s_2 \cdots s_{i-1} & \text{for } i = 2, 3, \dots, m \end{cases}$$

(see equations (2.29) and (2.30)). A calculation shows

$$\partial_v R_0(\mathbf{0}_m, v, u)|_{v=u} = -u \sum_{i=1}^m \pi_i b_{i,0} \frac{1}{w_i} w_i e^{-u^2/2w_i};$$

hence, the only critical trait is $u_c = 0$, and the only extinction equilibrium is

$$\begin{bmatrix} \mathbf{x} \\ u \end{bmatrix} = \begin{bmatrix} \mathbf{0}_m \\ 0 \end{bmatrix}.$$

Note that

$$\mathbf{P}(\mathbf{0}_m, v, 0)|_{v=0} = \begin{bmatrix} 0 & b_{2,0} & \cdots & b_{m-1,0} & b_{m,0} \\ s_1 & 0 & \cdots & 0 & 0 \\ 0 & s_2 & \cdots & 0 & 0 \\ \vdots & \vdots & & \vdots & \vdots \\ 0 & 0 & \cdots & s_{m-1} & 0 \end{bmatrix}$$

is primitive (Theorem 2.12).

Other calculations show

$$\partial_v^2 R_0(\mathbf{0}_m, v, 0)|_{v=0} = - \sum_{i=1}^m \pi_i b_{i,0} \frac{1}{w_i} < 0$$

and

$$\rho(T(\mathbf{0}_m, v, u_c)|_{v=u_c}) = \rho \left(\begin{bmatrix} 0 & 0 & \cdots & 0 & 0 \\ s_1 & 0 & \cdots & 0 & 0 \\ 0 & s_2 & \cdots & 0 & 0 \\ \vdots & \vdots & & \vdots & \vdots \\ 0 & 0 & \cdots & s_{m-1} & 0 \end{bmatrix} \right) = 0 < 1.$$

Hence, we can apply Theorem 5.19, provided θ is sufficiently small (the speed of evolution is not too fast). We conclude that the extinction equilibrium loses stability as

$$R_0(\mathbf{0}_m, 0, 0) = \sum_{i=1}^m \pi_i b_{i0}$$

increases through 1.

Also from Theorem 5.19, we can conclude (provided θ is sufficiently small) that positive equilibria bifurcate from the extinction equilibria provided $\kappa \neq 0$ and that the direction of bifurcation (and hence the stability of the bifurcating positive equilibria) is determined by the sign of κ . For example, suppose there are no component Allee effects (i.e.,

$$\partial_{x_k} \beta_i(\mathbf{0}_m, 0, 0) \leq 0$$

for all k and i and that at least one derivative is negative). Then from formula (5.20) for κ , it is clear that $\kappa > 0$. In this case, the bifurcation is forward and stable. Specific examples are obtained if each density factor has one of the forms

$$\frac{1}{1 + c_i(v - u)p_i} \quad \text{or} \quad \exp(-c_i(v - u)p_i),$$

where

$$p_i = \omega_i \cdot \mathbf{x} = \sum_{j=1}^m w_{ij}x_j, \quad \omega_i \in R_+^m, \quad \|\omega_i\| = 1$$

are weighted total population sizes. □

5.6. Applications

5.6.1. Early Versus Delayed Reproduction. The scheduling of reproduction is a central issue in the analysis of life history strategies for any biological population [119]. Over the course of their lifetimes, should individuals reproduce uniformly or perhaps be more reproductive earlier (or later) in their lives? The answer is intimately tied up with survival

probabilities. For example, an individual with little survival probability would probably want to put maximum effort into early reproduction. In this section, we use the methodology in this chapter to build a low-dimensional model, which we can use to consider this question and to determine what scheduling strategy natural selection will favor under differing survival probabilities.

We build a Darwinian version of an $m = 2$ extended Leslie model by classifying individuals by age, but only crudely: x_1 are the individuals less than 1-year-old and x_2 are individuals older than 1 year. Assume individuals become reproductively active within 1 year and construct a 2×2 Leslie model, using 1 year as the time unit, with fertility and transition matrices

$$\mathbf{F} = \begin{bmatrix} b_1 & b_2 \\ 0 & 0 \end{bmatrix} \quad \text{and} \quad \mathbf{T} = \begin{bmatrix} 0 & 0 \\ s_1 & s_2 \end{bmatrix}$$

with $b_i > 0$ and $0 < s_i < 1$.

We assume density dependence on fertility only and that both classes are affected the same way by total population size

$$\mathbf{F}(\mathbf{x}) = \begin{bmatrix} b_1\beta(\|\mathbf{x}\|) & b_2\beta(\|\mathbf{x}\|) \\ 0 & 0 \end{bmatrix},$$

where

$$\mathbf{x} = \begin{bmatrix} x_1 \\ x_2 \end{bmatrix}, \quad \|\mathbf{x}\| = x_1 + x_2,$$

and the positive-valued (twice continuously differentiable) factor $\beta(z)$ satisfies

$$\beta(0) = 1 \quad \text{and} \quad \partial_z \beta(0) < 0.$$

We know, from the general theorems in Chapter 3, that a forward-stable bifurcation of positive equilibria occurs as

$$R_0 = b_1 + b_2 \frac{s_1}{1 - s_2}$$

increases through 1 (causing the extinction equilibrium to destabilize). We refer to b_1 and b_2 , respectively, as the “early” and “late” fertility rates of an individual, and we assume each is determined by a trait v subject to natural selection.

We assume that an individual with trait v has a fertility rate that is a fraction $\varphi_i(v)$ of b_i , which we view as the largest possible fertility rate

available to individuals. Specifically, we take $\varphi_i(v)$ to have a normal type distribution centered at v_i with variance w_i :

$$\varphi_i(v) = \exp\left(-\frac{(v - v_i)^2}{2w_i}\right).$$

We assume $v_1 \neq v_2$ so that individuals can maximize either early reproduction or late reproduction, but not both. Without loss in mathematical generality, take $v_1 = 0$ as the reference point for early reproduction and choose a trait scale so that $v_2 = 1$ for later reproduction. For simplicity in this application, we assume equal variances $w_1 = w_2 = w$. Thus,

$$\varphi_1(v) = \exp\left(-\frac{v^2}{2w}\right) \quad \text{and} \quad \varphi_2(v) = \exp\left(-\frac{(v-1)^2}{2w}\right)$$

for which

$$\mathbf{F}(\mathbf{x}, v) = \begin{bmatrix} b_1 \exp\left(-\frac{v^2}{2w}\right) \beta(\|\mathbf{x}\|) & b_2 \exp\left(-\frac{(v-1)^2}{2w}\right) \beta(\|\mathbf{x}\|) \\ 0 & 0 \end{bmatrix}.$$

(In this model, u does not appear in the matrix entries and is left out of the argument list in \mathbf{F} .) The projection matrix for this model

$$(5.30) \quad \mathbf{P}(\mathbf{x}, v) = \begin{bmatrix} b_1 \exp\left(-\frac{v^2}{2w}\right) \beta(\|\mathbf{x}\|) & b_2 \exp\left(-\frac{(v-1)^2}{2w}\right) \beta(\|\mathbf{x}\|) \\ s_1 & s_2 \end{bmatrix}$$

leads to the Darwinian model equations

$$(5.31) \quad \begin{aligned} \mathbf{x}(t+1) &= \mathbf{P}(\mathbf{x}, v)|_{v=u(t)} \mathbf{x}(t) \quad \text{and} \\ u(t+1) &= u(t) + \theta \partial_v \ln r(\mathbf{x}(t), v)|_{v=u(t)}, \end{aligned}$$

where $r(\mathbf{x}, v)$ is the spectral radius (dominant eigenvalue) of $\mathbf{P}(\mathbf{x}, v)$. The projection matrix $\mathbf{P}(\mathbf{x}, v)$ is a Leslie matrix with

$$R_0(\mathbf{x}, v) = b_1 \exp\left(-\frac{v^2}{2w}\right) \beta(\|\mathbf{x}\|) + b_2 \exp\left(-\frac{(v-1)^2}{2w}\right) \beta(\|\mathbf{x}\|) \frac{s_1}{1-s_2}.$$

(See equation (2.29) in Section 2.3.)

We want to determine the existence and stability of equilibria $\text{col}(\mathbf{x}_e, u_e) \in R_+^2 \times R$ and the ESS status of the trait component u_e . We are also interested in the fractions $\varphi_1(u_e)$ and $\varphi_2(u_e)$ because they indicate, respectively, the effort directed toward early and late reproduction when at equilibrium.

Theorems 5.18 and 5.19 imply (if the speed of evolution is not too fast) that a forward-stable bifurcation of positive equilibria occurs at $R_0(\mathbf{0}_2, u_c) = 1$, where u_c is a critical point (i.e., a point $u = u_c$, where $\partial_v R_0(\mathbf{0}_2, v)|_{v=0} = 0$ or equivalently $\partial_v R_0(\mathbf{0}_2, v)|_{v=u} = 0$). We know the bifurcation is forward since the nonlinearities in $\mathbf{P}(\mathbf{x}, v)$ are both negative density effects (i.e., $\partial_z \beta(0) < 0$). The bifurcating positive equilibria have trait components $u_e \approx u_c$ for $R_0(\mathbf{0}_2, u_c) \gtrsim 1$; therefore, $\varphi_i(u_e) \approx \varphi_i(u_c)$. The properties of positive equilibria lying outside a neighborhood of the bifurcation point depend on the properties of the nonlinearity $\beta(z)$. We will consider only positive equilibria near the bifurcation point.

Our attention is then directed to critical traits, that is to say the roots $v = u_c$ of the equation $\partial_v R_0(\mathbf{0}_2, v)|_{v=u} = 0$ which (after a cancellation of the factor $-1/w$) is

$$b_1 u \exp\left(-\frac{u^2}{2w}\right) + b_2 (u - 1) \exp\left(-\frac{(u-1)^2}{2w}\right) \frac{s_1}{1-s_2} = 0.$$

Clearly, neither $u = 0$ or $u = 1$ are roots of this equation. By algebraically rewriting this equation for u as

$$h(u) = \delta,$$

where

$$\begin{aligned} \delta &:= b_1 \left(b_2 \frac{s_1}{1-s_2} \right)^{-1} \text{ and} \\ h(u) &:= \frac{1-u}{u} \exp\left(\frac{1}{w} \left(u - \frac{1}{2}\right)\right), \end{aligned}$$

we see that there are no roots for $u < 0$ or $u > 1$ (since $\delta > 0$ and $h(u)$ is negative). On the remaining interval $0 < u < 1$, some straightforward calculus shows that positive-valued function $h(u)$ is a monotonically decreasing function if

$$w > \frac{1}{4},$$

which we assume holds. Since

$$\lim_{u \rightarrow 0^+} h(u) = +\infty \quad \text{and} \quad h(1) = 0,$$

it follows that there is a unique root (critical point) $u_c(\delta)$ for each value of $\delta > 0$, namely

$$u_c(\delta) = h^{-1}(\delta).$$

As previously noted, stable positive equilibria exist (by bifurcation from the extinction equilibrium associated with a critical trait $u_c(\delta)$ provided evolution is not too fast) at least for $R_0(\mathbf{0}_2, u_c(\delta)) \gtrsim 1$. What life history characteristics do these equilibria have? Specifically, what are the relative values of $\varphi_1(u_c(\delta))$ and $\varphi_2(u_c(\delta))$?

Note that

$$u_c(0) = 1 \quad \text{and} \quad \lim_{\delta \rightarrow +\infty} u_c(\delta) = 0.$$

Also note that

$$\begin{aligned} \varphi_1(u_c(0)) &< 1, & \varphi_2(u_c(0)) &= 1, \\ \lim_{\delta \rightarrow +\infty} \varphi_1(u_c(\delta)) &= 1, & \text{and} \quad \lim_{\delta \rightarrow +\infty} \varphi_2(u_c(\delta)) &< 1. \end{aligned}$$

For the positive equilibria

$$\text{col}(\mathbf{x}_e, u_e) \approx \text{col}(\mathbf{0}_2, u_c(\delta))$$

when

$$R_0(\mathbf{0}_2, u_c(\delta)) \gtrsim 1,$$

we have the following conclusions:

- $\delta \approx 0$ implies $\varphi_1(u_e) < 1$ and $\varphi_2(u_e) \approx 1$;
- $\delta \approx +\infty$ implies $\varphi_1(u_e) \approx 1$ and $\varphi_2(u_e) < 1$.

The quantity δ is the ratio between the maximal possible newborns produced by early reproduction b_1 and the (lifetime) expected newborns produced by late reproduction (i.e., $b_2 s_1 / (1 - s_2)$). Thus, we get the following not surprising result.

For small δ , late reproduction is maximized (and early reproduction is not), whereas for large δ , the opposite is true (i.e., early reproduction is maximized [and late reproduction is not]). That is to say, if births from early reproduction are low relative to those obtained from later reproduction, then the equilibrium trait u_e corresponds to late reproduction (and vice versa).

But is u_e an ESS trait (i.e., does the adaptive landscape

$$\ln \rho(\mathbf{P}(\mathbf{x}_e, v)),$$

or equivalently $\rho(\mathbf{P}(\mathbf{x}_e, v))$, have a global maximum at $v = u_e$)? The answer is yes, as we can see as follows. By Theorems 2.15 and 5.18 that

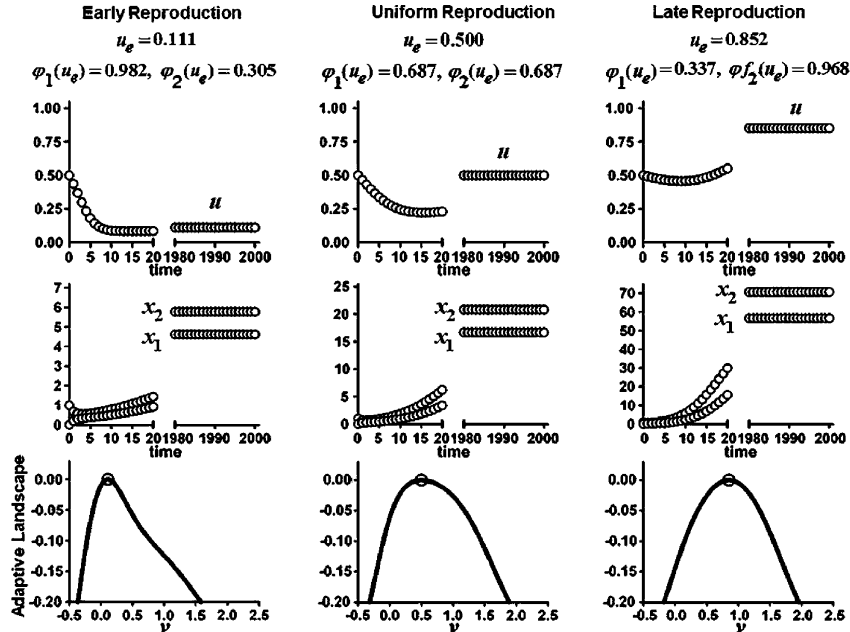


Figure 5.4. The time series of the solutions of the Darwinian model (5.30)–(5.31) with initial conditions $\mathbf{x}(0) = \text{col}(1, 0)$ and $u(0) = 0.5$ and parameter values $b_1 = 1$, $c = 1/100$, $s_1 = 1/5$, $s_2 = 3/4$, $w = 1/3$, and $\theta = 1/4$ are shown in three columns of plots for three values of b_2 . The left column with $b_2 = 0.5$ shows a trait equilibrium $u_e = 0.111$ (which gives $R_0(\mathbf{0}_2, u_e) = 1.104$) and a reproductive schedule with an emphasis on early reproduction. The center column with $b_2 = 1.25$ shows a trait equilibrium $u_e = 0.500$ (which gives $R_0(\mathbf{0}_2, u_e) = 1.375$) and a reproductive schedule with uniform reproduction schedule. The right column with $b_2 = 2.5$ shows a trait equilibrium at $u_e = 0.852$ (which gives $R_0(\mathbf{0}_2, u_e) = 2.272$) and a reproductive schedule with an emphasis on late reproduction. In all cases, the bottom row of plots shows that the equilibrium trait u_e lies at a global maximum on the adaptive landscape at equilibrium.

relate r_0 to R_0 , this is equivalent to asking whether

$$R_0(\mathbf{x}_e, v) = \left(b_1 \exp\left(-\frac{v^2}{2w}\right) + b_2 \exp\left(-\frac{(v-1)^2}{2w}\right) \frac{s_1}{1-s_2} \right) \beta_1(\|\mathbf{x}\|)$$

has a global maximum at $v = u_e$. As a function of v , the positive-valued and bounded function $R_0(\mathbf{x}_e, v)$ vanishes as $|v| \rightarrow +\infty$; therefore, its

maximum value must occur at a finite critical point. We have shown that when $w > 1/4$, there exists one and only one critical point, namely $v = u_c(\delta)$, which therefore must be the location of the global maximum.

We conclude that when $w > 1/4$, the trait component u_e is an ESS trait, at least for the positive equilibrium near the bifurcation point $R_0(\mathbf{0}_2, u_c(\rho)) \gtrapprox 1$.

The existence and analysis of equilibria outside a neighborhood of the bifurcation point depends on the properties of the nonlinear fertility density factor $\beta(|\mathbf{x}|)$. Figure 5.4 shows sample simulations that illustrate the conclusions we have obtained for this Darwinian model.

We have restricted our attention to the case when the variance of $\varphi_1(v)$ and $\varphi_2(v)$ satisfies $w > 1/4$. On the other hand, if $w < 1/4$, then it is possible that there exist more than one critical point, each of which can produce positive equilibria by bifurcation. Thus in this case, there is the possibility of multiple stable equilibria and ESS traits (and as a result, initial-condition dependent equilibration), which is a more complicated case that we do not consider here.

5.6.2. Coles’s Paradox: Semelparity Versus Iteroparity. Life history strategies of biological organisms crucially involve trade-offs in the allocation of resources and activities involving reproduction versus other processes that promote individual survival and growth. Although not always the case, frequently there are costs associated with reproduction that result in negative effects on survival [119]. Should an individual put so much effort into reproduction that it results in its death or should it allocate resources toward post-reproductive survival, at the expense of reproductive effort and output, so as to have more than one reproductive episode in its lifetime? In the first case, the population is semelparous, and in the second case, it is iteroparous. And which of these two strategies does evolution favor?

In a classic paper, Cole [22] argued that evolution should favor semelparity. However, given that iteroparity is common among biological species, this became known as Cole’s Paradox. In response, several authors pointed out that Cole did not adequately take into account newborn and adult survival probabilities [119]; in particular, see [16]. These

early resolutions of Cole's Paradox were based almost exclusively on linear dynamic models of population growth. Nonlinear density effects, however, can play a significant role in determining the circumstances when evolution will favor semelparity or iteroparity [120]. One purpose of this section is to demonstrate this assertion by means of a Darwinian model with a minimal number of density factors and simple trait dependencies. Since the modeling methodology of the Darwinian dynamic models in this chapter assume a continuous phenotypic trait (unlike the discrete, genotypic approaches most often been taken with regard to this issue), the argument put forth by Hughes [81] is relevant, namely that the binary classifications of either semelparity or iteroparity is often too crude to account for the life histories of natural populations (which often exhibit variability and plasticity in post-reproductive survival).

Fundamental to the issue of reproductive effort and survival are trade-offs. Increased effort and success in one activity (such as reproduction) often leads to decreased effort or success in another (such as survival) [119], [123]. To capture a trade-off between fertility and post-reproduction survival, we replace the inherent birth rate b_0 by $b_0\varphi$ in the basic linear equation equation (1.3) in Section 1.1, where φ is the fraction of the resource gathering activity that is allocated to reproduction and b_0 is the maximal possible newborn birth rate. We assume adult post-reproduction survival is proportional to the remaining fraction $1 - \varphi$ and equals $s_0(1 - \varphi)$, where s_0 is the maximal possible post-reproduction survival probability. In the absence of density effects, the population growth rate is

$$(5.32) \quad r = b_0 s \varphi + s_0 (1 - \varphi), \quad 0 \leq \varphi \leq 1.$$

(See Exercise 5.28.) We add nonlinear density effects by including a negative effect on fertility as described by a discrete logistic-type factor. If we ignore density effects on adult post-reproduction survival, then we have the population growth rate

$$r(x) = b_0 \varphi \frac{1}{1 + cx} + s_0 (1 - \varphi), \\ b_0, c > 0, \quad 0 < s_0 < 1.$$

We assume that the allocation fraction $\varphi = \varphi(v)$ and the intraspecific competition coefficient $c = c(v - u)$ depend on a trait v subject to

natural selection and on its population mean u . An individual's inherent fertility $b_0\varphi(v)$ depends on only v (and not u , because it is a density-free rate). The magnitude of the density effect on individual fertility, as measured by the coefficient $c(v - u)$, depends on how different the individual is from most other individuals (i.e., the typical individual with trait u). Then

$$r(x, v, u) = b_0\varphi(v) \frac{1}{1 + c(v - u)x} + s_0(1 - \varphi(v)).$$

In the example considered here, we make further assumptions on φ and c .

First, we assume there is a unique trait v_0 , where $\varphi(v)$ (and hence inherent fertility $b_0\varphi(v)$) is maximal and that $\varphi(v)$ is normally distributed around v_0 . Because a reference point and unit scale for the trait v can be arbitrarily chosen, we take $v_0 = 0$ and a standard deviation equal to 1, without loss in mathematical generality:

$$\varphi(v) = \exp\left(-\frac{1}{2}v^2\right).$$

Note that when $v = 0$, post-reproduction survival equals 0; therefore, we refer to 0 as the *semelparous trait*.

Second, we assume maximum competition occurs between like individuals so that an individual born with trait v experiences the greatest competition for resources when $v = u$, the population mean. Mathematically, we assume $c(z) \in C^2(R_+ : R_+)$ has a global maximum at $z = 0$. Specifically, we assume $c(z)$ is normally distributed with variance w :

$$(5.33) \quad c(z) = c_0 \exp\left(-\frac{1}{2w}z^2\right), \quad w > 0.$$

Under these assumptions and specifications, we have population growth rate

$$(5.34) \quad r(x, v, u) = b_0 \exp\left(-\frac{1}{2}v^2\right) \frac{1}{1 + c_0 \exp\left(-\frac{1}{2w}(v-u)^2\right)x} + s_0\left(1 - \exp\left(-\frac{1}{2}v^2\right)\right)$$

with which to construct the Darwinian equations (5.5) and (5.6):

$$(5.35) \quad \begin{aligned} x(t+1) &= b_0 \exp\left(-\frac{1}{2}u^2(t)\right) \frac{1}{1 + c_0 x(t)} x(t) \\ &\quad + s_0\left(1 - \exp\left(-\frac{1}{2}u^2(t)\right)\right) x(t) \quad \text{and} \\ u(t+1) &= u(t) + \theta \partial_v r(x(t), v, u(t))|_{v=u(t)}. \end{aligned}$$

Our goal is to study the existence and stability of positive equilibria and when their trait components are ESS traits.

The equilibrium equations are (after some simplifications in the trait equation)

$$\begin{aligned} x &= \left(b_0 \exp\left(-\frac{1}{2}u^2\right) \frac{1}{1+c_0x} + s_0 \left(1 - \exp\left(-\frac{1}{2}u^2\right)\right) \right) x \quad \text{and} \\ 0 &= u \left(b_0 \frac{1}{1+c_0x} - s_0 \right). \end{aligned}$$

If $b_0 \neq s_0$, then the only extinction equilibrium is $\text{col}(x, u) = \text{col}(0, 0)$. As we will see, we will eventually be interested in only $b_0 > 1$, so $b_0 \neq s_0$ is not a constraint for us. It is left as Exercise 5.30 to show that $R_0(0, 0) = b_0$ and to apply the general theorems in Section 5.3 to show that if

$$(5.36) \quad \theta < \theta^* := \frac{2}{1-s_0},$$

then a forward and stable bifurcation of positive equilibria occurs at $b_0 = 1$.

We can, however, obtain more in this example by an analysis of the equilibrium equations and a use of the Linearization Principle. The equations for a positive equilibrium are

$$\begin{aligned} 1 &= b_0 \exp\left(-\frac{1}{2}u^2\right) e^{-u^2/2} \frac{1}{1+c_0x} + s_0 \left(1 - \exp\left(-\frac{1}{2}u^2\right)\right) \quad \text{and} \\ 0 &= u \left(b_0 \frac{1}{1+c_0x} - s_0 \right). \end{aligned}$$

If

$$b_0 \frac{1}{1+c_0x} - s_0 = 0,$$

then the second equation is certainly satisfied, but the first equation reduces to $1 = s_0$, which is a contradiction to our assumption that $s_0 < 1$. Therefore, the second equilibrium equation implies $u = 0$ which, when placed into the first equation, yields

$$1 = b_0 \frac{1}{1+c_0x}$$

whose solution is $x = (b_0 - 1)/c_0$. Thus, *the positive equilibria of the model equations (5.35) are*

$$(5.37) \quad \begin{bmatrix} x_e \\ u_e \end{bmatrix} = \begin{bmatrix} \frac{b_0-1}{c_0} \\ 0 \end{bmatrix} \quad \text{for all } b_0 > 1.$$

Note that *all positive equilibria in this model have a semelparous mean trait $u = 0$* . Is $u = 0$ an ESS trait? To determine an answer to this question, we need to determine the stability of the equilibrium and whether the adaptive landscape at equilibrium $\ln r(x_e, v, u_e)$, or equivalently that $r(x_e, v, u_e)$, has a global maximum at $v = 0$. The answer is in the following theorem in which

$$w^* := \frac{1}{1 - s_0} \quad \text{and} \quad b_0^* := \frac{1}{1 - (1 - s_0)w}.$$

Theorem 5.21. *The positive equilibria (5.37) of the Darwinian model equations (5.35) are (locally asymptotically) stable if the speed of evolution θ is less than the threshold θ^* and are unstable if $\theta > \theta^*$.*

- (a) *If $\theta < \theta^*$ and $w > w^*$, then the semelparous trait $u_e = 0$ is an ESS for all $b_0 > 1$.*
- (b) *If $\theta < \theta^*$ and $w < w^*$, then the semelparous trait $u_e = 0$ is an ESS for b_0 on the interval $1 < b_0 < b_0^*$ but is not an ESS for $b_0 > b_0^*$.*

Proof. A straightforward calculation shows that the Jacobian associated with equations (5.35), when evaluated at the positive equilibrium, is a triangular matrix

$$\begin{pmatrix} \frac{1}{b_0} & 0 \\ * & 1 - (1 - s_0)\theta \end{pmatrix}$$

whose eigenvalues λ_1 and λ_2 appear along the diagonal:

$$\lambda_1 = \frac{1}{b_0} > 0 \quad \text{and} \quad \lambda_2 = 1 - (1 - s_0)\theta < 1.$$

Since $b_0 > 1$ for a positive equilibrium (5.37), we see that $|\lambda_1| < 1$ and that the Linearization Principle implies the equilibrium is (locally asymptotically) stable if $\lambda_2 > -1$. We conclude that the positive equilibria (5.37) are stable if $\theta < \theta^*$ and unstable if $\theta > \theta^*$.

To establish (a) and (b), we investigate whether or not $r(x_e, v, u_e)$, that is

$$\begin{aligned} r\left(\frac{b_0 - 1}{c_0}, v, 0\right) \\ = b_0 \exp\left(-\frac{1}{2}v^2\right) \frac{1}{1 + \exp\left(-\frac{1}{2w}v^2\right)(b_0 - 1)} + s_0 \left(1 - \exp\left(-\frac{1}{2}v^2\right)\right), \end{aligned}$$

has a global maximum at $v = 0$. For notational simplicity, let this function of v be denoted by $\Lambda(v)$. The question is whether or not $\Lambda(0) = 1$ is a global maximum of $\Lambda(v)$.

We begin by noting that $\lim_{v \rightarrow \pm\infty} \Lambda(v) = s_0 < 1$ and that, consequently, the global maximum must occur at a (finite) critical value v of $\Lambda(v)$. Critical values are the roots of $\partial_v \Lambda(v)$. A straightforward but tedious calculation (a computer algebra program helps) shows

$$\partial_v \Lambda(v) = v q(y(v)) \frac{1}{w((b_0 - 1)y(v) + 1)^2} \exp\left(-\frac{1}{2}v^2\right),$$

where we have defined

$$y(v) := \exp\left(-\frac{1}{2w}v^2\right)$$

and where $q(y)$ is the quadratic polynomial

$$\begin{aligned} q(y) := & -w(b_0 - s_0) + (b_0 - 1)(b_0 + (2s_0 - b_0)w)y \\ & + ws_0(b_0 - 1)^2 y^2 \end{aligned}$$

in y . Thus, the critical points of $\Lambda(v)$ are $v = 0$ and any roots of $q(y(v)) = 0$. The quadratic $q(y)$, whose graph is a concave upward parabola with a negative intercept, has a unique positive root which we denote by $y^* > 0$. The nonzero critical traits on the landscape are therefore obtained by solving the equation

$$y^* = \exp\left(-\frac{1}{2w}v^2\right)$$

for v . It follows that if $y^* > 1$, then there are no nonzero critical traits, but if $y^* < 1$, there exist exactly two nonzero critical traits

$$v = \pm\sqrt{-2w \ln y^*}.$$

The first case $y^* > 1$ occurs if and only if $q(1) < 0$, that is if and only if

$$q(1) = b_0((1 - (1 - s_0)w)b_0 - 1) < 0.$$

An inspection of this inequality shows it holds if and only if either

- (5.38)
- $w > w^*$ or
 - $w < w^*$ and $b_0 < b_0^*$.

In this case, $v = 0$ is the only critical point, and because $\Lambda(v)$ is a positive-valued and bounded function that satisfies $\lim_{|v| \rightarrow +\infty} \Lambda(v) = 0$,

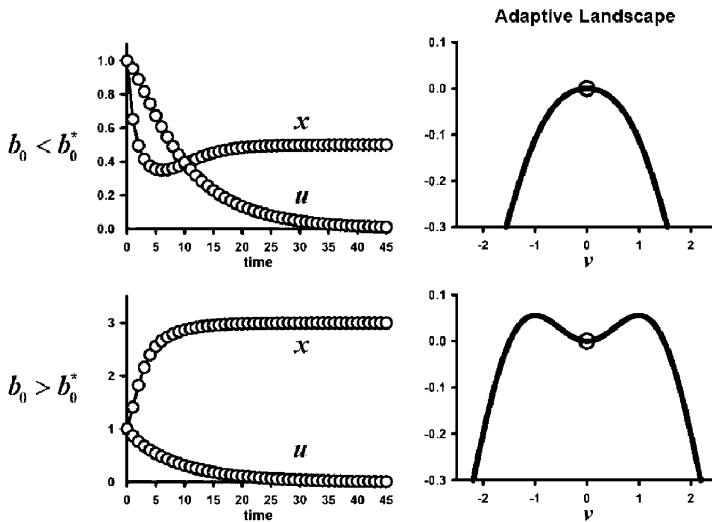


Figure 5.5. A sample solution of the Darwinian model equations (5.35) with initial conditions $x(0) = u(0) = 1$ are shown for each case $y^* > 1$ and $y^* < 1$. In both cases, parameter values are $w = 1$, $c_0 = 1$, and $s_0 = 0.5$ for which $b_0^* = w^* = 2$. In the top row, $b_0 = 1.5 < b_0^*$, and in the bottom row, $b_0 = 4 > b_0^*$. The right column shows the adaptive landscape $\ln r(x_e, v, u_0)$ at the equilibrium, which are seen to have a global maximum at $v = 0$ in the top row and not to have a global maximum at $v = 0$ in the bottom row.

it follows that the global maximum occurs at $v = 0$. By the ESS Maximum Principle, $v = 0$ is an ESS in this case.

The second case $y^* < 1$ occurs if and only if $q(1) > 0$, that is if and only if

$$(5.39) \quad w < w^* \quad \text{and} \quad b_0 > b_0^*.$$

In this case, $\Lambda''(0) > 0$, and a local minimum occurs at $v = 0$. By the ESS Maximum Principle, $v = 0$ is not an ESS in this case. \square

For the model considered here, we found the following.

All positive equilibria have a semelparous mean trait $u = 0$, but this trait is not necessarily an ESS. It is not an ESS if the width w of the trait-dependent intraspecific competition coefficient $c(v - u)$ is small and the

inherent fertility rate b_0 is large. Otherwise, $u = 0$ is an ESS, which is in agreement with Cole's assertion.

See Figure 5.5 for numerical examples of these two possibilities.

We have considered here a model with a minimal number of features and special assumptions (no population structure, a logistic-type density dependence in fertility, a normal distribution for φ , and so on). For more elaborate models from which more complicated conclusions are possible, see [35], [37], [45], [68].

5.6.3. Evolution and Complex Dynamics. In Section 1.2.3, we saw that the Ricker equation

$$x(t+1) = b_0 e^{-cx(t)} x(t)$$

with fitness function

$$\ln r(x) = \ln(b_0 \exp(-cx))$$

has a forward-stable bifurcation at $b_0 = 1$ and that there exists a unique positive equilibrium

$$x_e = \frac{1}{c} \ln b_0$$

for each $b_0 > 1$ which is (locally asymptotically) stable for $1 < b_0 < e^2$ and unstable for $b_0 > e^2$. We also saw that as $b_0 > e^2$ increases, there occurs a cascade of period-doubling bifurcations and, ultimately, complicated nonperiodic and “chaotic” attractors.

The occurrence of complex attractors—by which we simply mean nonequilibrium attractors—is not uncommon in discrete population models. Do such dynamics occur in biological populations? It has been rigorously demonstrated, by long-term replicated and controlled laboratory experiments, that a beetle population will indeed follow such a model-predicted route-to-chaos [50], [41], [23], [51], [52], [53]. Other experiments have also shown populations with chaotic dynamics [4], [5], [6], [71], [126].

However, unequivocal evidence for deterministic complex and chaotic dynamics in natural populations is rare [113], [134]. Several hypotheses have been offered for why this is the case, including the difficulty caused by the presence of noise in data, the lack of long-term data sets, and the damping effects of interacting species in food webs. Another hypothesis is that evolution selects against population oscillations

and complex dynamics. It is this latter question that we will address here by making use of a Darwinian version of the Ricker equation (5.9) in Example 5.1.

Assume that inherent fertility has a normal distribution as a function of an evolving trait v (scaled and referenced to have mean 0 and standard deviation 1) and that the intraspecific competition coefficient is again given by (5.33). The resulting fitness function

$$\ln r(x, v, u) = \ln\left(b_0 \exp\left(-\frac{1}{2}v^2\right) \exp\left(-c_0 \exp\left(-\frac{1}{2w}(v-u)^2\right)x\right)\right)$$

produces the Darwinian Ricker model

$$(5.40) \quad \begin{aligned} x(t+1) &= b_0 \exp\left(-\frac{1}{2}u^2(t)\right) \exp(-c_0 x(t)) x(t) \\ u(t+1) &= (1-\theta)u(t). \end{aligned}$$

We can analyze this model in the way we analyzed the similar Darwinian discrete logistic (5.23) in Section 5.4. From the equilibrium equations

$$\begin{aligned} x &= b_0 \exp\left(-\frac{1}{2}u^2\right) \exp(-c_0 x) x \quad \text{and} \\ u &= (1-\theta)u, \end{aligned}$$

we get, in addition to the extinction equilibrium $\text{col}(x, u) = \text{col}(0, 0)$, the positive equilibria

$$(5.41) \quad \begin{bmatrix} x_e \\ u_e \end{bmatrix} = \begin{bmatrix} \frac{1}{c_0} \ln b_0 \\ 0 \end{bmatrix}, \quad b_0 > 1.$$

The Jacobian

$$J(x, u) = \begin{bmatrix} b_0 e^{-\frac{1}{2}u^2} (1 - xc_0) e^{-xc_0} & -b_0 ue^{-u^2/2} e^{-c_0 x} x \\ 0 & 1 - \theta \end{bmatrix}$$

evaluated at these two equilibria gives

$$\begin{aligned} J(0, 0) &= \begin{bmatrix} b_0 & 0 \\ 0 & 1 - \theta \end{bmatrix}, \\ J(x_e, u_e) &= \begin{bmatrix} 1 - \ln b_0 & 0 \\ 0 & 1 - \theta \end{bmatrix}, \quad b_0 > 1. \end{aligned}$$

The eigenvalues λ_i of these diagonal matrices appear along their diagonals.

For both Jacobians, $1 - \theta$ is an eigenvalue, and by the Linearization Principle, both equilibria are unstable if the speed of evolution is too fast (i.e., if $\theta > 2$). In this case, it turns out $\lim_{t \rightarrow \infty} x(t) = 0$ for all

positive, nonequilibrium solutions and **evolutionary suicide** occurs (see Exercise 5.29).

If $\theta < 2$, then the extinction equilibrium $\text{col}(0, 0)$ loses stability as b_0 increases through 1, and the positive equilibrium is stable for $1 < b_0 < e^2$. In this case, this Darwinian version of the Ricker equation has the same equilibrium existence and stability properties as the nonevolutionary Ricker equation. But is $u = 0$ an ESS?

Theorem 5.22. *Suppose $\theta < 2$ in the Darwinian Ricker model (5.40). For $1 < b_0 < e^2$, the positive equilibrium (5.41) is (locally asymptotically) stable.*

- (a) *If $w > 2$, then $u_e = 0$ is an ESS.*
- (b) *If $w < 2$, then $u_e = 0$ is an ESS for $1 < b_0 < e^w$ and not an ESS for $e^w < b_0 < e^2$.*

Proof. As a function of v , the adaptive landscape at equilibrium

$$\ln r(x_e, v, 0) = \ln b_0 - \frac{1}{2}v^2 - e^{-v^2/(2w)} \ln b_0$$

approaches $-\infty$ as $v \rightarrow \pm\infty$; hence, its global maximum occurs at a finite critical point. Critical points are the roots of the derivative

$$\partial_v \ln r(x_e, v, 0) = v \left(-1 + \frac{\ln b_0}{w} \exp\left(-\frac{1}{2w}v^2\right) \right).$$

Clearly $v = 0$ is a critical point. If it is the only critical point, then the global maximum of the adaptive landscape must occur there, and $v = 0$ is an ESS. Other possible critical points are roots of the parenthetical factor, which are

$$v_{\pm} := \pm \sqrt{2w \ln\left(\frac{\ln b_0}{w}\right)}$$

provided $b_0 > e^w$.

- (a) If $w > 2$, then for $1 < b_0 < e^2$ the only critical trait on the adaptive landscape is $v = 0$, which is therefore at the global maximum.
- (b) Suppose $w < 2$. A calculation shows that the second derivation

$$\partial_v^2 \ln r(x_e, v, 0)|_{v=0} = -1 + \frac{1}{w} \ln b_0$$

is positive for $b_0 > e^w$, which implies $v = 0$ is a local minimum and therefore is not an ESS. By symmetry, the global maximum must occur at both critical points v_{\pm} (since the landscape is an even function of v).

□

Figure 5.6 shows simulation examples that illustrate the conclusions given by Theorem 5.22.

Note that in the Darwinian Ricker model (5.40), a population at equilibrium has trait component $u_e = 0$, which implies that the inherent population growth rate r_0 equals b_0 . From Theorem 5.22, we draw

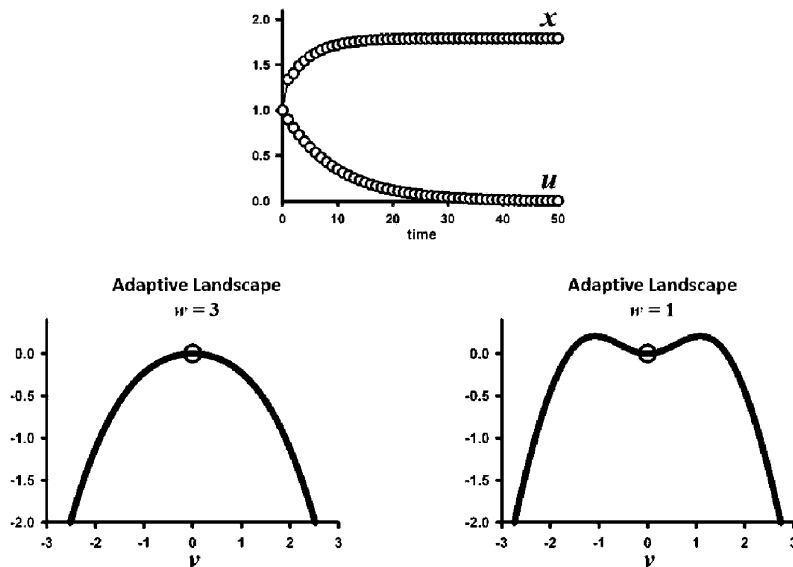


Figure 5.6. Shown are the time series plots of the solution of the Darwinian Ricker model (5.40) with parameters $b_0 = 6$, $c_0 = 1$, and $\theta = 0.1$ and initial conditions $x(0) = u(0) = 1$. The solution and its time series plots are independent of w , but the adaptive landscape is not, as seen with two sample plots with $w = 3$ and $w = 1$. At $v = 0$, a global maximum occurs when $w = 3$ (Theorem 5.22(a)), and a local minimum occurs with $w = 1$ (Theorem 5.22(b)).

the following conclusions.

- When $\theta < 2$ and $w > 2$, the equilibrium trait $u_e = 0$ is an ESS for b_0 on the entire interval $1 < b_0 < e^2$. In this case, we conclude that this Darwinian Ricker model predicts that evolution has no effect on the onset of complex (nonequilibrium) dynamics.
- If $\theta < 2$ and $w < 2$, then the threshold for the onset of complex (nonequilibrium) dynamics remains at $b_0 = e^2$, but evolution will not favor the non-ESS trait $u_e = 0$ for those values of b_0 near the threshold. Instead, evolution favors mutants with traits at $u = v_{\pm} \neq 0$, where the inherent birth rate is reduced to $b_0 \exp(-v_{\pm}/2w) < b_0$ away from the threshold e^2 . In this sense, evolution selects against complex dynamics in this case when the width w of the distribution of competition coefficients (5.22) is sufficiently narrow.

In Theorem 5.22, it is assumed that the speed of evolution is not too fast (i.e., $\theta < 2$). What happens in this model when the speed of evolution θ exceeds 2? We saw previously that, in this case, all equilibria are unstable, including the extinction equilibrium. Nonetheless, it turns out in this case that all populations go extinct (evolutionary suicide occurs).

Theorem 5.23. Suppose the speed of evolution $\theta > 2$ in the Darwinian Ricker model (5.40). Then evolutionary suicide occurs, in the sense that $\lim_{t \rightarrow \infty} x(t) = 0$ for all initial conditions $x(0) \geq 0$ and $u(0) \neq 0$.

Proof. The trait equation for $u(t)$ in (5.40) is uncoupled from the population equation for $x(t)$ and is a simple linear difference equation whose solution is

$$u(t) = (1 - \theta)^t u(0).$$

Thus, the equation for $x(t)$ becomes

$$x(t+1) = b_0 \exp\left(-\frac{1}{2}(1-\theta)^{2t} u^2(0)\right) \exp(-c_0 x(t)) x(t)$$

(a nonautonomous difference equation). Some straightforward calculus shows that

$$0 \leq \exp(-c_0 x) x \leq \frac{1}{c_0} e^{-1} \quad \text{for } x \geq 0$$

from which we have the inequality

$$(5.42) \quad 0 \leq x(t+1) \leq b_0 \exp\left(-\frac{1}{2}(1-\theta)^{2t} u^2(0)\right) \frac{1}{c_0} e^{-1}$$

for all $t \in \mathbf{Z}_+$. Since $(1-\theta)^2 > 1$, it follows that the exponent on the right side satisfies

$$-\frac{1}{2} \lim_{t \rightarrow \infty} (1-\theta)^{2t} u^2(0) = -\frac{1}{2} \lim_{t \rightarrow \infty} ((1-\theta)^2)^t u^2(0) = -\infty,$$

and as a result, we get from (5.42) that

$$0 \leq \lim_{t \rightarrow \infty} x(t+1) \leq b_0 \lim_{t \rightarrow \infty} \exp\left(-\frac{1}{2}(1-\theta)^{2t} u^2(0)\right) \frac{1}{c_0} e^{-1} = 0.$$

□

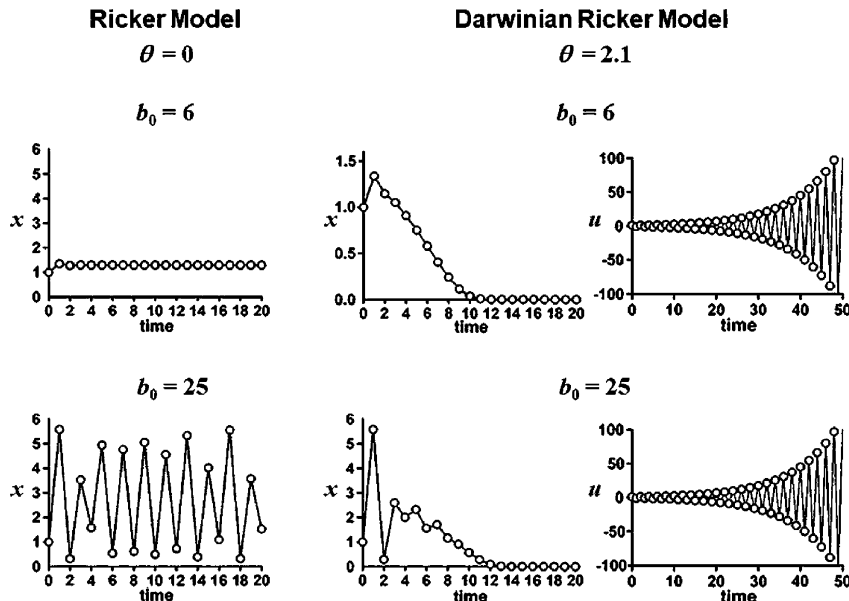


Figure 5.7. The time series for a sample solution with initial conditions $x(0) = u(0) = 1$ (and $c_0 = 1$) of the Darwinian Ricker model (5.40) is shown for two values of b_0 when $\theta > 2$. Both show the population going extinct, whereas the nonevolutionary Ricker model with the same parameter values and initial condition (see the column of plots on the left) does not predict extinction, namely survival with equilibrium dynamics when $b_0 = 6$ and nonequilibrium dynamics when $b_0 = 25$.

Figure 5.7 illustrates examples of evolutionary suicide when the nonevolutionary Ricker equation predicts equilibrium dynamics and when it predicts complex (chaotic) dynamics.

The Darwinian Ricker model considered here was based on specific submodels for the trait dependence of the coefficients. Other submodels can lead to different conclusions. For example, in [36], a hierarchical dependence $c(v - u) = c_0 \exp(w(v - u))$ is used in place of (5.22) with the result that, except for high-speed evolution, the b_0 threshold for the onset of nonequilibrium, complex dynamics is larger than e^2 ; in this sense, evolution selects against complex dynamics. We conclude that the relationship between evolution and complex dynamics is a complicated one and is significantly dependent on the nature of the trait dependency of the coefficients in the Ricker equation.

5.7. Concluding Remarks

In this chapter, we studied a method for including evolution by Darwinian principles into a population model. To use this method, a modeler describes how (at least some) vital rates depend on a (continuous) phenotypic trait that is subject to natural selection and constructs an expanded dynamical system that includes the population dynamics and the dynamics of the population mean trait. In our presentation of the method, we used (as is commonly done) the logarithm of the spectral radius of the population projection matrix as the fitness function [3], [129]. We looked at some theorems that generalized the basic results in Chapter 3 concerning the stability properties of an extinction equilibrium and the bifurcation of positive equilibria that occurs when it destabilizes. Under the assumption of primitivity of the inherent projection matrix, we saw how the general basic bifurcation theorem for nonevolutionary models, that relates the stability of the bifurcating positive equilibrium to the direction of bifurcation (Chapter 3), holds for a general Darwinian model, provided the speed of evolution is not too fast. We also introduced the notion of an ESS trait and the ESS Maximum Principle. Several applications of this modeling methodology and analysis appearing in Section 5.6 illustrate how a stable equilibrium might or might not be associated with an ESS trait and hence indicate a trait favored by evolution.

As seen in Section 3.6, there are applications in which the inherent population projection matrix is not primitive. We saw there that the basic principle that the direction of bifurcation of equilibria (upon destabilization of an extinction equilibrium) determines their stability does not necessarily hold in this case and that, furthermore, other (nonequilibrium) attractors can result from the bifurcation. In general, the bifurcation scenario in the imprimitive case can be extraordinarily complicated, especially in higher-dimensional structured population models, and it is not well understood except in special cases. The same is, of course, true for evolutionary versions of an imprimitive population model. For examples and applications of some imprimitive Darwinian models, see [127], [128].

5.8. Exercises

Exercise 5.24. Show, with methods used in Example 5.5, that the Darwinian Ricker model (5.9) has a unique extinction equilibrium for all $b_0 > 0$ and that it has a positive equilibrium if and only if $b_0 > 1$ (in which case it is unique).

Exercise 5.25. Show, with methods used in Example 5.5, that the Darwinian semelparous juvenile-adult model in Example 5.2 has a unique extinction equilibrium for all $b_0 > 0$ and that it has a positive equilibrium if and only if $b_0 > 1/s_1$ (in which case it is unique).

Exercise 5.26. Apply Lemma 5.7 and Theorem 5.8 to the Darwinian Ricker model (5.9). Then apply Theorem 5.11.

Exercise 5.27. Show that the trait component $u = 0$ of the solution of equations (5.21) with initial condition $\text{col}(x(0), u(0)) = (8, 1)$ shown in Figure 5.1 is an ESS.

Exercise 5.28. Consider the linear population model equation

$$x(t+1) = rx(t)$$

with r given by (5.32), $b_0 > 0$, $0 < s_0 < 1$, and $0 \leq \varphi \leq 1$.

- (a) If $b_0 < 1$, prove that the population goes extinct for all initial conditions $x(0) \geq 0$.

- (b) Suppose $b_0 > 1$. Show that as a function of the allocation fraction φ , fitness $\ln r$ is maximized when $\varphi = 1$ (i.e., the population is semelparous and, in this case, survives by growing exponentially for all initial conditions $x(0) > 0$).

Exercise 5.29. Assume $\theta > 2$ in the Darwinian discrete logistic model (5.23). For all initial conditions

$$\text{col}(x(0), u(0)) \neq \text{col}(x_e, 0)$$

with $x(0) > 0$, prove that $\lim_{t \rightarrow \infty} x(t) = 0$.

Exercise 5.30. Use Corollary 5.12 to show that a forward and stable bifurcation of positive equilibria occurs at $b_0 = 1$ in the model (5.35) if $\theta < 2/(1 - s_0)$.

Exercise 5.31. Construct and analyze a Darwinian model as done in Section 5.6.2 but using instead

$$\varphi(v) = \frac{1}{1 + v^2} \quad \text{and} \quad c(v - u) = c_0 \frac{1}{1 + \frac{1}{2w}(v - u)^2}.$$

Compare your results with those in Theorem 5.21.

Exercise 5.32. Consider a Darwinian version of the juvenile-adult model with fertility and transition matrices

$$\mathbf{F}(\mathbf{x}, v, u) = \begin{bmatrix} 0 & b_2 \frac{1}{1 + c_0 x_2} \\ 0 & 0 \end{bmatrix} \quad \text{and}$$

$$\mathbf{T}(\mathbf{x}, v, u) = \begin{bmatrix} 0 & 0 \\ s_1 \exp\left(-\frac{v^2}{2}\right) & s_2 \exp\left(-\frac{v^2}{2w}\right) \end{bmatrix}.$$

- (a) Show that $u_c = 0$ is the only critical trait and find a formula for R_0 .
- (b) Apply Theorem 5.8 to show that the extinction equilibrium $\text{col}(\mathbf{0}_2, 0)$ loses stability as R_0 increases through 1 if $\theta < 2(2 - s_2)$.
- (c) Use Theorem 5.19 to prove that a forward-stable bifurcation of positive equilibria from the extinction equilibrium $\text{col}(\mathbf{0}_2, 0)$ occurs at $R_0 = 1$ if $\theta < 2(2 - s_2)$.
- (d) Find formulas for the positive equilibria and use them, and the Linearization Principle, to show that there is a unique, positive equilibrium for all $R_0 > 1$ and that it is stable if $\theta < 2(2 - s_2)$.

- (e) Use the ESS Maximum Principle to show that the trait $u = 0$ associated with a positive equilibrium is an ESS if $\theta < 2(2 - s_2)$.

Appendix A

Appendices

A.1. Jury Conditions for 2×2 Matrices

Let $\text{tr} M = m_{11} + m_{22}$ and $\det M = m_{11}m_{22} - m_{21}m_{12}$ denote the trace and the determinant of a 2×2 matrix $\mathbf{M} = [m_{ij}]$. Both eigenvalues of \mathbf{M} satisfy $|\lambda| < 1$ if and only if $|\text{tr } \mathbf{M}| < 1 + \det \mathbf{M} < 2$ or equivalently

$$(A.1) \quad |\text{tr } \mathbf{M}| < 1 + \det \mathbf{M} \quad \text{and} \quad \det \mathbf{M} < 1.$$

These inequalities can be viewed geometrically by showing that they are satisfied if and only if the point $(\text{tr } \mathbf{M}, \det \mathbf{M})$ lies inside the triangle shown in Figure A.1. This so-called trace-determinant condition for $m = 2$ dimensional matrices states that its two eigenvalues lie inside the unit complex disk if and only if the point $(\text{tr } \mathbf{M}, \det \mathbf{M})$ lies inside the triangle. If an entry in \mathbf{M} is changed so as to cause the point $(\text{tr } \mathbf{M}, \det \mathbf{M})$ to leave the inside of the triangle, then an eigenvalue \mathbf{M} will move from inside to outside of the unit disk in the complex plane. More specifically, if the point $(\text{tr } \mathbf{M}, \det \mathbf{M})$ moves across the lower-left side of the triangle, then one eigenvalue leaves the unit circle through $+1$, whereas if it moves across the lower-right side of the triangle, then one eigenvalue leaves the unit circle through -1 . On the other hand, if the point leaves the triangle through the top of the triangle, then a complex pair of eigenvalues leaves the complex unit circle. (If the point leaves the triangle through the bottom-corner of the triangle, then both eigenvalues of \mathbf{M} leave the unit circle: one through $+1$ and one through -1 . If the point leaves the triangle through the left- or right-corner, then both

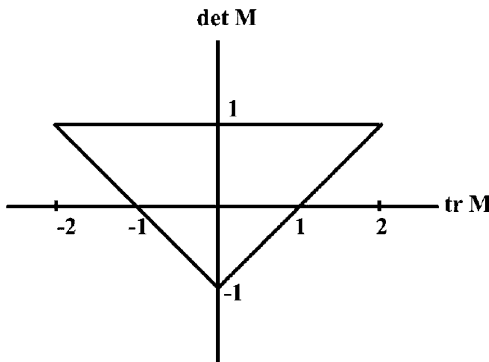


Figure A.1. The inequalities (A.1) in the Jury stability criteria geometrically place the point $(\text{tr } \mathbf{M}, \det \mathbf{M})$ inside the displayed triangle. Points outside the triangle correspond to instability.

eigenvalues leave the unit disk at $+1$ or -1 , respectively.) Thus, when \mathbf{M} is the Jacobian evaluated at an equilibrium of a nonlinear equation, different types of bifurcations occur as an eigenvalue leaves the triangle and the equilibrium destabilizes. Although other technical conditions are needed to assure that a bifurcation occurs and to determine whether it is forward or backward (or stable or unstable), one expects the following: if an eigenvalue leaves the inside of the triangle through the

- (a) top, then a Neimark–Sacker occurs;
- (b) lower-right side, then a period-doubling bifurcation occurs;
- (c) lower-left side, then an equilibrium bifurcation occurs.

In case (a), an invariant loop is created. In case (b), cycles of period 2 are created. In case (c), a tangent (aka blue-sky or saddle-node), pitchfork, or transcritical bifurcation of equilibria occurs.

The Jury conditions (A.1) can be equivalently rewritten as the following three conditions, relating to the three sides of the triangle in Figure A.1 and the different types of bifurcations associated with them:

- $$(A.2) \quad \begin{aligned} (a) \quad & 0 < 1 - \det M; \\ (b) \quad & 0 < 1 + \det M + \text{tr } M; \\ (c) \quad & 0 < 1 + \det M - \text{tr } M. \end{aligned}$$

A.2. The Linearization Principle

In this section, we give a proof of Theorem 1.10. By the Mean Value Theorem,

$$f(x) - x_e = f(x) - f(x_e) = \partial_x f(\xi)(x - x_e)$$

for some number ξ between x and x_e (i.e., satisfying $|\xi - x_e| \leq |x - x_e|$).

First, suppose $|\partial_x f(x_e)| < 1$. Then $|\partial_x f(x)| < 1$ for x near x_e since $\partial_x f(x)$ is continuous. More specifically, if we choose a number α between $|\partial_x f(x_e)|$ and 1 (i.e., a number satisfying $|\partial_x f(x_e)| < \alpha < 1$), then there exists an interval of x values, say $|x - x_e| \leq \delta^*$ where $\delta^* < \delta$, on which $|\partial_x f(x)| \leq \alpha < 1$.

We begin by addressing the stability of the equilibrium x_e . If the initial condition $x(0)$ satisfies

$$|x(0) - x_e| \leq \delta^*,$$

then

$$|x(1) - x_e| = |f(x(0)) - f(x_e)| = |\partial_x f(\xi_1)| |x(0) - x_e|$$

for some ξ_1 between x_e and x_0 (i.e., satisfying $|\xi_1 - x_e| \leq |x - x_e|$). It follows that

$$|x(1) - x_e| \leq \alpha |x(0) - x_e| \leq \delta^*.$$

This inequality allows us to repeat this same argument using $x(2)$ in place of $x(1)$. Thus, for some ξ_2 between x_e and x_0 (i.e., satisfying $|\xi_2 - x_e| \leq |x - x_e|$), we have

$$|x(2) - x_e| = |f(x(1)) - f(x_e)| = |\partial_x f(\xi_2)| |x(1) - x_e|;$$

hence,

$$|x(2) - x_e| \leq \alpha^2 |x(0) - x_e| \leq \delta^*.$$

For purposes of induction, suppose for a $t \geq 1$ that

$$|x(t-1) - x_e| \leq \alpha^{t-1} |x(0) - x_e| \leq \delta^*.$$

Then, repeating the previous argument, we have

$$|x(t) - x_e| = |f(x(t-1)) - f(x_e)| = |\partial_x f(\xi_t)| |x(t-1) - x_e|$$

for some ξ_t between x_e and x_0 ; hence,

$$(A.3) \quad |x(t) - x_e| \leq \alpha^t |x(0) - x_e| \leq \delta^*.$$

By induction inequality, (A.3) holds for all $t \in \mathbb{Z}_+$.

Given any $\varepsilon > 0$, let $\delta(\varepsilon) = \min\{\delta^*, \varepsilon\}$. Then for any initial condition satisfying $|x(0) - x_e| \leq \delta(\varepsilon)$, the inequality (A.3) holds; hence,

$$|x(t) - x_e| \leq \alpha^t |x(0) - x_e| \leq 1 \cdot \min\{\delta^*, \varepsilon\} \leq \varepsilon$$

for all $t \in Z_+$. This shows x_e is stable. Finally, we note that (A.3) implies $\lim_{t \rightarrow \infty} |x(t) - x_e| = 0$ when $|x(0) - x_e| \leq \delta^*$. That is to say, the stable equilibrium x_e is locally attracting and hence is locally asymptotically stable.

Second, suppose $|\partial_x f(x_e)| > 1$. Then $|\partial_x f(x)| > 1$ for x near x_e since $\partial_x f(x)$ is continuous. More specifically, if we choose a number α between $|\partial_x f(x_e)|$ and 1, then there exists an interval of x values, say $|x - x_e| \leq \varepsilon$ where $\varepsilon < \delta$, on which $|\partial_x f(x)| \geq \alpha > 1$.

Suppose for purposes of reaching a contradiction that x_e is stable. Then there exists a $\delta(\varepsilon)$ such that $|x(0) - x_e| \leq \delta(\varepsilon)$ implies

$$(A.4) \quad |x(t) - x_e| \leq \varepsilon \text{ for all } t \in Z_+.$$

However, reasoning analogously as in (a), we inductively conclude that $|x(0) - x_e| \leq \delta^*$ implies

$$|x(t) - x_e| \geq \alpha^t |x(0) - x_e| \text{ for all } t \in Z_+.$$

For an initial condition $x(0) \neq x_e$, this contradicts (A.4) for large t , specifically for

$$t > \ln(\varepsilon |x(0) - x_e|^{-1}) / \ln \alpha.$$

This contradiction means that the assumption that x_e is stable is false.

A.3. The Implicit Function Theorem

Let $\mathbf{g} \in C^q(\Omega : \Theta)$, where Ω and Θ are open sets in $R^{n+m} = R^n \times R^m$ and R^m , respectively. We write $\mathbf{g} = \mathbf{g}(\boldsymbol{\mu}, \mathbf{x})$ for $\boldsymbol{\mu} \in \Omega$ and $\mathbf{x} \in \Theta$ and consider the equation $\mathbf{g}(\boldsymbol{\mu}, \mathbf{x}) = \mathbf{0}_m$ to be solved for \mathbf{x} as a function of $\boldsymbol{\mu}$. We denote the Jacobian of \mathbf{g} with respect to \mathbf{x} by

$$J_{\mathbf{x}} \mathbf{g}(\boldsymbol{\mu}, \mathbf{x}) = \left[\partial_{y_j} g_i(\boldsymbol{\mu}, \mathbf{x}) \right].$$

Theorem A.1. *Assume there exists $(\boldsymbol{\mu}_0, \mathbf{x}_0) \in R^{n+m}$ such that $\mathbf{g}(\boldsymbol{\mu}_0, \mathbf{x}_0) = \mathbf{0}_m$ and the Jacobian $J_{\mathbf{x}} \mathbf{g}(\boldsymbol{\mu}, \mathbf{x})$ evaluated at $(\boldsymbol{\mu}_0, \mathbf{x}_0)$ is invertible. Then in a neighborhood N of $\boldsymbol{\mu}_0$, there exists a unique function $\mathbf{x} = \xi(\boldsymbol{\mu}) \in C^q(U : \Theta)$ such that $\xi(\boldsymbol{\mu}_0) = \mathbf{x}_0$ and $\mathbf{g}(\boldsymbol{\mu}, \xi(\boldsymbol{\mu})) = \mathbf{0}_m$.*

The derivatives of $\xi(\mu)$ at $\mu \in N$ can be calculated by implicit differentiation of $\mathbf{g}(\mu, \xi(\mu)) = \mathbf{0}_m$. For example, the first order derivatives are

$$(A.5) \quad \partial_{\mu_i} \xi(\mu) = -J_x^{-1} \mathbf{g}(\mu, \xi(\mu)) \partial_{\mu_i} \mathbf{g}(\mu, \xi(\mu)).$$

A.4. Mean Trait Dynamics

In this section, we follow [129] to give a derivation of the trait equation (5.6). Suppose a population x has mean phenotypic trait u and contains k subpopulations x_j with mean traits $u_j \in \Lambda$:

$$x = \sum_{j=1}^k x_j.$$

The frequency of phenotype j is

$$q_j = \frac{x_j}{x},$$

and the population mean is, by definition,

$$u = \sum_{j=1}^k q_j u_j.$$

The differences

$$\Delta u_j = u_j - u$$

measure the variability within the population. Note that

$$\begin{aligned} u &= \sum_{j=1}^k q_j (u + \Delta u_j) \\ &= \sum_{j=1}^k q_j u + \sum_{j=1}^k q_j \Delta u_j \\ &= u + \sum_{j=1}^k q_j \Delta u_j, \end{aligned}$$

which implies

$$(A.6) \quad \sum_{j=1}^k q_j \Delta u_j = 0.$$

We want to determine how u changes due to the population density dynamics. It is assumed that the population and each subpopulation changes according to the equation (5.5). It follows that u changes in time

because the frequencies q_j change in time, while u_j remains unchanged. Thus,

$$\begin{aligned} u(t+1) &= \sum_{j=1}^k q_j(t+1) u_j \\ &= \sum_{j=1}^k \frac{x_j(t+1)}{x(t+1)} u_j \\ &= \sum_{j=1}^k \frac{r(x(t), v, u(t))|_{v=u_j(t)} x_j(t)}{r(x(t), v, u(t))|_{v=u(t)} x(t)} u_j, \end{aligned}$$

and

$$\begin{aligned} u(t+1) - u(t) &= \sum_{j=1}^k \frac{r(x(t), v, u(t))|_{v=u_j(t)} x_j(t)}{r(x(t), v, u(t))|_{v=u(t)} x(t)} u_j \\ &\quad - \sum_{j=1}^k q_j(t) u_j \\ &= \sum_{j=1}^k \left(\frac{r(x(t), v, u(t))|_{v=u_j(t)}}{r(x(t), v, u(t))|_{v=u(t)}} - 1 \right) q_j(t) u_j \end{aligned}$$

or

$$\begin{aligned} u(t+1) - u(t) \\ = \frac{\sum_{j=1}^k (r(x(t), v, u(t))|_{v=u_j(t)} - r(x(t), v, u(t))|_{v=u(t)}) q_j(t) u_j}{r(x(t), v, u(t))|_{v=u(t)}}. \end{aligned}$$

To obtain the so-called first order trait dynamics, we use the first order Taylor approximation

$$r(x, v, u)|_{v=u+\Delta u_j} - r(x, v, u)|_{v=u} \approx \partial_v r(x, v, u)|_{v=u} \Delta u_j$$

to obtain

$$(A.7) \quad u(t+1) = u(t) + \theta(t) \frac{\partial_v r(x(t), v, u(t))|_{v=u(t)}}{r(x(t), v, u(t))|_{v=u(t)}},$$

where, by virtue of (A.6),

$$\begin{aligned}\theta(t) &= \sum_{j=1}^k \Delta u_j q_j(t) u_j \\ &= \sum_{j=1}^k \Delta u_j q_j(t) (u + \Delta u_j) \\ &= u \sum_{j=1}^k \Delta u_j q_j(t) + \sum_{j=1}^k q_j(t) (\Delta u_j)^2 \\ &= \sum_{j=1}^k q_j(t) (\Delta u_j)^2\end{aligned}$$

is the variance of the phenotypes from the mean u .

Suppose we add the assumption that the phenotypes in the population are symmetrically distributed around the mean u (i.e., for each j , there is an i such that $\Delta u_j q_j(t) = -\Delta u_i q_i(t)$) [129]. In fact, according to Lande [96], “most commonly, phenotypic characters have a normal distribution” (or can be transformed to a normal distribution). Then

$$(A.8) \quad \sum_{j=1}^k \Delta u_j q_j(t) (\Delta u_j)^2 = 0.$$

The difference

$$\theta(t+1) - \theta(t) = \sum_{j=1}^k (q_j(t+1) - q_j(t)) (\Delta u_j)^2$$

equals

$$\sum_{j=1}^k \left(\frac{r(x(t), v, u(t))|_{v=u_j(t)} x_j(t)}{r(x(t), v, u(t))|_{v=u(t)} x(t)} - q_j(t) \right) (\Delta u_j)^2,$$

which we can rewrite as

$$\frac{\sum_{j=1}^k \left(r(x(t), v, u(t))|_{v=u_j(t)} - r(x(t), v, u(t))|_{v=u(t)} \right) q_j(t) (\Delta u_j)^2}{r(x(t), v, u(t))|_{v=u(t)}}.$$

To first-order this term,

$$\frac{\partial_v r(x(t), v, u(t))|_{v=u(t)}}{r(x(t), v, u(t))|_{v=u(t)}} \sum_{j=1}^k \Delta u_j q_j(t) (\Delta u_j)^2 = 0$$

by (A.8). Thus, using first order trait dynamics, we have that $\theta(t+1) = \theta(t)$ (i.e., the variance remains constant in time), and the trait equation (A.7) becomes (5.6).

Bibliography

- [1] P. A. Abrams, ‘Adaptive Dynamics’ vs. ‘adaptive dynamics’, *Journal of Evolutionary Biology* **18** (2005), 1162–1165.
 - [2] A. S. Ackleh, H. Caswell, R. A. Chiquet, T. Tang, and A. Veprauskas, *Sensitivity analysis of the recovery time for a population under the impact of an environmental disturbance*, *Nat. Resour. Model.* **32** (2019), no. 1, e12166, 22, DOI 10.1111/nrm.12166. MR3915788
 - [3] M. Barfield, R. D. Holt, and R. Gomulkiewicz, *Evolution in stage-structured populations*, *The American Naturalist* **177** (2011), no. 4, 397–409.
 - [4] L. Becks, F. Hilker, H. Malchow, K. Jürgens, and H. Arndt, *Experimental demonstration of chaos in a microbial food web*, *Nature* **435** (2005), 1226–1229, DOI <https://doi.org/10.1038/nature03627>.
 - [5] L. Becks and H. Arndt, *Transitions from stable equilibria and back in an experimental food web*, *Ecology* **89** (2008), 3222–3226.
 - [6] E. Beninca, J. Huisman, R. Heerkloss, K. Johnk, P. Branko, E. Van Nes, M. Cheffer, and S. Ellner, *Chaos in a long-term experiment with a plankton community*, *Nature* **451** (2008), 822–825, DOI <https://doi.org/10.1038/nature06512>.
 - [7] A. Berman and R. J. Plemmons, *Nonnegative matrices in the mathematical sciences*, Classics in Applied Mathematics, vol. 9, Society for Industrial and Applied Mathematics (SIAM), Philadelphia, PA, 1994. Revised reprint of the 1979 original, DOI 10.1137/1.9781611971262. MR1298430
 - [8] H. Bernardelli, *Population waves*, *Journal of the Burma Research Society* **31** (1942), part 1, 1–18.
 - [9] F. Brauer and C. Castillo-Chávez, *Mathematical models in population biology and epidemiology*, Texts in Applied Mathematics, vol. 40, Springer-Verlag, New York, 2001, DOI 10.1007/978-1-4757-3516-1. MR1822695
 - [10] F. Brauer, C. Castillo-Chavez, and Z. Feng, *Mathematical models in epidemiology*, Texts in Applied Mathematics, vol. 69, Springer, New York, 2019. With a foreword by Simon Levin, DOI 10.1007/978-1-4939-9828-9. MR3969982
 - [11] M. G. Bulmer, *Periodical insects*, *American Naturalist* **111** (1977), 1099–1117.
 - [12] S. Busenberg and K. Cooke, *Vertically transmitted diseases*, Biomathematics, vol. 23, Springer-Verlag, Berlin, 1993. Models and dynamics, DOI 10.1007/978-3-642-75301-5. MR1206227
 - [13] H. Caswell, *Matrix population models: Construction, analysis, and interpretation*, 2nd ed., Sinauer Associates, Inc. Publishers, Sunderland, Massachusetts, 2001.
 - [14] H. Caswell, *Sensitivity analysis: matrix methods in demography and ecology*, Demographic Research Monographs, Springer, Cham, 2019, DOI 10.1007/978-3-030-10534-1. MR3930559
-

- [15] B. Charlesworth, *Evolution in age-structured populations*, 2nd ed., Cambridge Studies in Mathematical Biology, vol. 13, Cambridge University Press, Cambridge, 1994, DOI 10.1017/CBO9780511525711. MR1294137
- [16] E. L. Charnov and W. M. Schaffer, *Life-history consequences of natural selection: Cole's result revisited*, The American Naturalist **107** (1973), no. 958, 791–793.
- [17] N. R. Chitnis, *Using mathematical models in controlling the spread of malaria*, ProQuest LLC, Ann Arbor, MI, 2005. Thesis (Ph.D.)—The University of Arizona. MR2707899
- [18] N. Chitnis, J. M. Cushing, and J. M. Hyman, *Bifurcation analysis of a mathematical model for malaria transmission*, SIAM J. Appl. Math. **67** (2006), no. 1, 24–45, DOI 10.1137/050638941. MR2272613
- [19] N. Chitnis, J. M. Hyman, and J. M. Cushing, *Determining important parameters in the spread of malaria through the sensitivity analysis of a mathematical model*, Bull. Math. Biol. **70** (2008), no. 5, 1272–1296, DOI 10.1007/s11538-008-9299-0. MR2421498
- [20] R. A. Chiquet, B. Ma, A. S. Ackleh, N. Pal, and N. Sidorovskaya, *Demographic analysis of sperm whales using matrix population models*, Ecological Modeling **248** (2013), 71–79.
- [21] T. J. Clark and A. D. Luis, *Nonlinear population dynamics are ubiquitous in animals*, Nature Ecology & Evolution **4** (2020), 75–81.
- [22] L. C. Cole, *The population consequences of life history phenomena*, The Quarterly Review of Biology **29** (1954), no. 2, 103–137.
- [23] R. F. Costantino, R. A. Desharnais, J. M. Cushing, and Brian Dennis, *Chaotic dynamics in an insect population*, Science **275** (1997), 289–391.
- [24] R. F. Costantino, J. M. Cushing, B. Dennis, R. A. Desharnais, and S. M. Henson, *Resonant population cycles in temporally fluctuating habitats*, Bulletin of Mathematical Biology **60** (1998), no. 2, 247–275.
- [25] R. F. Costantino, R. A. Desharnais, J. M. Cushing, B. Dennis, S. M. Henson, and A. A. King, *The flour beetle *Tribolium* as an effective tool of discovery*, Advances in Ecological Research **37** (2005), 101–141.
- [26] F. Courchamp, L. Berec, and J. Gascoigne, *Allee effects in ecology and conservation*, Oxford University Press, Oxford, Great Britain, 2008.
- [27] J. M. Cushing, *A strong ergodic theorem for some nonlinear matrix models for the dynamics of structured populations*, Natur. Resource Modeling **3** (1989), no. 3, 331–357, DOI 10.1111/j.1939-7445.1989.tb00085.x. MR1025700
- [28] J. M. Cushing, *An introduction to structured population dynamics*, CBMS-NSF Regional Conference Series in Applied Mathematics, vol. 71, Society for Industrial and Applied Mathematics (SIAM), Philadelphia, PA, 1998, DOI 10.1137/1.9781611970005. MR1636703
- [29] J. M. Cushing, *Nonlinear semelparous Leslie models*, Math. Biosci. Eng. **3** (2006), no. 1, 17–36, DOI 10.3934/mbe.2006.3.17. MR2188279
- [30] J. M. Cushing, *Three stage semelparous Leslie models*, J. Math. Biol. **59** (2009), no. 1, 75–104, Springer Nature, DOI 10.1007/s00285-008-0208-9. MR2501473
- [31] J. M. Cushing, *Matrix models and population dynamics*, Mathematical biology, IAS/Park City Math. Ser., vol. 14, Amer. Math. Soc., Providence, RI, 2009, pp. 49–149, DOI 10.1090/pcms/014/04. MR2522049
- [32] J. M. Cushing, *On the relationship between r and R_0 and its role in the bifurcation of stable equilibria of Darwinian matrix models*, J. Biol. Dyn. **5** (2011), no. 3, 277–297, DOI 10.1080/17513758.2010.491583. MR2818158
- [33] J. M. Cushing, *Backward bifurcations and strong Allee effects in matrix models for the dynamics of structured populations*, J. Biol. Dyn. **8** (2014), no. 1, 57–73, DOI 10.1080/17513758.2014.899638. MR3271017
- [34] J. M. Cushing, *On the fundamental bifurcation theorem for semelparous Leslie models*, Dynamics, games and science, CIM Ser. Math. Sci., vol. 1, Springer, Cham, 2015, pp. 215–251. MR3644916
- [35] J. M. Cushing, *Discrete time darwinian dynamics and semelparity versus iteroparity*, Math. Biosci. Eng. **16** (2019), no. 4, 1815–1835, DOI 10.3934/mbe.2019088. MR4030661

- [36] J. M. Cushing, *A Darwinian Ricker equation*, Progress on difference equations and discrete dynamical systems, Springer Proc. Math. Stat., vol. 341, Springer, Cham, [2020] ©2020, pp. 231–243, DOI 10.1007/978-3-030-60107-2_10. MR4219152
- [37] J. M. Cushing, *A bifurcation theorem for Darwinian matrix models and an application to the evolution of reproductive life-history strategies*, J. Biol. Dyn. **15** (2021), no. suppl. 1, S190–S213, DOI 10.1080/17513758.2020.1858196. MR4263451
- [38] J. M. Cushing and J. Li, *On Ebenman's model for the dynamics of a population with competing juveniles and adults*, Bulletin of Mathematical Biology **51** (1989), no. 6, 687–713.
- [39] J. M. Cushing and Z. Yicang, *The net reproductive value and stability in matrix population models*, Natural Resource Modeling **8** (1994), 297–333.
- [40] J. M. Cushing, B. Dennis, R. A. Desharnais, and R. F. Costantino, *Moving toward an unstable equilibrium: Saddle nodes in population systems*, Journal of Animal Ecology **67** (1998), no. 1, 298–306.
- [41] J. M. Cushing, R. F. Costantino, B. Dennis, R. A. Desharnais, and S. M. Henson, *Chaos in ecology: Experimental nonlinear dynamics*, Theoretical Ecology Series, vol. 1, Academic Press (Elsevier Science), New York, 2003, ISBN: 0-12-1988767.
- [42] J. M. Cushing and S. M. Henson, *Stable bifurcations in semelparous Leslie models*, J. Biol. Dyn. **6** (2012), no. suppl. 2, 80–102, DOI 10.1080/17513758.2012.716085. MR2994280
- [43] J. M. Cushing, S. M. Henson, and J. L. Hayward, *An evolutionary game-theoretic model of cannibalism*, Nat. Resour. Model. **28** (2015), no. 4, 497–521, DOI 10.1111/nrm.12079. MR3423350
- [44] J. M. Cushing and A. P. Farrell, *A bifurcation theorem for nonlinear matrix models of population dynamics*, J. Difference Equ. Appl. **26** (2020), no. 1, 25–44, DOI 10.1080/10236198.2019.1699916. MR4065246
- [45] J. M. Cushing and K. Stefanko, *A Darwinian dynamic model for the evolution of post-reproduction survival*, J. Biol. Systems **29** (2021), no. 2, 433–450, DOI 10.1142/S0218339021400088. MR4274354
- [46] C. Darwin, *The origin of species*, 6th ed., Murray, London, 1872.
- [47] N. V. Davydova, O. Diekmann, and S. A. van Gils, *Year class coexistence or competitive exclusion for strict biennials?*, J. Math. Biol. **46** (2003), no. 2, 95–131, DOI 10.1007/s00285-002-0167-5. MR1963068
- [48] N. V. Davydova, O. Diekmann, and S. A. van Gils, *On circulant populations. I. The algebra of semelparity*, Linear Algebra Appl. **398** (2005), 185–243, DOI 10.1016/j.laa.2004.12.020. MR2121350
- [49] J. H. P. Dawes and M. O. Souza, *A derivation of Holling's type I, II and III functional responses in predator-prey systems*, J. Theoret. Biol. **327** (2013), 11–22, DOI 10.1016/j.jtbi.2013.02.017. MR3046076
- [50] B. Dennis, R. A. Desharnais, J. M. Cushing, and R. F. Costantino, *Nonlinear demographic dynamics: Mathematical models, statistical methods, and biological experiments*, Ecological Monographs **65** (1995), no. 3, 261–281.
- [51] B. Dennis, R. A. Desharnais, J. M. Cushing, and R. F. Costantino, *Transitions in population dynamics: Equilibria to periodic cycles to aperiodic cycles*, Journal of Animal Ecology **66** (1997), 704–729.
- [52] B. Dennis, R. A. Desharnais, J. M. Cushing, S. M. Henson, and R. F. Costantino, *Estimating chaos and complex dynamics in an insect population*, Ecological Monographs **71** (2001), no. 2, 277–303.
- [53] R. A. Desharnais, R. F. Costantino, J. M. Cushing, S. M. Henson, and B. Dennis, *Chaos and population control of insect outbreaks*, Ecology Letters **4** (2001), no. 3, 229–235.
- [54] R. A. Desharnais, S. M. Henson, R. F. Costantino, and B. Dennis, *Capturing chaos: A multidisciplinary approach to nonlinear population dynamics*, Journal of Difference Equations and Applications (2023), DOI 10.1080/10236198.2023.2260013.
- [55] O. Diekmann, M. Gyllenberg, H. Huang, M. Kirkilionis, J. A. J. Metz, and H. R. Thieme, *On the formulation and analysis of general deterministic structured population models. II. Nonlinear theory*, J. Math. Biol. **43** (2001), no. 2, 157–189, DOI 10.1007/s002850170002. MR1860461

- [56] O. Diekmann and S. A. van Gils, *Invariance and symmetry in a year-class model*, Bifurcation, symmetry and patterns (Porto, 2000), Trends Math., Birkhäuser, Basel, 2003, pp. 141–150. MR2014364
- [57] O. Diekmann, *A beginner's guide to adaptive dynamics*, Mathematical modelling of population dynamics, Banach Center Publ., vol. 63, Polish Acad. Sci. Inst. Math., Warsaw, 2004, pp. 47–86. MR2076953
- [58] O. Diekmann and S. A. van Gils, *On the cyclic replicator equation and the dynamics of semelparous populations*, SIAM J. Appl. Dyn. Syst. **8** (2009), no. 3, 1160–1189, DOI 10.1137/080722734. MR2551259
- [59] O. Diekmann, N. Davydova, and S. van Gils, *On a boom and bust year class cycle*, J. Difference Equ. Appl. **11** (2005), no. 4-5, 327–335, DOI 10.1080/10236190412331335409. MR2151678
- [60] D. Doak, P. Kareiva, and B. Klepetka, *Modeling population viability for the desert tortoise in the western Mojave Desert*, Ecological Applications **4** (1994), no. 3, 446–460.
- [61] Q. Dong and G. A. Polis, *The dynamics of cannibalistic populations: A foraging perspective*, in M.A. Elgar and B.J. Crespi (eds.), *Cannibalism: Ecology and evolution among diverse taxa*, Oxford University Press, Oxford, 1992, pp. 13–37.
- [62] S. Elaydi, *An introduction to difference equations*, 3rd ed., Undergraduate Texts in Mathematics, Springer, New York, 2005. MR2128146
- [63] S. N. Elaydi, *Discrete chaos*, 2nd ed., Chapman & Hall/CRC, Boca Raton, FL, 2008. With applications in science and engineering; With a foreword by Robert M. May; With 1 CD-ROM (Windows, Macintosh and UNIX). MR2364977
- [64] S. N. Elaydi and J. M. Cushing, *Discrete mathematical biology*, to appear, Springer, New York, NY.
- [65] M. A. Elgar and B. J. Crespi, *Cannibalism: Ecology and evolution among diverse taxa*, Oxford University Press, Oxford, 1992, ISBN: 9780198546504.
- [66] B. Ebenman, *Niche differences between age classes and intraspecific competition in age-structured populations*, J. Theoret. Biol. **124** (1987), no. 1, 25–33, DOI 10.1016/S0022-5193(87)80249-7. MR871409
- [67] B. Ebenman, *Competition between age classes and population dynamics*, J. Theoret. Biol. **131** (1988), no. 4, 389–400, DOI 10.1016/S0022-5193(88)80036-5. MR936313
- [68] A. P. Farrell, *How the concavity of reproduction/survival trade-offs impacts the evolution of life history strategies*, J. Biol. Dyn. **15** (2021), no. suppl. 1, S134–S167, DOI 10.1080/17513758.2020.1853834. MR4263449
- [69] A. B. Franklin, *Population regulation in Northern Spotted Owls: Theoretical implications for management*, in D. R. McCullough and R. H. Barrett (eds.), *Wildlife 2001: Populations*, Elsevier Applied Sciences, London, England, 1992, pp. 815–827.
- [70] P. Govindarajulu, R. Altwegg, and B. R. Anholt, *Matrix model investigation of invasive species control: Bullfrogs on Vancouver Island*, Ecological Applications **15** (2005), no. 6, 2161–2170.
- [71] D. Graham, C. Knapp, E. Van Vleck, K. Bloor, T. Lane, and C. Graham, *Experimental demonstration of chaotic instability in biological nitrification*, The ISME Journal **1** (2007), 385–393, DOI <https://doi.org/10.1038/ismej.2007.45>.
- [72] J. L. Hayward, L. M. Weldon, S. M. Henson, L. C. Megna, B. G. Payne, and A. E. Moncrieff, *Egg cannibalism in a gull colony increases with sea surface temperature*, Condor **116** (2014), 62–73.
- [73] K. Hellövaara, R. Väistönen, and C. Simon, *Evolutionary ecology of periodical insects*, Trends in Ecology and Evolution **9** (1994), no. 12, 475–480.
- [74] S. M. Henson and J. M. Cushing, *The effect of periodic habitat fluctuations on a nonlinear insect population model*, J. Math. Biol. **36** (1997), no. 2, 201–226, DOI 10.1007/s002850050098. MR1601788
- [75] S. M. Henson, J. M. Cushing, R. F. Costantino, B. Dennis, and R. A. Desharnais, *Phase switching in biological population*, Proceedings of the Royal Society **265** (1998), no. 22, 2229–2234.
- [76] S. M. Henson, R. F. Costantino, J. M. Cushing, B. Dennis, and R. A. Desharnais, *Multiple attractors, saddles, and population dynamics in periodic habitats*, Bulletin of Mathematical Biology **61** (1999), 1121–1149.

- [77] S. M. Henson, R. F. Costantino, J. M. Cushing, B. Dennis, and R. A. Desharnais, *Basins of attraction: Population dynamics with two locally stable 4-cycles*, Oikos **98** (2002), 17–24.
- [78] S. M. Henson, R. F. Costantino, J. M. Cushing, R. A. Desharnais, B. Dennis, and A. A. King, *Lattice effects observed in chaotic dynamics of experimental populations*, Science **294** (2002), no. 19, 602–605.
- [79] W. A. Hoffman, *Fire and population dynamics of woody plants in a neotropical savanna: Matrix model projections*, Ecology **80** (1999), no. 4, 1354–1369.
- [80] R. A. Horn and C. R. Johnson, *Matrix analysis*, Cambridge University Press, Cambridge, 1985, DOI 10.1017/CBO9780511810817. MR832183
- [81] P. W. Hughes (2017), *Between semelparity and iteroparity: Empirical evidence for a continuum of models of parity*, Ecology and Evolution **7** (2017), no. 20, 8232–8261.
- [82] J. Impagliazzo, *Deterministic aspects of mathematical demography*, Biomathematics, vol. 13, Springer-Verlag, Berlin, 1985. An investigation of the stable theory of population including an analysis of the population statistics of Denmark, DOI 10.1007/978-3-642-82319-0. MR795278
- [83] H. Inaba, *Age-structured population dynamics in demography and epidemiology*, Springer, Singapore, 2017, DOI 10.1007/978-981-10-0188-8. MR3616174
- [84] M. Iannelli and A. Pugliese, *An introduction to mathematical population dynamics*, Unitext, vol. 79, Springer, Cham, 2014. Along the trail of Volterra and Lotka; La Matematica per il 3+2, DOI 10.1007/978-3-319-03026-5. MR3288300
- [85] J. Jacobs, *Cooperation, optimal density, and low density thresholds: Yet another modification of the logistic model*, Oecologia **64** (1984), 389–395.
- [86] D. Kamerow, *The world's deadliest animal*, British Medical Journal (online) (2014), vol. 348, DOI 10.1136/bmjj.g3258.
- [87] A. A. King, R. F. Costantino, J. M. Cushing, S. M. Henson, R. A. Desharnais, and B. Dennis, *Anatomy of a chaotic attractor: Subtle model predicted patterns revealed in population data*, Proceedings of the National Academy of Sciences **101** (2003), no. 1, 408–413.
- [88] B. Kipchumba, *Construction and analysis of a Leslie matrix population model for Amboseli elephants*, Masters thesis, Applied Mathematics, University of Nairobi, 2013.
- [89] R. Kon, *Competitive exclusion between year-classes in a semelparous biennial population*, Mathematical Modeling of Biological Systems, Volume II, Birkhäuser, Boston-Basel-Berlin, 2008, pp. 75–85.
- [90] R. Kon, *Age-structured Lotka-Volterra equations for multiple semelparous populations*, SIAM J. Appl. Math. **71** (2011), no. 3, 694–713, DOI 10.1137/100794262. MR2796085
- [91] R. Kon, *Non-synchronous oscillations in four-dimensional nonlinear semelparous Leslie matrix models*, J. Difference Equ. Appl. **23** (2017), no. 10, 1747–1759, DOI 10.1080/10236198.2017.1365144. MR3740677
- [92] R. Kon, Y. Saito, and Y. Takeuchi, *Permanence of single-species stage-structured models*, J. Math. Biol. **48** (2004), no. 5, 515–528, DOI 10.1007/s00285-003-0239-1. MR2067114
- [93] R. Kon and Y. Iwasa, *Single-class orbits in nonlinear Leslie matrix models for semelparous populations*, J. Math. Biol. **55** (2007), no. 5–6, 781–802, DOI 10.1007/s00285-007-0111-9. MR2350560
- [94] M. Kot, *Elements of mathematical ecology*, Cambridge University Press, Cambridge, 2001, DOI 10.1017/CBO9780511608520. MR2006645
- [95] U. Krause, *Positive dynamical systems in discrete time*, De Gruyter Studies in Mathematics, vol. 62, De Gruyter, Berlin, 2015. Theory, models, and applications, DOI 10.1515/9783110365696. MR3309532
- [96] R. Lande, *Natural selection and random genetic drift in phenotypic evolution*, Evolution **30** (1976), no. 2, 314–334.
- [97] R. Lande, *A quantitative genetic theory of life history evolution*, Ecology **63** (1982), 607–615.
- [98] J. P. LaSalle, *The stability of dynamical systems*, Regional Conference Series in Applied Mathematics, Society for Industrial and Applied Mathematics, Philadelphia, PA, 1976. With an appendix: “Limiting equations and stability of nonautonomous ordinary differential equations” by Z. Artstein. MR481301

- [99] L. P. Lefkovitch, *The study of population growth in organisms grouped by stage*, Biometrics **21** (1965), 1–18.
- [100] P. H. Leslie, *On the use of matrices in certain population mathematics*, Biometrika **33** (1945), 183–212, DOI 10.1093/biomet/33.3.183. MR15760
- [101] P. H. Leslie, *Some further notes on the use of matrices in population mathematics*, Biometrika **35** (1948), 213–245, DOI 10.1093/biomet/35.3-4.213. MR27991
- [102] S. A. Levin and C. P. Goodyear, *Analysis of an age-structured fishery model*, J. Math. Biol. **9** (1980), no. 3, 245–274, DOI 10.1007/BF00276028. MR661430
- [103] E. G. Lewis, *On the generation and growth of a population*, Sankhya **6** (1942), 93–96.
- [104] C.-K. Li and H. Schneider, *Applications of Perron-Frobenius theory to population dynamics*, J. Math. Biol. **44** (2002), no. 5, 450–462, DOI 10.1007/s002850100132. MR1908132
- [105] X.-Z. Li, J. Yang, and M. Martcheva, *Age structured epidemic modeling*, Interdisciplinary Applied Mathematics, vol. 52, Springer, Cham, [2020] ©2020, DOI 10.1007/978-3-030-42496-1. MR4223785
- [106] D. O. Logofet, *Matrices and graphs: Stability problems in mathematical ecology*, CRC Press, Boca Raton, 2009.
- [107] D. Ludwig, D. D. Jones, and C. S. Holling, *Qualitative analysis of insect outbreak systems: The spruce budworm and forest*, Journal of Animal Ecology **47** (1978), 315–332.
- [108] F. Lutscher, *Integrodifference equations in spatial ecology*, Interdisciplinary Applied Mathematics, vol. 49, Springer, Cham, [2019] ©2019. With a foreword by Mark Lewis, DOI 10.1007/978-3-030-29294-2. MR3971004
- [109] P. Magal and S. Ruan (eds.), *Structured population models in biology and epidemiology*, Lecture Notes in Mathematics, vol. 1936, Springer-Verlag, Berlin, 2008. Mathematical Biosciences Subseries, DOI 10.1007/978-3-540-78273-5. MR2445337
- [110] J. A. Metz and O. Diekmann, *The dynamics of physiologically structured populations*, Lecture Notes in Biomathematics, vol. 68, Springer-Verlag, Berlin, 1986.
- [111] H. F. Mollet and G. M. Cailliet, *Comparative population demography of elasmobranchs using life history tables, Leslie matrices, and stage-based matrix models*, Marine and Freshwater Research **53** (2002), no. 2, 503–515.
- [112] Cynthia J. Moss, *The demography of an African elephant (*Loxodonta africana*) population in Amboseli, Kenya*, Journal of Zoology **255** (2001), no. 2, 145–156, DOI 10.1017/S0952836901001212.
- [113] J. N. Perry, R. H. Smith, I. P. Woiwod, and D. R. Morse, *Chaos in real data: The analysis of nonlinear dynamics from short ecological time series*, Kluwer Academic Publishers, Dordrecht, The Netherlands, 2000.
- [114] M. D. Pointer, M. J. G. Gage, and L. G. Spurgin, *Tribolium beetles as a model system in evolution and ecology*, Heredity **126** (2021), 869–883, DOI <https://doi.org/10.1038/s41437-021-00420-1>.
- [115] G. A. Polis, *The evolution and dynamics of intraspecific predation*, Annual Review of Ecology and Systematics **12** (1981), 225–251.
- [116] R. C. Rael, R. F. Costantino, J. M. Cushing, and T. L. Vincent, *Using stage-structured evolutionary game theory to model the experimentally observed evolution of a genetic polymorphism*, Evolutionary Ecology Research **11** (2009), 141–151.
- [117] W. E. Ricker, *Stock and recruitment*, Journal of the Fisheries Research Board of Canada **11** (1954), 559–623.
- [118] W. E. Ricker, *The historical development*, Fish Population Dynamics, L. A. Gulland (ed.), Wiley, London, 1975, pp. 1–26.
- [119] D. A. Roff, *The evolution of life histories, theory, and analysis*, Chapman & Hall, New York, 1992.
- [120] D. A. Roff, *Modeling evolution*, Oxford University Press, Oxford, 2010. An introduction to numerical methods. MR2599631
- [121] S. Schreiber, *Allee effects, extinctions, and chaotic transients in simple population models*, Theoretical Population Biology **64** (2003), 201–209.

-
- [122] H. L. Smith and H. R. Thieme, *Dynamical systems and population persistence*, Graduate Studies in Mathematics, vol. 118, American Mathematical Society, Providence, RI, 2011, DOI 10.1090/gsm/118. MR2731633
 - [123] S. C. Stearns, *The evolution of life histories*, Oxford University Press Inc., New York, 2004.
 - [124] M. B. Usher, *A matrix approach to the management of renewable resources, with special reference to selection forests*, Journal of Applied Ecology **3** (1966), 355–367.
 - [125] J. S. Vandergraft, *Spectral properties of matrices which have invariant cones*, SIAM J. Appl. Math. **16** (1968), 1208–1222, DOI 10.1137/0116101. MR244284
 - [126] D. Vayenas and S. Pavlou, *Chaotic dynamics of a food web in a chemostat*, Mathematical Biosciences **162** (1999), 69–84.
 - [127] A. Veprauskas, *Synchrony and the dynamic dichotomy in a class of matrix population models*, SIAM J. Appl. Math. **78** (2018), no. 5, 2491–2510, DOI 10.1137/17M1136444. MR3855397
 - [128] A. Veprauskas and J. M. Cushing, *A juvenile-adult population model: climate change, cannibalism, reproductive synchrony, and strong Allee effects*, J. Biol. Dyn. **11** (2017), no. suppl. 1, 1–24, DOI 10.1080/17513758.2015.1131853. MR3620961
 - [129] T. Vincent and J. Brown, *Evolutionary game theory, natural selection, and Darwinian dynamics*, Cambridge University Press, Cambridge, UK, 2005.
 - [130] G. F. Webb, *Theory of nonlinear age-dependent population dynamics*, Monographs and Textbooks in Pure and Applied Mathematics, vol. 89, Marcel Dekker, Inc., New York, 1985. MR772205
 - [131] P. A. Werner and H. Caswell, *Population growth rates and age versus stage-distribution models for teasel (*Dipsacus sylvestris* Huds.)*, Ecology **58** (1977), no. 5, 1103–1111.
 - [132] S. Wiggins, *Introduction to applied nonlinear dynamical systems and chaos*, 2nd ed., Texts in Applied Mathematics, vol. 2, Springer-Verlag, New York, 2003. MR2004534
 - [133] X.-Q. Zhao, *Dynamical systems in population biology*, CMS Books in Mathematics/Ouvrages de Mathématiques de la SMC, vol. 16, Springer-Verlag, New York, 2003, DOI 10.1007/978-0-387-21761-1. MR1980821
 - [134] C. Zimmer, *Life after chaos*, Science **284** (1999), no. 5411, 83–86.

Index

- 2-cycles, 28, 120
Synchronous, 137
- Adaptive landscape, 215
- Age-structured population, 45
- Allee effect
Allee component, 8, 19, 115
Strong Allee effect, 22, 119, 132, 220
Weak Allee effect, 22
- American bullfrog
Linear model, 77
Nonlinear model, 106
- Attractor, 4
- Axioms of natural selection, 203
- Backward bifurcation, 19, 110
- Basic bifurcation theorem
Darwinian matrix model, 217
Epidemic models, 183
 $m = 1$ dimensional equation, 21
Nonlinear matrix equation -
imprimitive Leslie model, 139
Nonlinear matrix equation -
primitive projection matrix, 109
- Basin of attraction, 14
- Beverton-Holt equation, 10
- Bifurcation, 4
+1, 123
-1, 125
Backward, 19, 110
- Direction, 21, 110
Forward, 19, 110
Local, 120
- Neimark-Sacker, 130
- Period-doubling, 29, 36, 125, 244
- Saddle-node, 125
Stable, 21
Tangent, 21
Transcritical, 5, 13, 123
Unstable, 21
- Bifurcation diagram, 5, 12, 112
- Cannibalism, 143, 148
- Canonical equation of evolution, 204
- Chaos, 29, 244
- Cicadas, 60, 154
- Cole's Paradox, 33, 237, 244
- Critical point, 16
- Critical trait, 214
- Cycle chain, 159
- Cycles, 244
- Darwinian dynamics, 205
Discrete logistic, 208, 216
Juvenile-adult model, 207, 209, 211,
212, 216
Nonlinear Leslie model, 229
Ricker, 208, 245, 246
Structured population, 208
- Density dependence, 7

- Density factor, 8, 98
 Negative, 92
 Normalization, 9, 98
 Positive, 92
- Density-free rates, 8
- Difference equation, 1, 2
 Linear, 7
 Nonlinear, 7
- Direction of bifurcation, 21, 110
- Discrete logistic equation, 10
- Disease-free equation, 168
- Disease-free equilibrium, 168
- Dominant eigenvalue, 53, 98
- Dynamic dichotomy, 140, 159
- Early versus late reproduction, 235
- Ebenman's model, 94, 108
- Elasticity, 73
- Elasticity matrix, 73
- Equilibrium, 4, 12
 Extinction, 4, 211
 Hyperbolic, 15
 Positive, 98, 211
 Survival, 91, 98, 211
- Equilibrium equation, 12
- Escape function, 169
- Escape probability, 169
- ESS Maximum Principle, 222
- Evergreen shrub model, 82
- Evolutionary game theory, 205
- Evolutionary stable strategy ESS, 221
 Darwinian Ricker, 248
 Semelparity, 241, 243
- Evolutionary suicide, 225, 246, 248
- Exchange of stability, 123
- Exponential population growth rate, 4
- Extinction equilibrium, 4
- Fertility matrix \mathbf{F} , 45
 Inherent, 97
- Fertility rate, 3
- Fisher's equation, 204
- Fitness, 4, 204, 209
- Flour beetles, 60, 75, 142
- Force of infection, 173
- Forward bifurcation, 19, 110
- Forward invariant, 9, 97
- Fundamental Theorem of Demography, 54
- Glaucous-winged gulls, 148
- Global asymptotic stability, 25, 99, 107
- Handling time, 33
- Herd immunity, 187, 189, 192
- Hysteresis, 24
- Imprimitive matrix, 54
- Inherent fertility matrix \mathbf{F} , 97
- Inherent population growth rate R_0
 Unstructured population, 25
- Inherent population growth rate r_0 ,
 103
 Darwinian model, 214, 228
 Unstructured population, 25
- Inherent rates
 Structured population, 97
 Unstructured population, 8
- Inherent reproduction number R_0
 Cannibalism model, 149
 Darwinian model, 228
 Definition of, 105
 Epidemic model, 172
 LPA model, 144
 Malaria model, 198
 Nonlinear Leslie model, 106
 Semelparous Leslie model, 155
 SI vaccination model, 188
 SIR vaccination model, 191
- Inherent transition matrix \mathbf{T} , 97
- Initial condition, 45
- Instability, 101
- Invariant loop, 122
- Invasion driven evolution, 202, 221
- Irreducible matrix, 49
- Iteroparous, 10, 33, 58, 237
- Jacobian, 99
- Juvenile-adult matrix model, 115
 Direction of bifurcation, 116
- Iteroparous, 58
- Linear, 57
- Nonlinear, 93, 103, 104, 111
- Semelparous, 58, 100, 139
- κ , 109, 183, 217

- Lande's equation, 204
Leslie matrix model, 46
 Ebenman's model, 94
 Extended, 47
 Irreducible, 59
 LPA model, 59
 Nonlinear, 105, 229
 Semelparous, 60, 154
Life cycle graph
 Definition, 49
 Strongly connected, 49
Linearization Principle
 For cycles, 128
 For equilibria, 15, 99
Local asymptotic stability, 14
LPA model, 59, 142

Malaria, 192
Malaria model, 193
Matrix equation
 Linear, 45
 Nonlinear, 96
 Solution of, 45
Matrix population model
 Definition, 2
 Leslie, 46, 47
 Usher or standard size structured, 47
Mosquitoes, 192

Next generation matrix, 61
Nonnegative matrix, 45
Normalized population distribution, 54

Orbit, 114

 p -cycle, 29, 122
 Hyperbolic, 31
Periodical insects, 154
Permanent immunity, 177
Perron eigenvalue, 54
Perron-Frobenius theory, 53, 97, 98,
 211
Persistent, 102
Phase plane, 114
Plasmodium, 192
Population growth rate r_0
 Structured population, 56, 98
 Unstructured population, 4
Population projection matrix \mathbf{P}
 Inherent or density-free, 97
 Linear, 45
 Nonlinear, 96
Post-reproduction survival, 31
Predation, 33
Predator saturation effect, 150
Prey discovery time, 33
Primitive matrix, 54

 R_0
 Epidemic model, 172
 Malaria model, 198
 Relation to r_0 , 228
 Structured population, 61, 105
 Unstructured population, 5
Repeller, 4
Reproduction number R_0
 Definition of, 61
 Leslie matrix, 64
 Unstructured population, 5
Ricker equation, 18

Saddle node, 125
Saddle-node bifurcation, 125
SAIR model, 178, 185
Semelparous, 10, 33, 58, 237
Sensitivity, 70
Sensitivity matrix, 71
SI Model, 168
 With vaccination, 188
SI model, 183
SIR Model, 175
 With vaccination, 189
Spectral radius, 54
Speed of evolution, 204
Spruce-Budworm, 33
Stability, 14, 98
Stable demographic distribution, 56
Stable node, 125
Standard size structured matrix model,
 47
Strictly dominant eigenvalue, 54
Structured population model, 1, 44
Survival rate, 3

Time series plots, 114
Tipping point, 21
Total population size, 98
Trade-offs, 149, 238

Trait (strategy) driven evolution, 202,
221

Transcritical bifurcation, 5, 13, 123

Transition matrix **T**, 45

Inherent, 97

Usher matrix model, 47

This book offers an introduction to the use of matrix theory and linear algebra in modeling the dynamics of biological populations. Matrix algebra has been used in population biology since the 1940s and continues to play a major role in theoretical and applied dynamics for populations structured by age, body size or weight, disease states, physiological and behavioral characteristics, life cycle stages, or any of many other possible classification schemes. With a focus on matrix models, the book requires only first courses in multivariable calculus and matrix theory or linear algebra as prerequisites.



The reader will learn the basics of modeling methodology (i.e., how to set up a matrix model from biological underpinnings) and the fundamentals of the analysis of discrete time dynamical systems (equilibria, stability, bifurcations, etc.). A recurrent theme in all chapters concerns the problem of extinction versus survival of a population. In addition to numerous examples that illustrate these fundamentals, several applications appear at the end of each chapter that illustrate the full cycle of model setup, mathematical analysis, and interpretation. The author has used the material over many decades in a variety of teaching and mentoring settings, including special topics courses and seminars in mathematical modeling, mathematical biology, and dynamical systems.

ISBN 978-1-4704-7334-1



9 781470 473341

STML/106



For additional information
and updates on this book, visit
www.ams.org/bookpages/stml-106

